

**SYNTHESIS AND PREPARATION OF  
POLYSACCHARIDE BASED MEMBRANES FOR  
THE PERVAPORATION SEPARATION OF LIQUID  
MIXTURE SYSTEMS OF INDUSTRIAL INTEREST**

by

Go Young Moon

A thesis  
presented to the University of Waterloo  
in fulfillment of the  
thesis requirement for the degree of  
Doctor of Philosophy  
in  
Chemical Engineering

Waterloo, Ontario, Canada, 2000

©Go Young Moon, 2000



**National Library  
of Canada**

**Acquisitions and  
Bibliographic Services**

395 Wellington Street  
Ottawa ON K1A 0N4  
Canada

**Bibliothèque nationale  
du Canada**

**Acquisitions et  
services bibliographiques**

395, rue Wellington  
Ottawa ON K1A 0N4  
Canada

*Your file Votre référence*

*Our file Notre référence*

The author has granted a non-exclusive licence allowing the National Library of Canada to reproduce, loan, distribute or sell copies of this thesis in microform, paper or electronic formats.

The author retains ownership of the copyright in this thesis. Neither the thesis nor substantial extracts from it may be printed or otherwise reproduced without the author's permission.

L'auteur a accordé une licence non exclusive permettant à la Bibliothèque nationale du Canada de reproduire, prêter, distribuer ou vendre des copies de cette thèse sous la forme de microfiche/film, de reproduction sur papier ou sur format électronique.

L'auteur conserve la propriété du droit d'auteur qui protège cette thèse. Ni la thèse ni des extraits substantiels de celle-ci ne doivent être imprimés ou autrement reproduits sans son autorisation.

0-612-60558-2

**Canada**

*The University of Waterloo requires the signatures of all persons using or photocopying this thesis. Please sign below, and give address and date.*

## ABSTRACT

Pervaporation membrane processes have been established as an important separation unit operation in chemical engineering processes. The pervaporation process is technologically mature for the dehydration of aqueous alcohol mixtures and is expected to find further progress in the organic/organic separations and the organic or water separation from water/organic mixtures.

Various pervaporation membranes made from natural polymers such as chitosan and alginate as well as EPDM rubber have been fabricated and investigated in terms of the permeation flux and separation factor in pervaporation experiments. Dense and thin film composite membranes were extensively investigated for the separation of water from aqueous alcohol mixtures, the separation of alcohols from alcohol/toluene mixtures, the separation of methanol from methanol/MTBE mixtures, and the separation of a model aroma compound from aqueous mixtures.

Sodium alginate membranes are known to be hydrophilic and suitable for dehydration applications. However, since sodium alginate is water soluble and mechanically brittle efforts to increase the mechanical strength of the alginate membrane have been made which include the metal ion crosslinking and the insolubilization reactions.

As part of research effort to increase the mechanical strength of alginate membranes, two ply composite membranes consisting of sodium alginate and chitosan

were prepared and the preparation parameters were analyzed by means of experimental design which lead to optimum membrane structure and preparation conditions.

Composite chitosan membranes were also prepared for the separation of aqueous alcohol mixtures and the pervaporation characteristics of dense and composite membranes were compared. In addition, it was shown that the coating of hydrophobic polysulfone substrate with hydrophilic polymers such as polyvinyl alcohol could enhance structural stability of the composite membrane.

The preparation and pervaporation performance study of the alginate composite membrane consisting of a chitosan layer sandwiched between the top alginate layer and polyvinylidene fluoride substrate layer were carried out for the separation of aqueous alcohol mixtures.

Chitosan membranes were chemically modified in acetic anhydride solution. Modified membranes (N-acetylated chitosan (or chitin)) were found to be much stronger than the chitosan membranes. The N-acetylation reaction made the chitosan membrane robust for the pervaporation separation of organic/organic mixtures such as alcohol/toluene mixtures while keeping its polar property.

Polyelectrolyte complex membranes with high hydrophilicity were developed from chitosan and anionic surfactants. The rheological properties of the casting solutions and also the pervaporation performance of the complex membranes for the separation of methanol/MTBE mixtures were extensively investigated. It was found that the resulting membrane thickness could be decreased because of a chain-coiling phenomenon induced by the interaction between cationic chitosan and anionic surfactant molecules.

Ethylene propylene diene monomer (EPDM) membranes were prepared to separate a model aroma compound from aqueous solution and the transport phenomenon of aroma compound was modeled based on the resistance-in-series model.

## ACKNOWLEDGMENTS

It has been said that it takes the village to raise the children. It is obviously true for the Ph.D. degree. I can say that research is like an endless journey through whole life trying to find the unknown. Now I just finished the first trip for another continuous journey.

I wish to carry my sincere appreciation to my supervisors, Professor R.Y.M. Huang and Professor R. Pal for their excellent guidance and invaluable advice throughout this study and during the preparation of the thesis. Especially Professor Huang and Mrs. Huang have been always generous for my family. It will be a long lasting and beautiful memory of Waterloo for my family.

I have had the pleasure to work and socialize with many brilliant and kind people whom I met in Waterloo. Some of them are Seon Wook Kim, Woo Young Won, Ping Hai Shao, and Amphai Chanachai and Panida Sampranpiboom who were visiting students from Thailand in the membrane laboratory. I pray for their future success.

Finally and most of all, my deep appreciation also goes to my beloved wife, Hyun Hong Seo. Her support and love never let me down and was always there when I needed it most. My parents and parents-in-law have provided me with endless encouragement and support. To all of them I dedicate this thesis.

# TABLE OF CONTENTS

**LIST OF TABLES**----- **xv**

**LIST OF FIGURES** ----- **xvii**

## **CHAPTER 1 INTRODUCTION**

**1.1 BACKGROUND**----- **1**  
**1.2 RESEARCH OBJECTIVES** ----- **5**  
**1.3 THE SCOPE OF THESIS**----- **6**

## **CHAPTER 2 BACKGROUND STUDY ON PERVAPORATION**

**2.1 CHARACTERISTICS OF PERVAPORATION MEMBRANE PROCESS** --- **10**  
**2.2 MATERIALS FOR THE PERVAPORATION MEMBRANE PROCESS**--- **15**  
    2.2.1 Approaches for the material selection in pervaporation membrane----- **16**  
    2.2.2 Materials for pervaporation ----- **21**  
**2.3 MASS TRANSPORT PHENOMENA IN PERVAPORATION MEMBRANE  
    PROCESSES** ----- **35**  
    2.3.1 Solution diffusion model ----- **35**  
    2.3.2 Pore flow model ----- **42**  
    2.3.3 The carrier transport mechanism----- **43**  
**2.4 PROCESS PARAMETERS IN PERVAPORATION MEMBRANE  
    PROCESSES** ----- **47**  
**2.5 CLASSIFICATIONS AND MODULES FOR PERVAPORATION**

<b>MEMBRANES</b>	<b>50</b>
2.5.1 Membrane classifications	50
2.5.2 Pervaporation modules	54
<b>2.6 THE MEASUREMENT OF THE DIFFUSION COEFFICIENT</b>	
<b>IN THE MEMBRANE</b>	<b>55</b>
2.6.1 Conventional measurements of diffusion coefficient	57
2.6.2 Inverse gas chromatography approach for the diffusion coefficient	67
<b>CHAPTER 3</b>	
<b>CHARACTERISTICS OF SODIUM ALGINATE MEMBRANES IN</b>	
<b>THE SEPARATION OF ALCOHOL MIXTURES BY</b>	
<b>PERVAPORATION</b>	
<b>3.1 SUMMARY</b>	<b>76</b>
<b>3.2 INTRODUCTION</b>	<b>76</b>
<b>3.3 EXPERIMENTAL</b>	<b>81</b>
3.3.1 Materials	81
3.3.2 Membrane preparation	81
3.3.3 Crosslinking solution	82
3.3.4 Pervaporation	82
<b>3.4 RESULTS AND DISCUSSION</b>	<b>84</b>
3.4.1 FT-IR measurement	84
3.4.2 Characteristics of sodium alginate membranes	86
3.4.3 Ionic crosslinking of sodium alginate membranes	87
3.4.4 Pervaporation of alcohol/water mixtures through sodium alginate membrane	93
3.4.5 Pervaporation of ionically crosslinked alginate membranes	98
3.4.6 Temperature effects	102
3.4.7 Pervaporation characteristics of alginate and alginic acid membranes for separating liquid/liquid mixtures rather than aqueous alcohol mixtures	106
<b>3.5 CONCLUSIONS</b>	<b>110</b>

## **CHAPTER 4**

### **NOVEL TWO PLY COMPOSITE MEMBRANES OF CHITOSAN AND SODIUM ALGinate FOR THE PERVAPORATION DEHYDRATION OF ISOPROPANOL AND ETHANOL**

<b>4.1 SUMMARY</b> .....	<b>111</b>
<b>4.2 INTRODUCTION</b> .....	<b>112</b>
<b>4.3 EXPERIMENTAL</b> .....	<b>115</b>
4.3.1 Materials.....	115
4.3.2 Two ply membrane preparation.....	115
4.3.3 Crosslinking solution.....	116
4.3.4 Pervaporation.....	117
4.3.5 Sorption.....	118
<b>4.4 RESULTS AND DISCUSSION</b> .....	<b>119</b>
4.4.1 Membrane morphology.....	119
4.4.2 Sorption.....	119
4.4.3 Effect of water content in insolubilization solution.....	125
4.4.4 Effect of time on crosslinking.....	126
4.4.5 A factorial design experiment for 95 wt% EtOH mixture.....	128
4.4.6 A factorial design experiment for 90 wt% PrOH mixture.....	132
4.4.7 Pervaporation experiments of the two ply membrane.....	136
<b>4.5 CONCLUSIONS</b> .....	<b>140</b>

## **CHAPTER 5**

### **CROSSLINKED CHITOSAN COMPOSITE MEMBRANE FOR THE PERVAPORATION DEHYDRATION OF ALCOHOL MIXTURES AND ENHANCEMENT OF STRUCTURAL STABILITY OF CHITOSAN/POLYSULFONE COMPOSITE MEMBRANES**

<b>5.1 SUMMARY</b> .....	<b>141</b>
<b>5.2 INTRODUCTION</b> .....	<b>142</b>
<b>5.3 EXPERIMENTAL</b> .....	<b>145</b>

5.3.1 Materials	145
5.3.2 Membrane preparation	146
5.3.3 Pervaporation	147
5.3.4 Scanning electron microscopy	150
5.3.5 Fourier transform infrared (FT-IR) measurement	150
<b>5.4 RESULTS AND DISCUSSION</b>	<b>150</b>
5.4.1 Water permeability of pretreated UF membranes	150
5.4.2 SEM pictures of the composite membranes	151
5.4.3 FT-IR	153
5.4.4 Pervaporation experiments of the composite membrane without binding polymer	155
5.4.5 Pervaporation experiments of the composite membrane with binding polymer	158
5.4.6 Pervaporation experiments of the composite membrane pretreated in PVA solution	162
5.4.7 Temperature effect	167
<b>5.5 CONCLUSIONS</b>	<b>170</b>

**CHAPTER 6**  
**PERVAPORATION DEHYDRATION OF AQUEOUS ETHANOL**  
**AND ISOPROPANOL MIXTURES THROUGH**  
**ALGINATE/CHITOSAN TWO PLY COMPOSITE MEMBRANES**  
**SUPPORTED BY POLY (VINYLIDENE FLUORIDE) POROUS**  
**MEMBRANE**

<b>6.1 SUMMARY</b>	<b>172</b>
<b>6.2 INTRODUCTION</b>	<b>173</b>
<b>6.3 EXPERIMENTAL</b>	<b>175</b>

6.3.1 Materials	175
6.3.2 Membrane preparation	176
6.3.3 Swelling and sorption experiments	177
6.3.4 Pervaporation	178
6.3.5 Infrared spectroscopy	178
6.3.6 Contact angle measurement	179
6.3.7 Scanning electron microscopy	179
<b>6.4 RESULTS AND DISCUSSION</b>	<b>180</b>
6.4.1 Surface characteristics of PVDF porous membrane and morphology of composite membrane	180
6.4.2 Sorption experiment	184
6.4.3 Infrared (IR) spectroscopy	186
6.4.4 Pervaporation experiments of aqueous ethanol mixtures	189
6.4.5 Pervaporation experiments of aqueous isopropanol mixtures	192
6.4.6 Temperature effects on the permeation flux	194
<b>6.5 CONCLUSIONS</b>	<b>199</b>

## **CHAPTER 7**

### **N-ACETYLATED CHITOSAN MEMBRANES FOR THE PERVAPORATION SEPARATION OF ALCOHOL/TOLUENE MIXTURES**

<b>7.1 SUMMARY</b>	<b>201</b>
<b>7.2 INTRODUCTION</b>	<b>202</b>
<b>7.3 Experimental</b>	<b>207</b>
7.3.1 Materials	207
7.3.2 Membrane preparation and N-acetylation reaction	207
7.3.3 Pervaporation experiment	209
7.3.4 FT-IR measurement	209
7.3.5 Scanning electron microscopy	210

<b>7.4 RESULTS AND DISCUSSION</b>	<b>210</b>
7.4.1 SEM and FT-IR measurement	210
7.4.2 Swelling behavior in water	214
7.4.3 Pervaporation of ethanol/toluene mixtures	216
7.4.4 Pervaporation of methanol/toluene mixtures	223
<b>7.5 CONCLUSIONS</b>	<b>225</b>

**CHAPTER 8**  
**CHITOSAN/ANIONIC SURFACTANT COMPLEX MEMBRANES**  
**FOR THE PERVAPORATION SEPARATION OF**  
**METHANOL/MTBE AND CHARACTERIZATION OF THE**  
**POLYMER/SURFACTANT SYSTEM**

<b>8.1 SUMMARY</b>	<b>226</b>
<b>8.2 INTRODUCTION</b>	<b>227</b>
<b>8.3 THEORY OF SURFACTANT/POLYMER BINDING</b>	<b>231</b>
<b>8.4 EXPERIMENTAL</b>	<b>233</b>
8.4.1 Materials	233
8.4.2 Membrane preparation	234
8.4.3 Pervaporation experiment	235
8.4.4 Rheological properties of chitosan/surfactant solutions	235
8.4.5 Scanning electron microscopy	236
8.4.6 Atomic force microscopy	236
<b>8.5 RESULTS AND DISCUSSION</b>	<b>238</b>
8.5.1 Scanning electron microscopy	238
8.5.2 Rheological properties of the polymer/surfactant solution	238
8.5.3 Atomic force microscopy (AFM) study of membrane surface	244
8.5.4 Pervaporation of methanol/MTBE mixture	247
8.5.5 Temperature effect on the pervaporation performance	255
<b>8.6 CONCLUSIONS</b>	<b>258</b>

**CHAPTER 9**  
**EPDM MEMBRANES FOR THE PERVAPORATION SEPARATION**  
**OF AROMA COMPOUND**

<b>9.1 SUMMARY</b> .....	<b>259</b>
<b>9.2 INTRODUCTION</b> .....	<b>260</b>
<b>9.3 RESISTANCE-IN-SERIES MODEL FOR THE ESTIMATION</b> <b>OF TRANSPORT PHENOMENON</b> .....	<b>262</b>
<b>9.4 EXPERIMENTAL</b> .....	<b>266</b>
9.4.1 Materials.....	266
9.4.2 Membrane preparation .....	268
9.4.3 Pervaporation .....	268
9.4.4 Scanning electron microscopy .....	269
<b>9.5 RESULTS AND DISCUSSION</b> .....	<b>271</b>
<b>9.6 CONCLUSIONS</b> .....	<b>287</b>

**CHAPTER 10**  
**ORIGINAL CONTRIBUTIONS TO RESEARCH AND**  
**RECOMMENDATIONS**

<b>10.1 ORIGINAL CONTRIBUTIONS TO RESEARCH</b> .....	<b>288</b>
<b>10.2 RECOMMENDATIONS FOR FUTURE WORK</b> .....	<b>290</b>

<b>NOMENCLATURE</b> .....	<b>292</b>
---------------------------	------------

<b>REFERENCE</b> .....	<b>295</b>
------------------------	------------

<b>APPENDIX</b> .....	<b>327</b>
-----------------------	------------

## LIST OF TABLES

Table 2.1 Characteristics of some important membrane processes -----	12
Table 2.2 Recent pervaporation research relevant to organic removal from aqueous organic mixtures (1999-2000) -----	32
Table 2.3 Recent pervaporation research relevant to organic/organic separation (except methanol/MTBE mixture) (1999-2000) – underlined component is the preferred permeant -----	34
Table 2.4 Models for the concentration dependence of diffusion coefficient in binary mixture-----	58
Table 4.1 Pervaporation experiment results for 95% ethanol-water mixture at 60 °C and factorial design matrix [CS:chitosan, AA:alginate]-----	129
Table 4.2 Estimated effects from a 2 <sup>3</sup> factorial design for 95% ethanol solution-----	130
Table 4.3 Pervaporation experiment results for 90% isopropanol-water mixture at 60 °C and factorial design matrix [CS:chitosan, AA:alginate]-----	134
Table 4.4 Estimated effects from a 2 <sup>3</sup> factorial design for 90% isopropanol solution --	135
Table 5.1 The list of the membrane (- : No; O : Yes)-----	148
Table 5.2 Water flux of polysulfone UF membranes pretreated in polymer solution (0.1 wt%)-----	149
Table 6.1 Contact angle values and adhesion works of water drops for PVDF membranes -----	182

Table 9.1 Analysis of EPDMs used in this study ----- 266

Table 9.2 Overall mass transfer resistance, boundary layer resistance and membrane  
resistance for EPDM membranes at 30 °C ----- 279

## LIST OF FIGURES

Figure 2.1 Solution-diffusion model for pervaporation-----	40
Figure 2.2 The pseudophase-change solution-diffusion (PPCSD) model-----	41
Figure 2.3 Pore flow model for pervaporation -----	44
Figure 2.4 Carrier transport mechanism for pervaporation-----	46
Figure 2.5 Plot of the Fermi function for $a=0.05326$ and $b=0.0001$ -----	63
Figure 2.6 Ideal permeation flux of the pervaporation membrane -----	66
Figure 3.1 The chemical structure of alginic acid -----	78
Figure 3.2 Alginate gel network formation by multivalent ions-----	80
Figure 3.3 A schematic diagram of the pervaporation apparatus; (1) temperature controller (2) feed tank (3) heating mantle (4) circulation pump (5) membrane cell (6) pressure gauge (7) cold trap (8) vacuum pump-----	83
Figure 3.4 FT-IR spectra of alginic acid and alginate membranes -----	85
Figure 3.5 Temperature dependence test of sodium alginate membrane for 90% EtOH feed mixture for 9 days -----	88
Figure 3.6 Consistency experiment of sodium alginate membrane for 90% PrOH feed mixture at 60 °C-----	89
Figure 3.7 Consistency experiment of alginic acid membrane for 90% PrOH feed mixture - at 60 °C-----	90
Figure 3.8 Comparison of pervaporation performance of sodium alginate (●: flux; ○: separation factor) and alginic acid (■: flux; □: separation factor) membranes	

for EtOH feed mixtures at 60 °C -----	91
Figure 3.9 Comparison of pervaporation performance of sodium alginate (●: flux; ○: separation factor) and alginic acid (■: flux; □: separation factor) membranes for PrOH feed mixtures at 60 °C -----	92
Figure 3.10 Pervaporation ionic crosslinking of sodium alginate membranes a) 90 wt% ethanol mixture, b) 90 wt% isopropanol mixture -----	95
Figure 3.11 a) Effect of ethanol feed concentration on the flux and separation factor at 50 °C for sodium alginate membrane, b) Water concentration in the permeate vs. water concentration in the feed -----	96
Figure 3.12 a) Effect of isopropanol feed concentration on the flux and separation factor at 50 °C for sodium alginate membrane, b) Water concentration in the permeate vs. water concentration in the feed -----	97
Figure 3.13 a) Effect of ethanol feed concentration on the flux and separation factor at 50 °C for crosslinked alginate membrane, b) Water concentration in the permeate vs. water concentration in the feed -----	100
Figure 3.14 a) Effect of isopropanol feed concentration on the flux and separation factor at 50 °C for crosslinked alginate membrane, b) Water concentration in the permeate vs. water concentration in the feed -----	101
Figure 3.15 a) Arrhenius plot of total permeation flux of 90% aqueous ethanol mixture, b) Dependence of separation factor on the temperature through sodium alginate and Ca <sup>2+</sup> crosslinked alginate membrane -----	104
Figure 3.16 a) Arrhenius plot of total permeation flux of 85% and 95% aqueous isopropanol mixture, b) Dependence of separation factor on the temperature	

through sodium alginate and Ca <sup>2+</sup> crosslinked alginate membrane -----	105
Figure 3.17 Pervaporation performance of sodium alginate (●) and alginic acid (◆) membrane for the separation of 90% acetic acid/10% water mixture at 25 °C -----	108
Figure 3.18 FT-IR of sodium alginate membranes before and after the pervaporation run for 90% acetic acid feed mixture at 25 °C -----	109
Figure 4.1 SEM picture of the cross-section of two-ply membrane -----	121
Figure 4.2 Water sorption (a) and sorption selectivity (b) versus ethanol content in the feed mixture at 60 °C-----	122
Figure 4.3 Water sorption (a) and sorption selectivity (b) versus isopropanol content in the feed mixture at 60 °C -----	123
Figure 4.4 Effect of water content in the H <sub>2</sub> SO <sub>4</sub> insolubilization solution for the conversion reaction of sodium alginate for the feed mixture of 95% EtOH at 60°C -----	124
Figure 4.5 Pervaporation data of the crosslinked two ply membrane (a) Type A crosslinking agent (H <sub>2</sub> SO <sub>4</sub> ) for 95 wt% EtOH mixture at 60 °C; chitosan side faces to the feed, (b) Type B crosslinking agent (HCHO) for 90 wt% PrOH mixture at 60 °C; alginate side faces to the feed -----	127
Figure 4.6 Pervaporation results of pure alginate, chitosan, and No.5 two ply membrane from a factorial design for ethanol-water mixture at 60 °C-----	137
Figure 4.7 Pervaporation results of pure alginate, chitosan, and No.6 two ply membrane from a factorial design for isopropanol-water mixture at 60 °C -----	138
Figure 5.1 SEM pictures of the composite membranes; a) and b) morphology of	

polysulfone substrates; c) cross-section of the chitosan/PSf composite membrane (Mem 4); d) cross-section of the chitosan/PSf composite membrane (Mem 9) -----	152
Figure 5.2 Characterization of the crosslinking nature of GA with sulfuric acid for chitosan membrane compared to those of GA with HCl and sulfuric acid crosslinking -----	154
Figure 5.3 Effect of feed concentration of the permeation flux at 50 °C for dense and composite membranes -----	156
Figure 5.4 Effect of feed concentration of the separation factor at 50 °C for dense and composite membranes -----	157
Figure 5.5 Effect of feed concentration of the flux at 50 °C for the composite membranes treated in various polymer solutions compared to that for the untreated Mem 3 -----	160
Figure 5.6 Effect of feed concentration of the separation factor at 50 °C for the composite membranes treated in various polymer solutions compared to that for the untreated Mem 3 -----	161
Figure 5.7 Effect of feed concentration on the flux at 50 °C through PVA treated (Mem 8) and untreated (Mem 4) composite membranes -----	163
Figure 5.8 Effect of feed concentration on the separation factor at 50 °C through PVA treated (Mem 8) and untreated (Mem 4) composite membranes -----	164
Figure 5.9 Thickness effect of the crosslinked composite membrane on the flux at 50 °C (Mem 8 : 10 $\mu\text{m}$ ; Mem 9 : 1 $\mu\text{m}$ ) -----	165
Figure 5.10 Thickness effect of the crosslinked composite membrane on the separation	

factor at 50 °C (Mem 8 : 10 μm ; Mem 9 : 1 μm) -----	166
Figure 5.11 Arrhenius plot of the flux vs. reciprocal of temperature through the composite membrane at 90 wt% isopropanol-----	168
Figure 5.12 Plot of the separation factor vs. reciprocal of temperature through the composite membrane at 90 wt% isopropanol-----	169
Figure 6.1 SEM photographs of the cross-section of the composite membrane; a) overview of the cross-section, b) adjacent view of top layer-----	183
Figure 6.2 The degree of swelling and sorption selectivity for various alginate and alginic acid membranes in 90 wt% ethanol (a) and isopropanol (b) mixtures at room temperature -----	185
Figure 6.3 FT-IR spectra of alginic acid membranes converted from sodium alginate membranes in H <sub>2</sub> SO <sub>4</sub> solutions of various concentrations -----	187
Figure 6.4 Effect of ethanol feed concentration on the flux through [(a) sodium alginate and alginic acid membranes, (b) sodium and cobalt alginate membranes] and (c) on the separation factor at 50 °C -----	191
Figure 6.5 Effect of isopropanol feed concentration on the flux through [(a) sodium alginate and alginic acid membranes, (b) sodium and cobalt alginate membranes] and (c) on the separation factor at 50 °C-----	193
Figure 6.6 Temperature effect on the flux through various alginate membranes (a) at 90% ethanol mixture (b) at 90% isopropanol mixture-----	196
Figure 6.7 Temperature effect (a) on the flux through alginic acid membrane (0.1M), (b)	

permeation activation energies according to the ethanol feed concentration -----	197
Figure 6.8 Temperature effect (a) on the flux through alginic acid membrane (0.1M), (b) permeation activation energies according to the isopropanol feed concentration -----	198
Figure 7.1 N-acetylation reaction of chitosan membrane to chitin membrane -----	206
Figure 7.2 SEM pictures of the chitosan/polyetherimide (PEI) composite membranes-----	212
Figure 7.3 FT-IR diagram of chitosan, natural chitin and acetylated chitosan membranes -----	213
Figure 7.4 Water sorption behavior of N-acetylated chitosan membranes according to the degree of acetylation -----	215
Figure 7.5 Pervaporation performance of pure chitosan membrane for 50% ethanol/50% toluene mixture at 50 °C -----	217
Figure 7.6 Comparison of the membrane performance between the dehydration application and organic-organic separation application of the chitosan membrane at 35 °C -----	218
Figure 7.7 Feed concentration effect on (a) total flux and (b) separation factor of N- acetylated membranes and pure chitosan membrane for ethanol/toluene feed mixture at 35 °C (AA : Acetic Anhydride)-----	221
Figure 7.8 Temperature effect on the total flux of 70% ethanol/30% toluene mixture -----	222
Figure 7.9 Feed concentration effect on total flux and separation factor of N-acetylated	

membrane and pure chitosan membrane for methanol/toluene mixtures at 35 °C (AA : Acetic Anhydride)----- 224

Figure 8.1 Tentative model of the formation of the chitosan-anionic surfactant complex in the solution. Surfactant molecules binding to chitosan chain according to the increase of the amount of surfactant from A (initiation of binding) to C (shrunk coil) ----- 229

Figure 8.2 Chemical structures of anionic surfactants; A) sodium dodecyl sulfate (SDS)- $C_{12}H_{25}NaO_4S$ , B) sodium laurate (SL)- $C_{12}H_{23}NaO_2$ , C) sodium stearate (SS)- $C_{18}H_{35}NaO_2$ , D) amphoteric sodium N-lauroyl sarcosinate (SLS)- $C_{15}H_{28}NNaO_3$ , and E) dioctyl sodium sulfosuccinate (DSS)- $C_{20}H_{37}NaO_7S$  ----- 230

Figure 8.3 Model to describe the polymer and surfactants association behavior in aqueous solution ----- 232

Figure 8.4 SEM picture of the composite membrane. (a) and (b) are the adjacent view and overview of the membrane cross-section without the addition of surfactant, respectively; (c) and (d) are the adjacent view and overview of the membrane cross-section with the addition of DSS surfactant, respectively ----- 237

Figure 8.5 Apparent viscosities of polymer solution with the addition of various surfactants at ambient temperature ----- 241

Figure 8.6 Surfactant (DSS) concentration effect on apparent viscosities of polymer solutions at ambient temperature ----- 242

Figure 8.7 Surfactant (SDS) concentration effect on apparent viscosities of polymer

solutions at ambient temperature -----	243
Figure 8.8 AFM topography [(a), (c) and (e)] and amplitude [(b), (d) and (f)] views of pure CS, modified CS with DSS 0.008% and modified CS with SDS 0.02% -----	245
Figure 8.9 AFM 3D views of pure CS membrane (a), DSS (0.008%) modified CS (b), and SDS (0.002%) modified CS (c) -----	246
Figure 8.10 Pervaporation performance of chitosan composite membranes complexed with various surfactants for 20% MeOH/80% MTBE at 25 °C -----	250
Figure 8.11 Surfactant (DSS) concentration effect on pervaporation performance at 25 °C -----	251
Figure 8.12 Surfactant (SDS) concentration effect on pervaporation performance at 25 °C -----	252
Figure 8.13 Feed concentration effect on permeation flux of pure chitosan and DSS complexed chitosan (CS-DSS) composite membrane at 25 °C -----	253
Figure 8.14 Feed concentration effect on MeOH concentration in the permeate of pure chitosan and DSS complexed chitosan (CS-DSS) composite membranes at 25 °C-----	254
Figure 8.15 Temperature effect on the permeation fluxes of pure, DSS modified, and SDS modified chitosan composite membranes for 20% MeOH/80% MTBE ---	256
Figure 8.16 Temperature effect on MeOH content in the permeate of pure, DSS modified, and SDS modified chitosan composite membranes for 20% MeOH/80%	

MTBE-----	257
Figure 9.1 Diagram of resistance-in-series model-----	263
Figure 9.2 Fabrication of EPDM thin film composite membranes-----	267
Figure 9.3 SEM pictures of the composite membranes (a) PAN supported membrane, (b) close view of PAN supported membrane and (c) PVDF supported membrane -----	270
Figure 9.4 Effect of substrates on the partial flux of ethyl butyrate (Mem 2 and Vistalon-8609)-----	272
Figure 9.5 Effect of substrates on separation factor (Mem 2 and Vistalon 8609)-----	273
Figure 9.6 Effect of feed concentration on the aroma flux in EPDM membranes (Kelton 514) at 30 °C-----	276
Figure 9.7 Water and organic flux for V-8609 EPDM membranes at feed concentration 600 ppm and 30 °C -----	277
Figure 9.8 Mass transfer resistances as a function of EPDM membrane thickness for Vistalon-8609 (a) and Kelton-514 (b) -----	278
Figure 9.9 Effect of feed flow rate on EB flux (V-8609 EPDM membranes at 30 °C)	281
Figure 9.10 Effect of feed flow rate on separation factor (V-8609 EPDM membranes at 30 °C) -----	282
Figure 9.11 Overall mass transfer resistance as a function of feed flow rate for K-514 EPDM membranes at 30 °C) -----	283
Figure 9.12 Effect of permeate pressure on the total flux (a) and on EB (ethyl butyrate) flux through EPDM membranes (Vistalon 8800) at 30 °C-----	284

Figure 9.13 Effect of permeate pressure on separation factor through EPDM membranes (Vistalon 8800) at 30 °C	285
Figure 9.14 Feed temperature effects on EB flux through two different EPDM membranes (membrane thickness 76 μm)	286

To my wife, Hyun Hong Seo who has been encouraging and dedicated to me during the study, my son, Justin Young Hyun Moon and my daughter, Sue Bin Moon with dad's hope that they grow up healthy and be good.

# CHAPTER 1

## INTRODUCTION

---

### 1.1 BACKGROUND

Membrane technology has been considered as an efficient and economic separation process in chemical industry. Depending on the separation mechanism, it can be classified into three processes using 1) the sieving mechanism, e.g., microfiltration and ultrafiltration, 2) the electrochemical mechanism, e.g., electro dialysis, and 3) the solubility mechanism, e.g., gas separation and pervaporation. In addition membrane modules are finding application niches in the fields of membrane distillation [Lawson and Lloyd, 1997] or membrane emulsification [Joscelyne and Trägårdh, 2000]. Among various membrane processes, dense pervaporation membranes that use the preferential selectivity of a component to the membrane material have attracted special interest for the separation of liquid/liquid mixtures.

Presently, the term pervaporation is widely used to designate a membrane process that makes liquid mixtures separated preferentially by phase change through the dense polymeric membranes. The pervaporation separation process distinguishes itself from other membrane processes because of the phase transition occurring during the mass transport. As a consequence of the phase change, the process is limited to volatile liquids

at operating condition and requires the input of the heat of vaporization of the permeating species. This vaporization heat, however, is the major thermal requirement of the process and good energy efficiency can be obtained if membrane selectivity is high and the process is applied to the selective removal of the minor component of the mixture. Although the pervaporation process is a more expensive process than other membrane processes due to the phase change, its main importance lies in applications where conventional separation processes fail, such as the separation of azeotropic mixture and close boiling point mixture. The term "pervaporation" was first coined by Kober [1917], a researcher of New York State's Dept. of Health, to describe the fact that a liquid in a collodion (cellulose nitrate) bag, which was suspended in the air, evaporated, although the bag was tightly closed. The first extensive research of pervaporation for the separation of the liquid mixture was conducted by Binning et al. [1958a, 1958b, and 1960]. However, pervaporation has been limited to a lab scale tool or a research curiosity because of the low productivity through non-porous membrane. This situation was changed greatly when Loeb and Sourirajan [1962] developed a method of phase inversion for the preparation of asymmetric cellulose acetate reverse osmosis membrane with high flux. Since then, driven by the need for environmentally sound, energy saving processes, great attention has been directed to the research and development of the pervaporation technology. The Sulzer Chemtech, formerly GFT Deutsche Carbon AG, of Germany launched the first commercial pervaporation process for the dehydration of ethanol in the sugar refinery of Bethenville, Marne, France in 1987. The dehydration membrane of Sulzer generally consists of a 1-2  $\mu\text{m}$  top layer of PVA, a 100  $\mu\text{m}$  of PAN porous

substrate, and a 100  $\mu\text{m}$  of nonwoven textile. By changing the PVA crosslinking, membranes can be tailored to handle different solvents or feed concentrations.

Thus pervaporation research should emphasize process development and the discovery of new application niche in chemical manufacturing and wastewater treatment industries.

Two applications of pervaporation have been commercialized to date. The first and most important application is water removal from aqueous alcohol solutions. The economical feasibility of the dehydration application by evaluating the separation of water from aqueous ethanol has been demonstrated industrially. The second application is the separation of the dilute dissolved organics such as trichloroethylene and phenol from the wastewater stream. Organic-organic separation is the most significant potential application for pervaporation membrane process. However no commercial systems have yet been reported for the separation of organic-organic mixtures with the exception of the pilot scale plant for the separation of methanol/MTBE by Air Products Co. and the production of high-octane gasoline by Exxon. Therefore, membrane materials and process design remain to be further developed and the separation of a variety of more industrially significant organic-organic mixtures will be realized in the near future.

Membrane performance is characterized by the permeation rate and separation factor. The permeation rate is a measure of amount of the preferentially separated amount that permeates through the dense membrane per unit membrane area and unit time. The permeation flux is expressed as follows.

$$J = \frac{Q}{At} \quad (1.1)$$

where  $Q$  is the amount of the permeate,  $A$  is the membrane area and  $t$  is the operating time. In some cases, permeability ( $P$ ), which is obtained by multiplying the flux with the membrane thickness, may be used as a normalized flux density (kg/m-hr). The separation factor,  $\alpha$ , achieved by a pervaporation process can be defined in the conventional way as

$$\alpha_{Water/Alcohol} = \frac{[Y_w / Y_A]}{[X_w / X_A]} \quad (1.2)$$

where  $X$  and  $Y$  are the weight fractions of the feed and permeate, respectively.

Although the pervaporation dehydration of ethanol-water mixtures is the most important application so far developed among the three main applications, the dehydration of other solvents including isopropanol, glycol, acetic acid, acetone, and pyridine has been also considered. In general, membrane materials can be elastomeric or glassy polymers. The choice of membrane material depends significantly on the intended application. Empirically, hydrophilic polymers such as PVA, polyacrylonitrile, and cellulose acetate are being used for the dehydration of organic-water mixtures because the hydrophilic functional group in the polymer backbone interacts with water molecules selectively by forming hydrogen bonding or dipole-dipole interaction. Among them, polysaccharides such as chitosan, alginic acid, and cellulose sulfate are receiving special attentions and are suitable for the dehydration purpose. They are classified into two types of polysaccharide, anionic and cationic polymers, and their ionic functional group of either anionic alginic acid or cationic chitosan can be easily modified into polyelectrolytes. The problems related to the polysaccharide membranes are water solubility and excessive swelling of the membrane caused by the plasticization action of water molecule. Swelling by the interaction between the permeant and the polymer is obviously beneficial from the point of enhanced flux. Excessive swelling of the

membrane, however, results in the increased sorption and diffusion of organic molecules, resulting in reduced separation efficiency. This can be solved by chemical crosslinking. It is worth pointing out that the proper choice of the membrane material and modifications such as crosslinking and heat treatments are crucial to the development of improved pervaporation membrane. Thus, great care has to be paid to the proper selection of materials and crosslinking agents. It can be noted that for the same material, the performances after crosslinking are quite different due to the different chemical nature and crosslinked structure depending on the crosslinking agent used. In this study, chitosan and sodium alginate that are good candidates for the pervaporation dehydration [Uragami et al., 1992, 1997] will be studied extensively by combining with other polymers and crosslinking. While uncrosslinked chitosan yields poor selectivity, chitosan membrane crosslinked with glutaraldehyde [Uragami et al., 1994] or sulfuric acid exhibited high separation factor with high permeation flux. In the applications of the pervaporation for organic/organic separation and organic separation from water the choice of membrane materials is critical.

## **1.2 RESEARCH OBJECTIVES**

The broad objective of this research was to synthesize novel pervaporation membranes in the forms of dense and composite membranes for the dehydration of aqueous organic mixtures, the separation of organic/organic mixtures, the concentration or separation of aroma compound from water. The membrane materials explored in this thesis were chitosan, sodium alginate and EPDM.

Specific objectives were as follows;

- to synthesize sodium alginate membranes for the dehydration of aqueous alcohol mixtures
- to synthesize novel two ply composite membranes consisting of chitosan and alginate for the dehydration of aqueous alcohol mixtures
- to synthesize the chitosan composite membranes which were mechanically robust
- to prepare composite membranes having two ply dense layers of alginate and chitosan for the dehydration of aqueous alcohol mixtures
- to synthesize N-acetylated chitosan composite membranes for organic/organic separation
- to prepare and characterize polyelectrolyte complex membranes consisting of chitosan and anionic surfactants for organic/organic separation
- to synthesize EPDM hydrophobic membranes for the separation of a model aroma compound from water and to model the transport phenomenon

### **1.3 THE SCOPE OF THESIS**

Chapter 1 presents an overview on pervaporation membrane technology and gives a brief introduction to membrane materials used in this research.

Chapter 2 reviews the published literatures on pervaporation membrane processes and on the methods to measure the diffusion coefficients of the solute through the dense polymeric membranes.

In Chapter 3 sodium alginate membrane is characterized for the separation of aqueous ethanol and isopropanol mixtures and is crosslinked by metal ions to prevent its dissolution in water.

Chapter 4 describes preparation of novel two ply membranes consisting of sodium alginate and chitosan. The preparation parameters are analyzed by means of experimental design which lead to the optimum membrane structure and preparation conditions.

In Chapter 5 composite chitosan membranes are prepared for the separation of aqueous alcohol mixtures and the pervaporation characteristics of dense and composite membranes are studied. In addition, it is shown that the structural stability of composite membrane can be enhanced by the coating of hydrophobic polysulfone substrate with hydrophilic polymers.

Chapter 6 is devoted to the preparation and pervaporation performance study of the alginate composite membrane buffered by chitosan layer between top alginate layer and polyvinylidene fluoride substrate layer for the separation of aqueous alcohol mixture.

Chapter 7 describes the synthesis of mechanically robust N-acetylated chitosan membranes for the separation of alcohol/toluene mixtures.

Chapter 8 presents synthesis and characterization of polyelectrolyte complex membranes of chitosan and anionic surfactants for the separation of methanol/MTBE mixtures.

In Chapter 9, EPDM membranes were prepared to separate an aroma compound from aqueous solution and the transport phenomenon was modeled based on the resistance-in-series model.

Finally, Chapter 10 presents the original contributions of this research and makes some recommendations for future work.

## CHAPTER 2

### BACKGROUND STUDY ON PERVAPORATION

---

Many reports and journal articles have been published extensively on the pervaporation membrane process since Binning et al. [1958ab, 1961] of American Oil Company, Texas, U.S.A. pioneered pervaporation membrane research on the separation of hydrocarbon mixtures through polyethylene film. There are many books [Noble and Stern, 1995; Hwang and Kammermeyer, 1975; Rautenbach and Albrecht, 1989; Huang, 1991; Wo and Sirkar, 1992] providing extensive theory and practical aspects of the various membrane processes. Although most of their books cover the pervaporation process in one of many chapters, the book edited by Huang [1991] is wholly concerned with the pervaporation membrane process and incorporates almost all aspects of the pervaporation up to 1991, including the basic principles of pervaporation, thermodynamic principles, materials, transport mechanism, and applications in addition to the industrial plant design.

The published papers before the early 1990's have been reviewed and well documented by Neel [1991]. A subsequent survey of pervaporation study until 1994 has been covered intensively in the dissertation of Feng [1994]. Currently most of pervaporation studies in academia are related to the discovery of new membrane materials, the surface modification of membrane material by means of grafting, and the

crosslinking of membrane for the enhancement of permselectivity and the new application of the pervaporation technology. In this section, significant membrane materials investigated for the pervaporation application will be reviewed and listed.

## **2.1 CHARACTERISTICS OF PERVAPORATION MEMBRANE PROCESS**

Membrane separation is one of the most advanced separation processes. It is available for many applications ranging from the medical field such as hemodialysis used for artificial kidney to large-scale industrial uses such as reverse osmosis and ultrafiltration used for desalination. Pervaporation is a membrane separation process for separating liquid mixtures. A phase change from the liquid of the feed side to the vapor of the down stream through the membrane makes the pervaporation unique among the relevant membrane processes.

Thus, the pervaporation is an energy intensive process compared to the other membrane processes. The economic feasibility of dehydrating solvents by evaluating the separation of water from alcohols such as ethanol and isopropanol was demonstrated on an industrial scale. The driving force of the selective separation arises from the difference of chemical potential (e.g., concentration gradient) through the dense membrane in the result of the low pressure applied to the downstream side. There are four energy-consuming operations in the industrial pervaporation processes (Colman et al., 1990); liquid side pumping, feed heating, permeate condensation, and permeate pumping. Under normal operating conditions pervaporation does not require feed side pressure. However, if the membranes are to be operated in the turbulent mode in order to reduce concentration

polarization, then there will be a feed side pumping requirements in order to overcome the pressure head loss. Permeating component penetrates through the membrane, and is removed in the vapor phase at the downstream side of low pressure. It is well recognized that the pervaporation flux is increased at as high a feed temperature as possible. Permeate is recovered and disposed in the condenser of the temperature range 0 to 10 °C. Thus, the energy requirement for this step is significant. Permeate pumping is to create the low pressure of the permeate side, which is mandatory for maintaining continuous operation. It is helpful to review some important membrane processes in order to understand the nature of the pervaporation process more clearly. Characteristics of some membranes are listed in Table 2.1 with that of the pervaporation process. It is recognized that the driving forces for preferential separations are explicitly the differences of chemical potentials for the relevant membrane processes as shown in Table 2.1.

*Reverse osmosis* membranes have no pores but allow material to diffuse up to molecular weights of about 25 to 100 daltons [Howell, 1990]. Osmosis process is driven by the pressure, on the order of 200 to 1,000 psig and separates the ionic solutes or macromolecules from aqueous mixtures based on their sizes, shape, and charges as well as the interactions with the membrane materials. It is much more energy efficient process compared to the energy intensive distillation and ion exchange required the strong chemicals. Reverse osmosis membranes are now being manufactured by the phase inversion method that was discovered by Loeb and Sourirajan [1962] in early 1960's, and salt removal from seawater is the main application. Reverse osmosis systems are being increasingly adapted for water softening where they are competitive with ion exchange

for high salt content water. Other common materials for RO membranes are cellulose acetate, polyamide, sulfonated polysulfone, and polybenzimidazole etc.

**Table 2.1 Characteristics of some important membrane processes**

Process	Application	Driving force	Permeating component
Nanofiltration	-For concentrating the solutions such as corn syrup (more than 1000 dalton)	-Pressure difference (around 100 psig)	Solvent
Reverse osmosis	-Aqueous low molecular mass solutions -Aqueous organic solutions	-Pressure difference (100-800 psi)	Solvent
Gas separation	-Gas mixture -Vapor-gas	-Pressure difference (1-80 psi) -Concentration gradient	Preferably permeating component
Vapor permeation	-Volatile vapor and gas mixture	-Concentration gradient	Preferably permeating component
Pervaporation	-Water-organic mixture -Organic-organic mixture	- $\Delta\mu$ (concentration, pressure, temperature)	Preferably permeating component

Theoretically reverse osmosis may also be used for separating organic or aqueous-organic mixtures. In practice, the concentration of an aqueous organic mixture by reverse osmosis is limited by the high osmotic pressures of such mixtures [Rautenbach and Albrecht, 1989]. Unlike reverse osmosis, pervaporation can concentrate aqueous-organic mixtures such as dehydration of alcohol. Thin film composite reverse osmosis membrane is exclusively reviewed by Perterson [1993] with emphasis on the chemistry and composition of various commercial membranes.

*Gas separation* is a membrane process to separate gas mixtures, unlike the pervaporation there is no phase change through the membrane. The separation is based on the fact that gases pass through thin membranes at different rates because their solubilities into the membrane and diffusivities through the membrane differ. It is widely accepted that the thermodynamic interaction between the gas molecules and the membrane is less pronounced than the case in pervaporation separation. Thin film composite membranes are widely used for the separation of gases on an industrial scale, which are similar to those used in pervaporation. Polymers for the gas separation must have their high permeability and selectivity for the gases to be separated. The polymers must also be processable into practical modules such as hollow fibers and spiral-wound types. Preferable polymers include polysulfone, polyimide, silicones, cellulose, polycarbonate and their derivatives. Separation of gas mixtures is dependent on the molecular size and the solubility of the gas preferentially separated. Like the separation mechanism of pervaporation membranes, the gas separation membranes do not have any visible pores, however they continuously generate transient free volume to accommodate the molecule separated through the polymer chain motion induced by thermal energy. Transport phenomena of gas separation and reverse osmosis as well as pervaporation processes are commonly described by the solution-diffusion model. Currently gas separation is of interest for nitrogen enrichment in air, CO<sub>2</sub> recovery from natural gas [Tabe-Mohammadi, 1999], hydrogen separation from ammonia purge gas, and oxygen enrichment in air [Koros and Fleming, 1993].

*Vapor permeation* process is the newest membrane process, and is closely related to the pervaporation process. In both processes vacuum on the permeate side is applied as

a driving force for the continuous separation. However, in vapor permeation the feed mixture is in a vapor phase unlike the liquid phase of the pervaporation. It is clear that vapor permeation and pervaporation is similar to each other from equation 2.1 and 2.2 [Kataoka et al., 1990].

$$\text{Pervaporation: } J = \frac{DC^m}{\delta\gamma^m} \left( \gamma_1 x_1 - \frac{P_2 x_2}{P_v} \right) \quad (2.1)$$

$$\text{Vapor permeation: } J = \frac{DC^m}{\delta\gamma^m} \left( \frac{P_1 x_1}{P_v} - \frac{P_2 x_2}{P_v} \right) \quad (2.2)$$

When the feed vapor of vapor permeation is equal to the concentration of feed liquid of pervaporation,  $x_i$ , in theoretical relation both fluxes become the same because  $y_i$  which is the mole fraction in vapor permeation can be expressed as the follows:

$$y_i = \frac{P_v x_i \gamma_i}{P_1} \quad (2.3)$$

The special advantages of vapor permeation compared with pervaporation are the potential savings by the lower required membrane area as well as the higher safety with respect to damages of the composite membranes by impurities in the feed [Sander and Janssen, 1991]. It was reported that the first commercial scale vapor permeation was launched in 1989 at Bruggemann Co. in Germany for the dehydration of ethanol. Vapor permeation and pervaporation were studied simultaneously [Uragami et al., 1988, 1990, 1991, 1992], and it is generally accepted that vapor permeation shows less permeation flux than that of pervaporation for most of applications.

Another interesting vapor (gas) separation membrane was successfully commercialized in order to recover expensive hydrocarbon from resin degassing vent streams of polymer manufacturing processes by MTR, company based in Menlo Park,

California although this process is close to the gas separation membrane. Their "reverse selective" membrane allows large hydrocarbon molecules to permeate much faster than smaller molecules such as nitrogen, hydrogen, or methane. The reverse selective effect is due to the higher solubility of large hydrocarbon molecules in the specific polymer.

## 2.2 MATERIALS FOR THE PERVAPORATION MEMBRANE PROCESS

As a good pervaporation material, the candidate material should have high permeation flux and separation factor for a particular application. However, since the increase in the permeability is frequently encountered with a decrease of the separation factor (so-called, trade-off phenomenon), the simultaneous enhancement of both parameters has been a challenge for material selection. According to the principle of the pervaporation separation, the permeability of component  $i$  is equal to the product of the solubility and diffusivity for component  $i$ .

$$P_i = D_i(c) \cdot S_i(c) \quad (2.4)$$

where  $P$ ,  $D$ , and  $S$  are the permeability, the diffusivity (function of concentration) of component  $i$  through the membrane, and the solubility (function of concentration) therein, respectively. This equation means that a size difference in the feed components is favored for the fast diffusion of small molecules. In principle, small molecules, which have similar chemical property with the membrane material, are facilitated to penetrate through the free volume in the membrane compared to the large molecules that their bulky structures act as physical barriers during diffusion. Also the shape and molecular weight of the permeants are governing factors for the diffusion process. The solubility

(sometime sorption) of specific component to be separated is governed by the chemical affinity between the component and the polymer although how this interaction is related to the selectivity and the permeability exactly is not clear yet due to the complex thermodynamics.

In summary, if the components to be separated have different size and shape, and the membrane has strong affinity to the specific component, the separation efficiency could be increased substantially. Currently, there is no known accurate method to select the membrane material. To obtain information and criterion concerning material selection, empirical trial and error permeation experiments are commonly used but are time-consuming. Several systematic approaches are now the only methods used by membranologists to deal with the selection of the adequate membrane materials for the specific separation system and are described in the following section.

### **2.2.1 Approaches for the material selection in pervaporation membrane**

#### *1) Solubility parameter approach.*

For the selection of a pervaporation membrane material capable of separating A and B components, the chemical nature of the membrane material M and the components A and B to be separated has been studied using solubility parameter approach for screening of various candidate materials [Mulder et al., 1982; Lee et al., 1989], synthesizing novel materials [Yamaguchi et al., 1992 and 1993; Ray et al., 1999], and correlating of pervaporation and sorption properties [Jonquieres et al., 1996; Wei and

Huang, 1994]. If two chemical species have strong affinity and solubility mutually, the difference in their solubility parameters  $\Delta_{CM}$  will be decreased.

$$\Delta_{CM} = \left[ (\delta_{dC} - \delta_{dM})^2 + (\delta_{pC} - \delta_{pM})^2 + (\delta_{hC} - \delta_{hM})^2 \right]^{\frac{1}{2}}$$

Lloyd and Meluch [1985] stated that  $\Delta_{AM} / \Delta_{BM}$  can be used as a measure of preferential sorption and thus as a membrane material selection index. For example, if preferential separation of component, *B* is desired while rejecting component, *A*, the membrane material should be selected to maximize the ratio  $\Delta_{AM} / \Delta_{BM}$  by maximizing  $\Delta_{AM}$  and by minimizing  $\Delta_{BM}$ . That is, it is desired that the membrane has a solubility parameter value close to that of the component separated. However, it must be pointed out at this stage that the solubility parameter and its use for quantifying physiochemical interactions is based on enthalpic considerations only; entropic considerations are neglected. Consequently, the solubility parameter may be misleading when diffusion contribution is comparatively significant and when the interactions between a component and the membrane material are influenced by the presence of the other component. Good examples for solubility parameter approach can be found in the work of Dagaonkar et al. [1998] and in the new synthetic membrane study for benzene/cyclohexane separation [Ray et al., 1997]. From the study of Dagaonkar et al. it was found that although organophilic membrane such as PDMS had high sorption selectivity to alkyl piperazines against water, total selectivity for alkyl piperazine was very low due to the fast diffusion of water and hindered diffusion of bulky alkyl piperazines. However, it is important to remember that although water is highly diffusive compared to most of organics, the permeability of organic can be much higher than that of water due to the high contribution of organic solubility in the membrane [Hoshi et al., 1999].

In spite of these limitations, the solubility parameter approach is still considered as a useful tool in the selection of polymer membrane materials and as far as the permeability prediction is concerned (selectivity cannot be predicted by solubility parameter).

2) *Surface thermodynamic approach.*

Lee et al. [1989] has adopted surface thermodynamic approach [Van Oss et al., 1983] or preferential sorption approach to test polymer materials which exhibit preferential organic permeation and compared the results with those of solubility parameter approach. The surface free energy difference between water, 1 and polymer, 3 in the presence of organic 2 is defined as equation 2.5.

$$\Delta F_{123} = \gamma_{31} - \gamma_{12} - \gamma_{23} \quad (2.5)$$

$$\gamma_{ij} = (\gamma_i^{0.5} - \gamma_j^{0.5})^2 / (1 - 0.015\gamma_i^{0.5}\gamma_j^{0.5}) \quad (2.6)$$

where a negative  $\Delta F_{123}$  implies preferential sorption of organic over water, interfacial tensions for the permeants and polymers were calculated from the equation 2.6 by Neumann et al. (1974).

Large values of  $\Delta F_{123}$  imply high separation factor of water (1) and organic (2) mixtures through the membrane (3). However, after considering Lee et al.'s work [1989] carefully the surface thermodynamics approach did not appear to correctly predict the pervaporation separation characteristics. In case of ethanol separation, although all materials show the negative  $\Delta F_{123}$  values, some of materials exhibit preferential water permeation tendency in real. Also in the separation of chloroform, the materials having large  $\Delta F_{132}$  values did not necessarily indicate the high separation factors. Because this approach emphasizes the interfacial behavior of the system, it seems that there are some

difficulties to predict the diffusion phenomenon of the pervaporation membrane since the solubility and the diffusivity jointly contribute to the transport of the component simultaneously.

### 3) *Polarity approach.*

Polarity is an intrinsic characteristic of polymeric material, which results from a nonuniform electron density distribution. The intensity of interaction of the polymer with water molecules depends largely on the polarity and determines the diffusion mechanism in polymers [Zaikov et al., 1988]. It has been suggested by Shimidzu and Yoshikawa [1991] and Yoshikawa et al. [1986] that membrane polarity can be expressed in terms of Dimroth's solvent polarity value ( $E_T(25\text{ }^\circ\text{C})$ ) that this is a good indicator for the membrane material selection. They stated that when the membrane polarity is close to that of water (63.1 kcal/mol), the membrane tends to be water selective. Relationship between separation factor and membrane polarity already exists. The separation factors of water-various alcohol through poly(maleimide-co-acrylonitrile) membranes tend to increase as the  $E_T(25\text{ }^\circ\text{C})$  value of the alcohol deviates from that of the membrane [Yoshikawa et al., 1984a], and the separation factor tends to decrease as the  $E_T(25\text{ }^\circ\text{C})$  value of the membrane deviates from that of water in the pervaporation of water-ethanol mixture through polymer membranes with maleimide functional group acting as a fixed carrier [Yoshikawa et al., 1984b]. Although the solubility parameter approach is a good indicator for the material selection, one must know the precise polymer structure in order to calculate solubility parameter, however no knowledge of the precise polymer structure is required by the use of membrane polarity approach. Thus, use of the  $E_T(25\text{ }^\circ\text{C})$  value

might be one of the promising parameters for use in the development of synthetic membranes for the separation of water-ethanol mixtures.

#### *4) Chromatographic approach.*

The strength and nature of the interactions between the permeating component and the membrane material can be determined by measuring the sorption of permeant by the polymer in binary systems. Chromatography measures similar physicochemical interactions between the binary permeating components and the polymer. 1) Liquid chromatography: If the carrier or mobile phase is the solvent B, the solute A is injected into the mobile phase and the interaction strength of A and the polymer is determined in the form of retention volume,  $V_A$  by the detector. Strong affinity between A and the polymer will delay the elution of A. This method has been extensively studied by Matsuura and Sourirajan [1978] for the material selections of reverse osmosis and ultrafiltration, and applied to PVA for reverse osmosis [Lang et al., 1994] and cellulose acetate [Gao and Bao, 1989] membranes. 2) Inverse gas chromatography: If the carrier is a gas and the solute is injected as a mobile phase into a injector of GC, the interaction between mobile phase, the solute and stationary phase, the polymer can be determined by the retention time and eluted peak. Inverse gas chromatography has not yet been studied for the pervaporation material selection process, however it is one of new techniques used to study the diffusion coefficient of a solute in a polymer [Pawlish, 1985, Bonifaci et al., 1994]. Therefore, this method might be an efficient way for the material selection of pervaporation separation membranes.

#### *5) Contact angle approach.*

It has long been recognized that polymers are classified into hydrophilic (containing more than 10 wt% water under normal condition), hydrophobic (the equilibrium water content at room temperature and 100% relative humidity does not exceed 2%) and intermediate (intermediate water values). However it is very difficult to find out a quantitative method for assigning a polymer to a specific class. Contact angle measurement can give rough idea at initial stage to select proper polymers for an intended separation. It must be pointed out that the surface properties of a polymer may not be same as its bulk properties. Farnard and Noh [1989] surveyed commercially available thin films in an effort to determine quickly which polymeric materials would give selective separation of the methanol or the hydrocarbons by measuring the contact angle of methanol with the surface of the membrane. This appears to be a simplified approach of the surface thermodynamics approach commonly used for characterizing the surface of modified or synthesized novel membranes. For example, this method was applied to the characterization of modified polysulfone ultrafiltration membranes [Nabe et al., 1997] and polyelectrolyte complex membranes [Lukas et al., 1997] rather than a good material screening method for the pervaporation separation processes.

### **2.2.2 Materials for pervaporation**

Potentially every available polymer including homopolymer, copolymer, and blend as well as modified polymer can be used for pervaporation membrane separation purposes. The most important requirements for a pervaporation membrane material are high flux, high separation efficiency, mechanical and chemical stability, and high

temperature resistance. Among the above requirements, high separation efficiency must be emphasized over the others since a low separation factor cannot be compensated for economically enough to compete with the conventional separation techniques in the separation market. It must be pointed out again that both the chemical nature and the physical structure of the membranes govern the permeation. There are three strategies to prepare the membrane materials for pervaporation applications; A) synthesis of new polymers or copolymers, B) modification of mother polymers using radiation grafting or plasma grafting, C) blending of mother polymers. Important membrane materials and characteristics of the materials according to the three main applications, namely dehydration of organics, organic removal from aqueous mixtures, and organic-organic separation will be reviewed in the following section.

*1) Dehydration of aqueous organic mixture.*

Currently dehydration is the major commercial application and research area for pervaporation. As industrial suppliers, crosslinked PVA composite membrane of Sulzer Chemtech, formerly GFT leads the market, and British Petroleum (Kalsep) is operating small plants mostly for water-isopropanol separation using the ion-exchange composite membranes. For the purpose of the dehydration of aqueous organic mixtures, candidate materials must have high water selectivity. In fact, since the molecular size of water (2 Å) is smaller than that of most of organic molecules, the diffusion of water through the membrane is less hindered sterically than that of organic molecules even though the polymer is a hydrophobic material. Thus, most of polymers available in the industry are preferentially water permeable. Polymers including hydrophilic groups such as  $-\text{COOH}$ ,  $-\text{OH}$ ,  $-\text{SO}_3^-$ ,  $\text{OSO}_3^-$ ,  $\text{R}_4\text{N}^+$ , and  $-\text{NH}_2$  have shown high affinity to water in solubility

parameter study. One of the most important pervaporation materials is polyvinyl alcohol (PVA). Substantial studies have been carried out by many research groups for the dehydration of alcohols [Ohya et al., 1992; Will & Lichtenthaler, 1992; Gref et al., 1993], the dehydration of phenol [Rhim et al., 1994], amines [Xie, et al., 1993], acetic acid [Huang and Yeom, 1991; Rhim et al., 1997], and ethylene glycol [Chen and Chen, 1998] and even for organic-organic separation [Wesslein et al., 1990; Yamasaki et al., 1997]. PVA has been favored as a polymer to be modified such as PVA/CD [Yamasaki et al., 1994a, 1994b; Miyata et. al., 1994], PVA copolymer [Chiang & Huang, 1991, 1993, 1998], sodium alginate/PVA [Yeom & Lee, 1998b; Jegal & Lee, 1996], and PVA/poly allyl amine [Park et al., 1994]. However, due to its strong hydrophilicity, it becomes water-soluble at elevated temperature. As an alternative, PVA is crosslinked chemically with the possible sacrifice of flux but the increase of separation factor in order to suppress excessive swelling arising from the plasticization action of water. Crosslinking agents, for example, amic acid [Huang & Yeom, 1991], low MW PAA [Rhim et al., 1994], monochloroacetic acid [Kang et al., 1990], glutaraldehyde [Yeom & Lee, 1996a; Kusumocahyo et al., 2000] have been tried to enhance the water permselectivity.

In addition to nonionic PVA membrane, ionic polysaccharide membranes show fairly good permselectivity in the dehydration application. Carboxymethylcellulose and alginic acid as anionic polyelectrolytes and chitosan as cationic polyelectrolyte are particularly well recognized as highly water permselective materials. Since the development of asymmetric cellulose acetate membrane for reverse osmosis by Loeb and Sourirajan, it was adapted in the gas separation in the early 1980s. The flexibility of cellulose derivatives was applied to pervaporation membranes [Huang & Jarvis, 1970].

Carboxymethylcellulose, sodium salt (CMC), which is water-soluble, has been tested for the dehydration of ethanol-water mixture with crosslinking reaction by Reineke et al. [1987]. They found that the counter ion exchange of CMC membrane blended with polyacrylic acid (PAA) sodium salt resulted in the increase of fluxes while maintaining high selectivities when  $\text{Cs}^+$  and  $\text{K}^+$  replaced the sodium salt. Although cellulose derivatives was studied for the purpose of dehydration [Balint et al., 1993; Kataoka et al., 1991; Deng et al., 1990], it has been searching for its significant adaptation in the organic-organic separation [Yang et al., 1998; Nguyen, 1997; Luo et al., 1997]. It is reported that cellulose acetate membrane of Air Products & Chemicals is suitable for recovering methanol from methyl t-butyl ether (MTBE) and butane in the production of MTBE as a high octane-enhancing agent in gasoline.

Chitosan is a partially deacetylated polymer of acetal glucosamine. Chitosan is usually prepared from chitin that has been found in various natural sources like crabshell, crayfish, and shrimp. It was shown that chitosan has excellent separation properties in pervaporation dehydration [Wong et al., 1996; Qunhui et al., 1995; Nawawi & Huang, 1997; Lee et al., 1997]. However, due to its high degree of swelling property in aqueous system chitosan membrane should be crosslinked with proper agents such as glutaraldehyde,  $\text{H}_2\text{SO}_4$ , sulfosuccinic acid [Jegal and Lee, 1999], or hexamethylene diisocyanate. Uragami et al. [1994] reported that the permeation rate and separation factor for water permselectivity through glutaraldehyde (GA) crosslinked chitosan membrane increased with GA content for aqueous ethanol mixtures. They stated that such an improvement was related to the inhibition of hydrogen bonds in the chitosan membrane due to the chemical modification. In a recent study, Lee et al. [1998]

examined the pervaporation characteristics of chitosan membranes having various deacetylation degrees. The permeation flux of chitosan membranes increases and the separation factor decreases because the removal of large acetyl group facilitates the mobility of the penetrants through the enlarged free volume. Chitosan having reactive hydroxyl and amino functional group as a cationic polymer can form a polyelectrolyte complex membrane with polyacrylic acid for ethanol-water separation [Shieh & Huang, 1997] and also can be blended to make chitosan/PVA membrane for isopropanol-water mixture [Nawawi & Huang, 1997]. Besides alcohol dehydration, studies for dimethyl sulfoxide dehydration was carried out by Uragami & Shinomiya [1992], and pervaporation separation of benzene/cyclohexane mixture through benzoylchitosan membrane was reported recently [Inui et al., 1998].

The effect of chitosan membrane preparation conditions on its separation performance was studied recently, chitosan membrane dissolved in acetic acid solution rather than formic, nitric and hydrochloric acid solutions showed the highest permeability because of the lower crystallinity [Matsuyama et al., 1999]. In another study, it was found that one could control the optimum crystallinity of the chitosan membrane for the improved separation index with the drying temperature [Ge et al., 2000].

Alginic acid that is extracted from seaweeds and is one of the natural polysaccharide, consist of D-mannuronic and L-guluronic acids that are flat and buckled ribbon-like in shape, respectively. Although alginic acid has some drawbacks including water-solubility [Mochizuki, 1990], mechanical weakness, and severe relaxation behavior [Yeom et al., 1996], it has high potential for the dehydration of aqueous organic mixtures when these obstacles are overcome using proper crosslinking. It is generally accepted that

the selective transport of water through most of hydrophilic polysaccharide membranes is achieved by hydrogen bonding between the membrane material and water molecules.

As another dehydration membrane, ion-exchange membranes that make use of coulombic interaction instead of hydrogen bonding have been applied for the separation of alcohol-water mixture. Cabasso and Liu [1985] reported that Nafion that is used for application in electrochemical separation can be used to efficiently separate alcohol-water mixtures by loading the membrane with the proper counter-ions. Similar results were obtained for CMV (cation exchange) and AMV (anion exchange) ion exchange membranes by Wenzlaff et al. [1985]. Significant pervaporation studies also were carried out for polyetherimide (PEI), Nylon, PAA, and PAN materials in dehydration applications.

Recently, polyelectrolyte membranes are gaining much attention in pervaporation dehydration [Schwarz et al., 1991]. Polyelectrolyte complexes can be formed as a result of coulombic interactions between two oppositely charged polyions. The distinguishing and unique properties of polyelectrolyte complexes are as follows [Michaels, 1965]: 1) insolubility in common solvents, 2) infusibility, 3) plastisizability by water and electrolytes, 4) highly specific, but limited water absorptivity, 5) transparency of flexible solids (when wet), 6) selectivity of ion sorption and ion exchange properties. It was reported that when complex had significant adsorptivity for water and slight adsorptivity for organic component, the water absorbed formed hydration with the ion site [Kurokawa et al., 1980]. This exceptional water selectivity makes the polyelectrolyte complex membranes one of the most promising membranes in the pervaporation dehydration. Richau et al. [1996] revealed that water molecules were transferred from one hydrogen

bonding site to another by fixed carrier mechanism (although they did not use this term) through cellulose sulfate and different polycation complexes, and the selectivity was governed by diffusion not by the sorption mechanism. Polysaccharide polymers have been used to prepare the complex membranes because of their ionic functional groups.

Shieh and Huang [1997] studied complex membranes consisting of cationic chitosan and anionic polyacrylic acid for the ethanol/water separation. In addition, several important relationships between membrane efficiencies or selectivities and surface characteristics using X-ray photoelectron spectroscopy (XPS) and contact angle measurements were found [Lukas et al., 1995, 1997]. A review paper extensively dealing with the hydrophilic membranes and relevant phenomena can be found elsewhere [Semenova et al., 1997].

## *2) Materials for organic removal from dilute organic aqueous mixtures.*

Pervaporation processes for organic (e.g., alcohols, ketones, esters, and chlorinated hydrocarbons etc.) and volatile organic compounds (VOC) (e.g., 1,1,1-trichloroethane (TCA), trichloroethylene (TCE), CCl<sub>4</sub>, chloroform, and phenol etc.) removal from water has attracted much interest these days in terms of energy savings, solvent reuse, and environmental pollution control. Pervaporation is also a potential cost-competitive alternative to traditional methods in this regard (e.g., air stripping or carbon adsorption, photolysis, and ozonization). In general, the more soluble and less volatile a permeant is in water, the lower its selectivity. Therefore, aromatics and chlorinated components such as benzene, toluene, xylene, TCE etc. exhibit high separation factor, while water-soluble and less volatile components such as alcohols, acetone, aldehydes, acetic acid, and ethylene glycol have much lower selectivities.

For instance, Blume et al. [1990] reported that pervaporation is a potentially economic method to recover low concentrations of organic solvents from aqueous streams. Dilute systems for pervaporation separation can be found in various industrial processes including continuous in situ removal of dilute alcohols during fermentation of biomass and solvent recovery from the industrial effluents. When pervaporation technology is applied to the separation of aqueous organic solutions, the permselectivity is mainly governed by the interaction between the membrane polymer and the component tends to be separated. Thus, for the purpose of organic removal, the polymers that have strong affinity with organic components (organophilic) should be selected. Elastomers as opposed to glassy polymers for the dehydration of organic-water mixtures may be suitable for the organic component removal due to their flexible polymer chain mobility and high free volume. Several elastomers showing reasonable permeability as well as organophilicity include ethylene-propylene-diene-monomer (EPDM), nitrile-butadiene rubber (NBR), styrene-butadiene rubber (SBR), polyethylene (PE), polybutadiene (PB), polyurethane (PU), polytetrafluoroethylene (PTFE), polydimethylsiloxane (PDMS), poly[1-trimethyl(silyl)-1-propyne] (PTMSP), poly[vinyltrimethylsilane] (PVTMS), etc.

Among them PDMS is the most well-known and extensively studied material because of its high vapor permeability, good thermal stability, and excellent film forming properties. Substantial studies have been carried out to preferentially separate ethanol from aqueous mixtures through PDMS membranes [Bruschke, 1990; Takegami et al., 1992; Uragami and Morikawa, 1992; Lai et al., 1994; Mauz et al., 1996; O'Brien & Craig, 1996], poly(1-trimethylsilyl-1-propyne)/PDMS copolymer [Nagase et al., 1990], peroxide crosslinked polybutadiene rubber [Yoshikawa et al., 1994], and

PDMS/polystyrene interpenetrating polymer network (IPN) [Miyata et al., 1996], and this application is useful in the fermentation process. As an example of non-alcohol separations, separation of acetic acid from water was attempted using PDMS [Deng et al., 1994] and silicone rubber [Bai et al., 1993]. Drioli et al. [1993] studied pyridine separation from pyridine/water mixtures using PDMS, cation-exchange material, and PVA, respectively, and revealed that only PDMS is preferentially permeable to pyridine. As one of efforts to enhance organic selectivity, hydrophobic fillers such as zeolite, silicalite, and carbon black etc. were incorporated into the PDMS membrane [Dotremont et al., 1995; Jia et al., 1992; Adnadjevlc et al., 1997; Vankelecom et al., 1995, 1997a, 1997b] and silicone rubber membrane [Hennepe et al., 1987]. The use of organic selective molecular sieves having organic transport channels through its pores resulted in the increase of the selectivity without any common trade off phenomena or with the slight increase of the permeability. The performance of zeolite filled membrane is influenced by the physicochemical properties of zeolite used, primarily the degree of hydrophobicity, as well as the sorption capacity for organic, the specific pore volume, specific area and mean crystallite size of the zeolite. Recently, Chen et al. [1998] reported silicone rubber membrane filled with more hydrophobic silicalite-I filler through the treatment of silicalite I by acid or under steam, which removed the remaining metallic impurities and resulted in enhanced selectivity to ethanol. Other studies were directed to VOC or dissolved organic removal [Nijhuis et al., 1991; Chandak et al., 1997; Brooks and Livingston, 1995; Watson and Payne, 1990]. Review paper exclusively dealing with pervaporation using adsorbent filled membrane can be found elsewhere [Ji & Sikdar, 1996].

Another interesting approach to control the permselectivity of organophilic membrane is to add more hydrophobic polymer additives, mostly copolymers, to the membrane. Miyata et al. [1997] showed that the selectivity of PDMS to ethanol could be enhanced by the addition of copolymers containing PDMS component which was selectively localized at the surface of the PDMS membrane which then increased its hydrophobicity. Improvement of the hydrophobicity of PDMS membrane such as the graft polymerization of a hydrophobic polymer onto PDMS surface [Mishima and Nakagawa, 1999] and addition crosslinking reaction [Yeom et al., 1999] was investigated in recent publications. Yamaguchi et al. [1994] prepared filling polymerized membranes by plasma-graft polymerization. They filled the micropores of a porous high-density polyethylene substrate that is inert to organic with the grafting monomers that selectively permeate chloroform or TCE. Schnabel et al. [1998] studied the VOC separation improvement through PDMS hollow fiber membrane of the coiled configuration. Another promising material having organophilicity is poly(1-trimethylsilyl-1-propyne) (PTMSP) that was originally developed for the gas separation. PTMSP membrane has also been known to preferentially permeate ethanol at pervaporation of aqueous ethanol and to be more ethanol selective than PDMS [Nagase et al., 1991; Ishihara et al., 1986]. Another interesting organoselective polymer which has strong potential for this application is polyether block amide (PEBA) produced by ATOCHEM in 1981. Further published papers regarding organic removal from dilute mixtures are summarized and listed in Table 2.2.

MTR (Membrane Technology & Research) has sold several plants in the 5-10-thousand gallon/day range for water pollution control based on the silicone rubber

composite membrane. As pointed out earlier in this part, the development of materials permselective for the water-soluble solvents such as alcohol and acetic acid as well as VOCs is in great demand by industry. Future prospects and performance of organophilic membrane process for wastewater treatment was thoroughly reviewed in the article of Lipnizki et al. [1999a].

### *3) Materials for organic-organic separation.*

Organic-organic separation is the least developed application among pervaporation applications mostly due to the lack of membrane materials and modules sustainable aggressive solvent mixtures under the severe operating conditions. In addition it is not easy to find the proper membrane materials which can permeate an organic component selectively over another organic component. However, for alcohol/organic mixture relatively hydrophilic or polar membrane can be adopted for the separation of the alcohol component. Considering commercialized processes, it is believed that the Separex Division of Air Products is operating a small pilot system for methanol/MTBE separation based on cellulose acetate membranes. Also, Ho et al. [1991, 1996] of Exxon Research & Engineering Co. reported hard/soft segment copolymer membranes for separating heavy catalytically cracked naphtha into aromatic-rich permeate and aromatic-lean retentate. In this membrane hard segments, which consist of polyimide, provide temperature stability and solvent resistance, while soft segments, which is polyadipate, govern selectivity and flux. They further improved the flux and separation factor via incorporating the soft segments (polysuccinate) having higher polarity than that of polyadipate. Unlike elastomeric material favored in organic separation from water, most of materials having high affinity with the organic to be separated can be selected for this purpose regardless

**Table 2.2 Recent pervaporation research relevant to organic removal from aqueous organic mixtures (1999-2000)**

<b>MEMBRANE MATERIAL</b>	<b>COMPONENT TO BE SEPARATED</b>	<b>RESEARCHER</b>
Polyoctylmethyl siloxane (POMS-PEI)	Aroma components	Olsson & Tragardh [1999]
Fluoroalkyl methacrylate grafted PDMS	TCE, Benzene, Toluene, Tetrachloroethylene etc.	Mishima & Nakagawa [1999, 2000]
Poly(n-butyl acrylate-co-acrylic acid) and poly(BA-co-2-hydroxy ethyl acrylate)	TCE	Hoshi et al. [1999]
PDMS	Organophosphorus compounds	Almquist and Hwang [1999]
PDMS	VOCs	Yeom et al. [1999]
Sulfonated phenylene oxide	n-Butanol	Boucher-Sharma et al. [1999]
PDMS, PDMS-zeolite and PEBA (commercial membranes)	MeOH, MTBE, acetates	Kujawski [2000]
Polyurethane	Phenol	Hoshi et al. [2000]
Styrene-butadiene-styrene block copolymer	TCA, TCE, and toluene	Dutta and Sirkar [1999]
PDMS	Butanol	Qureshi and Blaschek [1999b]
PDMS 1070-GFT	Ester flavor compound	Baudot and Marin [1999]
PDMS and PEBA	Aroma compounds	Baudot et al. [1999]
Silicalite filled PDMS	Acetic acid	Lu et al. [2000]
Polysiloxaneimide	VOCs	Chang et al. [2000]

of glassy or rubbery polymer. However, it is hard to find good membranes for specific applications and get them to work economically on the industrial scale. Wytcherley and McCandless [1992] reported the separation of meta- and para xylene by polypropylene (PP) membrane in the presence of  $\text{CBr}_4$ . At temperatures below  $5\text{ }^\circ\text{C}$ , the presence of 24 mol%  $\text{CBr}_4$  that makes molecular complex with p-xylene in the feed results in polypropylene membrane very selective for m-xylene although PP membrane is selective for p-xylene. Polymer-metal complex membranes of low-density polyethylene-graft-poly (acrylic acid)- $\text{Ag}^+$  (LLDPE-g-AA- $\text{Ag}^+$ ) [Yang and Hsiue, 1998], silicone rubber (SR-g-AA- $\text{Ag}^+$ ) [Yang and Hsiue, 1997], and PTMSP-g-AA- $\text{Ag}^+$  [Yang and Hsiue, 1996] as well as PVA- $\text{AgNO}_3$  [Ho and Dalrymple, 1994] with homogeneous  $\text{Ag}^+$  distribution for olefin/paraffin separation were extensively investigated.  $\text{Ag}^+$  coordinated onto the carboxylic acid facilitated olefin transport. Among three membranes of Yang and Hsiue's work, PTMSP-g-AA- $\text{Ag}^+$  membrane possesses high gas permeability and high olefin/paraffin selectivity. Although their work was for the gas separation, carrier facilitated transport membranes offer potential application possibility for the separation of organic/organic liquid mixtures from petroleum industry. It was found that the benzene permselectivity and permeability for a benzene/cyclohexane mixture were increased with the metal ion crosslinker in the MMA-MAA copolymer membranes [Inui et al., 1999]. Incorporated metal ions ( $\text{Fe}^{3+}$  and  $\text{Co}^{2+}$ ) into the membranes increased the hydrophilicity, in other word, benzene selectivity (hydrogen solubility of benzene is much higher than that of cyclohexane). Tanihara et al. [1995] investigated poly (ether imide) segmented copolymer for the separation of benzene/cyclohexane, benzene/n-hexane, and

acetone/cyclohexane mixtures. They found that rubbery polyether domain contributed to selective sorption and diffusion and glassy polyimide served for the matrix. Polyethylene oxide based copolymer showed good selectivity to benzene and acetone.

**Table 2.3 Recent pervaporation research relevant to organic/organic separation (except methanol/MTBE mixture) (1999-2000) – underlined component is the preferred permeant**

MEMBRANE MATERIAL	MIXTURES TO BE SEPARATED	RESEARCHER
Carboxylated polysulfone	<u>benzene</u> /cyclohexane	Yoshikawa et al. [1999a]
Copolymer of acrylonitrile	<u>methanol</u> /ethylene glycol	Ray et al. [1999]
Poly(hexamethylene sebacate)-based polyurethane	<u>styrene</u> /ethylbenzene	Cao & Kajiuchi [1999]
Poly(hexamethylene sebacate)	<u>styrene</u> /ethylbenzene	Cao et al. [1999]
Poly(glycidyl methacrylate)-grafted PE	<u>benzene</u> /cyclohexane	Wang et al. [1999]
Nylon 6-graft-poly(butyl methacrylate)	<u>benzene</u> /cyclohexane	Yoshikawa et al. [1999b]
Nylon 6-graft-poly(hexyl methacrylate)	<u>benzene</u> /cyclohexane	Yoshikawa and Tsubouchi [1999c]
Poly[bis(phenoxy)phosphazene]	<u>benzene</u> /cyclohexane	Sun et al. [1999]
Methyl methacrylate-methacrylic acid copolymer	<u>benzene</u> /cyclohexane	Inui et al. [1999]
Poly(vinyl chloride)-g-poly(butyl methacrylate)	<u>benzene</u> /cyclohexane	Yoshikawa and Tsubouchi [1999d]
SBR/natural rubber blend	<u>CCl<sub>4</sub></u> /acetone	George et al. [2000]

Hao et al. [1997] reported that sulfonyl-containing polyimide membrane was preferentially permeable to aromatics over aliphatic with rather low flux and high separation factor because sulfonyl group reduced the swelling and enhanced the affinity to the aromatic component. Extensive review papers for the benzene/cyclohexane mixture separation can be found with the emphasis on the previous membrane performance [Villaluenga and Tabe-Mohammadi, 2000].

High methanol separation from methanol/MTBE mixture through polystyrenesulfonate based membranes was reported by Chen and Martin [1995a]. Polystyrenesulfonate/ $\text{Al}_2\text{O}_3$  composite membrane shows extremely high separation factors (25,000 to 35,000) in the  $\text{Mg}^{2+}$  counter ion form (PSS- $\text{Mg}^{2+}$ ) for methanol/MTBE mixtures, and also the separation factor 400 was obtained at the azeotropic concentration of ethanol/water mixture [Chen et al., 1995b]. As promising materials for the separation of methanol/MTBE mixture, cellulose acetate and triacetate have been known to have good methanol selectivities [Yang et al., 1998; Cao et al., 1999]. Blend membranes of PAA and PVA were applied to separate alcohol/toluene mixture [Park et al., 1994]. Separation of toluene mixtures has been less studied due to the lack of polymeric materials that could tolerate the harsh chemical properties of toluene. In summary, methanol/MTBE is a well studied mixture among various organic/organic mixtures and other mixtures that have been studied are listed in Table 2.3.

### **2.3 MASS TRANSPORT PHENOMENA IN PERVAPORATION MEMBRANE PROCESSES**

### 2.3.1 Solution-diffusion model

As in reverse osmosis, vapor permeation, and gas separation, the solution-diffusion model was successfully applied to dense pervaporation membranes. The solution-diffusion model (see Figure 2.1) consists of three steps; 1) sorption of feed components into the swollen layer of the membrane at the liquid feed side; 2) diffusion of permeant through the unevenly swollen layer of the membrane; 3) desorption of permeant into the vapor phase at the vapor permeate side. One of the preconditions in solution-diffusion model is the existence of thermodynamic phase equilibrium at both membrane surfaces being in contact with the feed mixture and the permeate mixture. Mass transport through the pervaporation membrane is generally expressed by the following Fick's law and being the rate determining process for the total separation process.

$$J_i = -D_i \frac{\partial c_i}{\partial z} \quad (2.7)$$

Another popular form describing the flux of component  $i$  is the following,

$$J_i = \frac{P_i}{l} (p_{fi} - p_{pi}) \quad (2.7.1)$$

where  $J_i$  is the flux of component  $i$  ( $\text{kg}/\text{m}^2 \text{ hr}$ ),  $D_i$  is the diffusion coefficient, and  $\partial c_i / \partial z$  is the concentration gradient through the membrane  $p_{fi}$  and  $p_{pi}$  are the partial pressures of component  $i$  in the feed and permeate streams, respectively. Thus, from equation (2.7) the driving force of the pervaporation transport is the chemical potential difference across the membrane. The pressure on the feed side is maintained slightly above the atmospheric, and the pressure on the permeate side is kept far lower than the saturation vapor pressure of the permeant to maintain the chemical potential difference. At this stage, it is worth to

consider each step in the solution-diffusion model. Since the partial vapor pressures of the permeating components at the permeate side are significantly lower than those at the feed side, phase transition occurs somewhere inside the membrane. The enthalpy for the vaporization is supplied by the sensible heat of the feed mixture [Ito et al., 1997]. Generally, the desorption step is regarded as less important step because the rate is so fast that almost no mass transport resistance exists. However, desorption resistance on the surface of the permeate side should be considered for the total transport mechanism when a thin membrane is applied and/or at high permeate pressure condition [Yeom and Lee, 1997]. Sorption or solubility is generally dependent on several factors such as permeant condensability, the interaction between the permeant and the polymer, the morphology of polymer (crystalline or amorphous), and the concentrations of various components within the membrane. On the other hand, diffusivity depends on the size and shape of the permeant, the free volume, polarity and morphology of the polymer as well as the concentration of the permeant.

Heintz et al. [1991] introduced three special cases of the pervaporation process in terms of solubility and diffusivity: 1) Solubility coefficient  $S_i$  is independent of activity  $a_i$  and concentration  $c_i$ , and diffusion coefficient  $D_i$  is independent of the concentration. When the feed mixtures behave ideally, Henry's law is applied; 2) For non ideal mixture,  $S_i$  depends on the activity, and  $D_i = D_i(c_i)$ , diffusivity is the function of concentration. This is the real situation for the sorption process in pervaporation, but diffusion coupling of the components is not taken into account. This model is approximately valid in case of organic mixtures and membrane consisting of hydrophobic material such as PE. However, its application is not justified for hydrophilic membranes; 3)  $S_i$  depends not

only on the activity but also on the concentration  $c_j$  of the other components.  $D_i$  is dependent of  $c_j$  but coupling is still neglected (Heintz and Stephan, 1994a). This is the case where hydrophilic membranes are described. However, in most real pervaporation processes, interactions exist between both the component-component and membrane-the components. Heintz and Stephan [1994b] described the solution-diffusion model taking into account non-ideal multicomponent solubility effects, non-ideal diffusivity behavior, diffusion coupling and the influence of the porous support layer. In this work the authors emphasized the importance of UNIQUAC model calculations and accounting for diffusion coupling based on the Maxwell-Stefan theory.

Fels and Huang [1971] developed a theoretical interpretation for the permeation of binary organic liquid mixtures. This model is based on an extension of Fujita's free volume theory [1961] for diffusion of organic substances in polymers and takes into account the effect of one component of the mixture on the diffusion of the other component. However, disagreement between theory and experiment remains in this model mainly due to the complex mathematical equations with parameters that are difficult to determine experimentally and inaccuracies in the free volume parameters. Fels and Huang model was further improved by introducing the interaction parameter of the permeant and polymer [Rhim and Huang, 1989; Yeom and Huang, 1992]. Several relationships that correlate the concentration of the permeants inside the membrane with the diffusion coefficient have been reported including constant diffusivity [Lee, 1975; Kataoka et al., 1991], the linear relationship [Greenlaw et al., 1977a, 1977b; Rautenbach and Albrecht, 1984, 1985], and exponential relationship [Brun et al., 1985a, 1985b; Mulder et al., 1985; Aptel et al., 1974; Huang and Lin, 1968]. Interestingly, Blume et al.

[1990] interpreted the pervaporation process as the product of an evaporation separation step and a membrane permeation (diffusion) separation step both to facilitate the mathematical treatment and to understand the difference between pervaporation and evaporation.

$$\beta_{\text{pervap}} = \beta_{\text{evap}} \beta_{\text{mem}} \quad (2.8)$$

Equation (2.8) does not imply that the pervaporation process actually occurs as an evaporation step followed by a permeation step. Although the solution-diffusion model has been accepted by a number of researchers, further improvement is required to describe the coupling and phase change phenomena in pervaporation.

Very recently, Shieh and Huang [1998a, 1998b] proposed a pseudophase-change solution-diffusion (PPCSD) model that is assuming a combination of liquid and vapor permeation mechanisms in series (see Figure 2.2) by modifying the solution-diffusion model. The primary difference between the conventional solution-diffusion model and the PPCSD model are that the pressure within the membrane is not uniform throughout the membrane system and that a pseudophase change of permeant occurs within the membrane.

In summary, pervaporation transport can be well described by the solution-diffusion model. It is assumed that the feed mixture and the permeate are in equilibrium with their respective membrane surfaces, and a concentration gradient, the driving force for the selective separation, exists through the membrane.

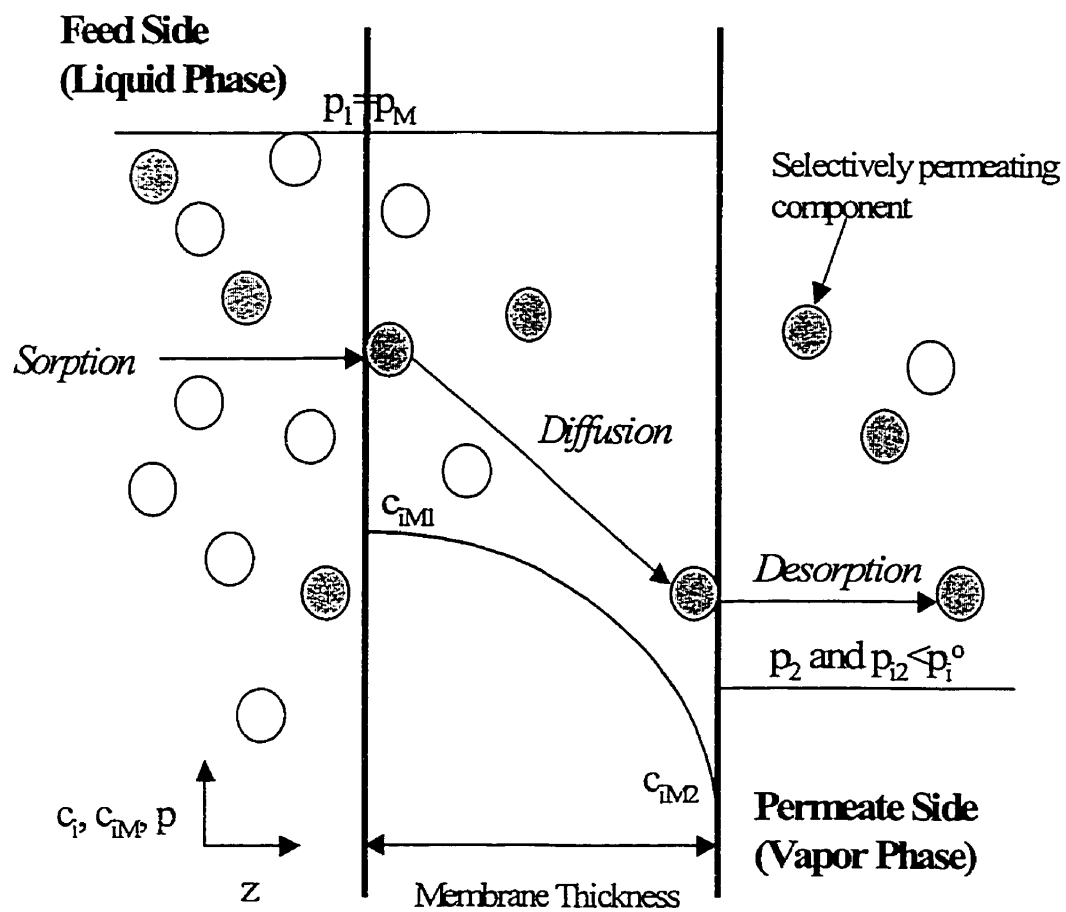


Figure 2.1 Solution-diffusion model for pervaporation

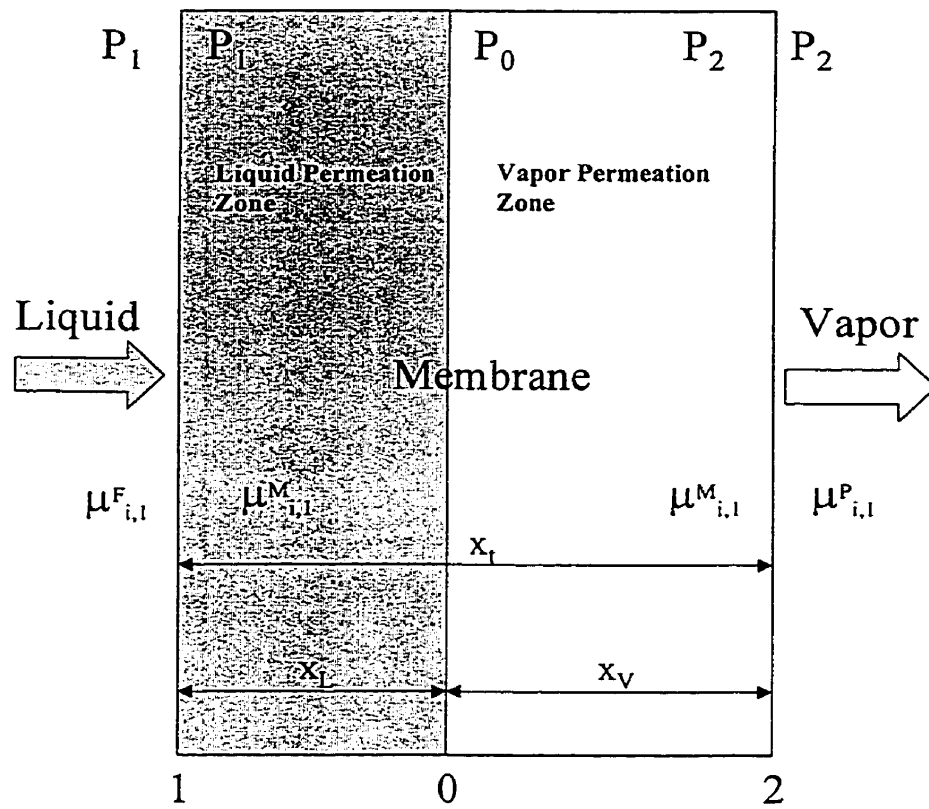


Figure 2.2 The pseudophase-change solution-diffusion (PPCSD) model

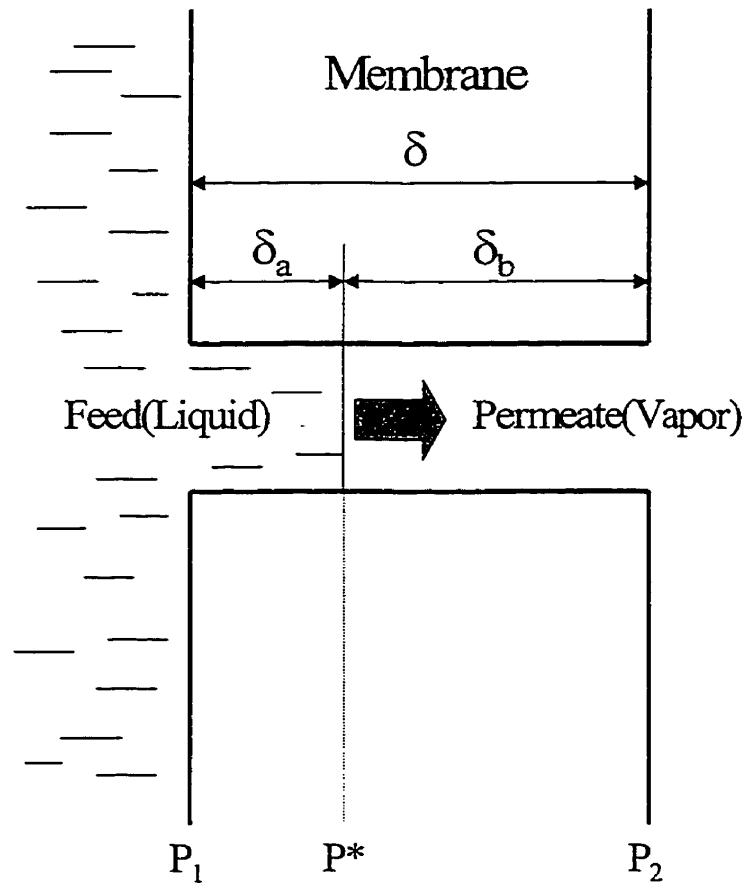
### 2.3.2 Pore flow model

Pervaporation transport theory based on the pore flow mechanism has been proposed first by Sourirajan et al. [1987] and has been described extensively by Okada et al. [1991a, 1991b]. Presumably this model creates a bundle of straight cylindrical pores (tortuous pores were simplified to straight pores in order to facilitate the derivation of equation) of length  $\delta$  penetrating across the active surface layer of the membrane normal to the membrane surface. Furthermore, it is assumed that the entire membrane is in an isothermal condition (see Figure 2.3). The pore is partially filled with liquid from the pore inlet to a distance  $\delta_a$  along the cylindrical axis. The rest of the pore ( $\delta_b$ ) is filled with vapor. The pore flow mechanism consists of the following three consecutive steps: 1) liquid transport from the pore inlet to the liquid vapor phase boundary; 2) evaporation at the phase boundary; 3) vapor transport from the phase to the pore outlet. There is a clear boundary separating liquid and vapor phases in the membrane [Matsuura, 1994]. That is, an imaginary phase that is in sorption equilibrium with the feed liquid and the permeant is established in the pore flow model. Tyagi et al. [1995] adopted this model to study the penetrant concentration profile inside the membrane showing concentration polarization. At this point, three differences can be noted between the solution-diffusion model and the pore flow model: 1) first, while no phase change inside the membrane occurs in the solution-diffusion model, a clear boundary of liquid and vapor exists inside the membrane at a certain distance from the surface that is in contact with liquid feed; 2) second, the concept of pore is different in both models. In the solution-diffusion model describing the liquid and gas transport through the dense polymer membrane, the

existence of pores is not dealt with. Effective membranes have no continuous passages but rely on the thermally agitated motion of chain segments comprising the polymer matrix to generate molecular-scale transient gaps in the matrix. The penetrants undergo random jumps through transient pore, but because of a higher concentration at the upstream side than the downstream side, a diffusion proceeds toward the downstream side [Koros and Fleming, 1993]; 3) third, driving forces for the transport are different. The mass transport is achieved by the concentration gradient according to the mathematical equations of solution-diffusion model, while the penetrant is driven by the pressure difference according to the transport equations based on the pore flow model. Consequently, considering the important fact that the equations of solution-diffusion model can be reduced to the ones based on the pore flow model, it is believed that both models represent the pervaporation transport properly but with different viewpoints of the polymer matrix.

### **2.3.3 The carrier transport mechanism**

The idea of fixed carrier membrane was coined during the design of novel synthetic membrane which a functional group was incorporated into a polymer structure as a carrier for transports of cations. In that sense, ion exchange membrane belongs to the fixed carrier membrane. Carrier membranes are classified into two types by an extensive state of carriers in the membrane [Shimidzu and Yoshikawa, 1991].

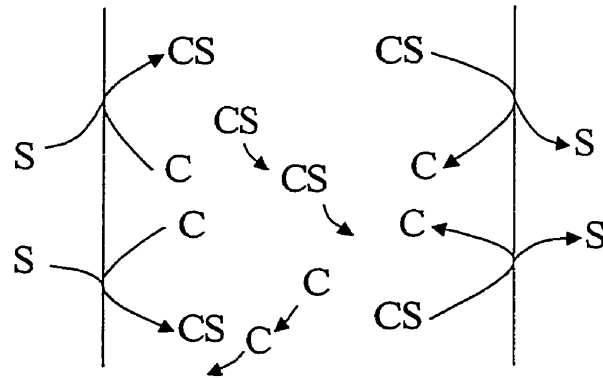
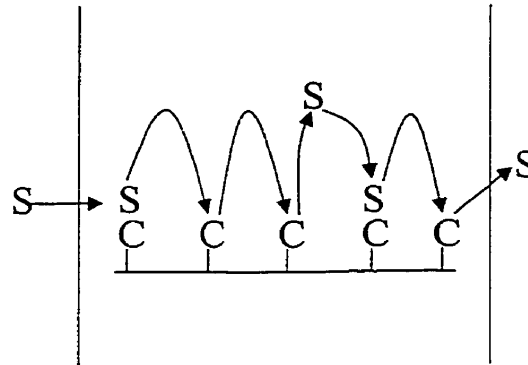


**Figure 2.3 Pore flow model for pervaporation**

1) Nonfixed carrier membrane (liquid membrane) – A membrane in which carrier is able to move.

2) Fixed carrier membrane – A membrane in which a carrier is fixed and impossible to diffuse.

A difference existing between nonfixed carrier and fixed carrier membranes is shown explicitly in Figure 2.4. In this figure, C represents a carrier such as imide group, carboxyl group and S is the transported component such as water in hydrophilic membrane. In fixed carrier membranes, much higher energy than in nonfixed carrier membranes is required since adsorption and desorption is repeated continuously when a transported component moves between fixed carriers. On the other hand, once a transported component forms a complex with a carrier in a nonfixed carrier membrane, the other components only can find the carriers after a previous component is released from the membrane. In this sense, a fixed carrier can achieve high selectivity because a transported component changes carriers many times during the transport. Fixed carrier membranes, in which carrier is fixed covalently to membrane matrix, have been developed since poly(maleimide-co-acrylonitrile) membranes containing pendent imide group as a carrier of water molecule was reported for the separation of water-ethanol mixture [Yoshikawa et al., 1984a]. Incorporating an imide group into a membrane caused a strong interaction with water through hydrogen bonding, and might lead to the enhanced permeation of water through this membrane.

**Nonfixed Carrier Membrane****Fixed Carrier Membrane**

**Figure 2.4 Carrier transport mechanism for pervaporation**

## 2.4 PROCESS PARAMETERS IN PERVAPORATION MEMBRANE PROCESSES

1) *Feed concentration.* As mentioned earlier, sorption and diffusion phenomena govern the mass transport through the pervaporation membrane. A change in feed concentration directly changes the sorption equilibrium at the membrane-feed mixture interface, and then the changed sorption equilibrium affects the concentration gradient inside the membrane. Additionally, the change of membrane dimension by swelling and coupling phenomena is closely relevant to the feed concentration; it is continuously critical to the flux and separation factor.

Concentration polarization has long been recognized as a major obstacle in continuous operation in the cases of microfiltration, ultrafiltration, and reverse osmosis processes. Selective permeation of a component leads to the accumulation of the retentate in front of the membrane, namely, in the boundary layer. Spontaneously the concentration of the more permeable component in the boundary layer is lower than that in the bulk fluid, while the opposite phenomenon occurs for the less permeable component. The polarization of the components generally causes a decrease in the flux of the preferentially permeating component and an increase in that of the less permeable component. This reduces the overall separation efficiency. Although concentration polarization is often found to be insignificant in pervaporation process [Heintz and Stephan, 1994b], Feng and Huang [1994] reported that the polarization is more severe in the pervaporation removal process of dilute phenol solutions using PEBA (polyether-block-polyamide) and PDMS membranes. When the feed concentration is considerably

high, the concentration polarization is unlikely to pose a severe problem to the separation performance. A generalized equation relating the modified Peclet number to the concentration polarization was proposed by Bhattacharya and Hwang [1997]. It is believed that the increase in the feed flow rate as the flow goes from laminar flow to turbulent flow reduces the concentration polarization in most cases [Dotremont et al., 1994]. Also the advantage of turbulent flow verifies why concentration polarization is negligible in gas separation process where Peclet number  $Pe < 1$  are typical in contrast to the liquid separation membrane processes. However, for the very high flux membranes used in industrial membrane processes for the separation of gas-vapor mixtures and in high pressure applications in the petrochemical industry concentration polarization could be significant [Ludtke et al., 1998]. Koops et al. [1994] reported that the selectivity of various pervaporation membranes decreases with decreasing membrane thickness below a limiting value of about  $15 \mu\text{m}$  while the selectivity of the same membranes for gas separation are independent of the thickness. The authors attributed this phenomenon to the defects in what induced from the feed solution.

2) *Feed and permeate pressures.* The driving force for pervaporation is provided by the vacuum which is applied to the permeate side. Thus the feed pressure hardly affect the permeation flux. Since permeate pressure is closely connected to the activity of the components at the permeate side of the membrane, it has a strong influence on the pervaporation characteristics. The maximum driving force can be obtained at zero vacuum pressure. Increasing the permeate pressure results in a decrease in driving force, decreasing the flux. It is generally observed that the selectivity is gradually reduced when permeate pressure is increased [Aptel et al., 1974; Rautenbach and Albrecht, 1985; Neel

et al., 1986]. However the opposite trend was also reported by Greenlaw et al. [1977b] for the hexane-heptane separation through polyethylene membrane. Shelden and Thomson [1978] of the same research group suggested that it relied on the nature of the experimental system studied. Recently in study of ester flavor recovery [Baudot and Marin, 1999], it was revealed that the selectivity can be significantly improved by the coupling of pervaporation with a flash condensation over the conventional total permeate condensation. In summary, the separation factor may increase or decrease with increasing permeate- pressure, depending on the relative volatility of the permeating components.

3) *Operating temperature.* It is commonly accepted that sorption and diffusion of the solvent in a polymeric membrane depend on the temperature. Diffusion rate of the permeant inside the polymer membrane is getting faster with the increase of temperature due to higher permeation energy and faster thermal motion of polymer chain segments. It is generally observed that the flux increases with the temperature increase but the separation factor decreases as the result of trade-off phenomenon commonly observed in pervaporation. However, an unusual phenomenon, in which the separation factor increases with the increase of the temperature, is also observed in natural polymer such as alginate [Yeom et al., 1996] because of the intrinsic relaxation behavior of the relevant polymer. The temperature dependence of the flux can be expressed by an Arrhenius type relationship:

$$J = A_p \exp\left(-\frac{E_p}{RT}\right) \quad (2.9)$$

where  $A_p$  and  $E_p$  are the pre-exponential factors and the apparent activation energy, respectively. Neel [1991] has reviewed the engineering aspects including above process parameters in detail.

## 2.5 CLASSIFICATIONS AND MODULES FOR PERVAPORATION MEMBRANES

### 2.5.1 Membrane classifications

Dense homogeneous films frequently used in the initial evaluation step to characterize the membrane performance suffer from very low permeation fluxes in practical applications. Reducing the membrane thickness is very crucial to improving permeation flux significantly, however dense homogenous membrane cannot be handled effectively in thickness control due to mechanical weakness. Two membrane types can be distinguished, viz. asymmetric and composite membranes. The difference between these two definitions is whether the materials consisting of the selective top layer and the supporting porous layer are the same materials or not. Their concepts and applications are reviewed in the following sections.

1) *Asymmetric membranes.* Asymmetric membranes which have a very thin selective layer (of the order of 0.1-1  $\mu\text{m}$ ) is supported by a porous substrate of the same material. In some books, the term “integrally skinned membrane” is often used instead of asymmetric membrane. Thin skin layer determines both the permeability and the selectivity of the membrane, whereas the porous substrate acts as a mechanical supporter. Cellulose acetate membranes in the reverse osmosis desalination application were reported as the first skinned membrane, and developed by Loeb and Sourirajan using the phase inversion technique. Phase inversion is now the most important process to prepare

asymmetric or symmetric membranes. The phase inversion mechanism was investigated extensively due to its importance. Two types of demixing occurring during immersion precipitation, namely, instantaneous and delayed demixing, were studied with regard to their effects on macrovoids [Smolders et al., 1992]. It was found that macrovoids were avoided and formed in case of delayed demixing and instantaneous demixing with some exceptions, respectively. Also polymeric additives suppresses the formation of macrovoids in the sub-layer, while the ultrafiltration type top layer consists of a closely packed layer of nodules [Boom et al., 1992]. Kim and Lee [1998] substantially investigated the effects of PEG additive on the structure of polysulfone porous membrane in the phase inversion process. In fact, asymmetric membranes for the pervaporation applications have been investigated by Feng and Huang [1993, 1996a] who reported asymmetric polyetherimide membrane prepared by the dry/wet phase inversion technique. It was revealed that the major variables involved in the membrane preparation included polymer concentration, additive content, solvent evaporation temperature and period were crucial to membrane performance. Symmetric and asymmetric membranes were compared with respect to their performance in pervaporation [Rautenbach and Albrecht, 1984]. They showed that the capacity of asymmetric membranes could be increased by facing the active skin layer to the feed side, and the pores should be fingerlike and in any case must be open at the permeate side. Defect free integrally skinned polysulfone hollow fiber membranes were developed by means of a triple orifice spinneret for the dehydration of acetic acid by pervaporation [Koops et al., 1992]. The formation of asymmetric pervaporation membranes was studied using nylon 4 [Lai et al.,

1994], polycarbonate [Lee et al., 1994], polyimide [Yanagishita et al., 1994, 1995], polyvinylidene fluoride (PVDF) [Jian and Pintauro, 1993, 1997] membranes.

Gas separation membrane with ultrathin skin layer is an important research topic because of its high productivity. Van't Hof et al. [1992] reported asymmetric polyethersulfone (PES) hollow fiber membrane having high selectivity by a dual-bath coagulation method. The first bath initiates the formation of a dense top layer and the second bath gives the actual polymer precipitation. Integrally skinned asymmetric gas separation membranes were prepared by dry/wet phase inversion technique in which the outmost region of the cast membrane undergoes phase separation induced by partially evaporating the solvent, while the bulk of the membrane is formed by solvent-nonsolvent exchange in methanol bath [Pinnau and Koros, 1991] and water bath [Pesek and Koros, 1993]. Membrane made by dry/wet phase inversion technique was superior to the membranes by dry or wet techniques in terms of selectivity.

It must be emphasized here that asymmetric membranes with high flux and optimum separation factor for pervaporation separation can be prepared by using the dry/wet phase inversion method through proper membrane preparation conditions.

2) *Composite membranes.* Since dense homogeneous membranes show low permeation rates, their industrial application is hindered. Composite membrane having a very thin selective layer supported by porous substrate was the breakthrough, which made the pervaporation process emerge on a commercial scale. The advantage of the composite membrane is that each layer can be optimized independently in terms of selectivity, permeation rate, and chemical, thermal and mechanical stability. The first commercial pervaporation membrane is the composite membrane manufactured by GFT

of Germany for alcohol dehydration. The GFT membrane consists of a crosslinked PVA skin layer supported by polyacrylonitrile substrate [Will & Lichtenthaler, 1992; Ohya et al., 1992]. In general, the supporting layer is prepared by phase inversion method. The structure of the support layer affects the performance of composite membrane significantly. If the pores of porous layer are too narrow, capillary condensation inside the pores cannot be avoided. With the Kelvin equation, (2.10) it can be calculated at what pressures capillary condensation occurs as a function of the pore radius [Koops et al., 1993].

$$\ln \frac{P}{P_o} = \frac{2 \cdot \gamma \cdot \bar{V}}{r \cdot RT} \cos \theta \quad (2.10)$$

where  $P$  and  $P_o$  are vapor pressure observed over curved surface in capillary and normal vapor pressures, respectively,  $r$  is the pore radius,  $\bar{V}$  is the molar volume of the liquid filled the capillary, and  $\theta$  is the contact angle. On the other hand, large pores cause difficulties in obtaining thin defect free top layer. It is frequently found that casting solution of top layer intrudes the pores and then reduces or blocks the pathways of the permeant [Vankelecom et al., 1999]. Ideal support membranes for the composite membranes possess a relatively high surface porosity to have the top layer mainly to be selective layer. When the surface porosity is low relatively, the top layer and the support layer control the separation properties concurrently. Several techniques can be used to prepare a composite membrane with a thin top layer; 1) dip coating, 2) solution casting, 3) plasma or UV initiated polymerization [Parthasarathy et al., 1994; Ulbricht and Schwarz, 1997]. In cases of dip coating and solution casting, polymer solution must have good wettability on the support polymer. Otherwise, each layer can be segregated again during the pervaporation operation.

### 2.5.2 Pervaporation modules

In practical applications, three types of membrane modules are used; 1) plate and frame, 2) spiral-wound, 3) hollow fiber, capillary and tubular. Significant reviews with regard to module design and characterization are contained in the book by Rautenbach & Albrecht [1989]. In most of pervaporation applications, feed mixtures containing hot, organic-solvent are involved. Thus, the seals and plastic components of the module should sustain severe chemical and thermal attack. Consequently, the first generation commercial pervaporation module installed by GFT have been made from stainless steel and are of the plate-frame design. However, since the membrane area per unit module volume is quite limited in the plate-frame module, several efforts have been made to switch to lower cost module designs. Pervaporation membranes of MTR (Membrane Technology and Research) and Air Products have been manufactured in spiral-wound modules, which is characterized by a high packing density ( $>900 \text{ m}^2/\text{m}^3$ ) and is commonly used by many membrane manufacturers. Moving from a plate frame module to a spiral wound module has improved the efficiency in organic removal applications. Meanwhile, the hollow fiber module is not used due to the technical reasons in pervaporation application in spite of its successful commercialization in reverse osmosis. Substantial studies were reported with respect to the hollow fiber pervaporation process on the basis of its potential [Sheng, 1994; Masawaki et al., 1992; Watanabe & Kyo, 1992; Feng & Huang, 1995; Nii et al., 1994].

Currently, the membrane separation as an industrial separation process has become more prevalent as various membrane modules have been developed. However, it must be pointed out that in many instances, the use of a membrane system alone is not desirable or feasible to carry out a complete industrial separation. As an alternative or strategy, the hybrid design concept is particularly well suited for membrane-based unit operations. It was found that hybrid processes might lower industrial separation costs significantly and result in more complete separation than are possible using conventional processes [Ray et al., 1991]. The overall aspects of pervaporation hybrid processes were extensively reviewed as industrialized cases such as distillation hybrid and reactor hybrid processes [Lipnizki et al., 1999b]. In the model study of ethanol production by a continuous fermentation-pervaporation, O'Brien et al. [2000] revealed that the incorporation of pervaporation unit into traditional fermentation plant costs slightly higher than the base case. However, with a modest improvement in either the permeation flux or separation factor, fermentation-pervaporation system could be cost-competitive.

## **2.6 THE MEASUREMENT OF DIFFUSION COEFFICIENT IN THE MEMBRANE**

As mentioned earlier, mass transport through the dense polymeric membrane is governed by the solution-diffusion mechanism. Diffusion is defined as the process in which components are transported from one part of a mixture (solid, liquid and gas) to another as a molecular motion. Diffusion of a component in the pervaporation membrane is considered thermodynamically irreversible because constant potential gradient is

maintained. In general, diffusion mechanism of a solvent such as alcohol and water in a polymeric membrane is described in the viewpoint of the ability of the polymer to physically accommodate the permeant. That is, the membrane continually provides randomly generated microvoids of molecular level for the permeant diffusion through the membrane [Frisch and Stern, 1983-1984]. Small molecules occupy the interchain space (free volume) between the macromolecules of the polymer. It has been widely accepted that the permeant size and shape effects dominate the diffusion mechanism in glassy or rubbery polymers. On the other hand, Watson et al. [1990, 1992] supposed that the diffusion process in silicone rubber is not dominated by permeant size effects, but is influenced to a significant extent by specific site, permeant-polymer interactions by expressing the diffusion coefficient as follows:

$$D = \frac{\lambda^2}{2\tau_0} \exp\left(-\frac{E}{RT}\right) \quad (2.11)$$

$$\tau_p = \tau_0 \exp\left(\frac{E}{RT}\right) \quad (2.12)$$

where the dwell time  $\tau_p$  at each site is determined by the strength of the permeant-polymer interaction,  $E$  is the activation energy characterizing the permeant-polymer physisorption bond,  $1/\tau_0$  is the vibration frequency of the bond and  $\lambda$  is the jump length. Equation 2.11 is identical to that of conventional diffusion theory, but the difference lies in the interpretation of  $E$  and  $\tau_0$  intimately concerns the permeant molecule. It must be mentioned that above authors merely emphasized the possibility that Van der Waals interactions might play an important role in the diffusion process especially in silicone rubber with the possibility in other polymers too. From above discussion, the size of the

permeant and its interaction with the polymer must be considered simultaneously to determine the diffusion coefficient [Brookes and Livingston, 1995; LaPack et al., 1994].

### 2.6.1 Conventional measurements of diffusion coefficient

Modelling allows one not only to explain but also to predict the behavior of a system under different experimental conditions when a set of relevant parameters such as the feed concentration, operating pressure, membrane thickness, and the diffusivity of the permeant are identified. Further more, mathematical modelling is essential for accurate scale-up.

The mass transport phenomenon through the dense polymeric membrane is well described by the solution-diffusion model. That is, the permeability  $P$  ( $= D \times S$ ) is the product of the solubility,  $S$  and the diffusivity,  $D$ .

When the membrane faces to the feed mixtures, the components in the feed mixture will be absorbed into the matrix of the membrane due to the concentration gradient through the membrane, and then the sorbed component will diffuse along the conceptual free volume in the polymeric membrane and eventually be desorbed into the permeate side. Desorption process is considered to be non-selective and swift, so this process is commonly not incorporated in the mass transport model.

Precise measurement of the solubility and diffusivity becomes of importance in estimating the mass transport phenomenon through the polymeric membrane reliably. In various applications of polymeric thin films such as the gas separation membrane, packaging barrier film, container and supercritical fluid ( $\text{CO}_2$ ) or foam processing,

**Table 2.4 Models for the concentration dependence of diffusion coefficient in binary mixture**

Models	Reference
$D_i = D_{i0}(C_i + B_{ji}C_j)$	Greenlaw et al., 1977a, 1977b; Shelden and Thompson, 1978; Rautenbach and Albrecht, 1985
$D_i = D_{i0} \exp(A_{ii}C_i + A_{ij}C_j)$	Brun et al., 1985a, 1985b
$\ln D_{im}^* = x_i \ln D_{ii}^* + \sum_{\substack{j=1 \\ j \neq i}}^n x_j \ln D_{ij}^*$	Bitter, 1991
$D_i = RTA_{di} \exp \left\{ - \left( \frac{f(0,T)}{B_i} + \frac{\beta_i(T)}{B_i} \phi_i + \frac{\beta_j(T)B_j}{B_i} \phi_j \right) \right\}^{-1}$	Yeom and Huang, 1992

aforementioned parameters should be measured accurately. Diffusion coefficients in the pervaporation membranes commonly depend on the concentration of the permeating component. Many researchers have been studying various relationships between the diffusion coefficient and the concentration of the permeating component either empirically or theoretically. Like the pervaporation separation, one considers that the binary permeation, diffusion coefficient of component  $i$  is affected by component  $j$  or vice versa. Significant models of diffusion coefficient are tabulated in Table 2.4.

In this section, methods to measure the diffusion coefficient experimentally in polymeric thin film are presented and reviewed.

1) *Electrogravimetric sorption (or desorption) experiment approach*

Sorption technique [Wong et al., 1998; Hernandez-Munoz et al., 1999] is a unique and advantageous method in measuring both solubility and diffusivity, especially when the diffusivity is very low. Solubility is the measurement of the concentration of sorbed species in the polymer matrix at the equilibrium state at given temperature and is vital in many areas such as chemical processing and the assessment of transport and distribution with organic compounds.

From the sorption experiment, solubility of the component  $i$  is estimated as follows,

$$\begin{aligned}
 w_i^f &= S_i \cdot a_i^f \\
 S_i &= \frac{M_\infty}{w} \cdot \frac{1}{a_i p_i^0} = \frac{M_\infty}{w} \cdot \frac{M_i}{c_i RT} \\
 w_i^f &= \frac{M_\infty}{w} \\
 a_i &= \frac{p_i}{p_i^0} \\
 p_i &= \frac{c_i RT}{M_i}
 \end{aligned} \tag{2.13}$$

where  $w_i^f$  is the weight fraction of component  $i$  at the surface membrane at the feed side,  $M_\infty$  is the amount of sorbed component in the membrane at equilibrium state,  $w$  is the dry weight of membrane,  $a_i^f$  is the activity of component  $i$  in the feed mixture,  $a_i$  is the activity of the component  $i$  in the membrane,  $p_i^0$  is the vapor pressure of pure component  $i$ ,  $p_i$  is the partial vapor pressure of  $i$ ,  $M_i$  is the molecular weight of  $i$ ,  $R$  is the gas constant. At very low concentration, Henry's law is applied and the solubility can be determined from the slope of the isotherm or from any data point using above equations.

There is a practical method to obtain the solubility of a solute in the membrane from swelling experiments [Yeom & Huang, 1992]

$$R = \frac{l - l_0}{l_0} \quad (2.14)$$

$$v = \frac{R^3 - 1}{R^3}$$

where  $R$  is the swelling ratio,  $l$  and  $l_0$  is the lengths of the swollen membrane and the dry membrane at specific condition.  $v$  is the volume fraction of the permeant in the swollen membrane and can be used as the solubility of the permeant in the membrane.

The kinetic characteristics of the sorption experiment make it possible to measure the diffusivity of the component through the dense polymeric membrane with the following relationship [Crank & Park, 1968].

$$\frac{M_t}{M_\infty} = 1 - \frac{8}{\pi^2} \sum_{n=0}^{\infty} \frac{1}{(2n+1)^2} \cdot \exp\left(-\frac{D(2n+1)^2 \pi^2 t}{\delta^2}\right) \quad (2.15)$$

$$\frac{M_t}{M_\infty} = \frac{4}{\delta} \left(\frac{Dt}{\pi}\right)^{\frac{1}{2}} + \frac{8}{\delta} (Dt)^{0.5} \sum_{n=0}^{\infty} (-1)^n \operatorname{ierfc}\left(\frac{n\delta}{2(Dt)^{0.5}}\right) \quad (2.16)$$

where  $M_t$  is the sorbed amount of the component  $i$  at time  $t$ ,  $D$  is the diffusivity,  $\delta$  is the membrane thickness. Equation 2.15 converges rapidly at moderate or long time, whereas equation 2.16 is converges at relatively short time.

When  $M_t/M_\infty \geq 0.5$ , equation 2.15 can be simplified to its first term of the summation with an error 0.001%.

$$-\frac{1}{\pi^2} \ln \left[ \left( 1 - \frac{M_t}{M_\infty} \right) \cdot \frac{\pi^2}{8} \right] = \frac{D \cdot t}{\delta^2} \quad (2.17)$$

Diffusivity can be obtained from the slope of the plot of left-hand side term vs.  $t$  at sufficiently long time.

When the half time ( $t_{1/2}$ ) sorption process is proceeded under well-controlled environment, it is assumed that diffusivity is constant, i.e., concentration independent and Fickian. That is, at  $M_t/M_\infty = 0.5$  above equation is simplified to the following.

$$D = 0.0489 \frac{\delta^2}{t_{0.5}} \quad (2.18)$$

Diffusivity is simply calculated when  $t_{0.5}$  is known from the experiment.

When  $M_t/M_\infty$  vs.  $\sqrt{t}$  is plotted at short time, diffusivity is calculated from the slope of the plot. One term simplified form of equation 2.16 can be written

$$\frac{M_t}{M_\infty} = \frac{4}{\delta} \left( \frac{Dt}{\pi} \right)^{0.5} \quad (2.19)$$

The momentum technique is also used to measure the diffusivity [Felder, 1978]. The momentum may be determined from the integration of the plot of  $M_t$  vs.  $t$  and diffusivity may be calculated from the following equation.

$$\tau_s = \int_0^{\infty} \left( 1 - \frac{M_t}{M_{\infty}} \right) dt \quad (2.20)$$

$$D = \frac{\delta^2}{12\tau_s}$$

There is a hybrid 1-term method which combines two first-terms of equation 2.15 and 2.16 in order to provide good approximation of sorption experiment over the entire time range [Balik, 1996]. A weighted sum of the two first term approximations is used, weighting function  $\phi(x)$  switch the equation from the short time equation 2.16 to the long time equation 2.15 at  $Dt/\delta^2 = 0.05326$ .

$$\frac{M_t}{M_{\infty}} = \phi(x)f(x) + (1 - \phi(x))g(x)$$

$$x = \frac{Dt}{\delta^2} \quad (2.21)$$

$$f(x) = 4\left(\frac{x}{\pi}\right)^{0.5}, \text{ short time approximation}$$

$$g(x) = 1 - \left(\frac{8}{\pi^2}\right)\exp(-\pi^2 x), \text{ long time approximation}$$

$$\phi(x) = \frac{1}{1 + \exp\left(\frac{x-a}{b}\right)}$$

$$a = 0.05326$$

$$b = 0.0001$$

The transition occurs from  $\phi(x)=1$  to  $\phi(x)=0$  at  $x=a$ . This is well-known Fermi function and plotted in Figure 2.5. In summary, sorption technique is preferred in very low diffusion coefficients and in high-pressure measurements, whereas the permeation approach is preferable for routine measurements especially at low and moderate penetrant activities [Felder, 1978].

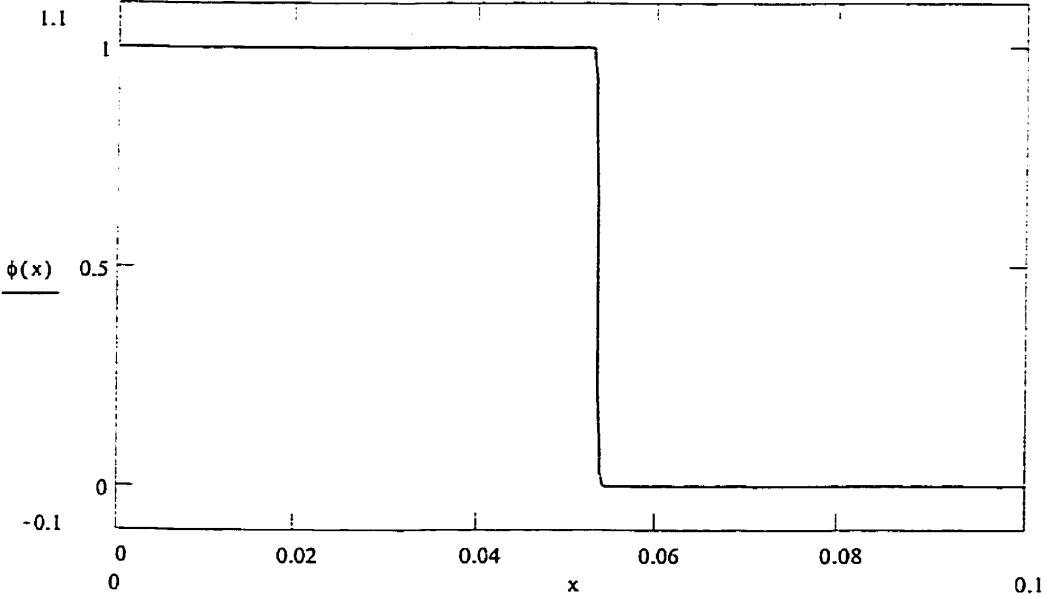


Figure 2.5 Plot of the Fermi function for  $a=0.05326$  and  $b=0.0001$

### 2) Permeation experiment approach

It seems that the measurement of diffusivity using pervaporation experiments is much more practical and more clearly represents the pervaporation process in the model if the experiments are well prepared. In this method, it is assumed that the solubility and diffusivity is independent of the concentration and that is, the concentration is constant through the membrane at any given time. From the Fick's first law,

$$J = -D \frac{dC}{dx}$$

B.C.

$$x = 0, C = C_1 \quad (2.22)$$

$$x = \delta, C = C_2$$

$$\therefore J = D \frac{(C_1 - C_2)}{\delta}$$

where  $C_1$  and  $C_2$  are the concentrations of the permeant on the surfaces of the feed side and permeate side, respectively. When diffusivity is measured from above equation, diffusivity here is independent of the concentration.

The above equation can be written in another form from the Henry's law (linear sorption isotherm),  $C = S \times p$

$$J = DS \frac{(p_1 - p_2)}{\delta} \quad (2.23)$$

where  $p_1$  and  $p_2$  are the partial vapor pressures of the permeant on the surfaces of both the feed and the permeate. From the permeability expression  $P = DS$  this equation is written

$$J = P \frac{(p_1 - p_2)}{\delta} \quad (2.24)$$

When  $P$  is known from the experiment, equation 2.24, provided that one of the diffusivity and the solubility is known, equation  $P=DS$  can be used to get the remaining parameter.

Unlike the steady state measurement, at the unsteady state condition Fick's second law can express the permeation characteristics.

$$\frac{dC}{dt} = D \frac{d^2C}{dx^2}$$

B.C.

$$C = C_1, x = 0, t \geq 0$$

$$C = 0, x = \delta, t \geq 0$$

$$C = 0, 0 < x < \delta, t = 0$$
(2.25)

From the boundary conditions this equation can be expressed as follows.

$$Q_t = \frac{DC_1 t}{\delta} - \frac{\delta C_1}{6} - \frac{2\delta C_1}{\pi^2} \sum_{n=1}^{\infty} \frac{(-1)^n}{n^2} \exp\left(\frac{-Dn^2\pi^2 t}{\delta^2}\right)$$
(2.26)

where  $Q_t$  is the total permeated amount of the permeant This is the equation modelling the experimental data. When  $t$  approaches  $\infty$ , further simplified expression is made and used to calculate the diffusivity.

$$Q_t = \frac{DC_1}{\delta} \left( t - \frac{\delta^2}{6D} \right)$$

$$I = \frac{\delta^2}{6D}$$
(2.27)

This is the so called time lag method to obtain the diffusivity from the intercept  $I$  of the plot of  $Q_t$  vs.  $t$  (Figure 2.6).

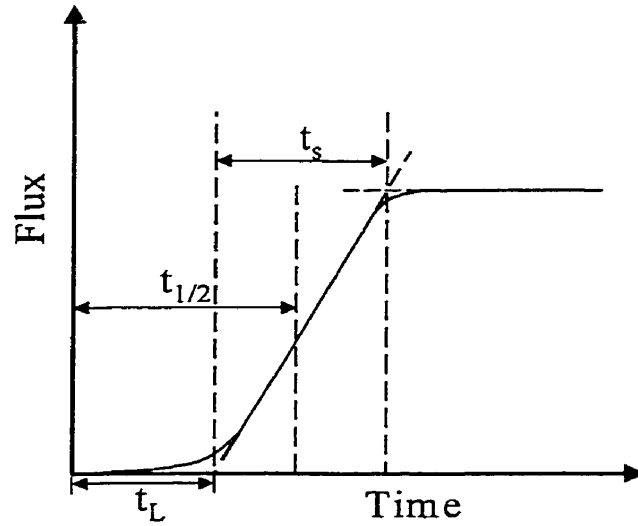


**Figure 2.6 Ideal permeation flux of the pervaporation membrane**

Watson et al. [1990, 1992] measured the diffusion coefficient in silicone rubber membrane using time-lag method. The permeant flux is given by

$$\frac{Q}{Q_s} = 1 + 2 \sum_{n=1}^{\infty} (-1)^n \exp(-n^2 \pi^2 D t / \delta^2) \quad (2.28)$$

where  $Q$  and  $Q_s$  are the fluxes at a certain time and steady state, respectively. They derived the two diffusion coefficients based on the two observed times.

$$\frac{D t_{1/2}}{\delta^2} = \frac{1}{7.21} \quad (2.29)$$

$$\frac{D t_s}{\delta^2} = \frac{1}{5.92} \quad (2.30)$$

### 2.6.2 Inverse gas chromatography approach for the diffusion coefficient

Conventional methods for measuring diffusion coefficient of the low molecular weight components in polymer such as the gravimetric vapor sorption or desorption depend on sorption and bulk equilibrium. These methods become increasingly unreliable when the diffusion is very slow or when the solvent is present in vanishingly small amounts. As an effective alternative, inverse gas chromatography (IGC) has been gaining much attention because of its convenience, economics of operation, and versatility. The word inverse means that the component of interest is the stationary polymer phase rather than the injected mobile substances. In principle, a variety of interesting physical and chemical properties, including the diffusion coefficient [Pawlish et al., 1987, 1988] and the solubility [Baltus et al., 1993] of the polymer as well as the activity coefficient [Bonifaci et al., 1994], the enthalpies of interaction, Flory-Huggins interaction parameter, crystallinity [Guillet and Stein, 1970; Gray and Guillet, 1971], adsorption isotherm [Kontominas et al., 1994], degree of fusion [Qin et al., 1995], and crosslinking [Tan et al., 1994] can be determined by studying the elution profiles of the injected volatile probe molecules of known properties through the chromatographic column containing the polymer. The principle of IGC technique is based on partitioning of a volatile substance between a mobile gas phase and a stationary polymer phase. Currently, IGC has proven to be a particularly important tool for the polymer surface/interface characterization. The most significant equipment in IGC technique is the form in which the stationary phase may be prepared in the chromatographic column. A column can be packed with a

polymer support mixture (packed column) or it may be coated on the wall with the polymer to create a capillary column. The proper preparation of each of these columns is extremely crucial to gaining reliable data. The free volume theory predicting diffusion in a solvent-polymer system and two types of chromatographic column for IGC experiment are reviewed below. IGC technique can be applied to measuring the diffusion coefficient of the permeants through the hydrophilic membranes.

1) *Free volume theory.* The free volume theory was originally developed by Cohen and Turnbull [1959] to consider the molecular transport in a liquid consisting of hard spheres by relating the self-diffusion coefficient to the free volume of the system. According to this theory, the free volume is defined as the volume within the cage of a molecule minus the volume of the molecule itself. One may imagine a “hole” opened up by thermal motions of molecules. The diffusion will occur only if another molecule jumps into the hole before the first molecule goes back to its previous hole.

Fujita [1961] was the first researcher to apply Cohen and Turnbull’s theory to self-diffusion in polymer systems. In Fujita’s study, the thermodynamic diffusion coefficient of the penetrant is defined as follows.

$$D = RTA_d \exp\left(-\frac{B_d}{f}\right) \quad (2.31)$$

where  $A_d$  and  $B_d$  are proportionality factors whose values are dependent on the size and shape of the diffusing molecule and may be independent of temperature and diluent concentration. In this equation,  $B_d$  can be taken to be the ratio between the size of the diffusing species and the size of the polymer chain segments [Huang and Rhim, 1990], and  $f$  is the fractional free volume of the system.

Vrentas and Duda [1977a, 1977b] extended the free volume theory of diffusion to account for the dependence of the solvent self-diffusion coefficient on the concentration and temperature in polymer solutions.

$$D_1 = D_{01} \exp\left(\frac{-\gamma(w_1 \hat{V}_1^* + w_2 \xi \hat{V}_2^*)}{\hat{V}_{FH}}\right) \quad (2.32)$$

$$\hat{V}_{FH} = w_1 K_{11} (K_{21} + T - T_{g1}) + w_2 K_{12} (K_{22} + T - T_{g2}) \quad (2.33)$$

$$D_{01} = D_0 \exp\left(-\frac{E}{RT}\right) \quad (2.34)$$

$$\xi = \frac{M_{j1} \hat{V}_1^*}{M_{j2} \hat{V}_2^*} \quad (2.35)$$

In these equations,  $\hat{V}_1^*$  is the specific critical hole free volume of component 1 required for a jump,  $w_1$  is the mass fraction of component 1,  $T_{g1}$  is the glass transition temperature of component 1, and  $\xi$  is the ratio of the critical molar volume of the solvent jumping unit to that of the polymer jumping unit,  $D_0$  is a constant preexponential factor,  $E$  is the energy per mole that a molecule needs to overcome attractive forces which hold it to its neighbors,  $T$  is the temperature. Also,  $K_{11}$  and  $K_{21}$  are free volume parameters for the solvent,  $K_{12}$  and  $K_{22}$  are free volume parameters for the polymer, and  $\gamma$  is an overlap factor which is introduced because the same free volume is available to more than one molecule. Finally,  $M_{ji}$  is the molar weight of a jumping unit of component  $i$ . Above equations are based on the following assumptions [Vrentas and Vrentas, 1993]:

(1) The partial specific volumes of the solvent and polymer are independent of composition so that there is no volume change on mixing. (2) All thermal expansion coefficients are adequately represented by average values over the temperature interval of

interest. (3) The parameter  $\gamma$  is the same over the complete concentration interval. (4)  $E$  is the same for all solvent concentrations.

If  $w_2 = 1$ , namely infinite dilute of solute which is the case for IGC, equation 2.32 reduces to the next expression which is essentially pure polymer.

$$D_1 = D_{01} \exp\left(\frac{-\gamma \hat{V}_2^* \xi}{K_{12}(K_{22} + T - T_{g2})}\right) \quad (2.36)$$

When the solvent chemical potential in the mixture is given by the Flory-Huggins equation, the mutual diffusion coefficient ( $D$ ) is related to the self-diffusion coefficient of solvent ( $D_1$ ) by the following equation.

$$D = D_1 (1 - \Phi_1)^2 (1 - 2\chi\Phi_1) \quad (2.37)$$

$$\Phi_1 = \frac{w_1 \hat{V}_1^0}{w_1 \hat{V}_1^0 + w_2 \hat{V}_2^0} \quad (2.38)$$

in which  $\Phi_1$  is the volume fraction of the solvent,  $\chi$  is the Flory-Huggins interaction parameter for a given polymer-solvent system, and  $\hat{V}_i^0$  is the partial specific volume of component  $i$ . Further experimental works of Vrentas and Duda's free volume theory may be found in the next papers for the reader's interest [Vrentas et al., 1985, 1986a, 1986b, 1988, 1989, 1990; Ganesh et al., 1992].

2) *Packed column*. For the preparation of a packed column, a polymer solution of known concentration is to be coated on a inert support particles such as glass bead with the uniform distribution of stationary phase on the support, and the supports coated with the polymer solution are dried and packed into the column.

The diffusion coefficient is determined by means of an analysis of the height equivalent to a theoretical plate (HETP) as a unit of column length sufficient to bring the

gas issuing from it into equilibrium with the solute in the immobile phase throughout the unit [Conder and Young, 1979], according to the van Deemter equation.

$$HETP = A + \frac{B}{V} + CV \quad (2.39)$$

where  $V$  is the linear velocity of carrier gas,  $A$  is the eddy diffusion which is null for capillary column and is related to the size of the support particles and the irregularity of packing,  $B$  depends on the longitudinal diffusion in the gas phase and on the tortuosity in the column, and  $C$  accounts for peak broadening, which is resulted from the mass transfer resistance in the stationary phase. The plate height HETP for linear non-ideal chromatography is determined from the width of the peak [Conder and Young, 1979].

$$HETP = L \cdot \left( \frac{\sigma_t}{t_r} \right)^2 = \frac{L}{5.54} \cdot \left( \frac{W_{1/2}}{t_r} \right)^2 \quad (2.40)$$

where  $L$  is the column length,  $\sigma_t^2$  is the peak variance,  $t_r$  is the retention time, and  $W_{1/2}$  is the measured peak width at half of the maximum height. Equation 2.39 is only valid for the symmetric peak that means the mass transfer resistance is very small or even negligible. When the relatively high flow rate is applied, the term  $B/V$  becomes negligible and  $A$  remains small. The term  $C$  is determined from the slope of a plot of HETP and  $V$ , and is related to the diffusion coefficient in the stationary phase by the following.

$$C = q \cdot \frac{K}{(K+1)^2} \cdot \frac{d^2}{D_s} \quad (2.41)$$

$$K = \frac{t_r - t_m}{t_m} \quad (2.42)$$

where  $D_s$  is the diffusion coefficient in the stationary phase,  $K$  is the partition coefficient,  $t_r$  and  $t_m$  are the retention time to the eluted peak maximum of the injected

solvent and the inert probe molecule such as methane and air. The terms of  $q$  and  $d$  must be determined empirically.  $q$  is the shape factor explaining the nonuniformity of the stationary film in the packed column,  $d$  is the film thickness at its deepest point.

Gray and Guillet [1973] did the pioneering work applying gas chromatography to the study of polymers. They used PE and natural rubber coated packed column to determine diffusion coefficient. The C term in the van Deemter equation was defined as follows by replacing  $q$  with  $2/3$  for a uniform film on a solid surface [Giddings, 1965].

$$C = \left(\frac{2}{3}\right) \left(\frac{K}{(1+K)^2}\right) \frac{d^2}{D_x} \quad (2.43)$$

The average thickness of the stationary polymer phase was taken to be

$$d = \left(\frac{W}{\rho}\right) / (3V/\bar{r}) \quad (2.44)$$

where  $W$  is the polymer weight coated onto the support with the density  $\rho$ ,  $\bar{r}$  is the average radius of the bead support, and  $V$  is the occupied volume of the beads in the column. Hawkes [1983] critically reviewed and modernized the van Deemter equation. It was reported that a shape factor  $q$  normally varies from  $2/15$  for the spherical particles to  $2/3$  for a uniform film. Hu et al. [1987] measured infinite dilution diffusion coefficients of volatile liquids in polystyrene and poly (vinyl acetate) at elevated temperature with the aid of the van Deemter equation. They assigned  $1/6$  to the shape factor  $q$  based on the experimental comparison with available data.

It must be pointed out that the main problem of the IGC technique using the packed column lies in the nonuniform distribution of the stationary phase within the column. Therefore, the shape factor,  $q$  can only be determined by the comparison of data gained in

IGC with the existing diffusion coefficients by other techniques. Additionally, modelling of transport in the polymer layer is difficult without many simplifying assumptions.

2) *Capillary column.* Unlike the packed column, a uniform distribution of polymer film can be achieved in the capillary column by coating the column wall with the static coating technique. Such simple film geometry makes the transport modeling of the injected solvent in the polymer layer easier and significantly improves the reliability of the data from IGC. Measurements of the diffusivity using capillary inverse gas chromatography (CCIGC) were carried out first by Pawlish et al. [1987, 1988]. They developed the following transport equations describing the elution process at the exit of the column and being solved in the Laplace domain.

$$\frac{cL}{c_0V} = \exp\left(\frac{1}{2\gamma}\right) \exp\left[-\left(\frac{1}{2\gamma}\right)(1+4\gamma\Psi)^{\frac{1}{2}}\right] \quad (2.45)$$

$$\Psi = S + (2S^{\frac{1}{2}}/\alpha\beta)\tanh(\beta S^{\frac{1}{2}}) \quad (2.46)$$

$$\alpha = \frac{R}{K\tau} \quad \gamma = \frac{D_g}{VL} \quad \beta^2 = \frac{\tau^2V}{D_pL}$$

where  $c$  is the mean gas phase solute concentration,  $c_0$  is the strength of the inlet impulse,  $L$  and  $R$  are the length and radius of the column, respectively,  $V$  is the mean speed of the carrier gas,  $K$  is the partition coefficient,  $\tau$  is the film thickness, and  $D_g$  and  $D_p$  are the gas phase and polymer phase diffusion coefficients. The elution profile of the injected probe molecule can be described and be predicted by the equation 2.45. The experimental data are regressed using equation 2.45 to obtain the diffusion and partition coefficients. CCIGC method has been extensively adopted for the study of solute diffusion in polymers due to it's a number of advantages [Arnold and Laurence, 1989,

1992; Vrentas et al., 1993; Baltus et al., 1993; Xie, 1993; Tihminlioglu et al., 1997; Surana et al., 1997].

### 2.6.3 Other methods

Many direct, accurate methods for measuring the solubility and diffusivity of the solvents through the polymeric thin films were explored and were shown to be efficient for practical applications. Among them, pulsed-field gradient (PFG)-NMR spectroscopy has been used to directly measure molecular or ionic self-diffusion coefficients in membranes [Volkov et al., 1995a, 1995b, 1998; Muzzalupo et al., 1999]. The main advantages of PFG-NMR method are as follows; it is possible to investigate the self-diffusion processes in the spatial scale from 0.1 to  $10^3 \mu\text{m}$ , which is crucial for the restricted diffusion; and also possible to separate the partial self-diffusion coefficients and solubilities in the case of complicated self-diffusion processes.

For molecules of diffusate undergoing unhindered isotropic Brownian motion, the evolution of spin echo amplitude is described by the following equation

$$A(2\tau, \tau_1, g) = A(2\tau, \tau_1, 0) \cdot \exp(-\gamma^2 g^2 \delta^2 t_d D_s) \quad (2.47)$$

where  $\gamma$  is gyromagnetic ratio,  $t_d$  is the diffusion time, and  $D_s$  is the self diffusion coefficient,  $\tau$  is the time interval between the first and second radio frequency (RF) pulses,  $\tau_1$  is the time interval between the second and the third ones,  $g$  is the amplitude of the gradient pulse. In experiment,  $\tau$  and  $\tau_1$  are fixed and  $A$  is analyzed as a function of  $g$  to obtain the diffusion coefficient.

Self-diffusion coefficient measured by means of NMR was described [Bitter, 1991] in Table 2.4.

## CHAPTER 3

# CHARACTERISTICS OF SODIUM ALGINATE MEMBRANES FOR THE PERVAPORATION DEHYDRATION OF ETHANOL-WATER AND ISOPROPANOL-WATER MIXTURES\*

---

### 3.1 SUMMARY

Alginate membranes for the pervaporation dehydration of ethanol-water and isopropanol-water mixtures were prepared and tested. The sodium alginate membrane was water soluble and mechanically weak but it showed promising performance for the pervaporation dehydration. To control the water solubility the sodium alginate membrane was crosslinked ionically using various divalent and trivalent ions. Among them the alginate membrane crosslinked with  $\text{Ca}^{2+}$  ion showed the highest pervaporation performance in terms of the flux and separation factors.

### 3.2 INTRODUCTION

Presently, the dehydration of organic mixtures is the most important application for pervaporation. Research efforts have been directed to the selection of proper membrane materials. A good pervaporation membrane material should have high permeation flux

---

\* Part of this chapter has been published in Journal of Membrane Science, 160(1999), 101-113

and separation factor for the pervaporation dehydration of alcohol. However, the simultaneous enhancement of both parameters has been a big challenge due to the trade-off phenomenon between flux and separation factor that is frequently encountered in pervaporation experiments. It has long been recognized that hydrophilic polymers are good dehydration membrane materials due to their strong affinity to water molecules. Major drawbacks of hydrophilic materials are its excessive swelling behavior resulting from the hydrogen bonding between the hydrophilic functional groups of the polymer and the water molecule, and water-soluble properties. Three-dimensional crosslinking of the membrane chain network is a generally accepted strategy to suppress the swelling and insolubilize the water-soluble membrane in water. Among the hydrophilic polysaccharide type polymers, alginate membrane has gained special interest because it showed the highest flux and separation factor among the hydrophilic materials tested for the pervaporation dehydration. Alginic acid has the same backbone and functional groups as carboxymethylcellulose [Muzzarelli, 1973], but has not been extensively studied for pervaporation applications. Alginic acid is a heteropolymer containing mannuronic acid and guluronic acid groups and is commonly found in the seaweeds. Its chemical formula is shown in Figure 3.1.

Uragami and Saito [1989] have carried out early studies of alginic acid membranes for the pervaporation dehydration. They converted sodium alginate to free alginic acid by immersing the membrane into HCl solution. Mochizuki et al. [1990] were also one of early researchers for alginic acid pervaporation membrane. They investigated the influences of counterions ( $\text{Li}^+$ ,  $\text{Na}^+$ ,  $\text{K}^+$ ,  $\text{Rb}^+$ , and  $\text{Cs}^+$ ) on the permeation rate. It was revealed that the alginate membrane neutralized by  $\text{Cs}^+$  ion had the highest flux. The

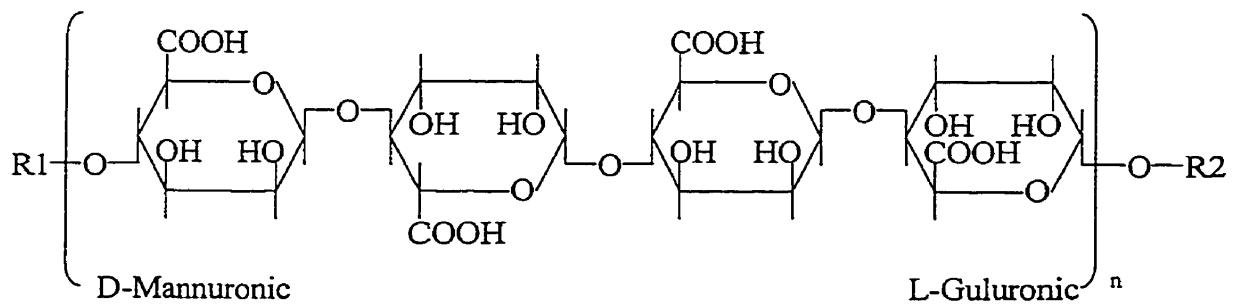


**Figure 3.1** The chemical structure of alginic acid

effect of the counter ion on the permeation flux was explained by the mobility of the alginate molecules, the water mobility of ion hydration cell and the crystallinity of the polymer. Recently, sodium alginate membranes have been studied by several research groups [Yeom et al., 1996b, 1998a, 1998b; Shi et al., 1996] because of their excellent pervaporation performance in spite of recognized drawbacks such as their water-soluble property and mechanical weakness. Sodium alginate membranes have also shown some interesting phenomena during the pervaporation. They showed a serious flux decline with operating time due to the occurrence of a significant relaxation process [Yeom et al., 1996b]. In general, the relaxation behavior of polymers is recognized in glassy polymers having rigid and bulky structure near the  $T_g$ . In case of sodium alginate membranes, its pervaporation performance was very sensitive to the preparation history, thus in this study careful and consistent preparation procedures have been maintained. An effort to overcome its mechanical weakness has been investigated by preparing a blend ion exchange membrane with cellulose cuoxam [Zhang et al., 1997]. Since sodium alginate is a water-soluble substance, insolubilization by crosslinking with glutaraldehyde [Yeom et al., 1998a] was also carried out. In principle, alginates form gels (or precipitate at low polymer concentrations) in the presence of divalent and trivalent ions such as  $Ca^{2+}$  and  $Al^{3+}$  [Yalpani, 1988]. This observation can be depicted through the chelate formation involving the carboxyl groups as shown in Figure 3.2. In this study the sodium alginate membranes were crosslinked and insolubilized by the solution technique using multivalent ion and dilute acid solutions. The pervaporation characteristics as well as the temperature dependence of sodium alginate membranes were explored for the pervaporation dehydration of ethanol-water and isopropanol-water mixtures.

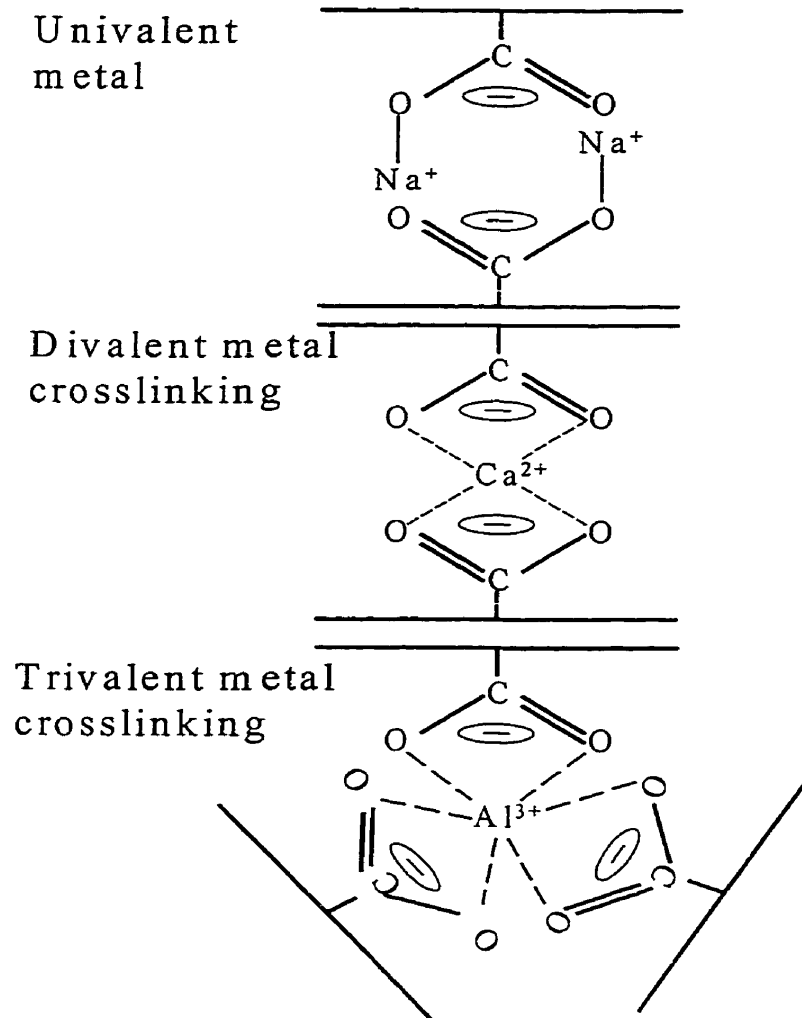


**Figure 3.2 Alginate gel network formation by multivalent ions**

### 3.3 EXPERIMENTAL

#### 3.3.1 Materials

Sodium alginate and cobalt (II) nitrate ( $\text{Co}(\text{NO}_3)_2 \cdot 6\text{H}_2\text{O}$ ) were purchased from Sigma Chemical Co., USA. The solution viscosity of a 2% sodium alginate was approximately 14,000 cps at 25 °C. Ethanol purchased from Commercial Alcohols Ltd, Toronto, ON and isopropanol from BDH Inc. were used as received.  $\text{H}_2\text{SO}_4$  (98%) and HCl (37%) were obtained from BDH Inc. Water was deionized and distilled before use. Calcium chloride was provided by Fisher Scientific, and all chemicals including zinc chloride, aluminium nitrate, manganous chloride, tetrahydrate ( $\text{MnCl}_2 \cdot 4\text{H}_2\text{O}$ ), and ferrous sulphate, heptahydrate ( $\text{FeSO}_4 \cdot 7\text{H}_2\text{O}$ ) were supplied from BDH Inc, Toronto, Canada.

#### 3.3.2 Membrane preparation

Sodium alginate was dissolved in deionized water to form a homogeneous solution of 1 wt% polymer. Sodium alginate solution was filtered to remove any undissolved solids and impurities. The membrane was prepared by casting the polymer solution onto a clean glass plate using a casting knife designed in this laboratory. The casting membrane was dried at room temperature for 24 hours in a dust free, environmentally controlled chamber. The dried membrane was peeled off from the plate, and then used for the pervaporation experiment or further treated for the crosslinking and insolubilization.

### 3.3.3 Crosslinking solution

Ionic crosslinking of sodium alginate membranes were performed by submerging the membranes into 0.1M solutions of various metal ions for 10 min, in succession, they were rinsed with water, then dried at room temperature for use. Alginate membrane was converted to free alginic acid membrane by immersion in 0.1M H<sub>2</sub>SO<sub>4</sub> solution consisting of isopropanol/water of 50/50 vol %.

### 3.3.4 Pervaporation

Pervaporation experiments were carried out for ethanol-water and isopropanol-water mixtures. The concentration of alcohol was varied from 70 to 95 wt%. A schematic diagram of the pervaporation apparatus is shown in Figure 3.3. The feed solution temperature in the tank was controlled to the desired value, and the feed solution was circulated using the feed pump. The membrane was placed on the porous stainless steel support and sealed. The effective area of the membrane in contact with the feed stream was 14.2 cm<sup>2</sup>. Pervaporation was initiated by switching on the circulation and vacuum pumps, the pressure at permeate side was maintained around 3 mbar. Permeate was collected in glass tubes which were immersed in liquid nitrogen. The pervaporation apparatus was run for at least 2 hours to reach the steady state before starting to measure permeate. When sufficient permeate (more than 0.3g) was collected in the cold trap, the vacuum valve was switched to the parallel trap to collect the other sample.

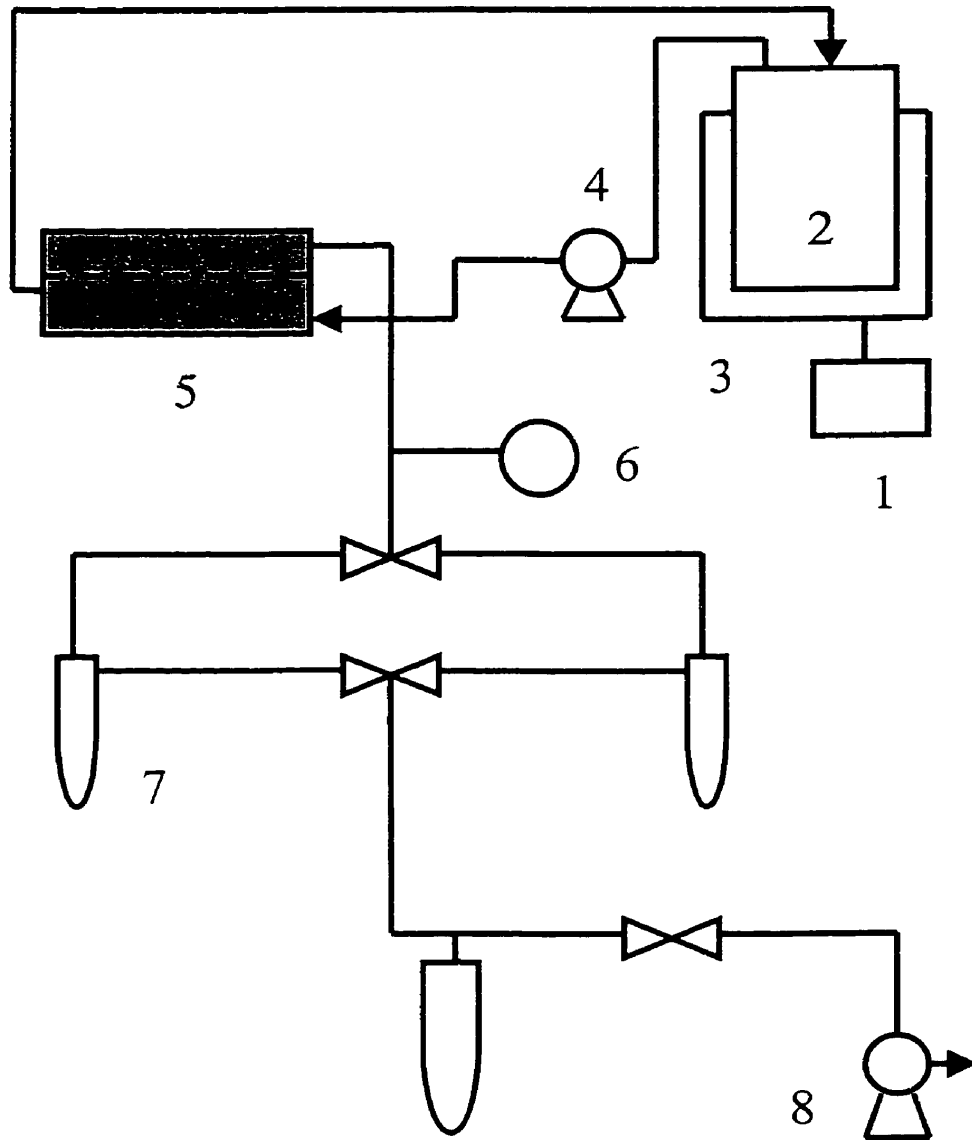


**Figure 3.3** A schematic diagram of the pervaporation apparatus; (1) temperature controller (2) feed tank (3) heating mantle (4) circulation pump (5) membrane cell (6) pressure gauge (7) cold trap (8) vacuum pump

The cold trap containing the permeate was warmed up to ambient temperature, then removed, and weighed to determine the flux and the contents were analyzed for the permeate composition. Separation factor was calculated by the following equation;

$$\alpha_{Water/Alcohol} = [Y_W / Y_A] / [X_W / X_A] \quad (1)$$

where X and Y are the weight fractions of the feed and permeate, respectively.

Analysis of the permeate composition was carried out by using a HP 5890 Gas Chromatography with a FID detector and Abbe Refractometer type 3T at 26.7 °C. The column used in GC analysis was 6' × 0.125" packed with Porapak T.

### 3.4 RESULTS AND DISCUSSION

#### 3.4.1 Fourier transform-infrared (FT-IR) measurement

Figure 3.4 shows IR spectra of sodium and cobalt crosslinked alginate membranes including alginic acid membranes converted by a dilute H<sub>2</sub>SO<sub>4</sub> and HCl solution. It was revealed that there was no crosslinking reaction between acids and sodium alginate membrane. The nature of conversion reaction of sulfuric acid was very similar to that of HCl from the IR spectra. The strong band at 1743 cm<sup>-1</sup> could be indicative of the free carboxyl group of alginic acid, whereas the bands at 1620 cm<sup>-1</sup> and 1416 cm<sup>-1</sup> were assigned to the presence of the salified carboxyl group. In detail, 1620 and 1416 cm<sup>-1</sup> bands are assigned to the antisymmetric and symmetric COO<sup>-</sup> stretching vibration of the salified carboxyl

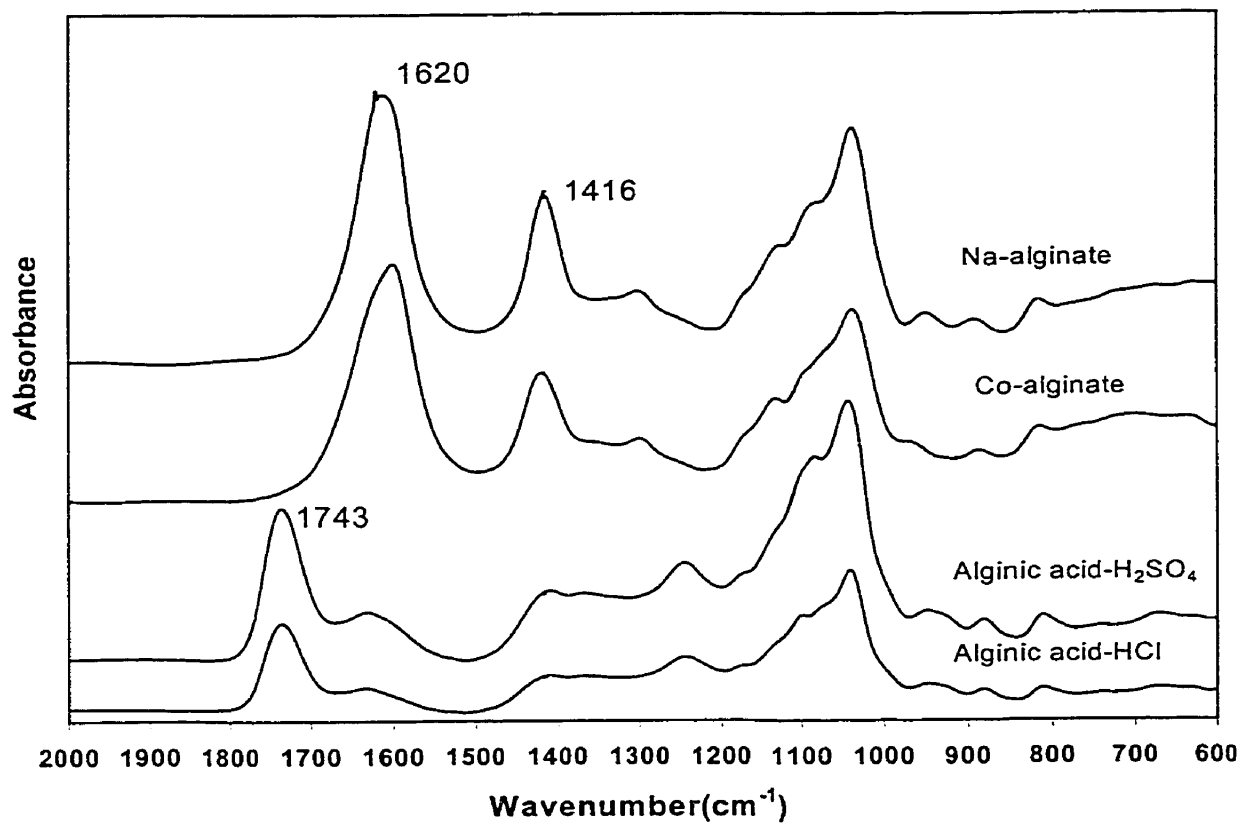


**Figure 3.4 FT-IR spectra of alginic acid and alginate membranes**

group, respectively. No direct evidence is available at present to assign the absorbance peak at  $1250\text{ cm}^{-1}$  of alginic acid membrane. Other studies [Yeom et al., 1998a; Tomihata & Ikada, 1997] on alginate membrane crosslinked with glutaraldehyde in the presence of HCl catalyst assigned the peak at  $1250\text{ cm}^{-1}$  to the formation of an acetal ring and ether linkage as a result of the reaction between the hydroxyl group of alginate and the aldehydes of glutaraldehyde. However, in this study, the conversion to alginic acid form was carried out in the  $\text{H}_2\text{SO}_4$  or HCl solution containing 50 vol% isopropanol.

### 3.4.2 Characteristics of sodium alginate membranes

As pointed out in introduction section, the pervaporation performance of sodium alginate membrane was not constant with the operating time of several days presumably due to the relaxation property. To investigate the pervaporation performance according to the change of operating time and temperature, alginate membrane was installed and operated from the range of  $40\text{ }^\circ\text{C}$  to  $70\text{ }^\circ\text{C}$  each day for 7 days. After exploring the temperature effect, the feed mixture was cooled down to the room temperature before the new trial. It is clear that alginate membrane is substantially affected by the operating condition as shown in Figure 3.5. After 6-day operation, the original flux trend was recovered and then it was dropped down in 9-day operation. This phenomenon can be explained by the relaxation behavior which the matrix of membrane repeats the relaxation and the close packing. When the matrix relax, polar channel which contributes to the continuous flow of water molecules is formed, and the close packing means that the matrix does not make

the open channel probably because of the strong internal or intra hydrogen bonding of -COONa groups.

The reliability of the pervaporation data sampling for alginate and alginic acid membranes was tested in terms of the pervaporation performance with time in Figure 3.6 and Figure 3.7. The pervaporation data acquired in this experiment was proven to be reliable at the given conditions for alginate and alginic acid membranes, respectively.

### 3.4.3 Ionic crosslinking of sodium alginate membranes

As mentioned earlier, multivalent ions can be used to crosslink alginate ionically. The crosslinking effect of various multivalent ions on the flux and separation factor is shown in Figure 3.10 for 90 wt% aqueous ethanol and 90 wt% aqueous isopropanol mixtures at 50 °C operating temperature. Six different metal ions including five divalent ions and one trivalent ion were tested to crosslink the alginate membranes. From Figure 3.10, it is clear that the ionic nature of counter cations in alginate ion exchange membrane affects the separation characteristic substantially. The highest separation performance is achieved by the  $\text{Ca}^{2+}$  crosslinking for both ethanol and isopropanol mixtures. Thus,  $\text{Ca}^{2+}$  crosslinked membranes were further evaluated in terms of the feed concentration and the temperature. It is interesting to note that converting alginate to free alginic acid membrane in isopropanol/water (50/50 vol%) solution in the presence of sulfuric acid lowered the membrane performance although the membrane was insolubilized in water and the mechanical stability was enhanced.

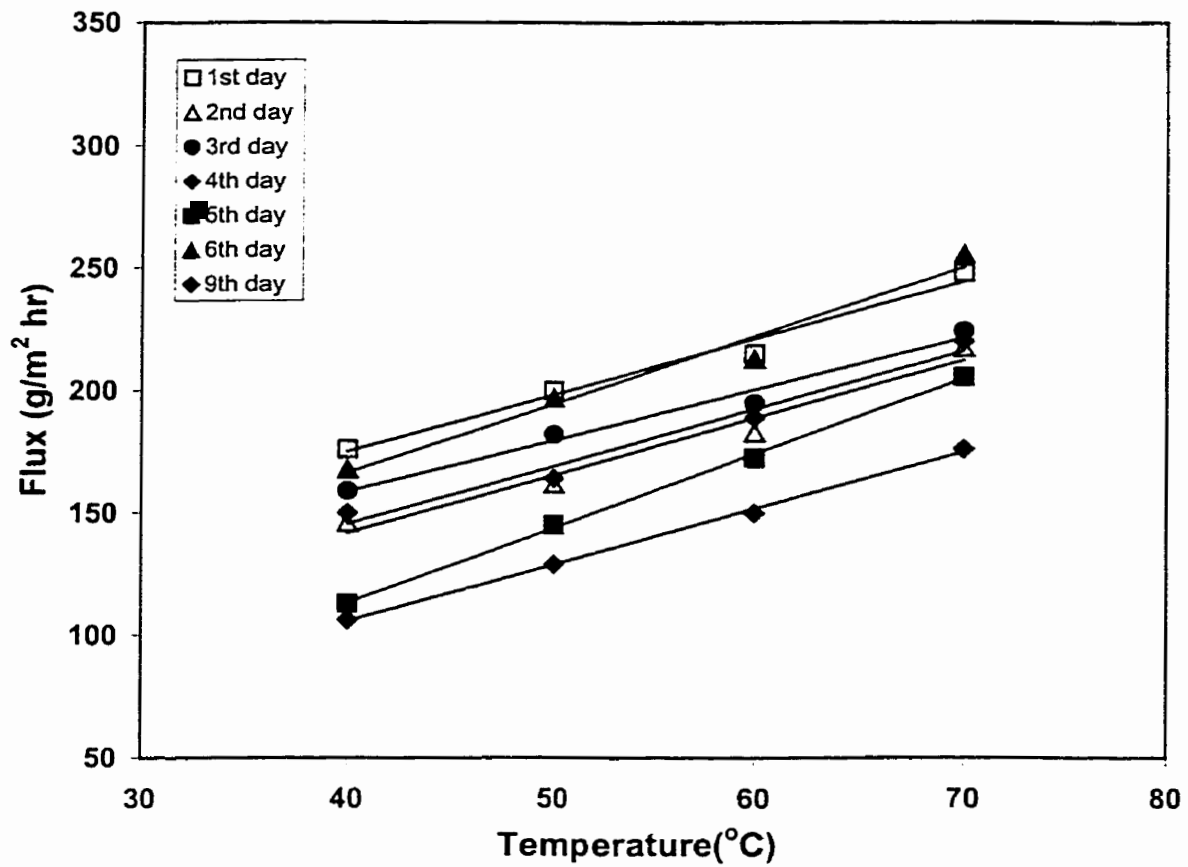


**Figure 3.5 Temperature dependence test of sodium alginate membrane for 90% EtOH feed mixture for 9 days**

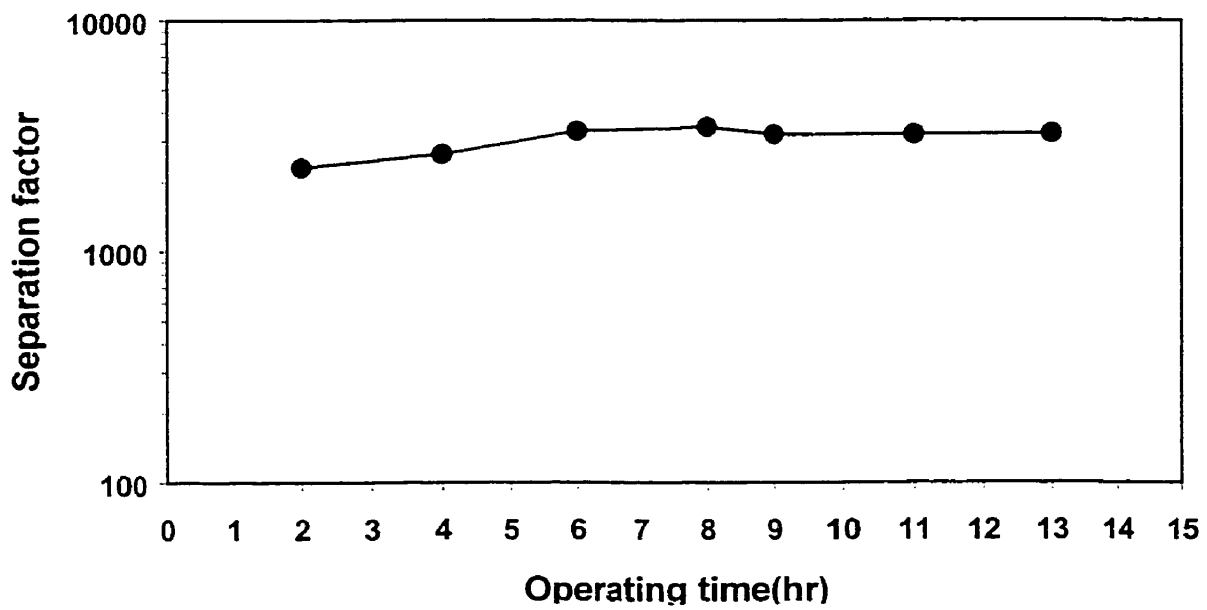
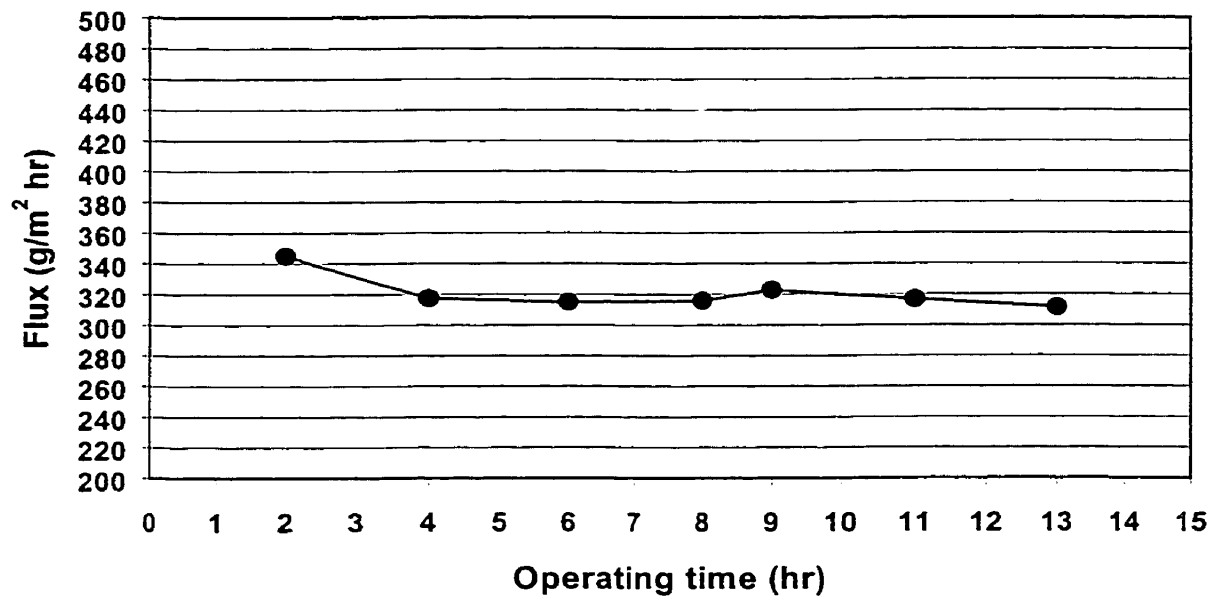


Figure 3.6 Consistency experiment of sodium alginate membrane for 90% PrOH feed mixture at 60 °C

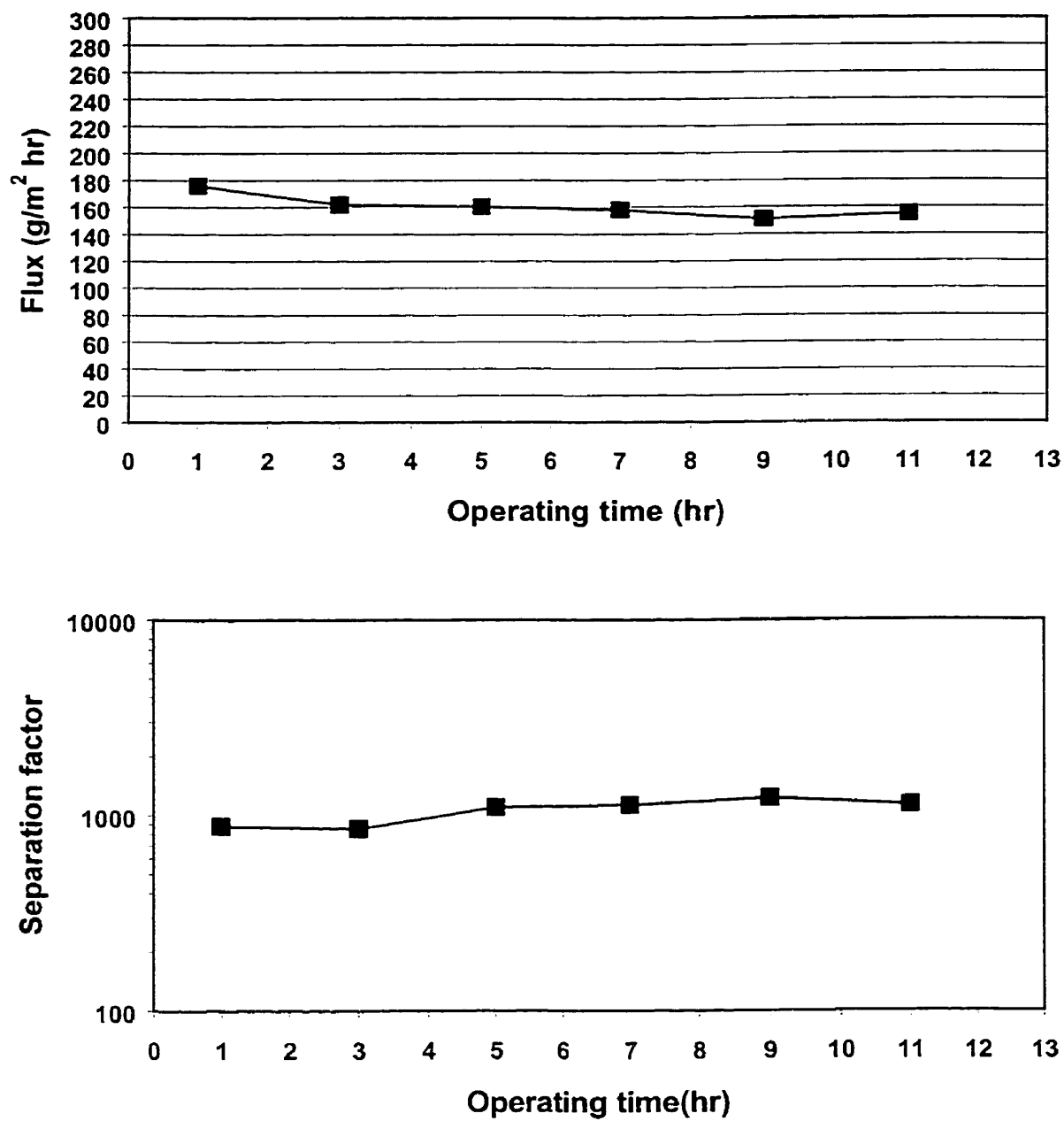


Figure 3.7 Consistency experiment of alginic acid membrane for 90% PrOH feed mixture at 60 °C

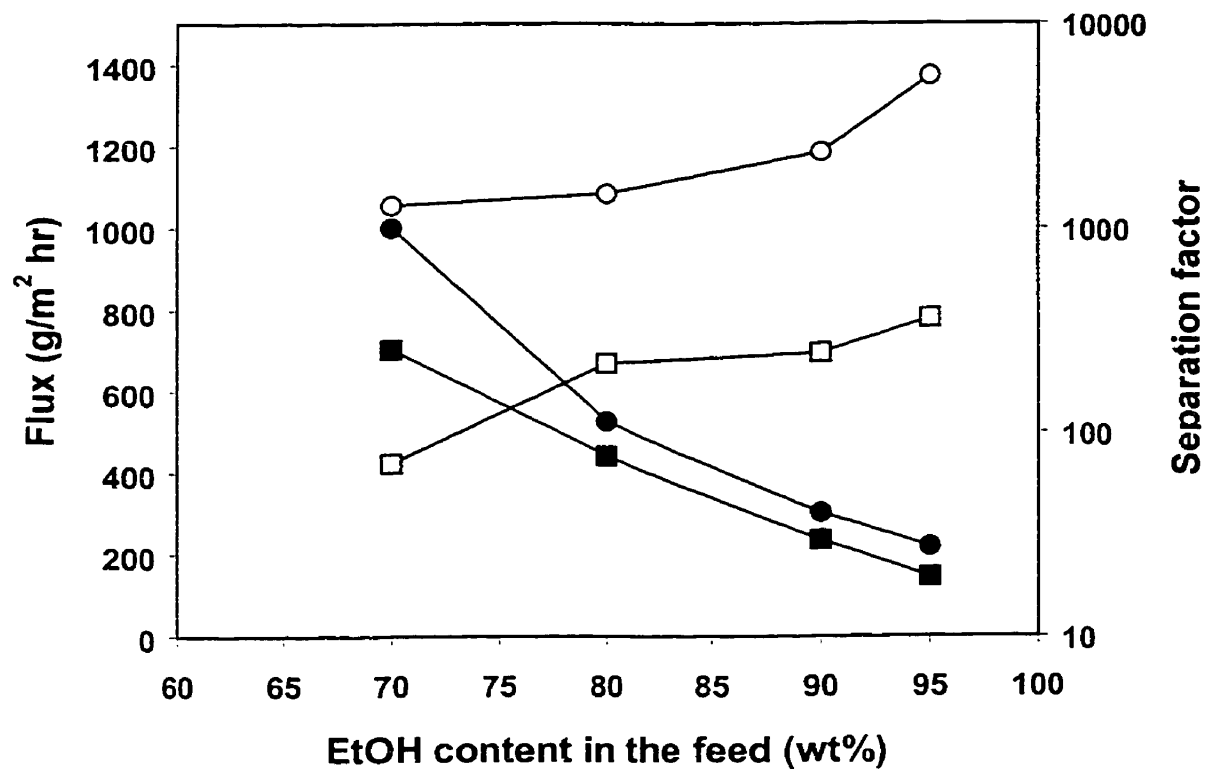
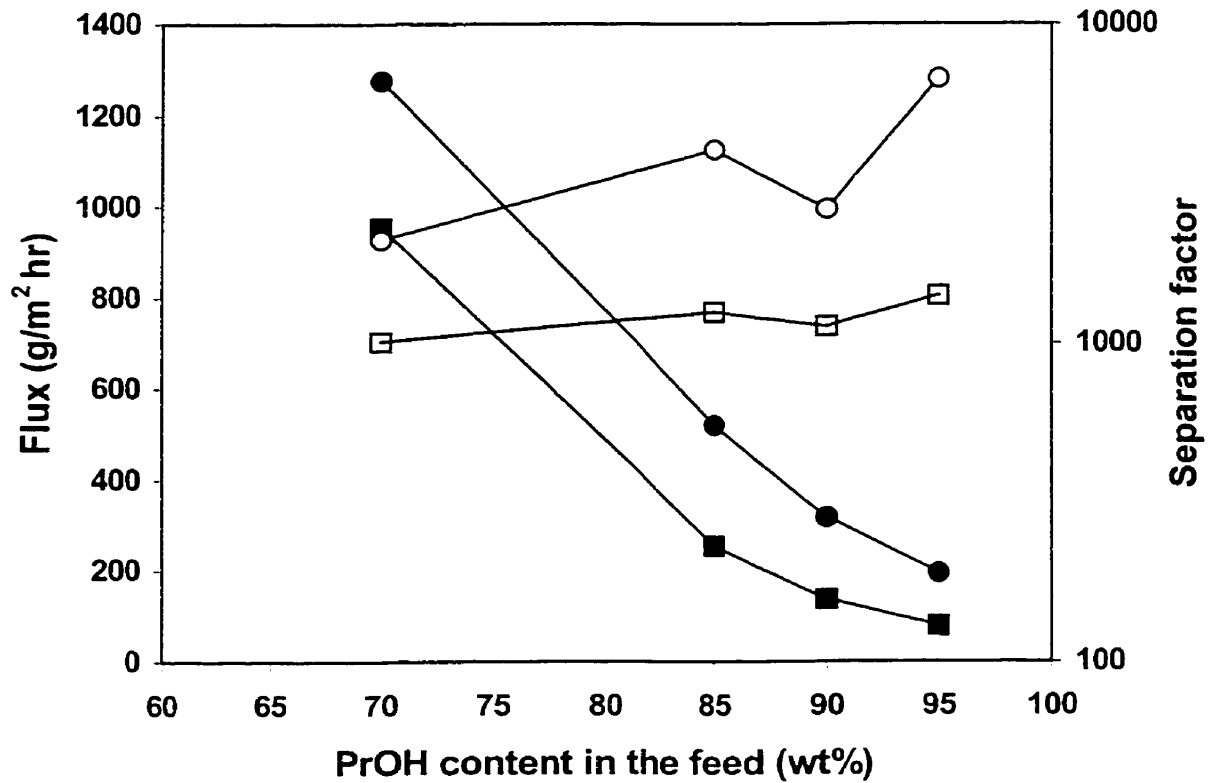


Figure 3.8 Comparison of pervaporation performance of sodium alginate (●: flux; ○: separation factor) and alginic acid (■: flux; □: separation factor) membranes for EtOH feed mixtures at 60 °C



**Figure 3.9** Comparison of pervaporation performance of sodium alginate (●: flux; ○: separation factor) and alginic acid (■: flux; □: separation factor) membranes for PrOH feed mixtures at 60 °C

To support this observation, an additional experiment was carried out. Figure 3.8 and 3.9 for ethanol and isopropanol feed mixtures, respectively show the pervaporation performance of sodium alginate membrane and alginic acid membrane converted in sulfuric acid solution. In these experiments it is apparent that sodium alginate membrane has superior water selectivity and flux to alginic acid membrane. Since sodium alginate is water soluble, one can imagine that sodium alginate membrane is more hydrophilic and has looser structure due to sodium ion than alginic acid membrane. This result can also be supported by the work of Hirai and Odani [1994] showing that water sorption amount of alginic acid film was lower than those of sodium and cobalt complex alginate. It was shown that the pervaporation separation performance for isopropanol mixture was much higher than that for the ethanol mixture. This can be attributed to the coupling phenomena between water and ethanol molecules, which is explained by the lower water content in the permeate in Figure 3.11b comparing to that of isopropanol mixture in Figure 3.12b. It is believed that higher permeation rate of isopropanol mixture results from the stronger plasticization action of water which is more strongly absorbed in the membrane compared to the coupled water from ethanol mixture to the membrane (see Figures 3.11a and 3.12a).

#### **3.4.4 Pervaporation of alcohol/water mixtures through sodium alginate membrane**

Figures 3.11a and 3.12a show the total permeation flux and separation factor as a function of feed concentration for sodium alginate membrane. Since sodium alginate has

hydrophilic functional groups, the high total flux and separation factor can be attributed to the strong affinity between sodium alginate membrane and water molecules.

The permeation flux increases constantly with the increase of water content in the feed. When the water content in the feed is increased, the selective interaction between water molecules and the hydrophilic alginate membrane was increased. This leads to the increased total permeation flux through easier diffusion of water molecules. For ethanol/water mixture, the highest separation factor for this sodium alginate membrane was observed at 90 wt% ethanol, while for isopropanol/water mixture it was at 85 wt% aqueous isopropanol mixture in the concentration ranges explored.

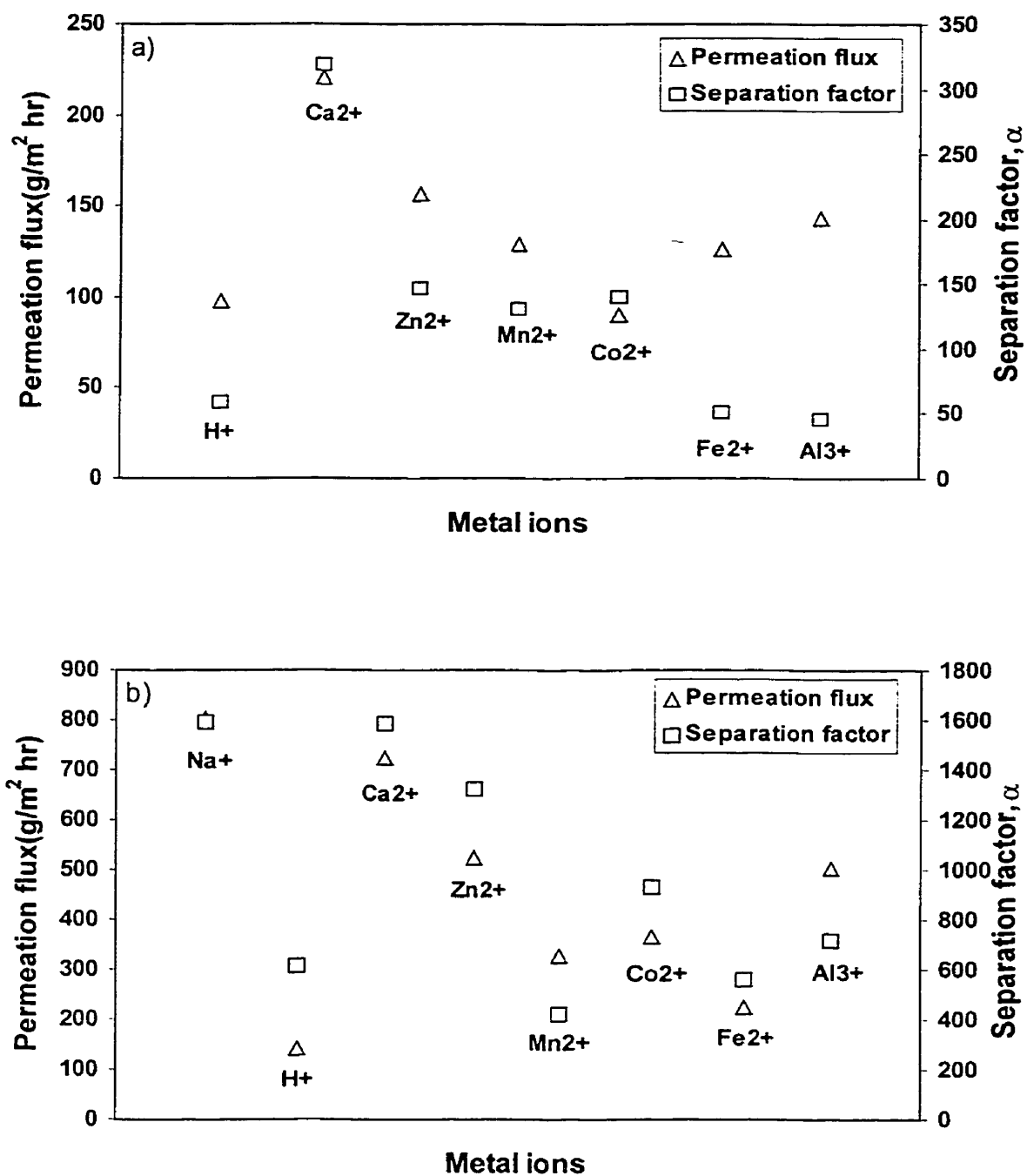


Figure 3.10 Pervaporation ionic crosslinking of sodium alginate membranes a) 90 wt% ethanol mixture, b) 90 wt% isopropanol mixture

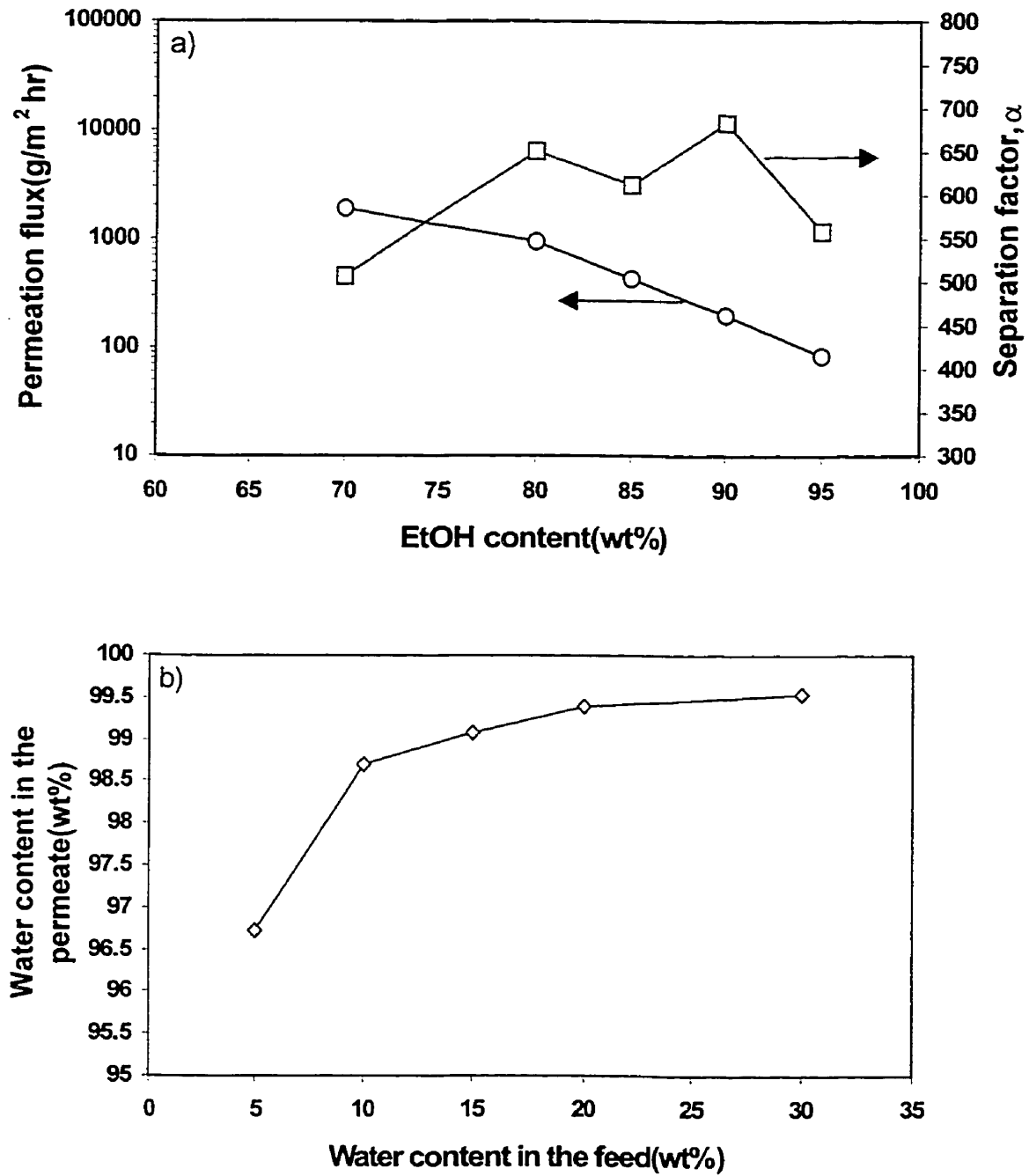


Figure 3.11 a) Effect of ethanol feed concentration on the flux and separation factor at 50 °C for sodium alginate membrane, b) Water concentration in the permeate vs. water concentration in the feed

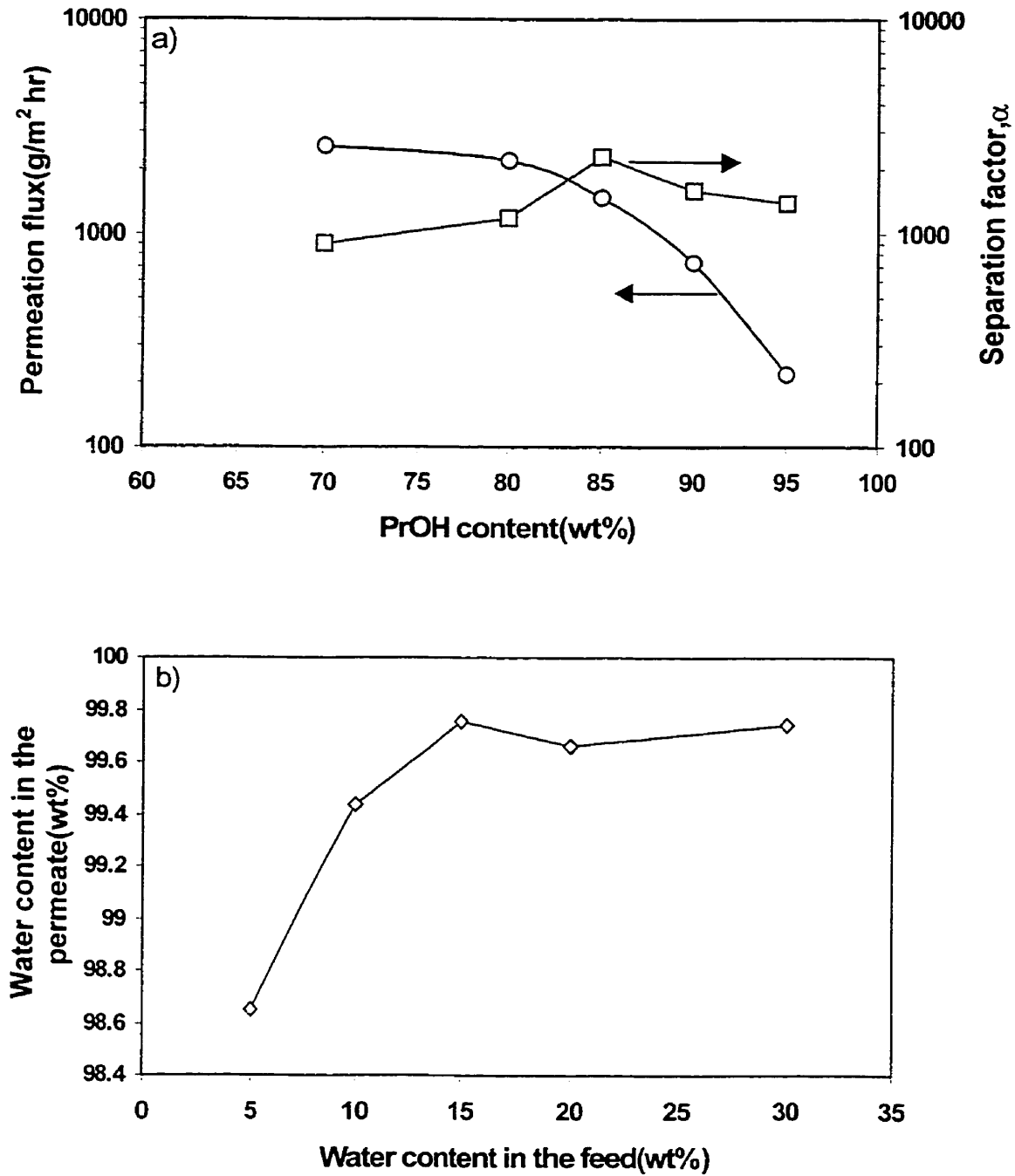


Figure 3.12 a) Effect of isopropanol feed concentration on the flux and separation factor at 50 °C for sodium alginate membrane, b) Water concentration in the permeate vs. water concentration in the feed

Figures 3.11b and 3.12b show water concentration in the permeate against water concentration in the feed mixture. It can be observed that the high separation factor for alcohol mixtures results from the high selective permeation of water through the sodium alginate membrane. Water concentration in the permeate remains over 99 wt% for 15 to 30 wt% water content in the feed. Another trend observed in these plots is that the water content in the permeate increases with increasing water concentration in the feed. This phenomenon cannot be explained by the swelling action resulting from the plasticization of water since the swelling of the membrane increases the alcohol concentration in the permeate as well as the water permeation flux. Thus, it is assumed that the transport phenomenon through sodium alginate membrane is mainly governed by strong interactions between water molecules and  $-\text{COONa}$  and  $-\text{OH}$  functional groups of alginate membrane acting as fixed carriers.

#### **3.4.5 Pervaporation of ionically crosslinked alginate membranes**

Generally, hydrophilic membranes having high water-permselectivity such as chitosan and polyvinyl alcohol (PVA) suffer from the low separation efficiency in spite of the high total permeation flux because of excessive swelling action of water. Crosslinking is widely used to achieve high separation factor with reasonable permeation flux. The GFT composite membrane which is the first commercialized pervaporation

membrane also consists of a crosslinked PVA top layer and polyacrylonitrile (PAN) support layer.

Sodium alginate membranes showed high permeation flux and reasonably high separation factor with increasing water content in the feed mixture. In this aspect, the crosslinking of sodium alginate membranes should be focussed not only on the further increase of separation factor but on the improvement of its insolubility in water and the enhancement of its mechanical strength. Figures 3.13 and 3.14 show the permeation flux, separation factor and water content in the permeate versus the feed concentration range from 70 wt% to 95 wt% for aqueous ethanol and isopropanol mixtures, respectively. It is generally accepted that the crosslinking of the polymeric membrane reduces the solubility and the diffusivity and thus results in significant reduction of chain mobility and free volume to accommodate the permeate during the diffusion process.

For aqueous ethanol mixtures, the total permeation flux constantly increased with increasing the water content in the feed like that of sodium alginate membrane. The permeation fluxes and separation factor of calcium crosslinked membrane were lower than those of the sodium alginate membrane except for the 95 wt% ethanol feed where the permeation flux of calcium crosslinked membrane was slightly higher. For isopropanol-water mixtures, the same trend as with ethanol/water mixtures was observed. The total permeation fluxes of sodium alginate membranes were higher than those of  $\text{Ca}^{2+}$  crosslinked alginate membranes because of the reduced chain mobility of crosslinked membrane except at 95 wt% aqueous isopropanol mixture. In principle, it can be expected that the separation factor would increase with resulting decreased flux after the crosslinking. The nature of crosslinking depends on the polymeric membrane and

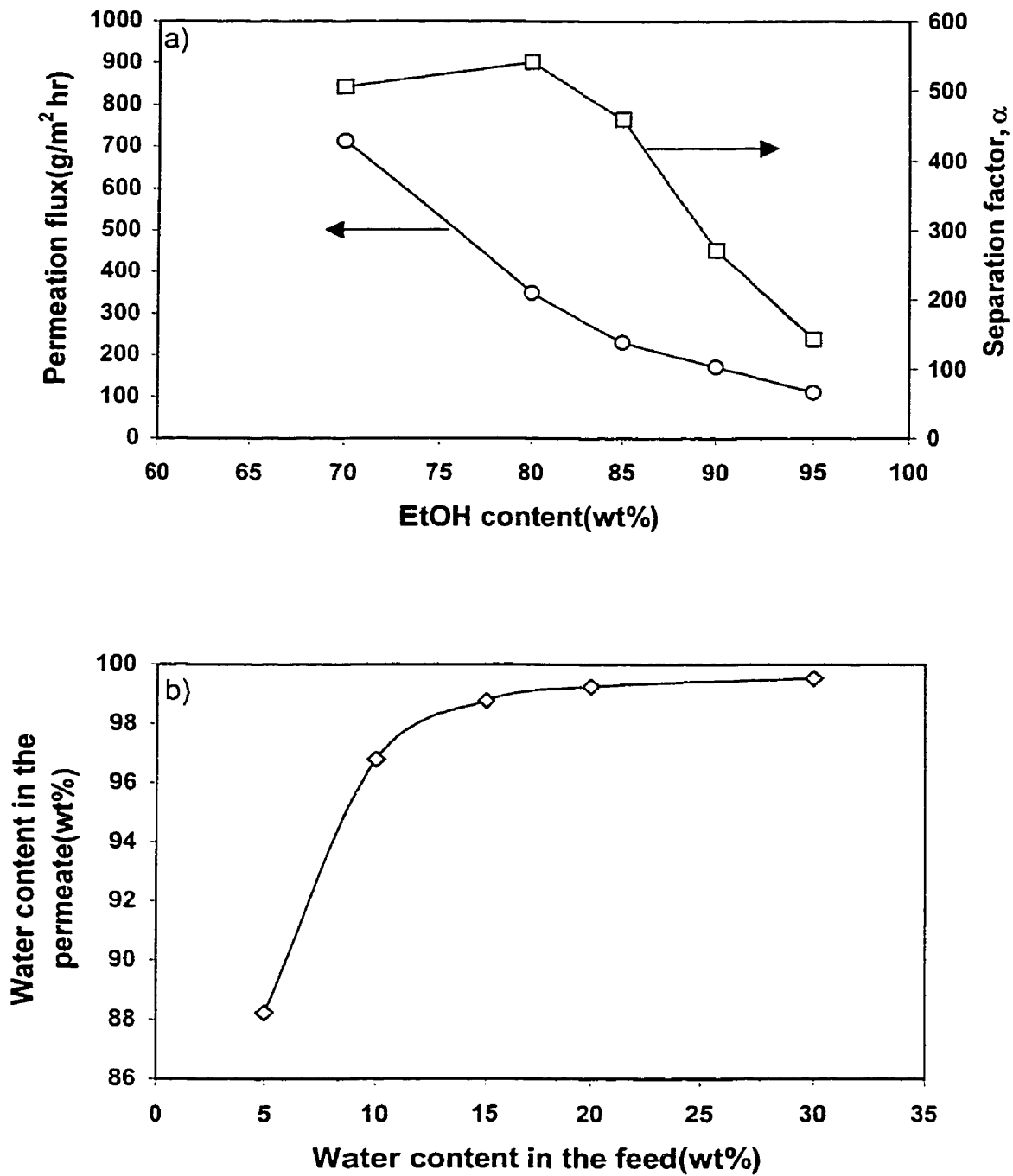


Figure 3.13 a) Effect of ethanol feed concentration on the flux and separation factor at 50 °C for crosslinked alginate membrane, b) Water concentration in the permeate vs. water concentration in the feed

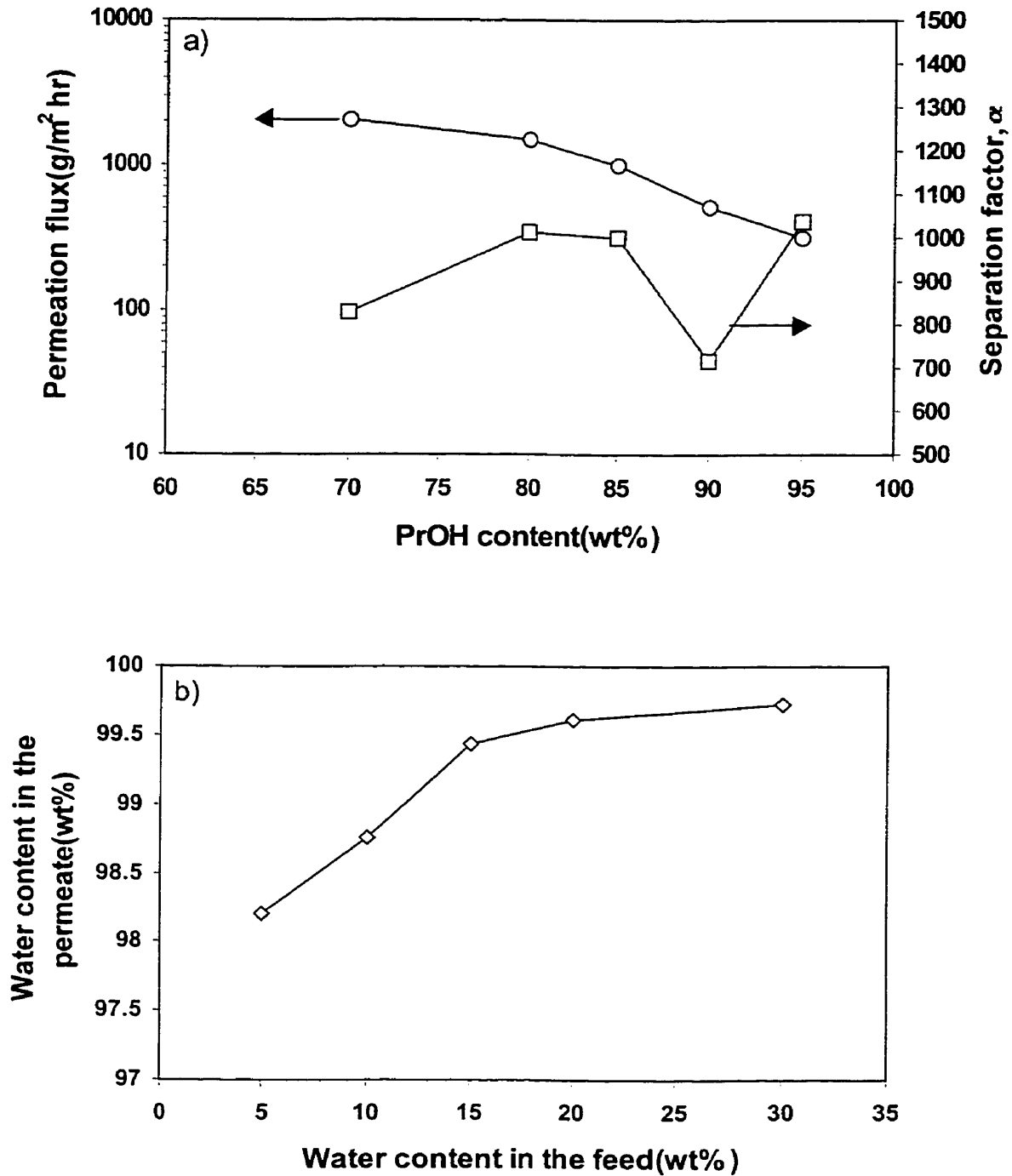


Figure 3.14 a) Effect of isopropanol feed concentration on the flux and separation factor at 50 °C for crosslinked alginate membrane, b) Water concentration in the permeate vs. water concentration in the feed

crosslinker used, Na<sup>+</sup> monovalent counterion membrane seems to have higher affinity and less steric hindrance to water than Ca<sup>2+</sup> divalent counterion crosslinked membrane for both alcohol mixtures. These large hydrophilicities and less hindrance of monovalent counterion membranes explain the higher separation efficiencies of sodium alginate membranes compared to those of calcium alginate membranes (see Figures 3.11b and 3.13b for ethanol mixture, Figures 3.12b and 3.14b for isopropanol mixture, respectively).

### 3.4.6 Temperature effects

Experimental data of temperature dependence of total permeation flux generally exhibits an Arrhenius relationship.

$$J = J_0 \exp(-E_p/RT) \quad (2)$$

where  $J_0$  and  $E_p$  are the pre-exponential factor and the apparent activation energy of permeation, respectively. Based on the solution-diffusion model, the activation energy of permeation can be expressed as follows.

$$E_p = E_D + \Delta H \quad (3)$$

where  $E_D$  and  $\Delta H$  are the activation energy of diffusion and the enthalpy of sorption of the permeant in the membrane, respectively. The total permeation flux of 90 wt% aqueous ethanol mixture is plotted against the reciprocal of the operating temperature in degree of Kelvin in Figure 3.15. The temperature range tested in this study was from 40 to 70 °C. The general tendency that the higher temperature, the higher permeation flux is still acceptable, while the separation factor is increasing with the temperature. The

activation energies of sodium alginate and calcium crosslinked alginate were calculated as 1.7 kJ/mol and 0.9 kJ/mol for 90 wt% aqueous ethanol mixture from the slope of Figure 3.15a. As observed in Figures 3.12a and 3.14a, the exceptionally higher flux of 95 wt% isopropanol mixture through calcium crosslinked membrane than that of sodium alginate membrane still holds for the tested temperature range (see Figure 3.16a), and the activation energy of the total permeation flux increases with increasing the water content in the feed mixture from 2.1 kJ/mol at 5 wt% water to 11.7 kJ/mol at 15 wt% water. Generally, the activation energy increases with the crosslinking density and with decreasing water content in the feed. However, the opposite observations were found in this study. This can be explained by the characteristic relaxation behavior of alginate membrane. This relaxation is much reduced after the calcium crosslinking, so the activation energy of calcium crosslinked membrane is lower than that of sodium alginate. In the cases of the activation energies for the feed mixtures having different water contents, the observation was rationalized as follows. When the feed mixture has higher water content, the membrane absorbs more water and the absorbed water acts as a plasticizer in the membrane. This plasticization action is much faster and larger for the membrane having higher water content in the feed. The facilitated relaxation behavior of this membrane causes the higher activation energy. Similar observation has been made by Yeom and Lee [1998a].

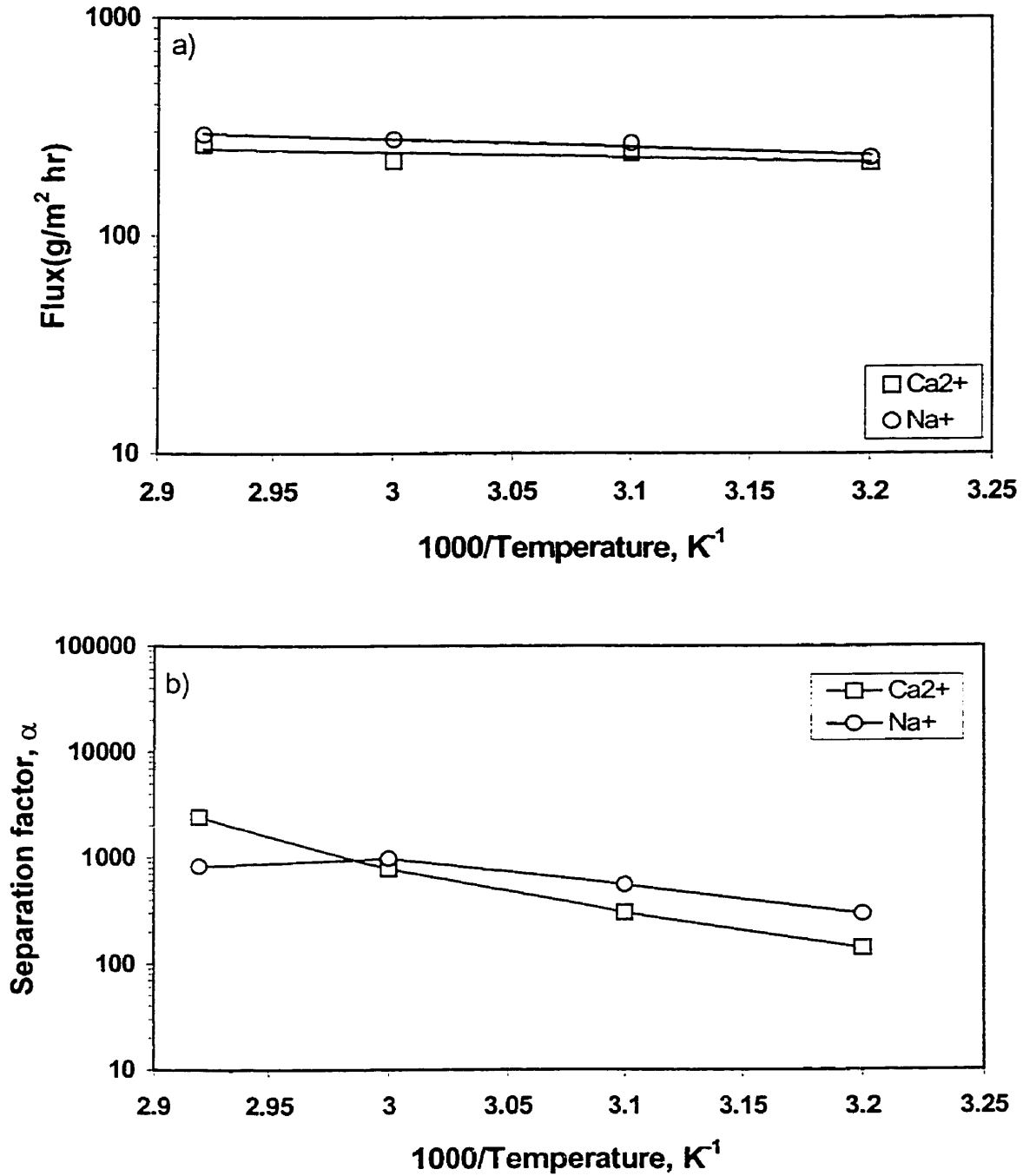


Figure 3.15 a) Arrhenius plot of total permeation flux of 90% aqueous ethanol mixture, b) Dependence of separation factor on the temperature through sodium alginate and Ca<sup>2+</sup> crosslinked alginate membrane

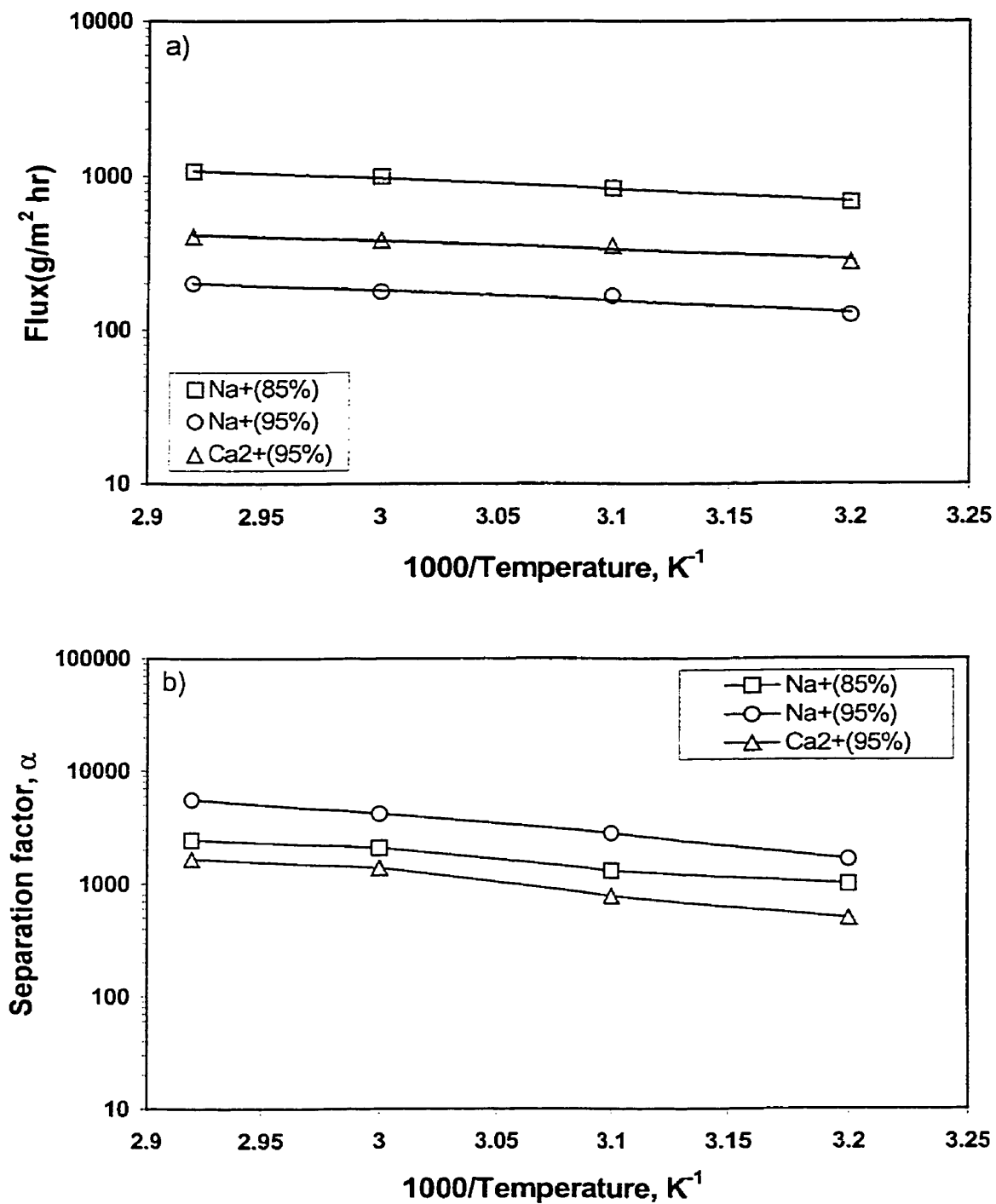


Figure 3.16 a) Arrhenius plot of total permeation flux of 85% and 95% aqueous isopropanol mixture, b) Dependence of separation factor on the temperature through sodium alginate and Ca<sup>2+</sup> crosslinked alginate membrane

### **3.4.7 Pervaporation characteristics of alginate and alginic acid membranes for separating liquid/liquid mixtures rather than aqueous alcohol mixtures**

Since alginate membrane showed the promising performance for the dehydration of aqueous alcohol mixture, it was tested for the separation of methanol/MTBE mixtures. However the flux was extremely small and it was judged that alginate membrane was not adequate for the separation of organic/organic mixtures, especially of alcohol/organic mixtures. The following statements can explain this potential judgment. As pointed out in early study, alginate membrane is quite brittle, that is, mechanically weak. This is due to weak inter molecular bonding. So when alginate membrane is exposed to the excess amount of water, alginate chain will form the hydrogen bonding with water molecule and eventually will be dissociated into the gel. With this postulation one can describe the transport phenomenon of water molecule based on the water flow channel along  $-\text{COONa}$  or  $-\text{COOH}$  groups in alginate or alginic acid molecular backbone. So the selective absorption of methanol into alginate membrane is very low and the diffusion of methanol is largely hindered because of the very small free volume available in alginate membrane. Besides, the swelling of alginate membrane in organic/organic mixture is pretty much low. Thus it was concluded that alginate membrane could not be applied to the selective removal of alcohol from organic/organic mixtures.

An interesting experiment has been carried out for aqueous acetic acid mixture. Sodium alginate membrane and alginic acid membrane converted in 2% sulfuric acid solution for 2 hours were tested for the separation of 90 wt% acetic acid solution. As shown in Figure 3.17 the flux of sodium alginate membrane increases with the operating

time with the initial drop at 3 hours, meanwhile the flux of alginic acid membrane is relatively constant during 11 hour operation. Also it can be recognized that the flux of alginic acid membrane is lower than that of alginate membrane like the case of 90 % isopropanol separation in Figure 3.6 and 3.7. The flux change of alginate membrane with the time explicit that the chemical property of the membrane keeps changing during the pervaporation operation. To investigate any structural change of membrane, FT-IR measurement has been carried out and presented in Figure 3.18. One can observe the peak at  $1620\text{ cm}^{-1}$  which is indicative of the salified carboxyl group of sodium alginate before the pervaporation. However, after the pervaporation experiment the peak at  $1620$  was weakened and the peak at  $1743$  was pronounced, which is similar to the peak of the alginic acid membrane converted in sulfuric acid solution. This observation clearly proves that sodium alginate membrane is gradually converted into alginic acid membrane during the pervaporation experiment. The peak between  $1100$  and  $1050\text{ cm}^{-1}$  is related to inter and intra hydrogen bonding and will be explained in detail in chapter 6. Intensity of the peak at around  $1100\text{ cm}^{-1}$  represents the degree of hydrogen bonding and that of alginic acid membrane converted in sulfuric acid is the highest and followed by alginic acid membrane (initially alginate membrane) converted in acetic acid feed mixture. Larger flux of alginate than that of alginic acid membrane is partially due to the less internal hydrogen bonding which suppresses the continuous sorption and diffusion of water molecule

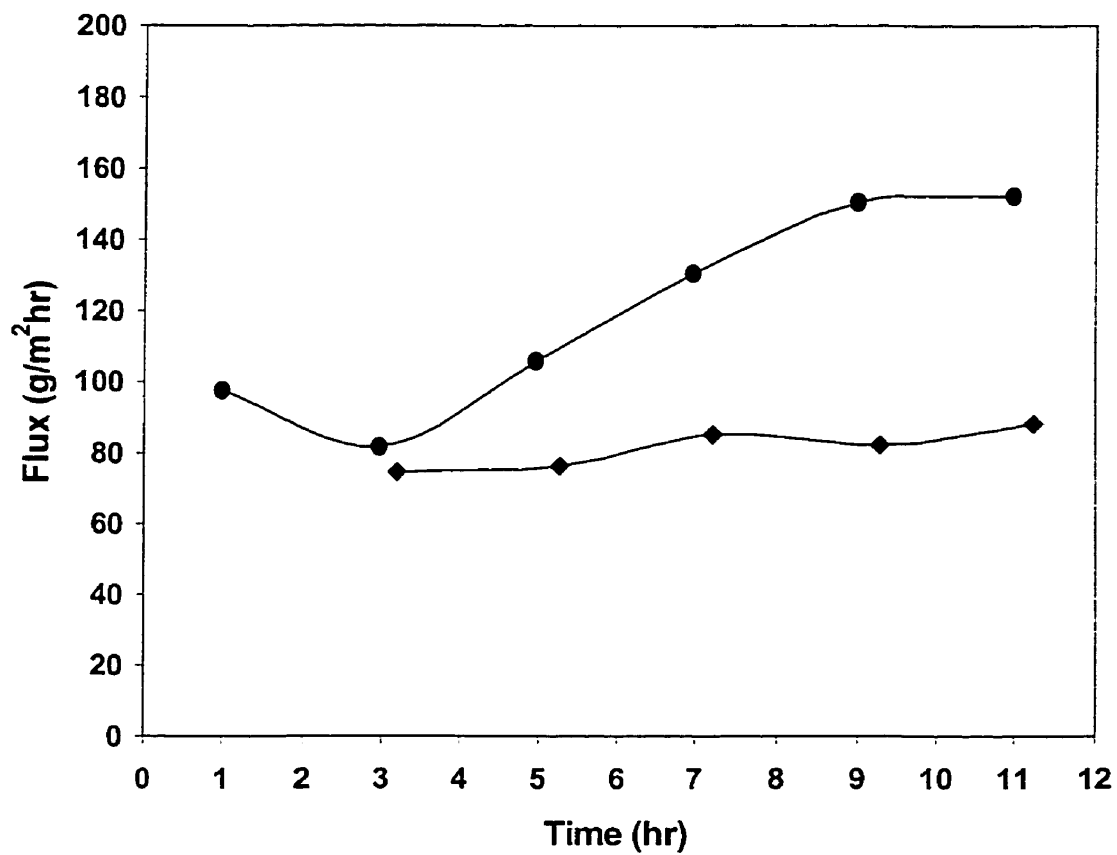


**Figure 3.17 Pervaporation performance of sodium alginate (●) and alginate (◆) membrane for the separation of 90% acetic acid/10% water mixture at 25 °C**

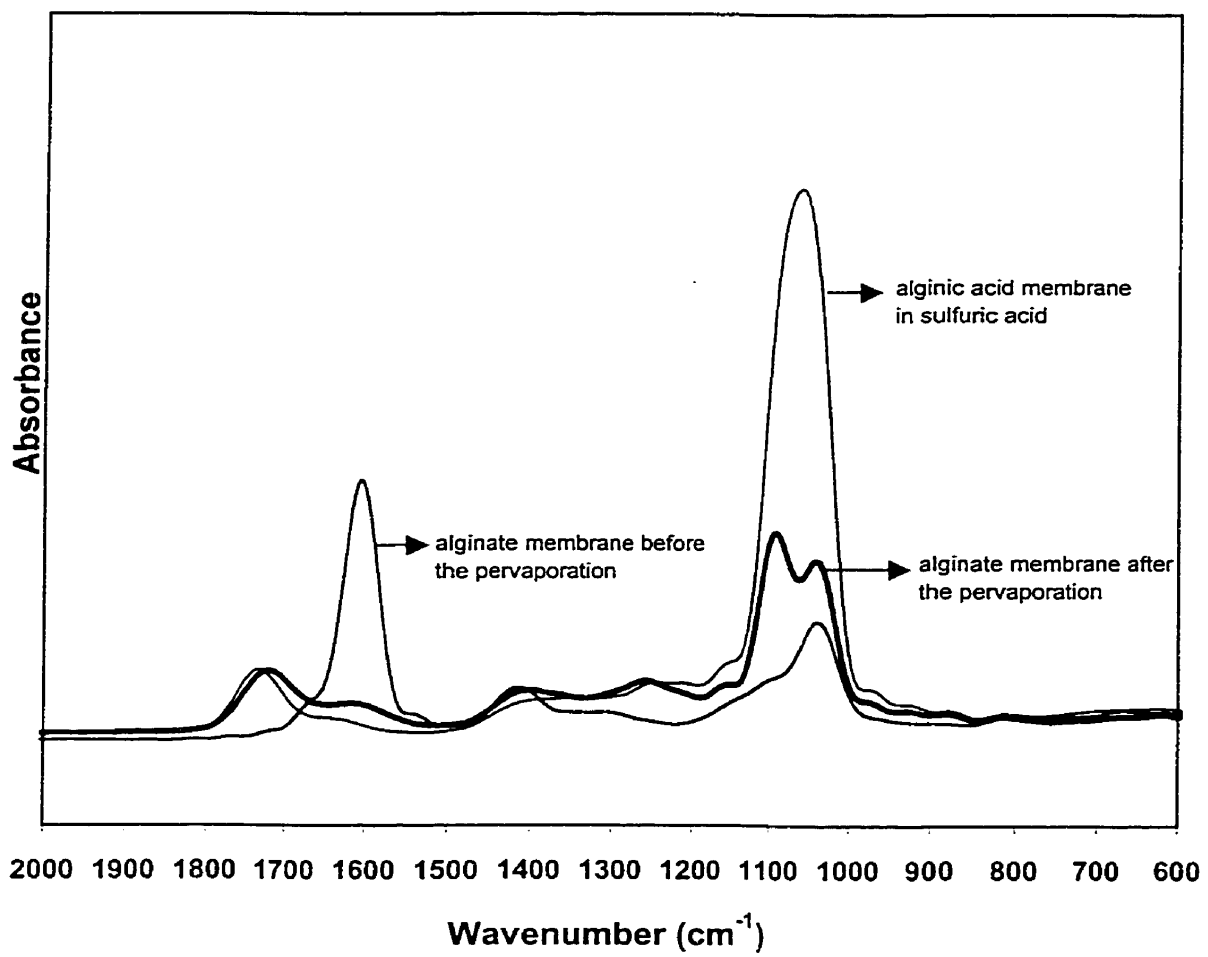


**Figure 3.18 FT-IR of sodium alginate membranes before and after the pervaporation run for 90% acetic acid feed mixture at 25 °C**

### 3.5 CONCLUSIONS

For the pervaporation separation of ethanol-water and isopropanol-water mixtures, sodium alginate membranes were prepared and tested at various feed concentrations, and the following results were obtained.

- 1) Sodium alginate membranes with an extremely high permeation flux and separation factor were prepared. It is believed that the sodium alginate membrane is one of the most promising pervaporation membrane materials.
- 2) Water-soluble sodium alginate membrane was successfully crosslinked using 6 different multivalent ions. Among them,  $\text{Ca}^{2+}$  divalent cation was the most effective for the separation of 90 wt% aqueous ethanol and isopropanol mixtures. Sulfuric acid was used to insolubilize alginate membrane by converting alginate into free alginic acid form. The nature of reaction between alginate and sulfuric acid was studied by FT-IR spectra and compared to the case of HCl.
- 3) Membranes crosslinked with  $\text{Ca}^{2+}$  always exhibited lower fluxes and separation factors than those of sodium alginate membrane except for 95 wt% ethanol mixture and 95 wt% isopropanol mixture. The decline in flux after crosslinking can be explained by closely packed membrane structure, whereas the drop of separation efficiency can be explained by the thermodynamic interaction difference between the permeating component and the counter ions, namely,  $\text{Na}^+$  and  $\text{Ca}^{2+}$ .

It was noticed that the separation characteristics of sodium alginate membrane are largely dependent upon the thermal history of membrane preparation.

## CHAPTER 4

# NOVEL TWO PLY COMPOSITE MEMBRANES OF CHITOSAN AND SODIUM ALGINATE FOR THE PERVAPORATION DEHYDRATION OF ISOPROPANOL AND ETHANOL\*

---

### 4.1 SUMMARY

Novel two ply dense composite membranes were prepared using successive castings of sodium alginate and chitosan solutions for the pervaporation dehydration of isopropanol and ethanol. Preparation and operating parameters namely polymers type facing to the feed stream, NaOH treatment for the regeneration of chitosan, and crosslinking system types were investigated using the factorial design method. It was shown that these parameters were all critical to the performance of the membrane in the form of the main and interaction effects. The pervaporation performance of the two ply membrane with its sodium alginate layer facing the feed side and crosslinked or insolubilized in sulphuric acid solution was compared with the pure sodium alginate and the chitosan membranes in terms of the flux and separation factors. It was shown that although its flux was lower than that of the pure sodium alginate and chitosan

---

\* Part of this chapter has been published in *Journal of Membrane Science*, 156(1999), 17-27

membranes, the separation factors at various alcohol concentrations were in between values for the two pure membranes.

For the dehydration of 90 wt% isopropanol-water mixtures the performance of the two-ply membrane which was moderately crosslinked in formaldehyde was found to match the high performance of the pure sodium alginate membrane. This two ply membrane had fluxes of 70 g/m<sup>2</sup> hr at 95% EtOH, 554 g/m<sup>2</sup> hr at 90% PrOH and separation factors of 1110 at 95% EtOH, 2010 at 90% PrOH and its mechanical properties were better than that of the pure sodium alginate membrane.

## 4.2 INTRODUCTION

Unlike other membrane processes that use porous barriers for separation, pervaporation is a membrane process that uses dense membrane barriers through which one of the liquid components permeates preferentially, and then evaporates as a vapor and is condensed on the downstream side. This phase change occurring through the dense membrane makes the pervaporation process unique among membrane separation processes. The driving force of this process is the difference of the component's chemical potential, hence vacuum is applied on the permeate side to maintain the driving force. The main applications of pervaporation are the dehydration of alcohol and organic solvents and the removal of organic solvents from water for environmental application. Dehydration of alcohols is presently the best-developed area of application. The separation of organic mixtures is the next challenge for pervaporation processes. For the dehydration of alcohol mixtures, new membrane materials, which contain hydrophilic

groups in the polymer structure, are preferred. Hydrophilic groups absorb water molecules preferentially, which leads to both high flux and high separation factors. However, the introduction of hydrophilic groups sometimes swells the membrane significantly due to its plasticization action which results in low selectivity [Huang, 1991]. Chitosan is the deacetylated form of chitin, which is the second most abundant biopolymer in nature. Chitosan has both reactive amino and hydroxyl groups that can be used for chemical reactions and salt formation. These hydrophilic groups are considered to play an important role in preferential water sorption and diffusion through the chitosan membrane. Chitosan membranes have been studied for the dehydration of alcohols [Uragami et al., 1990, 1994; Nawawi & Huang, 1997; Shieh & Huang, 1997] and dimethyl sulfoxide solutions [Uragami & Shinomiya, 1992], pervaporation separation of ethylene glycol from aqueous solutions [Feng & Huang, 1996b]. Amino functional group in chitosan is so reactive that chitosan membrane can be easily modified to N-alkyl chitosan membrane for the dehydration of ethanol [Uragami et al., 1997] and benzoylchitosan membrane for the separation of benzene/cyclohexane mixture [Inui et al., 1998]. From previous researches, chitosan has been proved to have good film forming properties, chemical resistance, and high permselectivity for water. Alginate, which is one of the polysaccharides extracted from seaweeds, has also been found to have excellent performance as a pervaporation membrane material for the dehydration of ethanol-water mixture [Shi et al., 1996; Uragami & Saito, 1989]. However very high hydrophilicity of alginate resulting from both its carboxylic and hydroxyl groups results in an unstable membrane in aqueous solution during pervaporation. It was pointed out that alginic acid membrane was not strong enough to operate in the 50% aqueous ethanol

concentration [Mochizuki et al., 1990]. Water solubility and mechanical weakness of alginic acid membrane has been a drawback in its possible use as a pervaporation material in spite of its excellent permselectivity for water. Also it was shown that alginate has a significant relaxation behavior during the subsequent processes of cooling and aging [Yeom et al., 1996b]. Recently, Yeom and Lee [1998a] crosslinked sodium alginate membrane with glutaraldehyde as a crosslinking agent and HCl catalyst in acetone solution. There are many crosslinking reactions that can be used to crosslink hydrophilic functional groups for this membrane. Among them ionic crosslinking has been of special interest since it is convenient to use and has good crosslinking efficiency.

In this study, pervaporation membranes consisting of chitosan and sodium alginate double layer that has not been studied previously was investigated. Preliminary experiments were carried out on the blending of alginate with chitosan, were unsuccessful due to the precipitating out of the alginate-chitosan electrolyte complex from the solution. This was the reason why we attempted the two ply membrane concept to improve the mechanical properties of the alginate-chitosan membrane. The purpose of this research is to study how to control and enhance the pervaporation flux and separation factor performance of a newly designed and robust two ply alginate-chitosan membrane for ethanol-water and isopropanol-water mixtures. Alginate that is mechanically unstable is used in combination with chitosan as a double layer ply membrane. Chitosan has fairly good properties as a membrane material with good mechanical strength and high water selectivity. Additive performance from both membrane materials was expected for this novel fabricating method. A factorial experimental design was carried out to identify important variables in membrane performance. By systematically altering one, two, three

or even more variables from one experiment to another, two level factorial design methods will give good estimates of the effects of variables from fewer experiments. It will also give additional information on interactions that the classical method of altering only one variable at a time could not achieve. In order to consider the possible interactions when this novel two ply membrane is fabricated and post treated in various crosslinking solutions, three factors a) polymer effect facing to the feed solution, b) NaOH solution treatment and c) crosslinking agent system were chosen in the factorial experiment.

### **4.3 EXPERIMENTAL**

#### **4.3.1 Materials**

Chitosan flakes (Flonac-N) of MW 100,000 (99% N-deacetylation degree) were obtained from Kyowa Technos Ltd, Chiba, Japan. Sodium salt of alginic acid was obtained from Sigma Chemicals Co. Acetic acid (glacial) was supplied by BDH Inc, Toronto, ON, Canada. Ethanol purchased from Commercial Alcohols Ltd, Toronto, ON and isopropanol from BDH Inc. were used as received. All chemicals including H<sub>2</sub>SO<sub>4</sub> (98%), HCl (37%), and Formaldehyde (37% content) were obtained from BDH Inc. Water was deionized and distilled before use.

#### **4.3.2 Two ply membrane preparation**

Sodium alginate was dissolved in water to form a homogeneous solution of 1.2 wt %. Chitosan solution was prepared by dissolving 1.2 wt% chitosan in 10 wt% aqueous acetic acid solution. Both sodium alginate and chitosan solutions were filtered to remove any undissolved solids and impurities. First, sodium alginate solution was cast onto a glass plate with the aid of a casting knife, in succession, chitosan solution was cast onto the alginate solution layer and spread on the surface of alginate layer homogeneously. However in the reverse casting order, sodium alginate did not make complete second layer on chitosan layer probably due to small spreading coefficient in this casting order. Thus chitosan was cast on the surface of alginate solution layer for the preparation of all membranes used. It is believed that there is no significant reaction between them because each layer can be separated after swelling with water. The resulting membrane was dried at room temperature for 24 hours. The dried membrane was peeled off from the plate, treated in 3 wt% NaOH solution containing 50 wt% ethanol solution for 24 hours at room temperature, washed thoroughly to completely remove NaOH, dried again at room temperature, and then immersed in the crosslinking solution. Because alginate is a water-soluble polymer and does not require NaOH solution treatment, this NaOH treatment was chosen as one of factorial design factors for the two ply membrane.

### **4.3.3 Crosslinking solution**

The crosslinking agent in this experiment should be effective for crosslinking both alginate and chitosan polymers. Among three types of crosslinking systems used, strictly speaking sulfuric acid acts as an ionic crosslinker for chitosan but as an insolubilizing

acid for alginate. Alginate is converted to free alginic acid form, which is insoluble in water, by sulfuric acid treatment. However, it was considered as a crosslinking agent in this study since the term crosslinking includes the insolubilization phenomenon. Type A ( $\text{H}_2\text{SO}_4$  crosslinking solution) consists of 3%  $\text{H}_2\text{SO}_4$  in 50 wt% acetone aqueous solution. The membrane was crosslinked for 12 hours in this solution. Two different formaldehyde solution were prepared with 6% formaldehyde, 0.5% HCl catalyst in 50% aqueous acetone solution (Type B) and 6% formaldehyde, 0.5%  $\text{H}_2\text{SO}_4$  catalyst in 100% acetone solution (Type C), respectively. Membranes in formaldehyde crosslinking solution were immersed for 24 hours.

#### 4.3.4 Pervaporation

Pervaporation experiments were carried out for ethanol-water and isopropanol-water mixtures. The concentration of alcohol was varied from 70 to 95 wt%. The alginate-chitosan two ply membranes were found to be mechanically stable during the alcohol dehydration runs and did not deteriorate like the pure alginate membranes due to the additive strength of the chitosan portion of the two ply membrane.

A schematic diagram of the pervaporation apparatus is shown in Figure 3.3. The feed solution temperature in the tank was controlled to the desired value, and the feed solution was circulated using the feed pump. The membrane was placed on the porous stainless steel support and sealed. The effective area of the membrane in contact with the feed stream was  $14.2 \text{ cm}^2$ . Pervaporation was initiated by switching on the circulation and vacuum pumps, the pressure at permeate side was maintained around 3 mbar. Permeate

was collected in glass tubes which were immersed in liquid nitrogen. The pervaporation apparatus was run for at least 2 hours to reach the equilibrium state before starting to measure permeate. When sufficient permeate was collected in the cold trap, the vacuum valve was switched to the parallel trap to collect the other sample. The cold trap containing the permeate was warmed up to ambient temperature, then removed, and weighed to determine the flux and the contents were analyzed for the permeate composition. Separation factor was calculated by the following equation;

$$\alpha_{Water/Alcohol} = [Y_W / Y_A] / [X_W / X_A]$$

where X and Y are the weight fractions of the feed and permeate, respectively.

Analysis of the permeate composition was carried out by using a HP 5890 Gas Chromatography with a FID detector and Abbe Refractometer type 3T at 26.7°C. The column used in GC analysis was 6' × 0.125" packed with Porapak T.

#### 4.3.5 Sorption

The steady state liquid uptake was measured to obtain sorption data for the pure alginate and chitosan membranes. The square shaped membranes were soaked into the various ethanol and isopropanol solutions for a period of 1 day for equilibrium measurements. After carefully blotting off the surface liquid with tissue paper as quickly as possible, they were put into glass tubes, which were connected to the pervaporation apparatus. The liquid absorbed in the membrane was collected in the cold traps, weighed, and analyzed by using GC to obtain the sorbed liquid amount and sorption selectivity. In analogy to the

pervaporation experiment, the sorbed amount and sorption selectivity are calculated as follows;

$$\text{Sorbed amount} = \frac{\text{total liquid amount sorbed(g)}}{\text{weight of dry membrane(g)}}$$

$$\alpha_{\text{water / alcohol}}^{\text{sorption}} = [C_W / C_A] / [X_W / X_A]$$

where C and X is the weight fractions of the permeate and feed components in the membrane at the equilibrium sorption, respectively.

## 4.4 RESULTS AND DISCUSSION

### 4.4.1 Membrane morphology

SEM photographs of the two ply membrane of sodium alginate and chitosan are shown in Figure 4.1. Note that the membrane is considered as a dense membrane in this experiment. The two-layer structure is clearly shown in this picture. This means that after the casting alginate and chitosan layers did not react with each other. The chitosan layer is thicker than alginate layer. The thickness of the two ply membrane tested in this research was 40-50  $\mu\text{m}$ , and that of alginate layer was less than 10  $\mu\text{m}$ .

### 4.4.2 Sorption

The pervaporation transport mechanism can be well interpreted by the solution-diffusion model. Thus, preferential sorption characteristics of each membrane layer were explored. Sorption, namely solubility of the membrane is caused by the interaction of

penetrating species and the membrane. The water sorption of pure alginate and chitosan membranes for ethanol-water mixture is shown in Fig. 4.2 where water amount sorbed in the membrane increases with water content in the mixture. From Fig. 4.2b it is observed that both membranes showed high sorption selectivity to water at equilibrium.

The hydrophilic groups in these membranes are responsible for the preferential water sorption. Alginate shows much higher water selectivity than chitosan. It is also shown that sorption selectivity decreases with increasing water concentration in the mixture. As membrane swelling increases with increasing water content, more ethanol molecules are sorbed together with water molecules. This is called sorption coupling. As shown in Fig. 4.3 sorption phenomena of alginate and chitosan membranes for the isopropanol mixture show similar trends with that of the ethanol mixture. An interesting observation is that for isopropanol mixture alginate absorbs more water than chitosan except at 95 wt% isopropanol mixture. Sorption selectivity of alginate is also much higher than that of chitosan in the isopropanol-water mixture. Alginate membrane shows extremely high water selectivity with the maximum occurring at 90 wt% isopropanol mixture. From these data, it is apparent that alginate and chitosan are excellent materials for the dehydration of ethanol and isopropanol alcohol mixtures. Their good dehydration properties will be further studied in the form of two ply membrane consisting of alginate and chitosan layers.

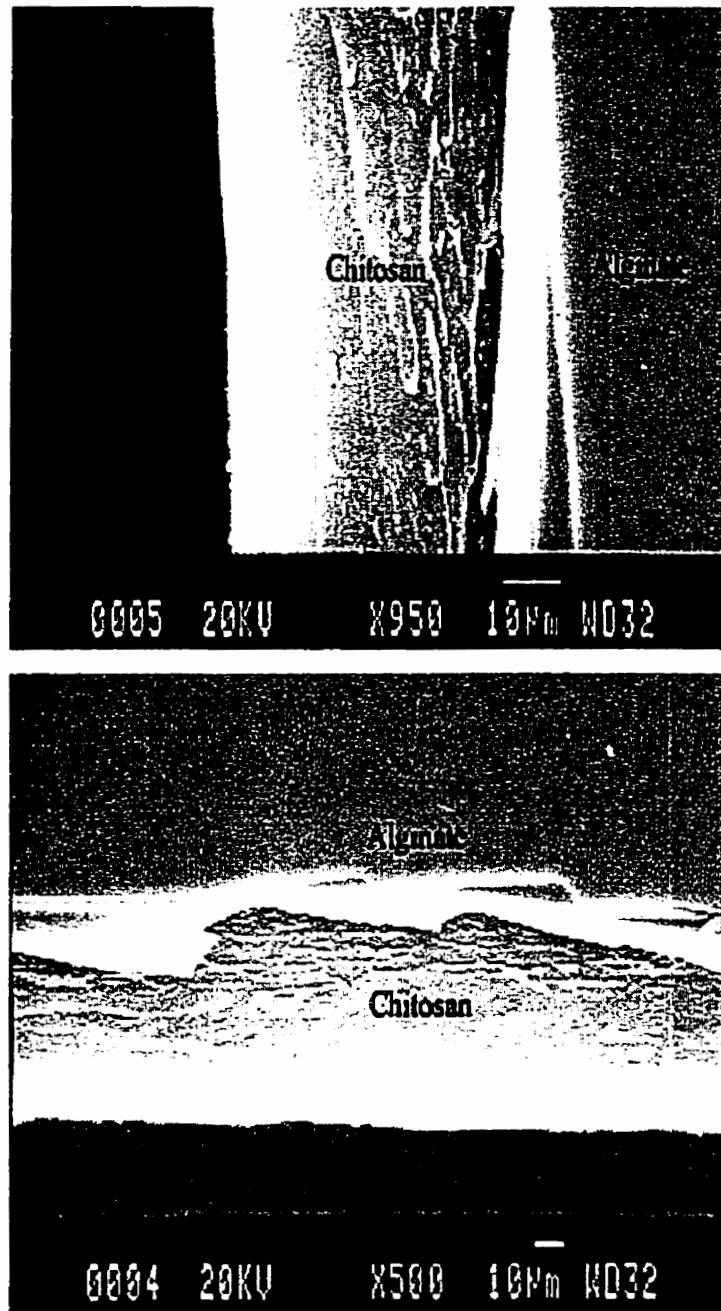
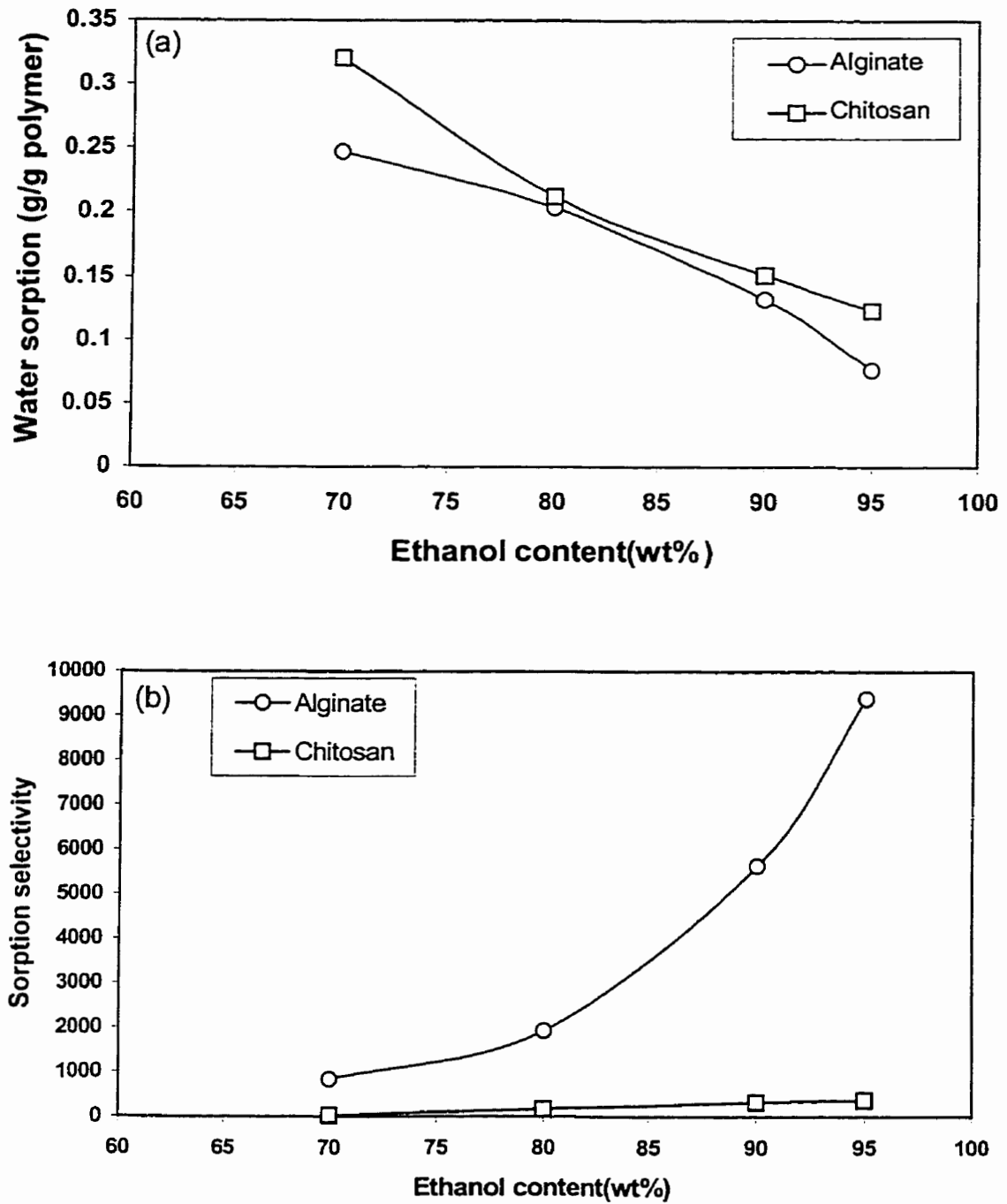


Figure 4.1 SEM picture of the cross-section of two-ply membrane



**Figure 4.2** Water sorption (a) and sorption selectivity (b) versus ethanol content in the feed mixture at 60°C

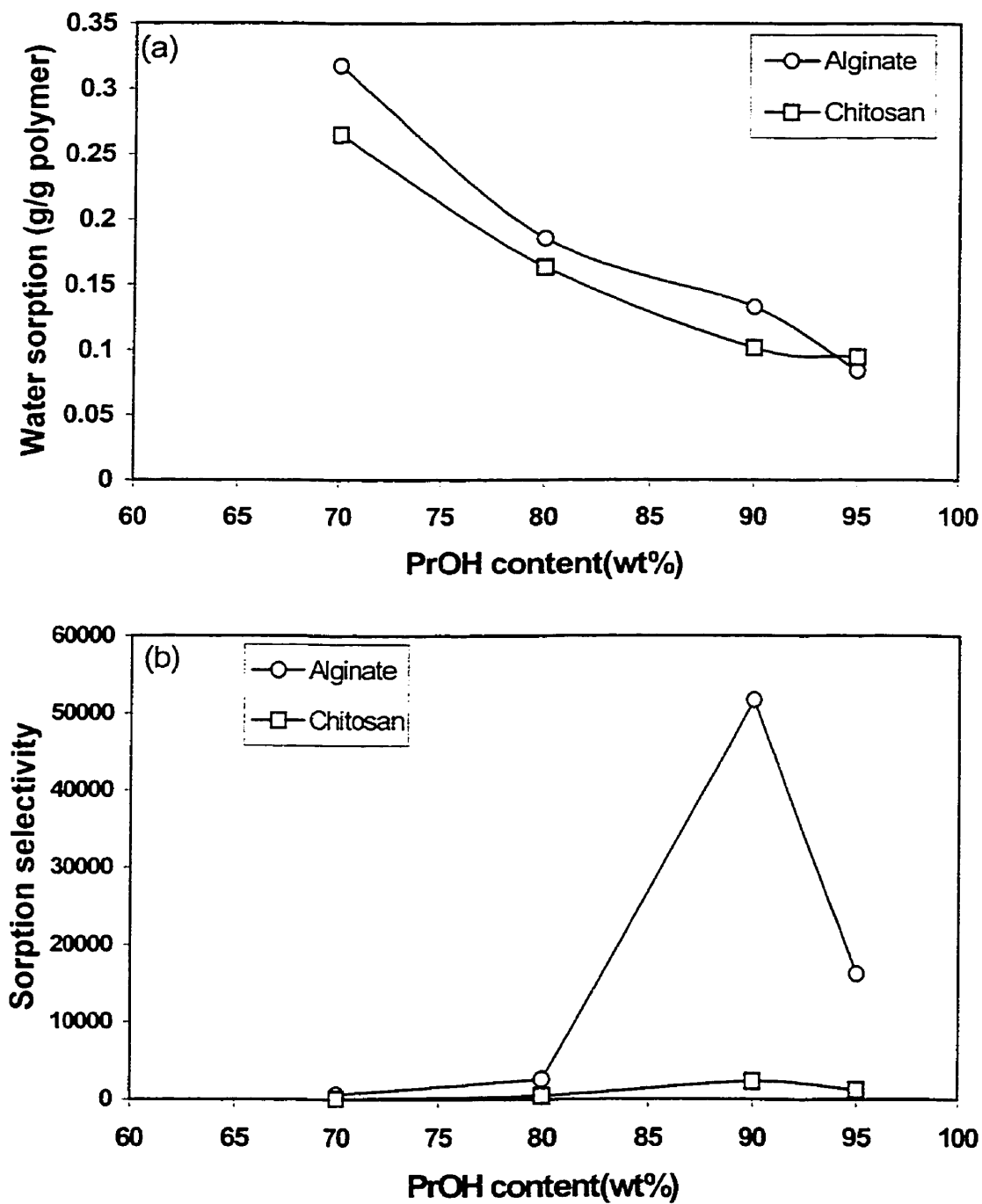


Figure 4.3 Water sorption (a) and sorption selectivity (b) versus isopropanol content in the feed mixture at 60°C

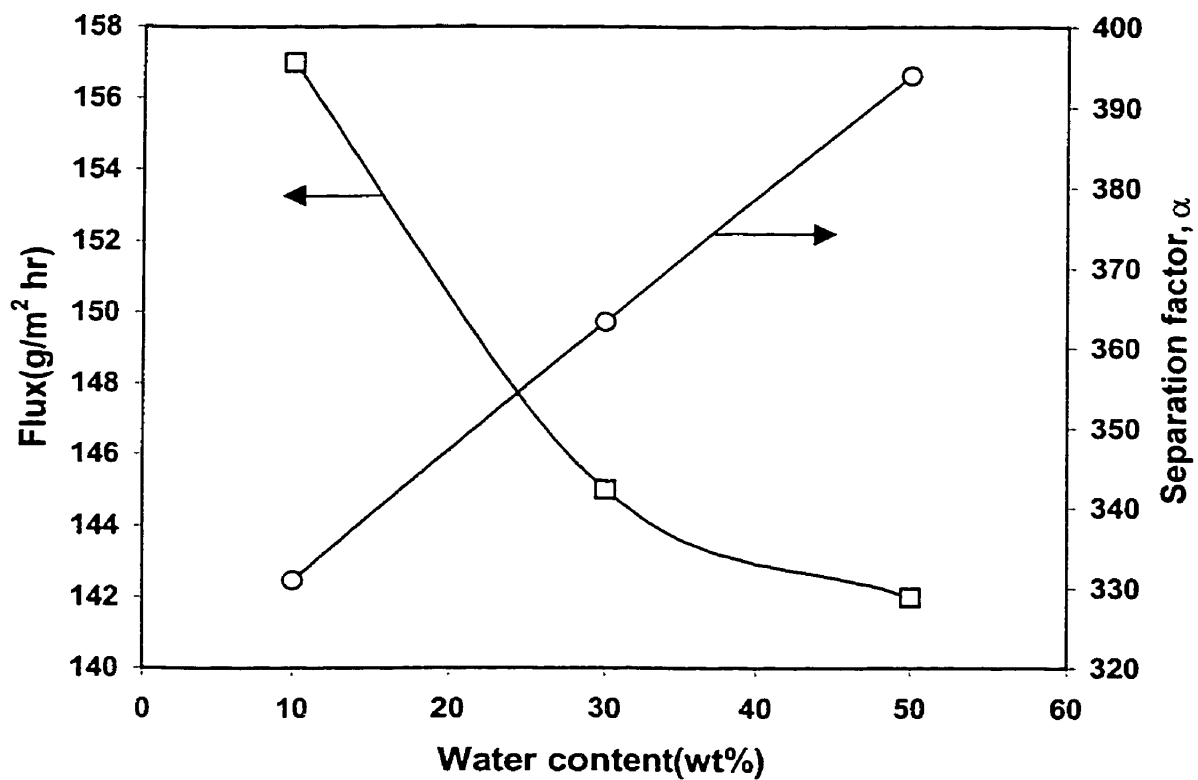


Figure 4.4 Effect of water content in the  $H_2SO_4$  insolubilization solution for the conversion reaction of sodium alginate for the feed mixture of 95% EtOH at 60°C

#### **4.4.3 Effect of water content in insolubilization solution**

The effect of water content in the insolubilization solution was investigated using sodium alginate membrane and H<sub>2</sub>SO<sub>4</sub> solution. It was revealed that flux decreased with increasing water content in the insolubilization solution while the separation factor increased (see Fig. 4.4). It is believed that dilute acid in solution diffused into the membrane easily under the condition of increased water content, the so-called by plasticization action that results in the enhanced conversion to free alginic acid.

#### **4.4.4 Effect of time on crosslinking**

One of the factors in two level factorial design experiments is the crosslinking agent type because the agents used in this study must satisfy both alginate and chitosan at the same time. Crosslinking reaction can be carried out through the use of crosslinking agent having two or more groups capable of reacting with the functional groups in the polymer chain. Preliminary experiments were done to select the proper crosslinking time for each crosslinking agent. It was difficult to find the optimum agent and its concentration to crosslink both alginate and chitosan simultaneously. Both polymers showed different crosslinking behavior for a certain agent. For example, glutaraldehyde was a very good agent for alginate, but chitosan became brittle using the same conditions. In principle, as the crosslinking density increases, the membrane becomes more compact and the polymer chains become rigid. Thus, penetrant molecules are less permeable due to the reduced free volume and increased penetration energy. The crosslinking time effect

for the membrane crosslinked with  $H_2SO_4$  solution is shown in Figure 4.5a. It must be pointed out again that the  $H_2SO_4$  crosslinking solution consists of 50 wt% acetone and 50 wt% water and acts as a ionic crosslinker for chitosan layer but as an insolubilizer for alginate layer. It seems that there is no simple relationship between crosslinking density and crosslinking time. Based on the pervaporation performance, a 12-hour crosslinking time was chosen as an optimum crosslinking time for further experiments. Another pervaporation experiment for the azeotropic mixture of 90wt % isopropanol was carried out with the membrane crosslinked in formaldehyde (Type B) catalyzed with HCl in 50wt% aqueous acetone as shown in Figure 4.5b. In this experiment, alginate side faced to the feed solution unlike Figure 4.5a in order to know polymer type dependence on the crosslinking time. This membrane also shows the random pervaporation performance at given conditions. For formaldehyde crosslinking agents (Type B and C) the membrane was immersed for 24 hours.

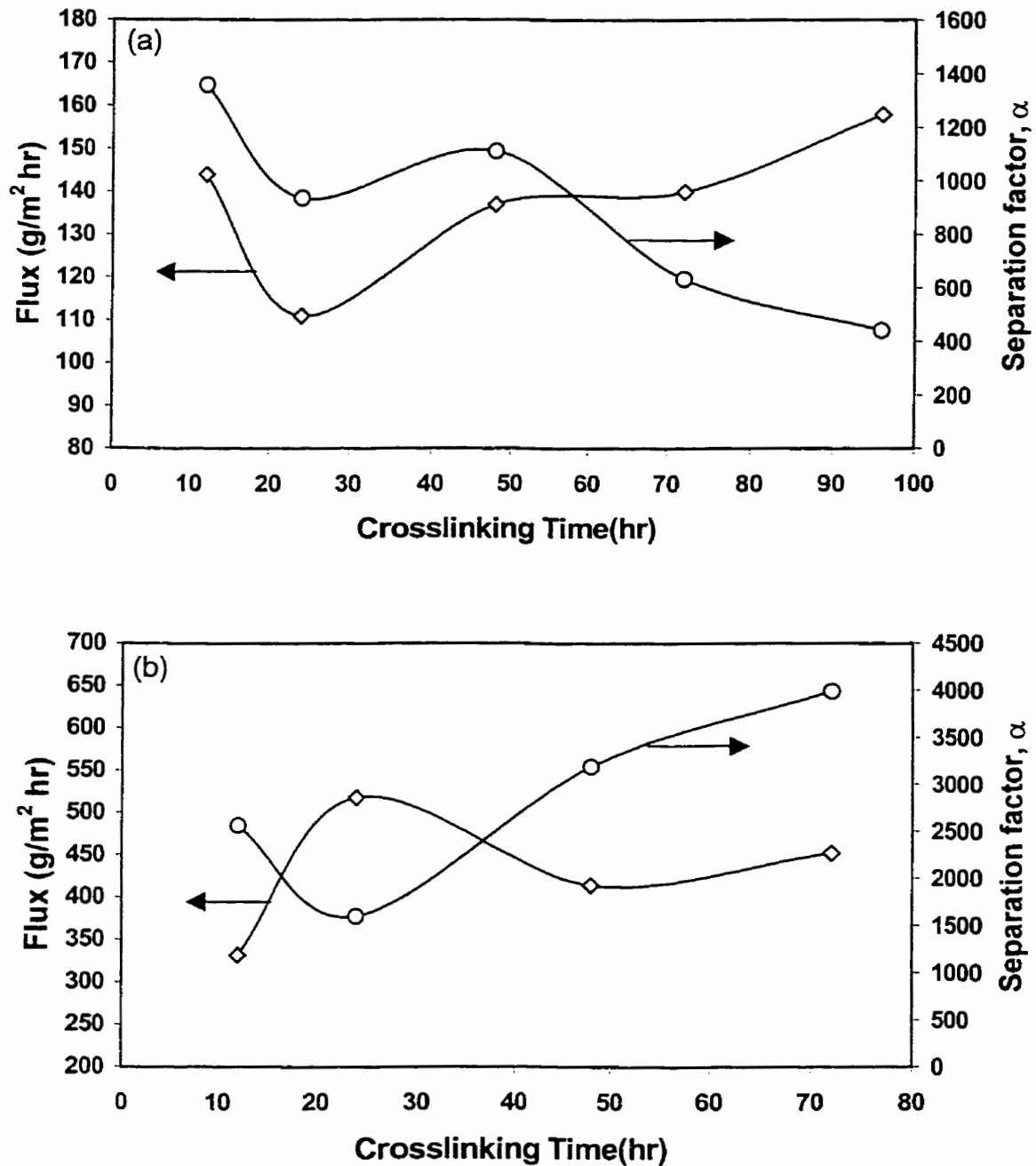


Figure 4.5 Pervaporation data of the crosslinked two ply membrane (a) Type A crosslinking agent (H<sub>2</sub>SO<sub>4</sub>) for 95 wt% EtOH mixture at 60°C; chitosan side faces to the feed, (b) Type B crosslinking agent (HCHO) for 90 wt% PrOH mixture at 60°C; alginate side faces to the feed

#### 4.4.5 A factorial design experiment for 95 wt% EtOH mixture

A  $2^3$  factorial experiment in which there are two qualitative variables; polymer type facing to the feed and crosslinking agent type and a single quantitative variable; NaOH treatment time was carried out. The response is the flux and separation factor. Table 4.1 shows the pervaporation results on the basis of design experiment and variables in the factorial design. Variables and levels have been chosen empirically based on the preliminary runs. Levels of each factor are coded with a minus sign and plus sign. A qualitative factor, for example, crosslinking agent type can be also designated using “-” and “+” notations. It is shown in Table 4.1 that the two ply membranes have fairly high permeation fluxes and separation factors, indicating that this membrane is a good hydrophilic dehydration membrane. Selectivity for water ranges from 70 to a thousand which can be considered fairly high.

In the two level factorial designs, the magnitude and direction of the factor effects can be examined, and the variables that are likely to be most important can be diagnosed [Feng & Huang, 1996a]. The main effect measures the average effect of each factor over all conditions of the other variables. On the other hand the factors which do not behave additively are said to interact. We find the main effect and interaction effect between the main effects from this factorial design. The data from a  $2^3$  design can be made to yield all eight “effects” by extending the algorithm of Yates [Box et al., 1978], and is presented in Table 4.2, where single letters symbolizes the main effects and the interaction effects are expressed by multiplying their respective factors.

No.	Factors			Flux(g/m <sup>2</sup> hr)	Separation factor
	A	B	C		
1	-	-	-	49	382
2	-	-	+	81	296
3	-	+	-	56	147
4	-	+	+	42	152
5	+	-	-	70	1112
6	+	-	+	94.4	208
7	+	+	-	59	1062
8	+	+	+	43	70.5
				Low(-)	High(+)
A	Polymer facing to the feed			CS	AA
B	NaOH treatment time			0hr	24hr
C	Crosslinking agent			Type A	Type C

**Table 4.1 Pervaporation experiment results for 95% ethanol-water mixture at 60°C and factorial design matrix [CS:chitosan, AA;alginate]**

Identification	Estimated effects	
	Flux (g/m <sup>2</sup> hr)	Separation factor
Average	61.8	428.7
A	9.6	369
B	-23.6	-141.5
C	6.6	-494
AB	-7.6	48
AC	-2.4	-453.5
BC	-21.6	1
ABC	1.4	-44.5

**Table 4.2 Estimated effects from a 2<sup>3</sup> factorial design for 95% ethanol solution**

From the results summarized in Table 4.2 we cannot make any firm decision whether the main effects are contributing to the membrane performance positively or negatively since occasionally real and meaningful interactions between the factors also should be considered. The effective way to detect the significant effects is to plot the effects on normal probability paper. If a point is far from a straight line going through the points for which the effect magnitudes are close to zero, then that effect can be considered to be significant on a comparative basis.

On the basis of Table 4.2 the following observations were obtained for the ethanol-water mixture:

- 1) A change in the polymer contacting the feed stream from chitosan to alginate enhances the permeation flux and separation factor. This agrees well with the fact that alginate has extremely high affinity to water as shown from previous sorption experiments. Note that the membrane explored here consists of two different polymers. It also can be assumed that most of separation performances depend on the properties of polymer absorbing the penetrant in the feed side. The water molecule is sorbed preferentially into the alginate layer, diffuses through a portion of alginate and chitosan layer along the hydrophilic, polar path, and is removed from the membrane in the form of vapor.
- 2) Except for main effect A, which is positive for both flux and separation factor responses, the effects C, AB, BC, ABC have opposite signs and the effects B and AC have negative signs for both flux and separation factor. The opposite signs can be explained by a trade-off phenomenon, which frequently occurs in pervaporation experiments. The flux can increase by sacrificing the separation factor or vice versa.

Based on the normal probability plot the significant effects for the fluxes are single effect A and interaction effect BC, whereas for separation factor interaction effect AC and single effect A were the most appreciable effects. This indicates that all factors involving this experiment contributed to the performance of membrane in the form of main effect and interaction effect over the experimental range investigated.

- 3) The effects of NaOH treatment (B) and crosslinking agent (C) cannot be interpreted separately because they interact significantly, and can best be analyzed using two-way tables [Box et al., 1978]. The interaction apparently arises from the difference of NaOH treatment effects for the crosslinking agents.
- 4) AC interaction effect is considered in the two-way table on separation factor response. The membrane shows the significant separation factor when the alginate side of the membrane crosslinked in type A faces to the feed stream. It must be pointed out here that considering only A, BC, and AC effects significant for the membrane performance can lead the experimenter to the wrong judgement.

#### 4.4.6 A factorial design experiment for 90 wt% PrOH mixture

Dehydration of isopropanol-water mixture especially for the 90% azeotropic composition arises from the demand in semi-conductor industry, where isopropanol is being used as cleaning agent for semi-conductor chips. Instead of Type C crosslinking agent, Type B that is formaldehyde catalyzed with HCl in 50 wt% aqueous acetone solution was used for the isopropanol application. The pervaporation results from a

factorial design experiment were obtained by following the same procedure as the ethanol-water mixture, and presented in Table 4.3 and 4.4.

The following observations are made for the isopropanol pervaporation system;

- 1) We were encouraged by the high flux and separation factor. It indicates that double layer membrane is a good pervaporation membrane for dehydration of isopropanol.
- 2) The two main effects A and C have the positive signs for both the flux and separation factor. Apparently these conditions should be considered when preparing double layer membrane as the significant parameters to enhance the flux and separation factor.
- 3) As far as the permeation flux is concerned, it was revealed that main effects A and B are the most significant effects for the high flux, whereas the interaction effect BC is the significant effect on the separation factor. The high flux can be achieved by the operating condition that the alginate side contacts with the feed stream.
- 4) Contrary to expectation, the crosslinking agent type did not appear as an important effect for the flux.
- 5) Considering the large number of parameters involved in the preparation of the two ply membranes, a factorial design experiment can be an efficient way to characterize the significance of each factor to the performance and to optimize the membrane. However, it should be noted that due to the linearity assumption of each factor in a factorial design, the extrapolation of results beyond the experimental ranges might cause unreliable results [Feng & Huang, 1996a; Chian & Fang, 1975; Guiver et al., 1989].

No.	Factors			Flux(g/m <sup>2</sup> hr)	Separation factor
	A	B	C		
1	-	-	-	198	2638
2	-	-	+	292	2094
3	-	+	-	221	1906
4	-	+	+	199	3991
5	+	-	-	324	3205
6	+	-	+	554	2011
7	+	+	-	279	2638
8	+	+	+	245	3466
				Low(-)	High(+)
A	Polymer facing to the feed			CS	AA
B	NaOH treatment time			0hr	24hr
C	Crosslinking agent			Type A	Type B

**Table 4.3 Pervaporation experiment results for 90% isopropanol-water mixture at 60°C and factorial design matrix [CS:chitosan, AA;alginate]**

Identification	Estimated effects	
	Flux (g/m <sup>2</sup> hr)	Separation factor
Average	289	2732.4
A	123	150.3
B	-106	513.3
C	67	294
AB	-71	-69.3
AC	31	-476.8
BC	-95	1162.8
ABC	-37	-151.8

**Table 4.4 Estimated effects from a 2<sup>3</sup> factorial design for 90% isopropanol solution**

#### 4.4.7 Pervaporation experiments of the two ply membrane

Figure 4.6 shows the pervaporation results at various ethanol concentrations of one of the double layer membranes (No.5) used in factorial design together with the pervaporation results of pure alginate and chitosan membranes. It is interesting to note that the alginate membrane shows higher flux than that of the chitosan membrane at feed concentrations of 90% and 95% ethanol. At azeotropic composition of ethanol, a flux of  $220 \text{ g/m}^2\text{-hr}$  and a separation factor of 5570 is achieved for alginate membrane. It means that alginate is an extremely water permselective material. In a previous sorption experiment, chitosan membrane showed higher solubility than that of alginate, but had lower separation factor than that of alginate. It is worth pointing out that solubility results in the static mode do not always agree with the pervaporation results in the dynamic operating mode due to the complicated interaction between the penetrating species and the membrane materials. The permeation flux of a double layer membrane has lower fluxes except for 80% ethanol feed than those of alginate and chitosan membranes. The flux and separation factor performance at azeotropic concentration reaches  $70 \text{ g/m}^2 \text{ hr}$  and 1110, respectively. Note that the No.5 membrane was crosslinked in  $\text{H}_2\text{SO}_4$  crosslinking agent. Normally, crosslinking reduces the chain mobility of the polymer and the free volume of the membrane resulting in decreased penetrant diffusion. The separation factors of both alginate and chitosan membranes decrease with the increase of water

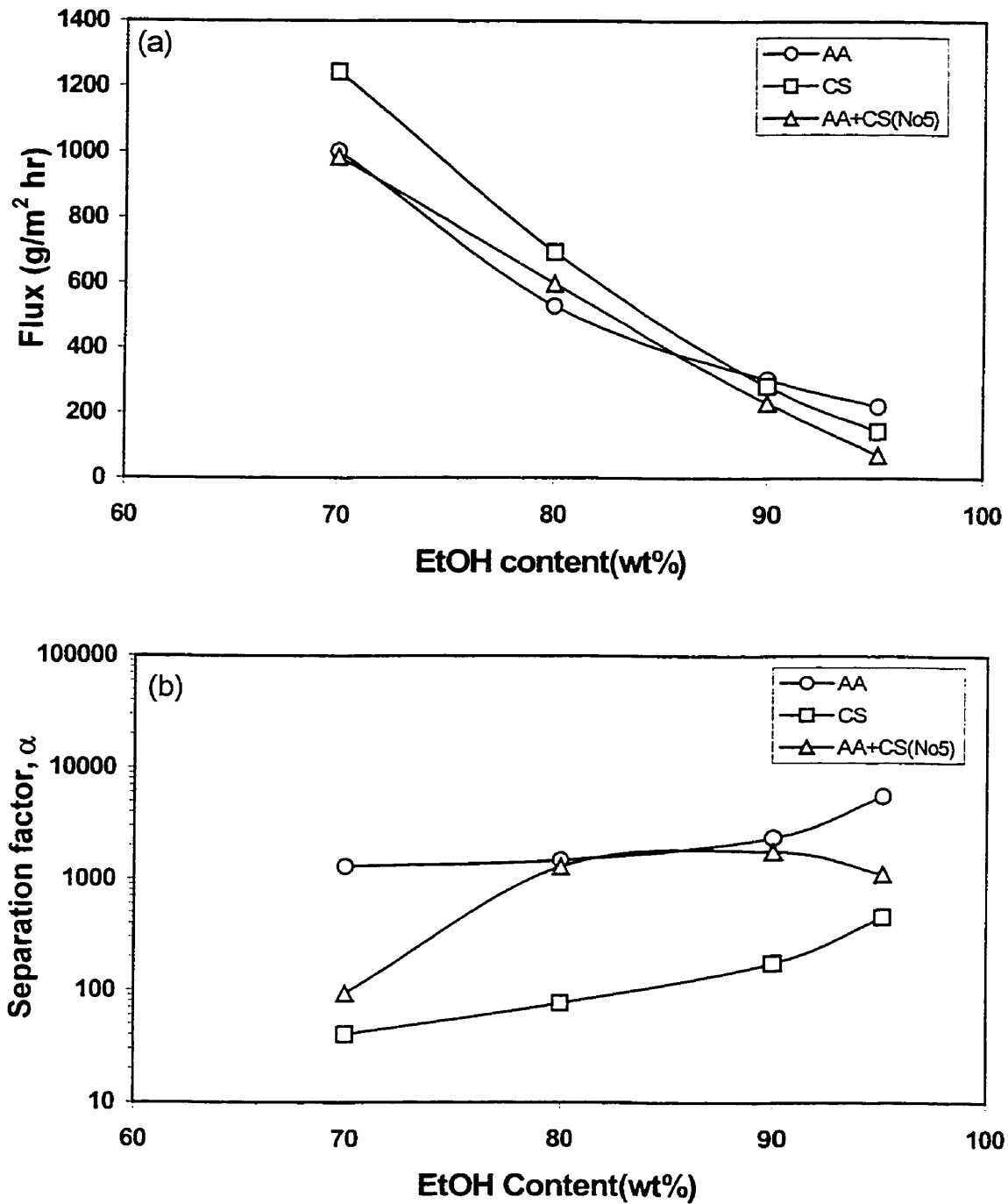


Figure 4.6 Pervaporation results of pure alginate, chitosan, and No.5 two ply membrane from a factorial design for ethanol-water mixture at 60°C

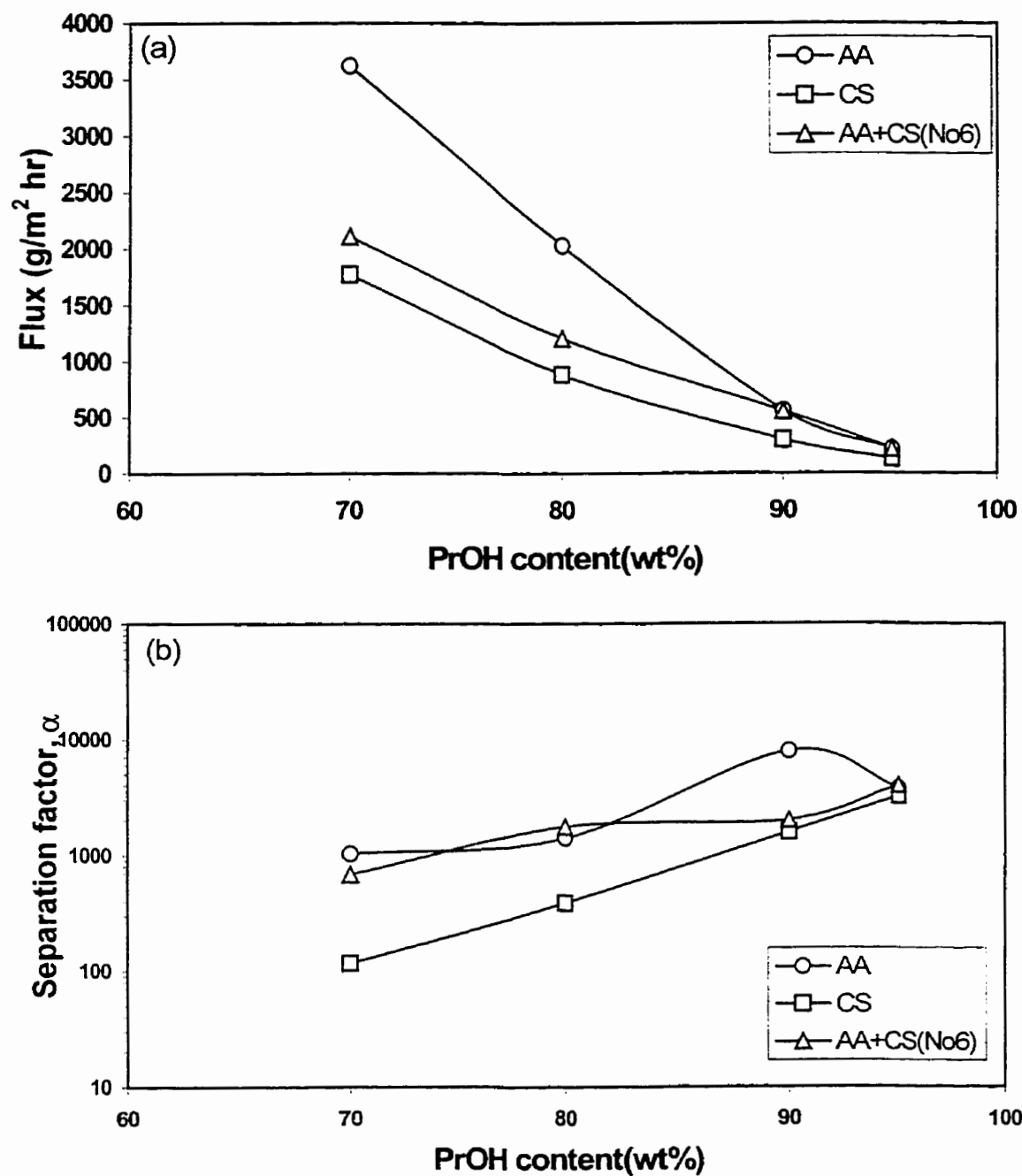


Figure 4.7 Pervaporation results of pure alginate, chitosan, and No.6 two ply membrane from a factorial design for isopropanol-water mixture at 60°C

content in the feed. These membranes are hydrophilic, and swell linearly with water content. Thus, more ethanol molecules coupled with water molecules diffuse through the membrane, resulting in decreased separation efficiency. Interestingly, the separation factors of No.5 double layer membrane lie between those of alginate and chitosan in spite of being crosslinked in a relatively strong crosslinking agent and levels off over 80 wt% ethanol concentration. It has also been previously postulated that crosslinked alginate has less affinity to water after glutaraldehyde crosslinking catalyzed with HCl [Yeom & Lee, 1998a].

Figure 4.7 shows the pervaporation results conducted at various isopropanol concentrations at 60°C for pure alginate, chitosan membrane, and No 6 double layer membrane. The No 6 membrane was crosslinked weakly in formaldehyde solution and the alginate side of the two sides contacts the feed stream. The flux performance (Figure 4.7a) of the two-ply membrane is analogous to that of pure alginate at 95% and 90% propanol concentrations. It is assumed that crosslinking density caused by formaldehyde solution (Type B) is not as strong compared to the H<sub>2</sub>SO<sub>4</sub> solution (Type A). This postulate is also supported by the separation factor results of No 6 membrane in Figure 4.7b. Unlike previous ethanol mixture the decrease of separation factor of No 6 is not significant compared to the separation factor of the alginate membrane. It means that the network change of polymer resulting from the crosslinking is not so significant. As shown in sorption selectivity data for isopropanol mixture in Figure 4.3b, a separation maximum at 90% mixture is observed in the pervaporation experiment. Presumably, the solubility of isopropanol is greatly hindered at 10% water concentration due to the interaction between isopropanol and alginate membrane. From all of the above

observations, it has been shown that the superior permselectivity of alginate polymer can be applied to the pervaporation membrane in the form of two-ply dense membrane.

#### 4.5 CONCLUSIONS

Two-ply dense membranes consisting of sodium alginate and chitosan were prepared for the pervaporation dehydration of ethanol-water and isopropanol-water mixtures. It was shown that the highly water permselective characteristic of alginate, which is water-soluble and mechanically weak can be made into dense two ply membrane consisting of alginate and chitosan with good flux, separation factors, and better mechanical properties. It was also shown that three factors including polymer type contacting the feed stream, NaOH treatment, and crosslinking agent type play important roles in the performance of this newly designed novel two-ply membrane in terms of the flux and separation factor. It was also revealed that the interaction effects are significant. It is apparent that a factorial experimental design is beneficial for the exploration of a large number of the membrane operating and preparing parameters. Further efforts will be directed to optimize this two ply membrane and verifying the benefits of the two-ply membrane. Further experiments might be carried out to test the tensile and mechanical properties of the two ply alginate-chitosan membrane.

## **CHAPTER 5**

# **CROSSLINKED CHITOSAN COMPOSITE MEMBRANE FOR THE PERVAPORATION DEHYDRATION OF ALCOHOL MIXTURES AND ENHANCEMENT OF STRUCTURAL STABILITY OF CHITOSAN/POLYSULFONE COMPOSITE MEMBRANES\***

---

### **5.1 SUMMARY**

Chitosan composite membranes having a microporous polysulfone substrate were prepared and tested for the pervaporation dehydration of aqueous isopropanol mixtures. When the composite membrane experienced excessive swelling at the feed mixture of high water content, the composite membranes were found to be segregated in structure due to the opposite characteristics to water of chitosan and polysulfone. Efforts to enhance the structural stability under various pervaporation operational conditions were made. The polysulfone substrate was immersed into hydrophilic binding polymer solutions such as polyvinyl alcohol, polyacrylic acid, and hydroxyethylcellulose before the casting of chitosan layer to increase the affinity between the thin chitosan layer and porous polysulfone layer which resulted in increased geometrical stability of the

---

\*Part of this study has been published in Journal of Membrane Science, 160(1999), 17-30

chitosan/polysulfone composite membranes. The chitosan layer was crosslinked with glutaraldehyde and  $H_2SO_4$  in acetone solution to control the permselectivity.

## 5.2 INTRODUCTION

The pervaporation membrane process is governed by the chemical nature of the polymer membrane and its physical structure, the physicochemical properties of the mixture to be separated, and the feed component-component and component-membrane interactions [Feng & Huang, 1997]. Dehydration of alcohol is the best-developed area of the pervaporation application processes. For this purpose, good membrane material should have high flux, high separation efficiency, and long term stability to maintain its original permselectivity under operating condition. Since a trade-off between the flux and separation factor exists, much effort has been made to achieve high fluxes and separation factors simultaneously.

One of the characteristics of pervaporation processes is the fact that it is a rate-controlled process. Thus, asymmetric and composite membrane structures have been introduced into the membrane. The basic idea is to reduce the flow resistance by depositing thin and dense active layers on the supporting microporous ultrafiltration (UF) membrane. Asymmetric membranes are also called integrally skinned asymmetric membranes because commonly they consist of the same material. Most of industrial interest for pervaporation membrane is directed to the development of composite membranes that have very thin and dense skin layers on the top of the asymmetric UF membrane so that the flux can be increased significantly. However, unlike homogeneous asymmetric membranes, they consist of two different materials. The GFT membrane

which is the first commercialized pervaporation membrane used in the dehydration of aqueous ethanol mixture, is composed of polyvinyl alcohol (PVA) thin layer and microporous polyacrylonitrile (PAN) substrate which offers little resistance to the flow of permeate. In this research, chitosan has been chosen as the active skin layer material and polysulfone as the microporous supporting material. Chitosan is the partially deacetylated polymer of chitin, which is found in a wide range of natural sources like crab and shrimp shells. Recently many investigations [Uragami et al., 1994, 1997; Nawawi & Huang, 1997; Volkov et al., 1998; Ren & Jiang, 1998; Qunhui et al., 1995] have been directed to chitosan as a pervaporation membrane material due to its extremely high affinity to water, good film forming properties, functional groups which are easy to modify, and good mechanical and chemical stability. Polysulfone is one of the most common UF materials, which can withstand a pH range of 0.5-3.0, temperature to 85 °C, and 25 mg/L of free chlorine on the continuous operation, and has excellent chemical, mechanical and biological stability. Recently several studies of chitosan or chitosan blend/polysulfone composite membrane have been carried out to dehydrate ethanol-water mixtures [Shieh & Huang, 1997] and isopropanol-water mixtures [Nawawi & Huang, 1997] and to remove ethylene glycol from aqueous systems [Feng & Huang, 1996b]. Chitosan/polyethersulfone composite membrane was also studied for alcohol-water mixture [Lee et al., 1997].

Chitosan and polysulfone are good materials for preparing composite membranes, however the structural stability of this composite membrane is not acceptable to endure the long experimental conditions because they have opposite characteristics with respect to affinity for water. Note that chitosan is an extremely hydrophilic material, whereas

polysulfone is a hydrophobic material. That means significant differences of surface tension between these two materials resulting in the segregation of these two layers under swollen conditions. The goals of this study are to enhance the structural stability of chitosan/polysulfone composite membrane over a wide range of temperature and feed concentration conditions and to control the permselectivity of the composite membrane through combined glutaraldehyde and  $H_2SO_4$  crosslinking.

Currently there are two methods for surface modification of polysulfone membrane. First, sulfonation of the chemical structure [Bunn & Rose, 1993; Chen et al., 1996; Kerres et al., 1996] improves the hydrophilicity of polysulfone membrane with a controlled level of sulfonation. Secondly, modification of surface can be achieved by physical adsorption (that is, coating) of hydrophilic polymer onto the surface of the polysulfone UF membrane, followed by the crosslinking of this thin coating layer. This study applied the coating technique to modify polysulfone to reduce the hydrophobicity of polysulfone. Hence, it is expected that the separation tendency of top layer and supporting layer can be significantly reduced as the result of the increased affinity via hydrophilic binding polymer. Several investigators [Millesime et al., 1994; Kim et al., 1988; Brink & Romijn, 1990] tried to produce high protein rejection rate and less fouling through the surface by the surface modification of polymer coating in UF applications. Three water-soluble polymers, namely polyacrylic acid (PAA)-anionic, polyvinylalcohol (PVA)-nonionic, and hydroxyethylcellulose (HEC)-nonionic were used to coat the polysulfone substrate. Ionically crosslinked polyacrylic acid membranes [Huang et al., 1983; Habert et al., 1979a, 1979b; Zhao & Huang, 1990] have been studied extensively in various applications due to its strong hydrophilicity. PVA is the primary pervaporation material

that was first commercialized by the GFT Carbone Lorraine A.G. Co., and also has been studied intensively [Huang & Rhim, 1993a, 1993b; Yeom & Huang, 1992] by other investigators. Crosslinking is one of the efficient strategies to control the permselectivity of the pervaporation membrane. In principle, crosslinking enhances the selectivity with sacrifice of the permeation flux, namely the so-called trade-off phenomenon. The membrane becomes more compact due to the crosslinking density increase and the polymer chains become more rigid. Thus, penetrant molecules are less permeable due to the reduced free volume and increased penetration energy. Various crosslinking agents have been used to crosslink chitosan material like glutaraldehyde [Uragami et al., 1994; Suto & Ui, 1996; Goto et al., 1994], H<sub>2</sub>SO<sub>4</sub> [Ren & Jiang, 1998; Lee et al., 1997], formaldehyde [Zhang et al., 1997], hexamethylene diisocyanate [Nawawi & Huang, 1997], and epichlorohydrin [Wei et al., 1992]. In this study we used glutaraldehyde with sulfuric acid in aqueous acetone for the crosslinking of chitosan thin layer.

## **5.3 EXPERIMENTAL**

### **5.3.1 Materials**

Chitosan flakes (Flonac-N) with MW 100,000 and 99% N-deacetylation degree were donated by Kyowa Technos Inc, Japan. Polysulfone (Udel P-3500) was obtained from Amoco performance products, Inc., USA in powder form. PVA (MW 108,000), polyacrylic acid (MW 4,000,000), and hydroxyethylcellulose (HEC) were purchased from Polyscience, Inc. Dimethylformamide (DMF), acetic acid (glacial), aluminium

nitrate ( $\text{Al}(\text{NO}_3)_3 \cdot 9\text{H}_2\text{O}$ ), and HCl as well as  $\text{H}_2\text{SO}_4$  were supplied by BDH Chemicals Co., Toronto, ON, and ethylene glycol (monomethyl ether) from Sigma Chemical Co. Glutaraldehyde (25%) was purchased from Sigma Chemical, Co. A non-woven polyester fabric from Veratec division of International Paper Co., USA was used as the backing material for the composite membrane. Water was de-ionized and distilled before use.

### 5.3.2 Membrane preparation

Polysulfone UF membrane were prepared via the wet phase inversion technique from the casting solution containing 14 wt% polysulfone, 10 wt% ethylene glycol, and 76 wt% N,N-dimethylformamide (DMF). The casting solution was cast onto a polyester non-woven fabric held on a glass plate with the aid of a casting knife made in this laboratory. The cast film was immediately immersed into a coagulation bath consisting of aqueous DMF. The resulting membrane was washed in de-ionized water thoroughly and air-dried completely at ambient temperature. Initial microporous polysulfone membrane showed a pure water permeation rate of  $268 \text{ kg/m}^2 \text{ hr}$  at transmembrane pressure of 100 psi and operating temperature  $22 \text{ }^\circ\text{C}$ . Most of the water flux tests were performed in replicate to achieve precision in the flux. To test the binding effect of four hydrophilic polymer solutions, the first polysulfone UF membrane was immersed in 0.1 wt% polyacrylic acid (PAA) solution for 1 hr and crosslinked in the 10 wt%  $\text{Al}(\text{NO}_3)_3 \cdot 9\text{H}_2\text{O}$  aqueous solution for 12 hr. The second polysulfone UF membrane was soaked in 0.1 wt% PVA binding solution for 1 hr. and crosslinked in 80 wt% aqueous acetone solution containing 1.6 wt% glutaraldehyde and 0.05 wt% HCl for 12 hours. The third membrane was pretreated in

0.1 wt% HEC for 1 hr., followed by crosslinking in 1 wt% H<sub>2</sub>SO<sub>4</sub> solution containing 80% acetone for 1 hour. Finally, polysulfone membranes coated with three hydrophilic polymers were washed in water thoroughly to remove the unreacted crosslinking agents, treated in both ethanol and hexane solutions for 2 hr each in succession, and dried at ambient temperature for the further use. Chitosan solutions consisting of 1.0 wt% chitosan for dense membrane and 0.5 wt% chitosan for the composite membrane in 10 wt% and 7 wt% aqueous acetic acid solutions for dense and composite membranes, respectively were filtered to remove any undissolved solids and impurities. Dense membrane was prepared by casting the polymer solution onto a clean glass plate using a casting knife designed in this Lab. For the preparation of composite membranes, the solution casting technique was used, however, when the polysulfone UF membrane is treated in dilute polymer solution, dip coating technique was applied to reduce the top layer thickness. Dense and composite membranes were treated in 3 wt% NaOH solution containing 50 wt% ethanol solution for 24 hours at room temperature, washed thoroughly to completely remove NaOH, dried at room temperature. Dense and composite membranes were crosslinked in the crosslinking solution consisting of 0.5 wt% glutaraldehyde and 0.05 wt% H<sub>2</sub>SO<sub>4</sub> in 80% acetone solution for 20 minutes, and then washed in deionized water thoroughly to remove any possible remnant. The membranes prepared and tested in this experiment are all listed in Table 5.1.

### 5.3.3 Pervaporation

Pervaporation apparatus and experiment was described in detail in chapter 3.

Membrane Number	Crosslinking	Dense membrane	Composite membrane		Binding polymer		
			1 $\mu$	10 $\mu$	PAA	PVA	HEC
Mem 1	-	O	-	-			
Mem 2	O	O	-	-			
Mem 3	-	-	-	O	-	-	-
Mem 4	O	-	-	O	-	-	-
Mem 5	-	-	-	O	O	-	-
Mem 6	-	-	-	O	-	O	-
Mem 7	-	-	-	O	-	-	O
Mem 8	O	-	-	O	-	O	-
Mem 9	O	-	O	-	-	O	-

**Table 5.1. The list of the membranes (- : No ; O : Yes)**

<i>Binding polymer-Crosslinking agent</i>	<i>Water flux(kg/m<sup>2</sup> hr)</i>
Untreated	268
Polyacrylic acid(PAA)- Al(NO <sub>3</sub> ) <sub>3</sub> ·9H <sub>2</sub> O	187
Polyvinylalcohol(PVA)-Glutaraldehyde	124
Hydroxyethylcellulose(HEC)-H <sub>2</sub> SO <sub>4</sub>	100

**Table 5.2. Water flux of polysulfone UF membranes pretreated in polymer solution (0.1 wt%)**

### **5.3.4 Scanning electron microscopy**

Scanning electron microscopy was used to study the cross section morphology of the various composite membranes and to measure the thickness of the membrane. Cryogenic fracturing of the membrane was done after freezing the samples in liquid nitrogen. All specimens were coated with a conductive layer (400Å) of sputtered gold. A Jeol JSM 805 scanning electron microscopy was used for the specimens at 20kV.

### **5.3.5 Fourier transform infrared (FT-IR) measurement**

A BOMEM Michelson series 100 FT-IR spectrometer was used to identify and characterize structural changes in the crosslinked chitosan membranes. The experiments were run with air as the background, and the resolution and number of scans were 4.0 cm<sup>-1</sup> and 16, respectively. Films were sandwiched between rectangular holders having a hole. The sample thickness was about 10µm.

## **5.4 RESULTS AND DISCUSSION**

### **5.4.1 Water permeability of pretreated UF membranes**

Water fluxes of the polysulfone UF membranes pretreated in the four binding polymer solutions were measured using ordinary reverse osmosis test equipment and are presented in Table 5.2. Water flux measurements could be an indicator of the changes of the UF membrane pores and surfaces. Membranes tested were crosslinked in the proper solution

after coating to prevent the dissolution from the water during the water permeation tests and pervaporation experiments. Water permeation rates decreased from 268 kg/m<sup>2</sup> hr of untreated UF polysulfone membrane to 187, 124 and 100 kg/m<sup>2</sup> hr for the membranes treated with PAA, PVA and HEC solutions as a result of the change of the membrane surface and pores. The binding polymer molecules penetrate into the pores of polysulfone membrane and are coated on the pore wall. Thus, it is believed that the pore size was reduced or even some pores were blocked. Also polymer molecules may be adsorbed on the surface of the membrane and form thin hydrophilic polymer layer. The above factors are considered to account for the decrease of the water permeation rates through the coated polysulfone UF membrane.

#### **5.4.2 SEM pictures of the composite membranes**

Scanning electron micrographs of the typical composite membranes are presented in Figure 5.1. It is obvious from the pictures that chitosan thin layer was properly cast on the top of the polysulfone substrate. Figure 5.1a and 5.1b show the morphology of polysulfone UF membrane prepared by wet phase inversion technique. Polysulfone substrate consists of microvoids in the form of honeycomb (Figure 5.1a) as well as bulbous macrovoids (Figure 5.1b) that is frequently found in the process of instantaneous demixing in wet phase inversion. The macrovoids do not span the entire width of the membrane as in the case of ultrafiltration membrane structures where the macrovoids are believed to be formed by intrusion of nonsolvent through defects in the skin layer during wet phase separation [Cabasso et al., 1977]. Figure 5.1c and 5.1d show the cross- section

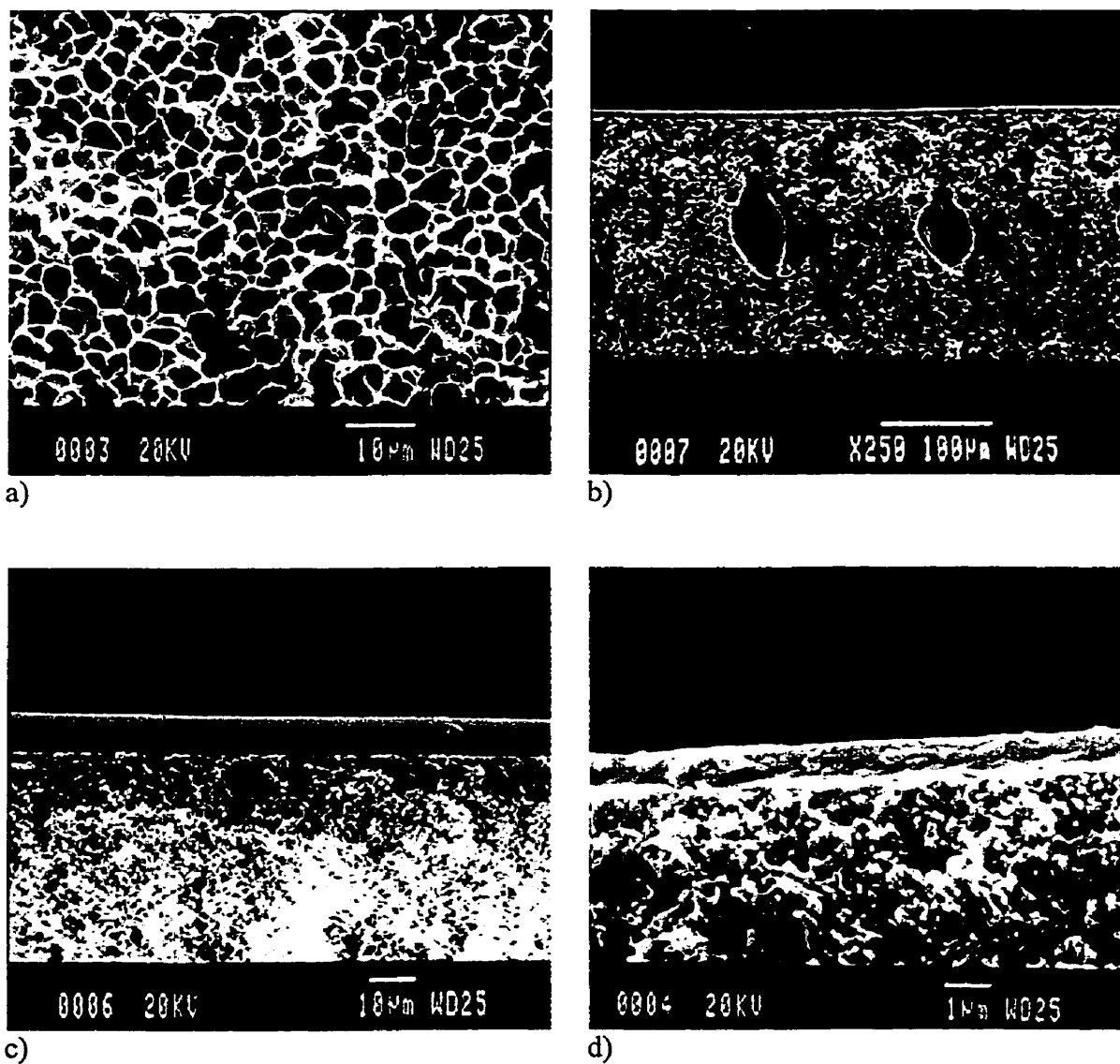


**Figure 5.1 SEM pictures of the composite membranes; a) and b) morphology of polysulfone substrates; c) cross-section of the chitosan/PSf composite membrane (Mem 4); d) cross-section of the chitosan/PSf composite membrane (Mem 9)**

of the composite membrane treated in dilute PVA solution after the chitosan layer casting. Chitosan layer thickness was approximately 10  $\mu\text{m}$  from SEM photo of Figure 5.1c without binding polymer treatment, where the solution casting method (pouring the chitosan solution on the polysulfone layer) was used because the poor wettability of hydrophilic chitosan against the hydrophobic polysulfone substrate restricts the dip coating method. The thickness of top layer could be reduced by dip coating method (immersing the polysulfone into the chitosan solution) when polysulfone membrane is treated in PVA polymer solution (Figure 5.1d).

### 5.4.3 FT-IR

IR spectra have been used to understand the crosslinking nature of glutaraldehyde (GA) with  $\text{H}_2\text{SO}_4$  which is used in this study. In general, GA crosslinking has been used with HCl catalyst. In this case, it is believed that HCl does not participate in the crosslinking reaction directly. However, when  $\text{H}_2\text{SO}_4$  is used instead of HCl, it is expected that  $\text{H}_2\text{SO}_4$  plays a role as a crosslinker and catalyst for GA crosslinking. In Figure 5.2, the bands at 1650 and 1560  $\text{cm}^{-1}$  which are representing amino I and amino II functional groups in chitosan [Aspinall, 1982; Chavasit et al., 1988] were shifted to the lower wavenumber when the membrane was crosslinked with three crosslinking agents, namely, GA with HCl,  $\text{H}_2\text{SO}_4$ , and GA with  $\text{H}_2\text{SO}_4$ . However, in the case of GA with HCl the shifting of the band is less pronounced and the relevant peaks are flattened. From the FT-IR peaks, it can be concluded that the nature of GA crosslinking with  $\text{H}_2\text{SO}_4$  is close to that of  $\text{H}_2\text{SO}_4$  crosslinking although a brown color, one of characteristics of GA crosslinking has been

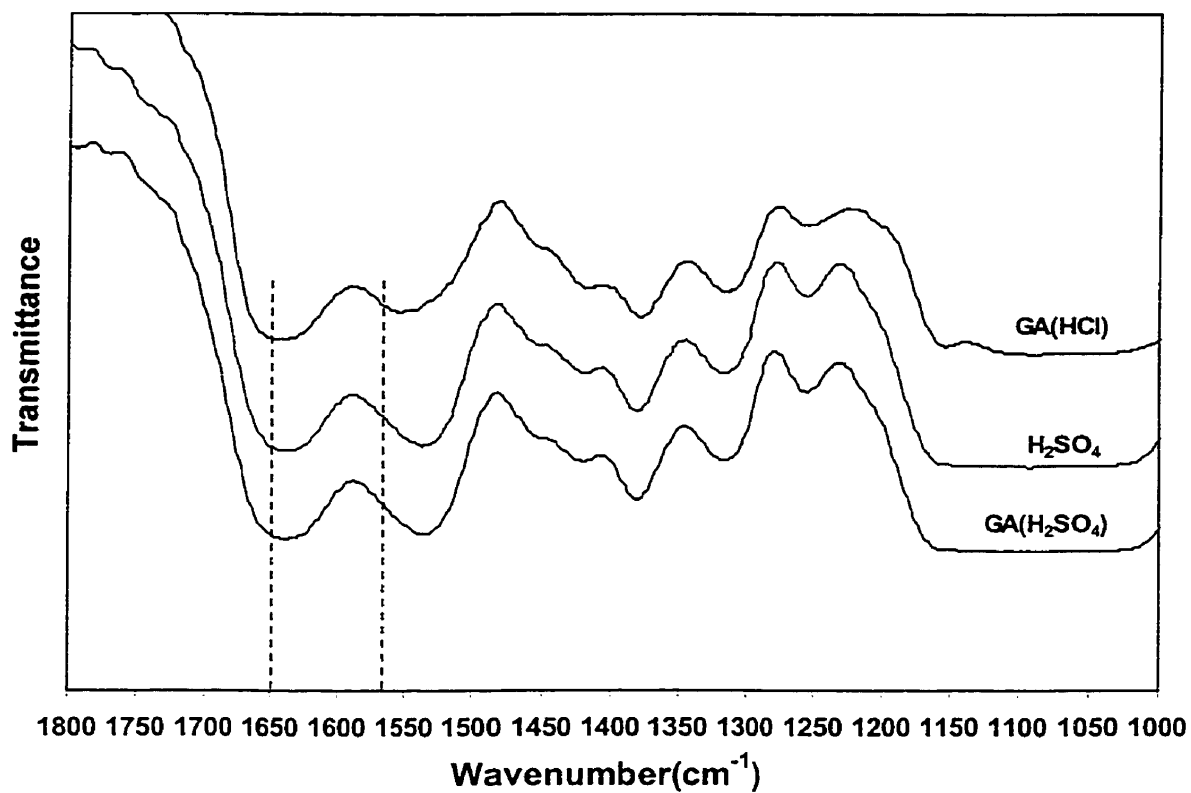


**Figure 5.2** Characterization of the crosslinking nature of GA with sulfuric acid for chitosan membrane compared to those of GA with HCl and sulfuric acid crosslinking

observed after crosslinking. This phenomenon explains that  $H_2SO_4$  function as an independent crosslinker rather than a catalyst for GA.

#### **5.4.4 Pervaporation experiments of the composite membrane without binding polymer**

The permeation flux and separation factor characteristics of isopropanol-water mixtures through four membranes including dense, crosslinked dense, composite and crosslinked composite membranes are compared in Figure 5.3 and 5.4. Crosslinking of chitosan membrane reduced the permeation flux, but increased the separation factor for both dense and composite membranes. This phenomenon can be explained by closely packed chain structure due to three-dimensional crosslinking. However, it should be pointed out that the chemical crosslinking changed not only the physical density but also the chemical nature such as hydrophilicity of the membrane. The thermal mobility of polymeric chains apparently dropped and the absolute free volume to diffuse the permeants through the membrane decreased due to the crosslinking. Thus, water molecules having relatively small molecular size can diffuse through the crosslinked membrane easily rather than isopropanol molecules having large molecular size. It was observed that the composite membrane was more effective than dense membrane in terms of the flux when isopropanol concentration is over 90 wt%. This interesting tendency seems to be the result of the thickness difference between the selective top layer of the composite membrane and dense membrane. The thickness of the composite membrane was approximately 10  $\mu m$ , whereas that of dense chitosan membrane was 20-40  $\mu m$ . Above

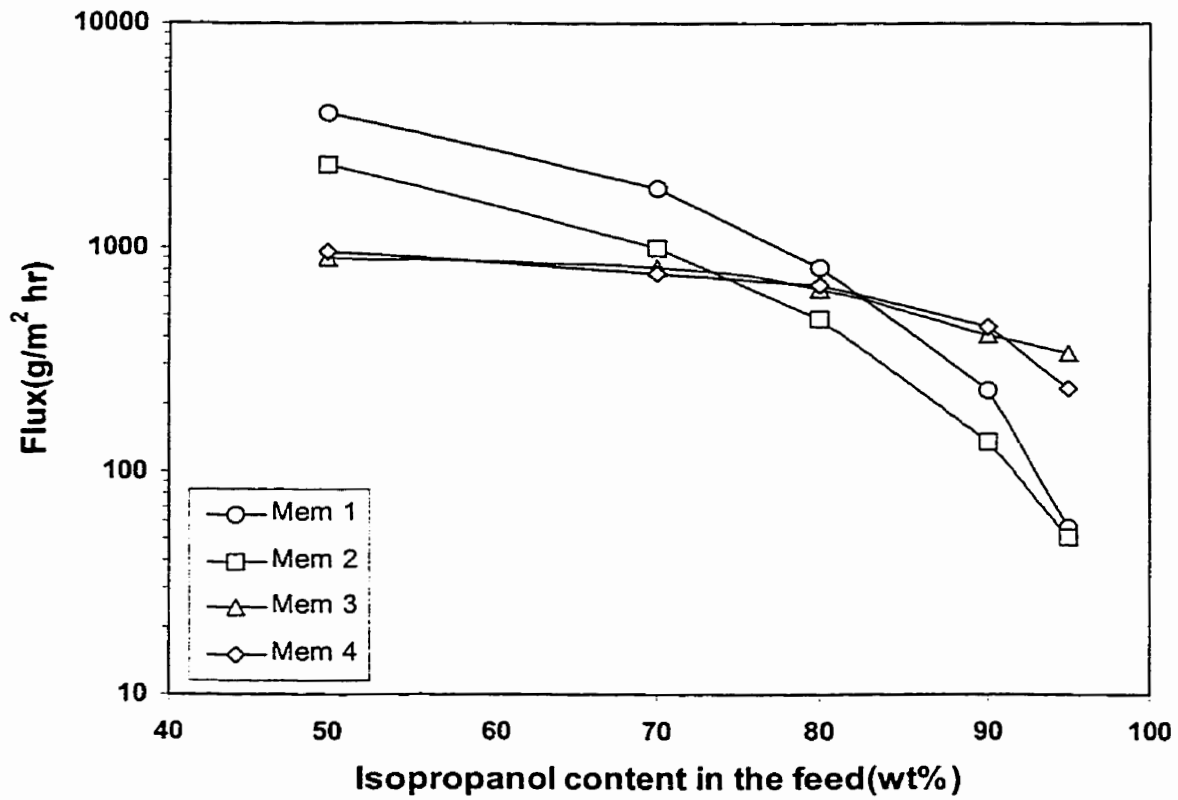


**Figure 5.3 Effect of feed concentration on the permeation flux at 50 °C for dense and composite membranes**

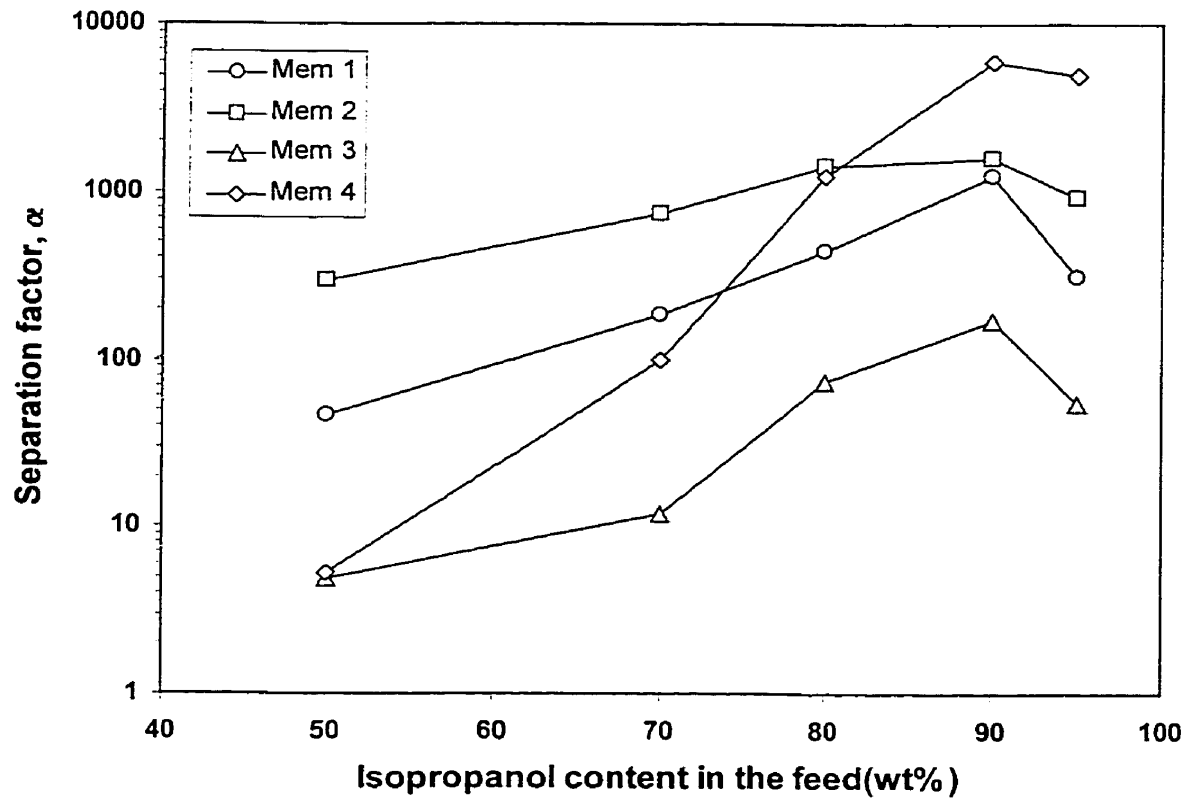


**Figure 5.4 Effect of feed concentration on the separation factor at 50 °C for dense and composite membranes**

90 wt% isopropanol concentration, membrane thickness was a dominant factor because the swelling was not significant at lower water concentration. Therefore, the fluxes of the composite membrane were much larger than those of the dense membranes when the water content in the feed was less than 20 wt% water concentration in the feed.

However, increasing the water content in the feed caused large swelling of the membrane by the plasticization of water that took over the permeation process for the dense membranes, whereas the swelling of chitosan top layer in the composite membrane is greatly depressed because it is anchored to the substrate. For crosslinked membranes, the flux of crosslinked composite membrane is still larger than that of crosslinked dense membrane because the membrane thickness continues to control the permeation as the result of the hindered swelling after crosslinking. In general, the separation factors of the crosslinked membrane were higher than those of non-crosslinked membranes. High separation factors of 4942 and 5912 and fluxes of 236 and 446 for 90 and 95 wt% isopropanol concentrations in the feed were obtained for the crosslinked composite membrane. High separation factors and fluxes are the required properties for successful composite membrane in the pervaporation application.

#### **5.4.5 Pervaporation experiments of the composite membrane with binding polymer**

As mentioned before, the treatment of polysulfone (PSf) substrate in dilute polymer solutions significantly changed the surface properties of the PSf membrane. It was noted that the spreading of chitosan solution during the solution casting on the PSf substrate was faster on the pretreated PSf substrate than on the untreated PSf substrate. Also, the

structural stability of the chitosan/PSf composite membrane was greatly increased as a result of the increased affinity between chitosan top layer and PSf substrate. This was confirmed with the pervaporation experiments for 90% water mixture. The composite membrane without binding polymer was eventually separated after the pervaporation operation at the feed mixture of 90 wt% water which is considered as an extreme swelling condition. However, in the case of the composite membrane treated in binding polymer solution, the structural integrity was maintained even under the forced swelling condition. Figures 5.5 and 5.6 show the permeation fluxes and the separation factors through the composite membranes pretreated in various polymer solutions such as polyvinyl alcohol, polyacrylic acid, and hydroxyethyl cellulose without crosslinking the chitosan layers. It is interesting to note the flux increase for the composite membrane pretreated in dilute binding solutions specially for the composite membrane treated in PVA solution in addition to the structural stability. Many aspects of binding polymer solutions can affect the permeability and selectivity of the pretreated composite membranes. Possible factors are as follows; the molecular weight of binding polymer, the amount of adhesion of binding polymer onto polysulfone substrate, the selection of crosslinking agents for these hydrophilic binding polymers and the extent of compatibility with chitosan. In previous experiments, PVA showed complete compatibility with chitosan over the whole blend ratio and crosslinking agent for PVA is well studied. The exceptional performance of the composite membrane pretreated in PVA solution was further evaluated for the crosslinked composite membranes in the next section.

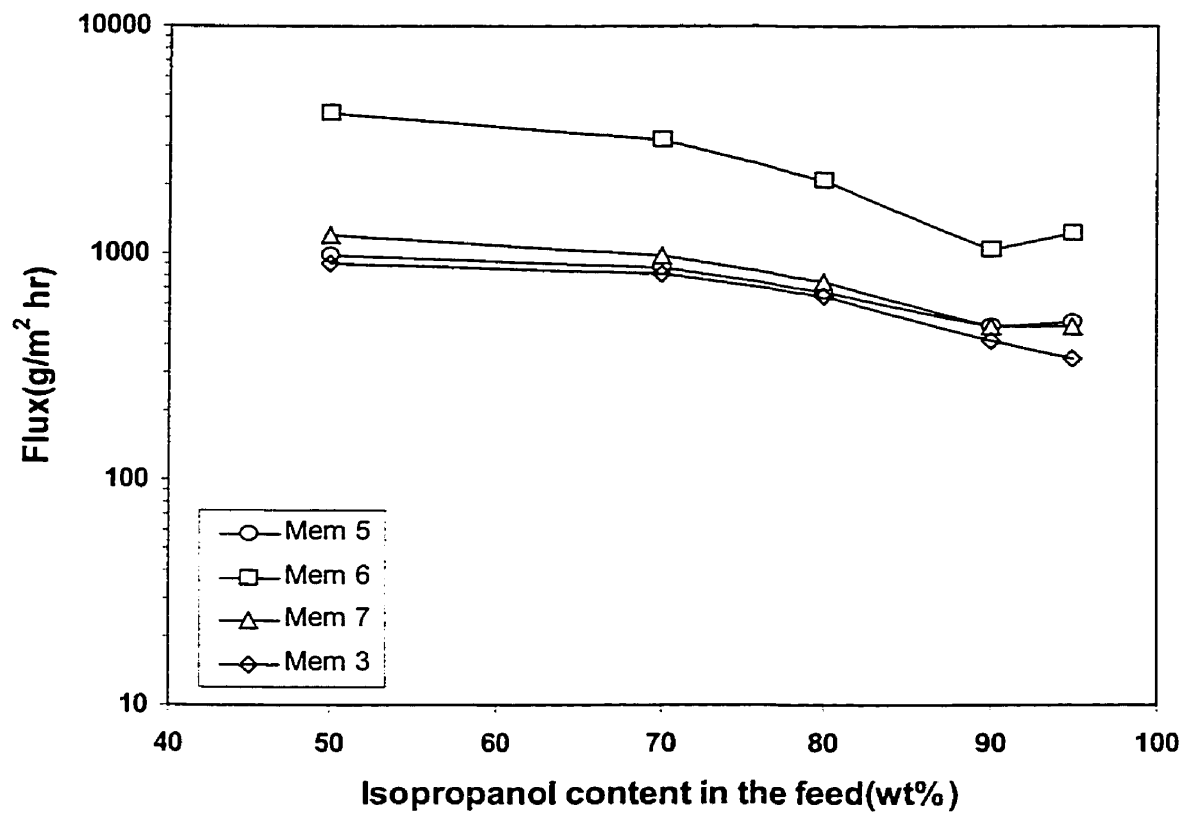
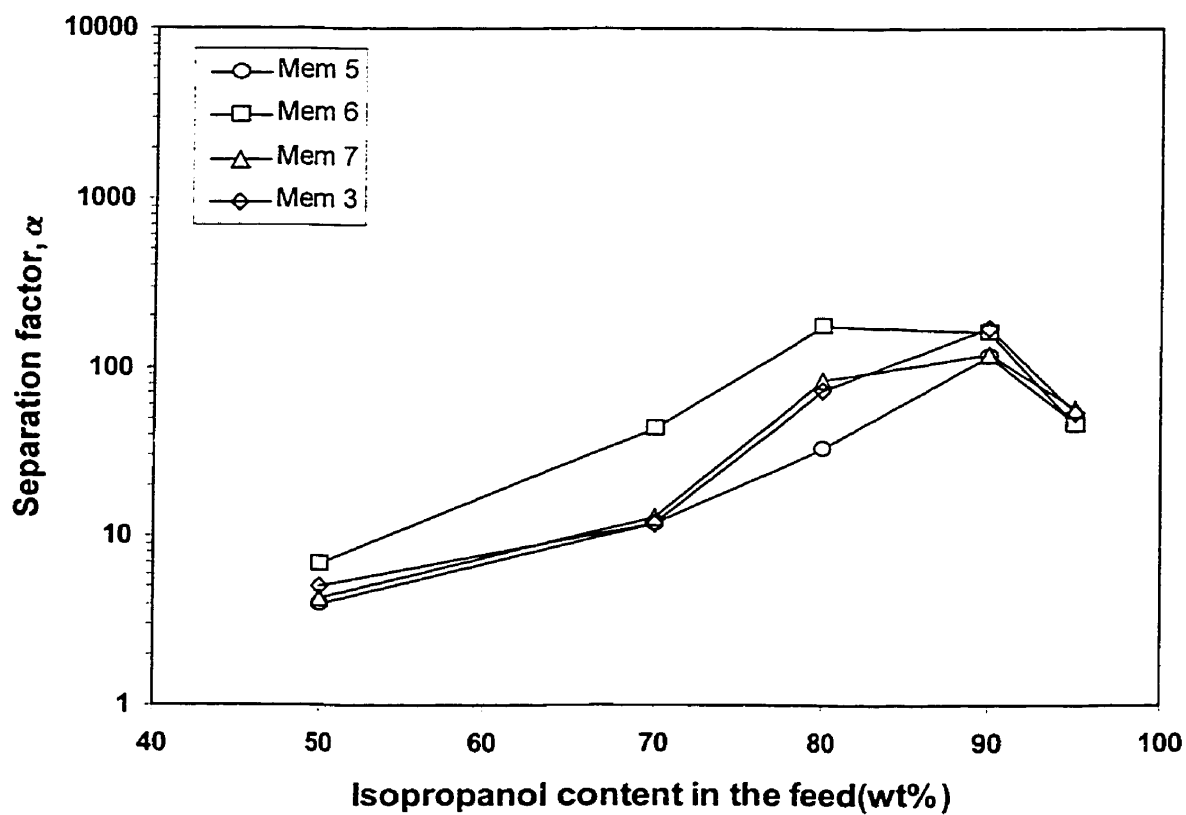


Figure 5.5 Effect of feed concentration on the flux at 50 °C for the composite membranes treated in various polymer solutions compared to that for the untreated Mem 3



**Figure 5.6** Effect of feed concentration on the separation factor at 50 °C for the composite membranes treated in various polymer solutions compared to that for the untreated Mem 3

#### **5.4.6 Pervaporation experiments of the composite membrane pretreated in PVA solution**

The pervaporation separations of isopropanol-water mixtures through the crosslinked chitosan/PSf composite membranes are compared in Figures 5.7 and 5.8. It is clear that the permeation fluxes of the composite membranes pretreated in PVA solution (Mem 8) are larger than that of the untreated composite membrane (Mem 4). This proves the existence of a resistance barrier between the selective chitosan top layer and the PSf substrate in a typical chitosan/PSf composite membrane. Very thin PVA coating applied to the surface or the pore of the substrate reduced the interface resistance. The separation factor exhibits the common trade-off phenomenon in Figure 5.8. In the case of uncrosslinked membrane, the separation factor of Mem 6 (PVA treated) is slightly higher than that of Mem 3 (untreated). However, in the crosslinked membranes it is controvertible that the separation factor of Mem 8 treated in PVA solution is much lower than that of untreated Mem 4 though affirmative aspects such as the increase of the flux and the structural stability were achieved by the pretreatment. It seems that the crosslinking reaction of the composite membranes plays an important role on the permselectivity.

Thickness reduction effects for the composite membrane top layer are presented in Figures 5.9 and 5.10. One of benefits of the pretreatment of substrate in PVA solution is the thickness reduction of top thin layer by changing the casting technique. In Figure 5.9, Mem 9 (1  $\mu\text{m}$ ) of the composite membrane was achieved by the dip coating method which was not used for the untreated PSf substrate because of the poor wettability of

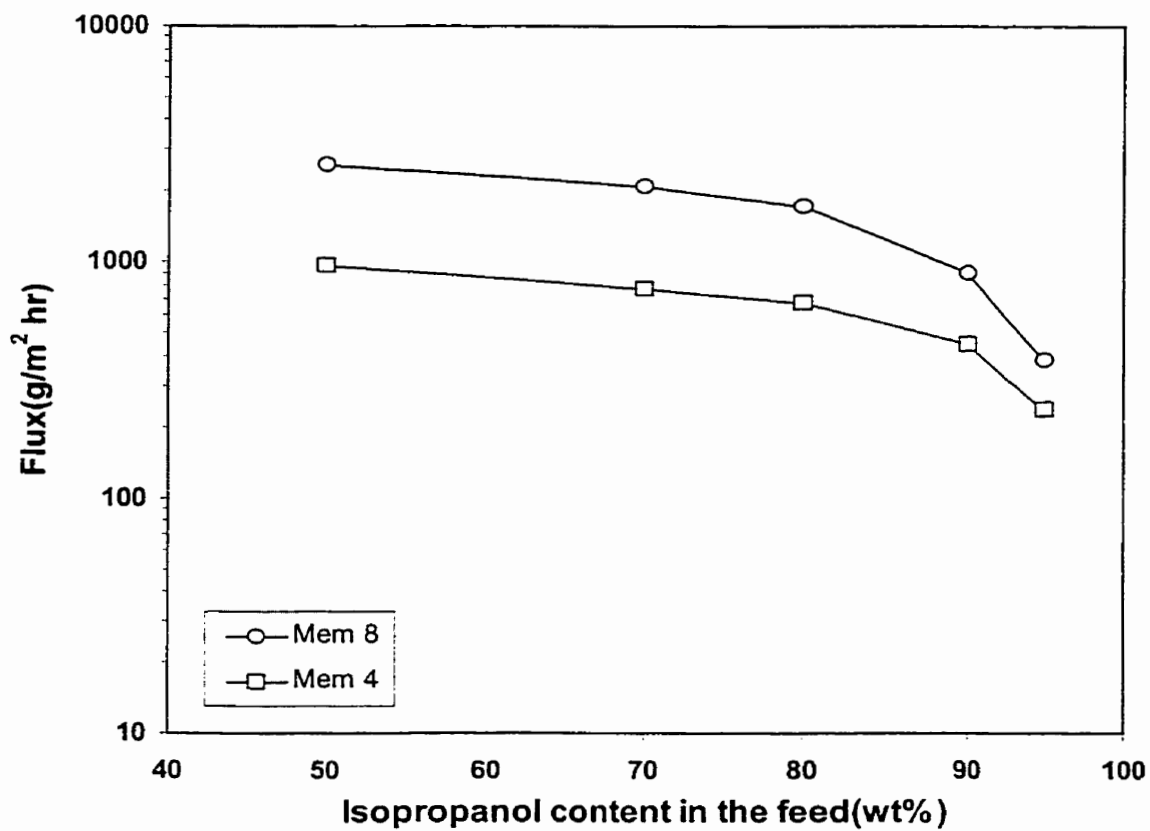
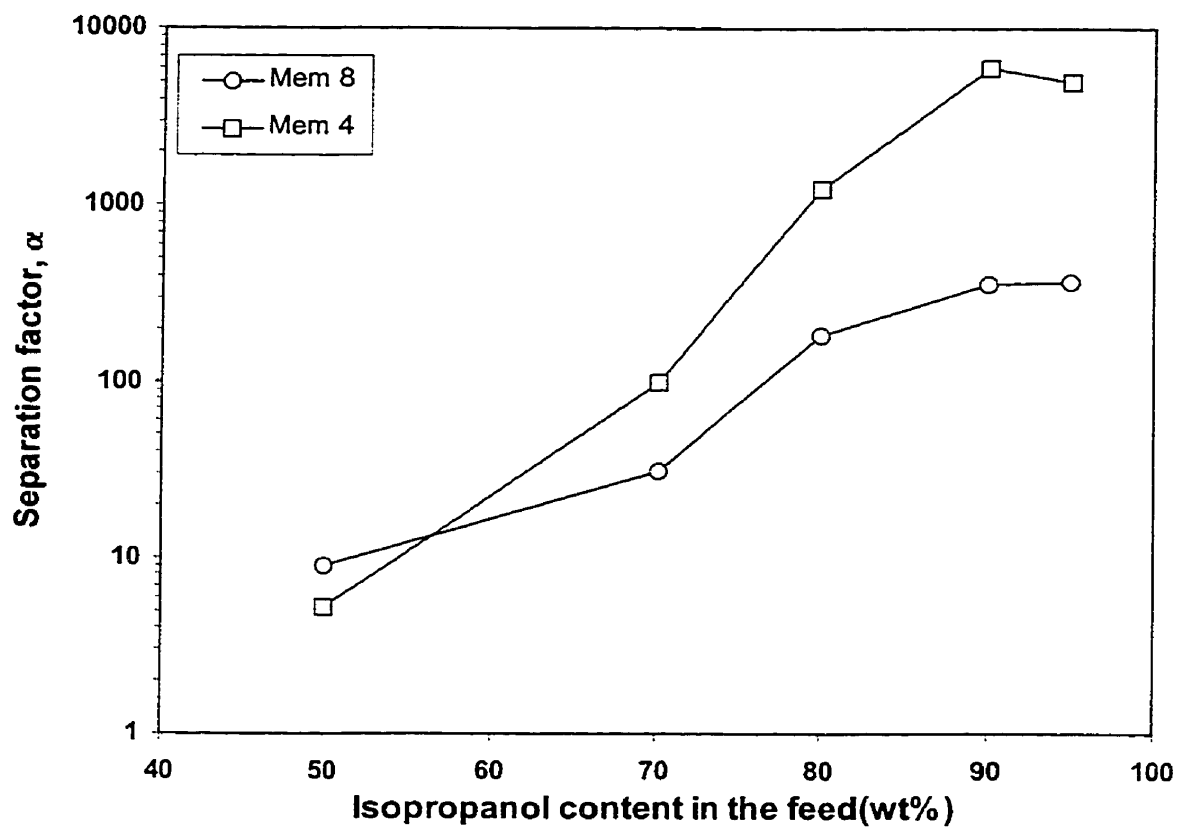
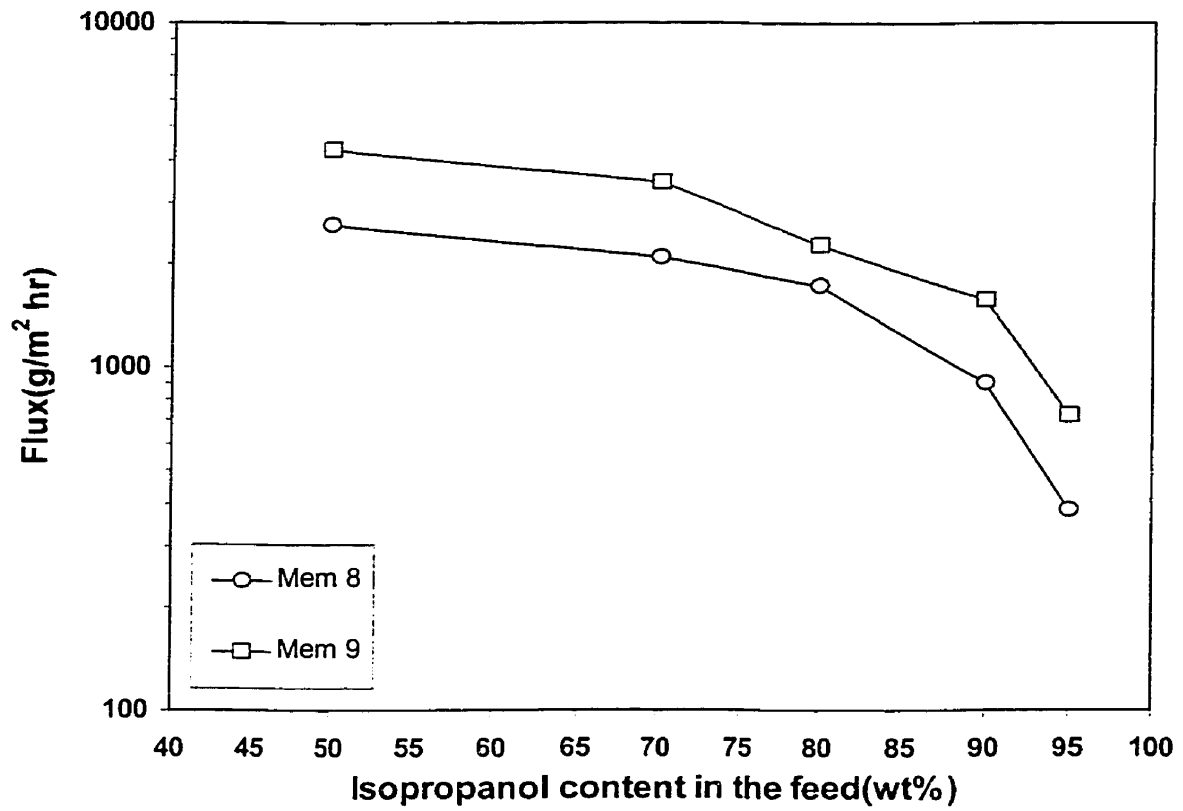


Figure 5.7 Effect of feed concentration on the flux at 50 °C through PVA treated (Mem 8) and untreated (Mem 4) composite membranes



**Figure 5.8 Effect of feed concentration on the separation factor at 50 °C through PVA treated (Mem 8) and untreated (Mem 4) composite membranes**



**Figure 5.9 Thickness effect of the crosslinked composite membrane on the flux at 50 °C (Mem 8 : 10  $\mu\text{m}$  ; Mem 9 : 1  $\mu\text{m}$ )**

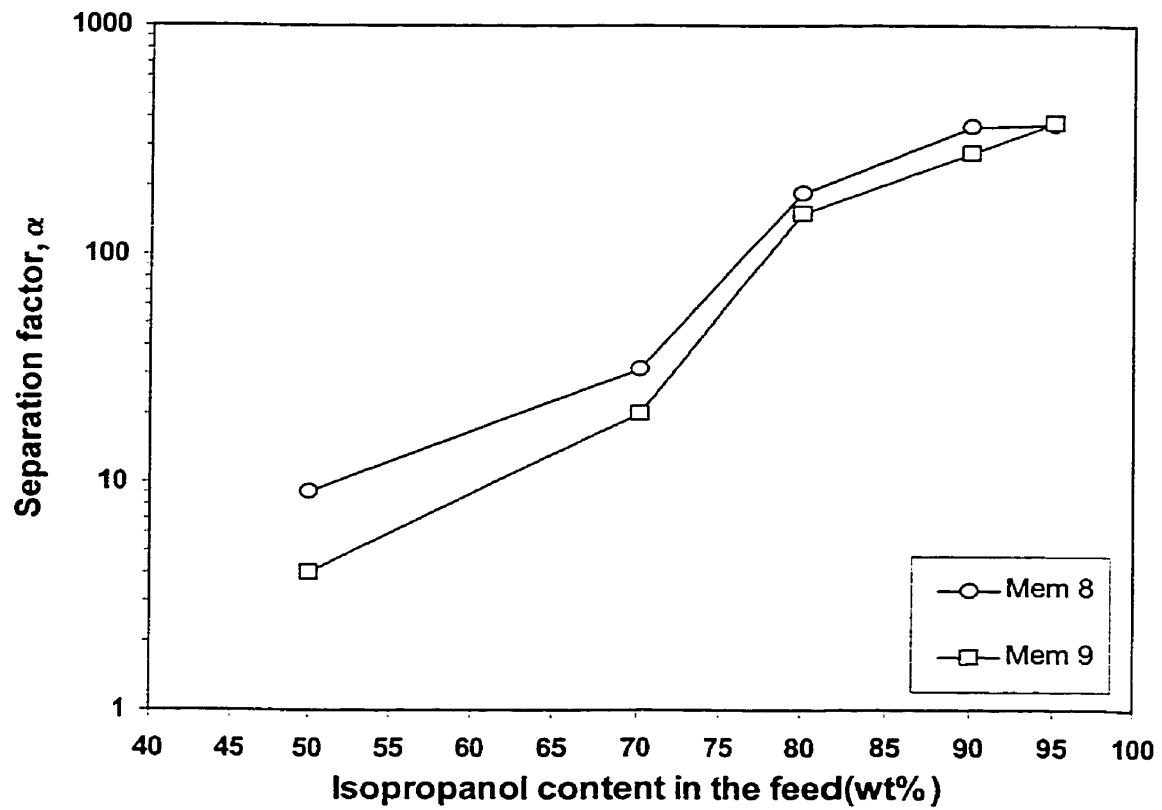


Figure 5.10 Thickness effect of the crosslinked composite membrane on the separation factor at 50 °C (Mem 8 : 10  $\mu\text{m}$  ; Mem 9 : 1  $\mu\text{m}$ )

chitosan solution. The permeation flux of Mem 9 (1  $\mu\text{m}$ ) composite membrane is much larger than that of Mem 8 (10  $\mu\text{m}$ ) composite membrane. As a rule of thumb, the permeation flux is inversely proportional to the membrane thickness. However, simultaneously decreasing the membrane thickness reduced the selectivity because the swelling of Mem 9 is much larger and fast than that of Mem 8.

#### **5.4.7 Temperature effect**

In principle, the effect of temperature on flux is positive. This is due to the increased thermal motion of the chain with increasing temperature that accelerates the diffusion of the permeants. A crosslinked composite membrane without PVA binder (Mem 4) has slightly higher sorption and diffusion activation energy than that of uncrosslinked composite membrane (Mem 3) due to the hindered diffusion in more dense structure as shown in Figure 5.11.

The flux increase with temperature is significant for the composite membrane treated in PVA solution (Mem 8). It can be also observed that the activation energy of the PVA bound composite membrane is higher than that of untreated composite membrane, suggesting that the existence of another interface (namely, coating) between chitosan and PSf substrate layers. The temperature effect of various composite membranes on the separation factor is shown in Figure 5.12. It can be seen that the separation factor increased with the temperature unexpectedly with the exception of the untreated composite membrane. It is usually assumed that the separation factor decreased with the increase of the temperature because the enlarged free volume of the membrane caused by

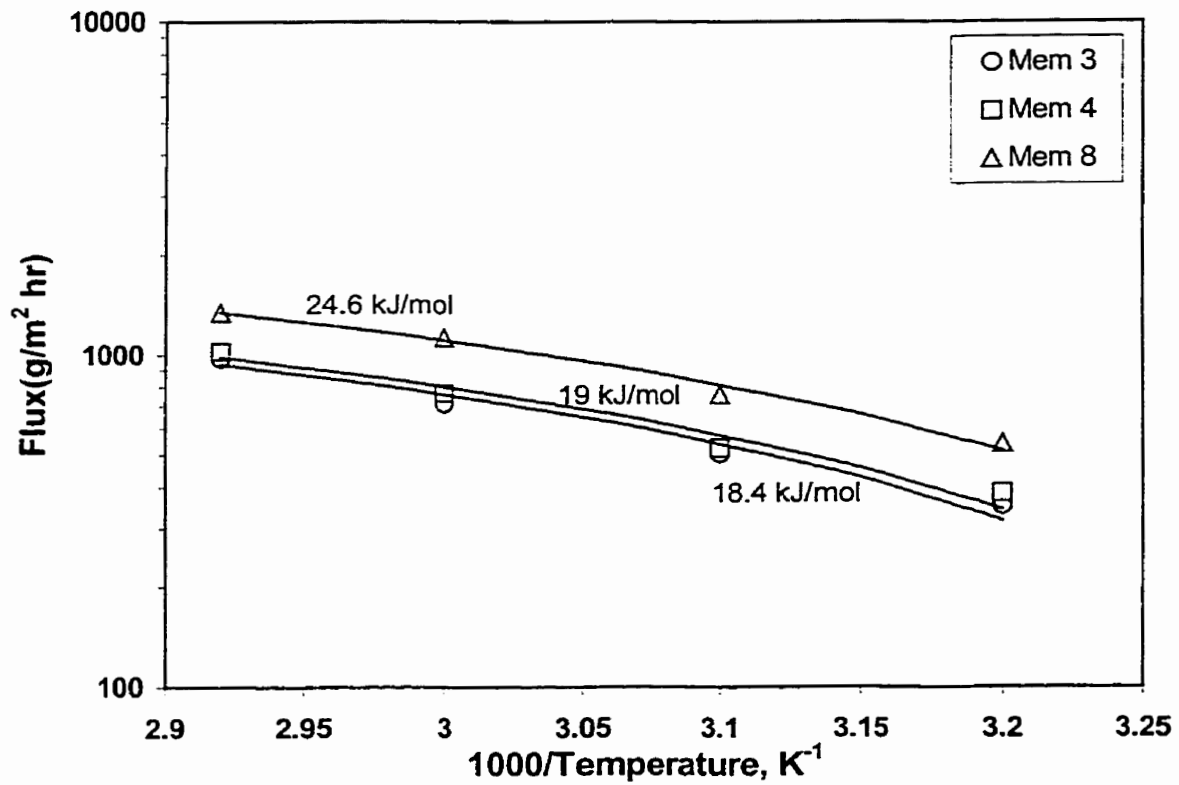
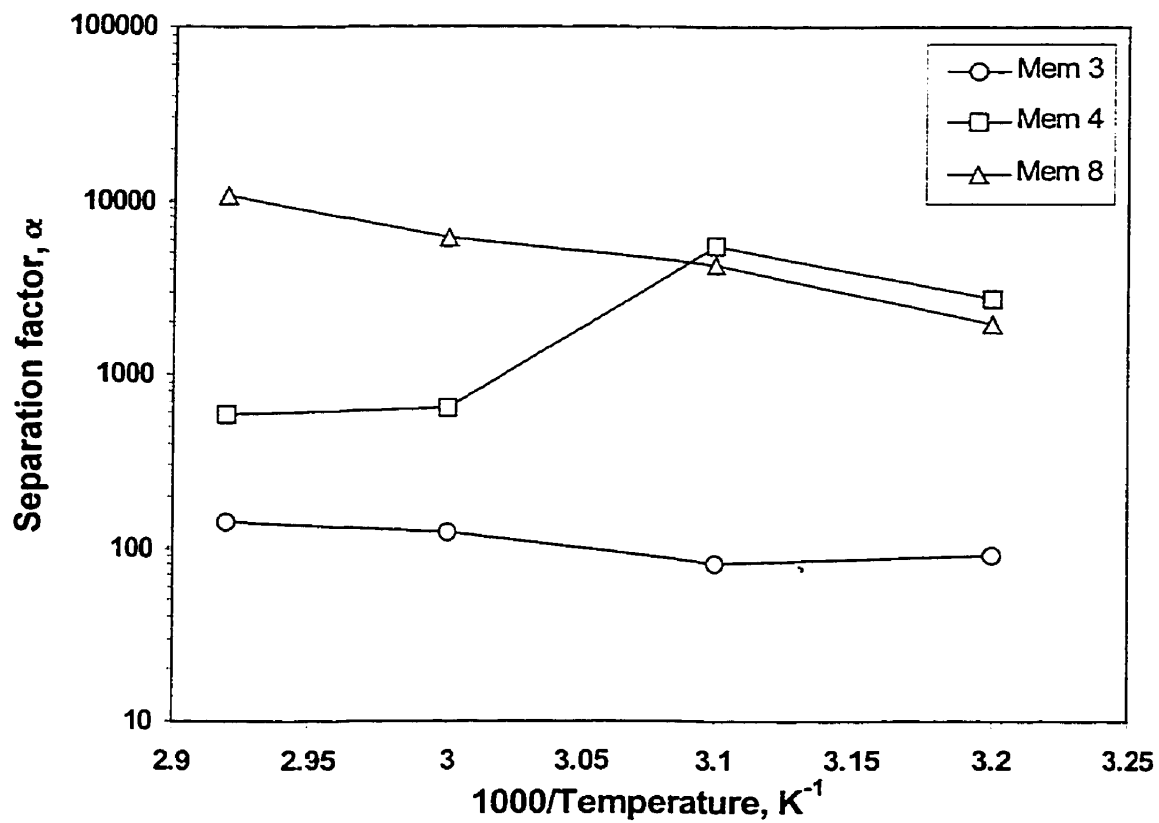


Figure 5.11 Arrhenius plot of the flux vs. reciprocal of temperature through the composite membranes at 90 wt% isopropanol



**Figure 5.12** Plot of the separation factor vs. reciprocal of temperature through the composite membranes at 90 wt% isopropanol

the temperature increase facilitates the transport of the feed mixtures. No direct explanation is available for above unusual phenomenon. However, it might be related to the feed mixture of 90 wt% alcohol and the material property, so called relaxation behavior. Chitosan membrane may experience two phenomena during the pervaporation operation. One is the swelling which depends on the feed concentration, and the other is the intrinsic relaxation behavior which was mainly studied in alginate membrane [Yeom et al., 1996b; Yeom & Lee, 1998a] but also potential for the polysaccharides such as chitosan. At the high isopropanol feed, the swelling of the chitosan is not so intense, whereas the polymer chains get packed slowly with the increase of temperature. The free volume of this packed membrane is still big enough to permeate water molecules but restricts the transport of relatively big isopropanol molecules. Thus, the increase of temperature only promotes the transport of water, which results in the increased flux and separation factor.

## 5.5 CONCLUSIONS

The following results have been obtained from the pervaporation experiment.

- Chitosan/PSf composite membrane has been prepared and crosslinked for the separation of isopropanol/water mixture. The crosslinking nature of glutaraldehyde with  $H_2SO_4$  has been investigated using FT-IR spectra.
- It was shown that the poor wettability of PSf substrate could be improved by immersion of substrate into dilute polymer solution before the top layer casting. Structural stability of the composite membrane was improved in this way. In addition to

structural stability, the permeation flux also increased due to the reduced hydrophobicity of PSf layer by coated ultrathin PVA layer.

It is believed that the porous substrate in the composite membrane acts not only as a mechanical support but also as part of selective layer affecting the pervaporation performance. Measurement of mechanical properties of the porous material and also of the composite membrane can be an interesting research topic in the future.

## CHAPTER 6

# PERVAPORATION DEHYDRATION OF AQUEOUS ETHANOL AND ISOPROPANOL MIXTURES THROUGH ALGINATE/CHITOSAN TWO PLY COMPOSITE MEMBRANES SUPPORTED BY POLY (VINYLIDENE FLUORIDE) POROUS MEMBRANE\*

---

### 6.1 SUMMARY

Composite membranes consisting of an active alginate layer and supporting chitosan layer on top of the base porous blended polyvinylidene fluoride (PVDF) membrane were prepared and tested for pervaporation dehydration applications. Efforts to enhance the surface properties of PVDF by blending with relatively hydrophilic polymethyl methacrylate (PMMA) were carried out and evaluated by contact angle measurements. Various modifications for the alginate/chitosan composite membranes such as converting to the free acid form and crosslinking with cobalt ion were investigated. They were then compared for the pervaporation dehydration of ethanol/water and isopropanol/water mixtures and the temperature effect on the permeation flux was also investigated.

---

\* Part of this study has been published in *Journal of Membrane Science*, 167(2000), 275-289

## 6.2 INTRODUCTION

The principle of the pervaporation membrane separation process is relatively simple. The minor component of the liquid mixture is preferentially separated with phase change through polymeric dense membranes at efficiencies considerably better than those obtained in other separation processes such as distillation, adsorption and fractional crystallization processes. Its advantages are particularly apparent when azeotropic mixtures are to be separated. Areas where the pervaporation separation process is beginning to have large impacts are in the dehydration of aqueous organic mixtures, the removal of organic (especially environmental pollutants) from organic/water mixtures, and the separation of organic/organic mixtures.

Currently, polysaccharides have been gaining much attention as pervaporation membrane materials for the dehydration of aqueous organic systems. In particular sodium alginate has been explored for the pervaporation dehydration of alcohol due to its extremely high water selectivity, while chitosan has been investigated due to its excellent chemical and mechanical stability as well as its high hydrophilicity. Although sodium alginate shows strong hydrophilicity, it has not been used as a thin film membrane material for pervaporation dehydration because of its water solubility and mechanical weakness. Its applicability as a new pervaporation membrane is increasing these days after ionic crosslinking and insolubilization treatment. However, concerns about its mechanical weakness remain. It is believed that alginate, being polyanionic forms a polyelectrolyte complex when it contacts chitosan, which is polycationic. It is clear that chitosan and sodium alginate cannot form the homogeneous blend because the oppositely charged

functional groups form the precipitates upon the ionic reaction. Very recently, Zhang et al. [2000] reported the homogeneous blend membranes from carboxymethylated chitosan (CMC)/alginate solutions. This is because CMC is no longer cationic but nonionic. The chitosan/alginate polyelectrolyte complex was studied mainly in controlled delivery systems for macromolecular drugs [Huguet et al., 1994; Hari et al., 1996; Chandy et al., 1994; Lee et al., 1997; Wheatly et al., 1991]. It was recognized that the chitosan layer increased the stability of alginate capsules or controlled the diffusion rates of the encapsulated materials. Recently Yeom et al. [Yeom et al., 1998c] synthesized a  $\text{Ca}^{2+}$  crosslinked alginate membrane having a polyelectrolyte complex layer with chitosan for the recovery of anionic surfactant by the reverse osmosis (RO) process, and demonstrated the existence of ionic interactions that stabilizes the alginate separation performance. As a part of an effort to enhance the mechanical strength for pervaporation applications, we reported the preparation of novel two ply membranes consisting of alginate and chitosan in a previous publication [Moon et al., 1999]. Chitosan and sodium alginate solutions were cast in succession, and preparation and operating parameters such as polymer types facing to the feed stream, NaOH treatment for the regeneration of chitosan, and crosslinking system types were investigated using a factorial design method. As a continuation of the two ply membrane research program, we prepared another pervaporation membrane which consists of an active hydrophilic alginate layer buffered by chitosan which is hydrophilic with good film forming properties on top of a modified poly(vinylidene fluoride) (PVDF) porous membrane. It is known that PVDF is a hydrophobic and chemically inert fluoropolymer which can tolerate high temperature feed solutions. In the ultrafiltration process, fouling and concentration polarization are the

major limitations to broad PVDF application. It is generally recognized that more hydrophilic membranes tend to have less fouling and exhibit high flux, high rejection ratio and slow flux declines. There are various techniques to make UF membrane more hydrophilic such as blending, the introduction of hydrophilic functional group into the membrane surface, plasma treatment and coating [Musale & Kulkarni, 1998] as well as self-organizing blend of an amphiphilic comb polymer [Hester et al., 1999]. Among the many attempts to make PVDF more hydrophilic, blending strategy is reported to be the most feasible method [Nunes & Peinemann, 1992]. In the present investigation, the morphology of the porous PVDF layer, the hydrophilicity change resulting from the blending and the pervaporation characteristics of this new alginate/chitosan two ply composite membrane are reported in detail.

## **6.3 EXPERIMENTAL**

### **6.3.1 Materials**

Sodium alginate and cobalt(II) nitrate were obtained from Sigma Chemical Co. Chitosan flakes (Flonac-N) of MW 100,000 and 99% N-deacetylation degree were donated by Kyowa Technos Inc, Japan. Poly(vinylidene fluoride) of MW 350,000 and poly(methyl methacrylate) of MW 75,000 were purchased from Polyscience Inc., USA in powder forms. H<sub>2</sub>SO<sub>4</sub> was supplied by BDH Chemicals Co., Toronto, ON. Calcium chloride was provided by Fisher Scientific. A non-woven polyester fabric from Veratec division of

International Paper Co., USA was used as the backing material for the composite membrane. Water was de-ionized before use.

### 6.3.2 Membrane Preparation

Sodium alginate was dissolved in water to form a homogeneous solution of 0.5 wt %. Chitosan solution was prepared by dissolving 0.5 wt% chitosan in dilute aqueous acetic acid solution. Both sodium alginate and chitosan solutions were filtered to remove any undissolved solids and impurities.

Poly(vinylidene fluoride) membranes were prepared via the wet phase inversion technique from casting solution containing 15 wt% PVDF, 1 wt% poly(methyl methacrylate), and 84 wt% N,N-dimethylformamide (DMF). In order to increase the wettability of chitosan solution on top of the PVDF porous membrane relatively hydrophilic PMMA was blended with PVDF and the blending ratio was evaluated in terms of hydrophilicity using contact angle measurements. The casting solution for porous support membrane was poured onto a polyester non-woven fabric held on a glass plate with the aid of a casting knife made in this laboratory. The cast film was immediately immersed into a coagulation water bath. The resulting membrane was washed in de-ionized water thoroughly and air-dried completely at ambient temperature. The initial microporous poly(vinylidene fluoride) membrane showed a pure water permeation rate of  $89 \text{ kg/m}^2 \text{ hr}$  at transmembrane pressure of 100 psi and operating temperature  $22 \text{ }^\circ\text{C}$ . Water flux tests were performed in replicate to achieve precision in the flux. Finally, for the preparation of composite membranes, the dip coating technique

was used. At first, chitosan solution poured onto the PVDF membranes which was glued to the bottom of a glass container, excessive chitosan solution was removed from the glass container after 10 minutes, and then the composite membranes were dried completely. After the drying of the chitosan layer, 0.5% alginate solution was added into the glass container again to get double top layers in the same way with the addition of chitosan solution. The alginate layer of the composite membranes were further insolubilized in sulfuric acid solutions containing 50 vol% isopropanol for 10 minutes at room temperature, washed thoroughly to completely remove the remnant solvents, then dried at room temperature. Originally there was a special consideration for the interface layer because of the possibility of polyelectrolyte complex formation between polyion layers [Schamagl et al., 1996]. However, since the chitosan layer before the casting of alginate layer was dried, the possible formation of polyelectrolyte is believed to be minimal in this study. Crosslinking of the alginate layer of the composite membranes was carried out by immersing them into the crosslinking solution consisting of 0.1M cobalt nitrate for 10 minutes, and then washed in deionized water thoroughly to remove any possible remnant.

### **6.3.3 Swelling and Sorption experiments**

The steady state liquid uptake was measured in order to obtain sorption data for the alginic acid membranes, sodium, and cobalt alginate membranes respectively. The square shaped membranes were soaked into the 90 wt% ethanol and isopropanol solutions for the equilibration period of 1day. After carefully blotting off the surface liquid with tissue

paper as quickly as possible, they were put into glass tubes, which were connected to the pervaporation apparatus. The liquid absorbed in the membrane was collected in the cold traps, weighed, and analyzed by using GC to obtain the sorbed liquid amount and sorption selectivity. In analogy to the pervaporation experiment, the degree of swelling and sorption selectivity are calculated as follows;

$$\text{Swelling degree} = \frac{W_s - W_d}{W_d} \times 100$$

$$\alpha_{\text{water / alcohol}}^{\text{sorption}} = [C_W / C_A] / [X_W / X_A]$$

where  $W_d$  and  $W_s$  indicate the weight of the dry and swollen membranes, respectively and  $C$  and  $X$  is the weight fractions of the permeate and feed components in the membrane at the equilibrium sorption, respectively.

#### 6.3.4 Pervaporation

The pervaporation experiment was carried out using the apparatus and method described in chapter 3.

#### 6.3.5 Infrared spectroscopy

FT-IR spectroscopy was conducted on the membranes before and after the treatment using sulfuric acid as an attempt to detect the new chemical bonds or the change of chemical bonds caused by the insolubilization treatment of alginate membranes and compared to the chemical bonds of the alginate membranes. A BOMEM Michelson series 100 FT-IR spectrometer was used. The experiments were run with air as the

background, and the resolution and number of scans were  $4.0 \text{ cm}^{-1}$  and 16, respectively. Films were sandwiched between rectangular holders, whose insides were circularly cut. The sample thickness was about  $10 \text{ }\mu\text{m}$ .

### 6.3.6 Contact angle measurement

In order to make the chitosan solution spread over easily on the top of the supporting PVDF membrane, PMMA which is relatively hydrophilic and miscible with PVDF was solution-blended with PVDF to form the blended PVDF membrane. Contact angle measurements for the investigation of the wetting behaviour and the surface energy properties of blended PVDF membrane were carried out using the Video Contact Angle 2500 System of ASC products, USA. Water drop images were frozen in 10 sec after the dropping of water on the membrane surface and angle values were obtained, to get reliable data 10 contact angle values were measured for each membrane. Also the work  $w_A$  necessary to pull water from a square meter of membrane surface can be calculated as follows;

$$w_A = \gamma_w (1 + \cos \theta)$$

where  $\gamma_w$  is water surface tension ( $7.28 \times 10^{-2} \text{ N/m}$ ).

Contact angle values and adhesion data are presented in Table 6.1.

### 6.3.7 Scanning electron microscopy

Scanning electron microscopy was used to study the cross section morphology of the composite membranes and to measure the thickness of the membrane. Cryogenic fracturing of the membrane was done after freezing the samples in liquid nitrogen. All specimens were coated with a conductive layer of sputtered gold. A Hitachi S-570 scanning electron microscopy was used for the specimens at 15kV.

## **6.4 RESULTS AND DISCUSSION**

### **6.4.1 Surface characteristics of PVDF porous membrane and morphology of composite membrane**

In a previous paper [Huang et al., 1999a], we reported a chitosan composite membrane supported by a polysulfone porous membrane. Since polysulfone had opposite wetting properties compared to the hydrophilic chitosan top layer material, the structural stability of the composite membrane was weakened after a long pervaporation operating time, and then eventually the chitosan top layer became separated from the support layer. To overcome this noticeable drawback of polysulfone as a supporting membrane, polysulfone membrane was soaked in dilute polyvinylalcohol (PVA) solution before casting the chitosan layer. This PVA thin coating significantly increased the membrane stability as well as being able to reduce the top layer thickness by increasing the chitosan wettability on top of the modified polysulfone. In this study, PVDF was used as the porous support material. As a usual ultrafiltration membrane, polyvinylidene fluoride (PVDF) has been known to be relatively hydrophobic. Its hydrophobicity contrasts with

the hydrophilicity of chitosan. Thus the blending of PVDF with a more hydrophilic polymer was tried to improve compatibility with the top layer casting material. It is known that PVDF and PMMA are completely miscible with each other and form a homogeneous blend. The changed surface property was measured in terms of hydrophilicity using contact angle measurements. In Table 6.1, it is shown that the addition of PMMA into the matrix of PVDF improved the hydrophilicity of blended PVDF membrane. The contact angle of a cobalt crosslinked alginate membrane was measured for comparison as shown in this table.

When one prepares a composite membrane for pervaporation dehydration, the similar hydrophilicity or chemical affinity between the support membrane and the top layer has several advantages such as improved structural stability and reduced top layer thickness resulting from the easy spreading of the top layer solution. However, although the hydrophilicity of supporting membrane was improved with the blending, as shown in Table 6.1, the surface properties of the alginate top layer and the PVDF supporting membranes are still substantially different. The problem occurring from the difference of surface properties was examined for the morphological study of the composite membrane using SEM. SEM photographs are shown in Figure 6.1. The thin top layer consisting of chitosan below the alginate is clearly shown to be supported by the porous PVDF membrane. Total thickness of top layer is approximately 5  $\mu\text{m}$  and that of the chitosan layer occupies less than 2  $\mu\text{m}$ . Here the alginate layer is the permselective layer, whereas the chitosan layer plays potential roles for the following reasons. First when the alginate membrane is not crosslinked or even crosslinked, it may collapse after a long pervaporation operation time because of its natural water-solubility. However, in

combination with the chitosan barrier this can be improved because chitosan has good film forming properties and relatively good mechanical strength. Secondly in preparing the composite membrane, the blended PVDF is still hydrophobic in spite of the improved hydrophilicity due to the blending. Thus the chitosan layer makes the casting and spreading of the next alginate layer much easier. The direct casting of the alginate layer without the chitosan buffer layer can lead to a thick alginate top layer which can eventually be separated in the swollen state from the porous PVDF membrane.

Type of membrane	Contact angle	Adhesion work( $\times 10^2$ )
15% PVDF	75°	9.16 N/m
15% PVDF/1% PMMA	71°	9.65 N/m
PMMA	67°	10.12 N/m
Cobalt crosslinked alginate	55°	11.45 N/m

**Table 6.1 Contact angle values and adhesion works of water drops for PVDF membranes**

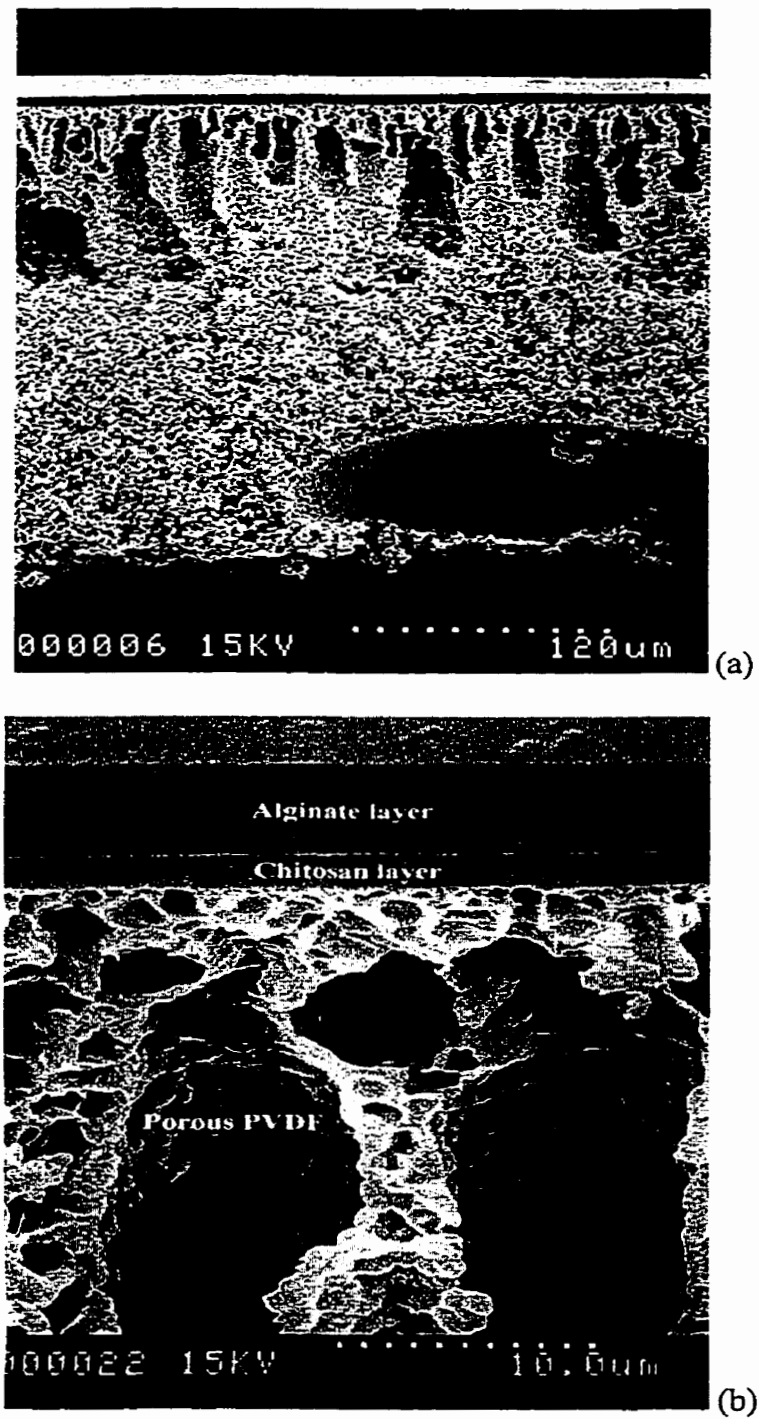


**Figure 6.1 SEM photographs of the cross-section of the composite membrane; a) overview of the cross-section, b) adjacent view of top layer**

### 6.4.2 Sorption experiment

The sorption properties of the various alginate membranes have been investigated for 90 wt% ethanol and isopropanol mixtures at room temperature and are presented in Figure 6.2. The five membranes tested are sodium alginate and cobalt crosslinked alginates, and three different alginic acid membranes which were converted from sodium alginates by using different concentrations of sulfuric acid solutions. It has long been recognized that the sorption properties are helpful for the selection of proper membrane materials and subsequent chemical treatment because the pervaporation properties of the membranes partly rely on sorption characteristics. However, it must be pointed out first that the sorption data does not always necessarily correspond to the permeability data because the diffusion phenomenon through the membrane also significantly contributes to the permeability. Some knowledge was obtained with sorption experiment and can be rationalized as follows. For the ethanol mixture, the swelling degrees of sodium alginate membrane are much higher than those of crosslinked and free acid form membranes because the structures of crosslinked and converted membranes are more packed than that of the sodium alginate membranes. For sorption selectivity, selectivities of crosslinked alginate membranes with divalent ions are higher than those of the others. Thus, crosslinked membranes show lower flux and higher separation factors than their uncrosslinked membrane counterparts. It was found that sodium and crosslinked alginate membranes follow this rule of thumb. When sodium alginate membranes are converted to its free acid form, the sorption ability and selectivity decreased although the alginic acid membranes are insoluble in water and mechanically robust compared to sodium alginate.

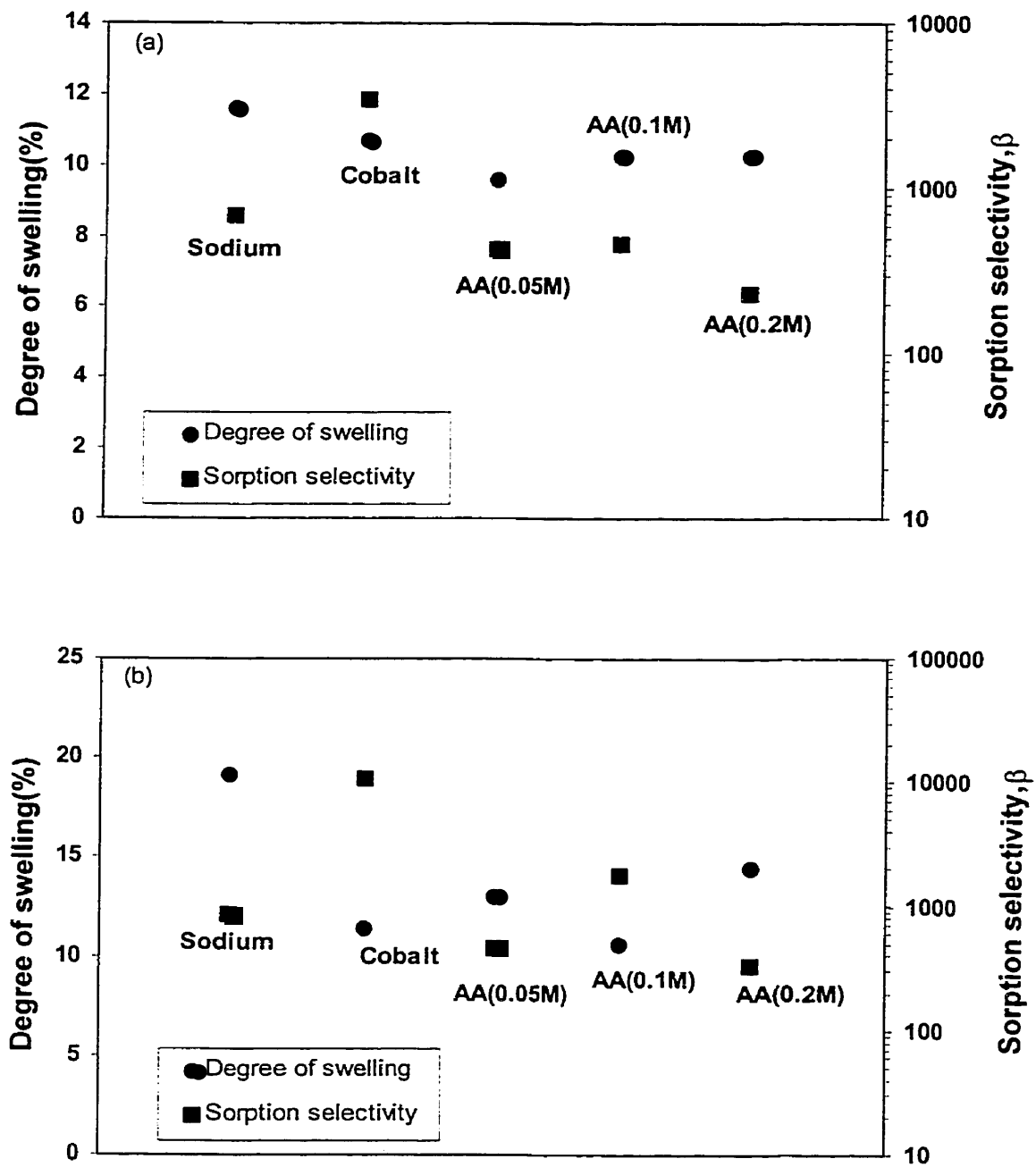


Figure 6.2 The degree of swelling and sorption selectivity for various alginate and alginate membranes in 90 wt% ethanol (a) and isopropanol (b) mixtures at room temperature

Among the three different alginic acid membranes, those converted with 0.1M sulfuric acid solution appeared to be more water selective than acid membranes converted with 0.05M and 0.2M sulfuric acid solutions.

For the 90% isopropanol mixture, the sodium alginate membrane has the highest swelling degree as found for the ethanol mixtures. The general trend for the isopropanol sorption experiments is almost similar to that for the ethanol mixture. The selectivity of the cobalt crosslinked membrane is the highest like that found for the ethanol mixture. It is believed that the crosslinker type and interaction between crosslinked membrane and feed mixture affect the separation performance of the membrane. The highest sorption selectivity among alginic acid membranes was achieved for alginic acid membrane converted in 0.1 M sulfuric acid solution as found for the ethanol mixture. However, it is interesting to note that the affinity to water is much higher than the sodium alginate membrane. The sorption experiment for ethanol and isopropanol mixtures show that the permselectivities of alginic acid membranes are not superior to the sodium alginate salt membranes.

#### **6.4.3 Infrared (IR) spectroscopy**

In previous sorption experiment, three alginic acid membranes converted in different sulfuric acid concentrations which revealed different sorption characteristics were studied. IR spectroscopy has been applied to detect possible functional group or configuration difference between these membranes. It was reported that the strong band at  $1743\text{ cm}^{-1}$  could be indicative of the free carboxyl group of alginic acid, whereas the bands at  $1620$  and that at  $1416\text{ cm}^{-1}$  was assigned to the presence of the salified carboxyl

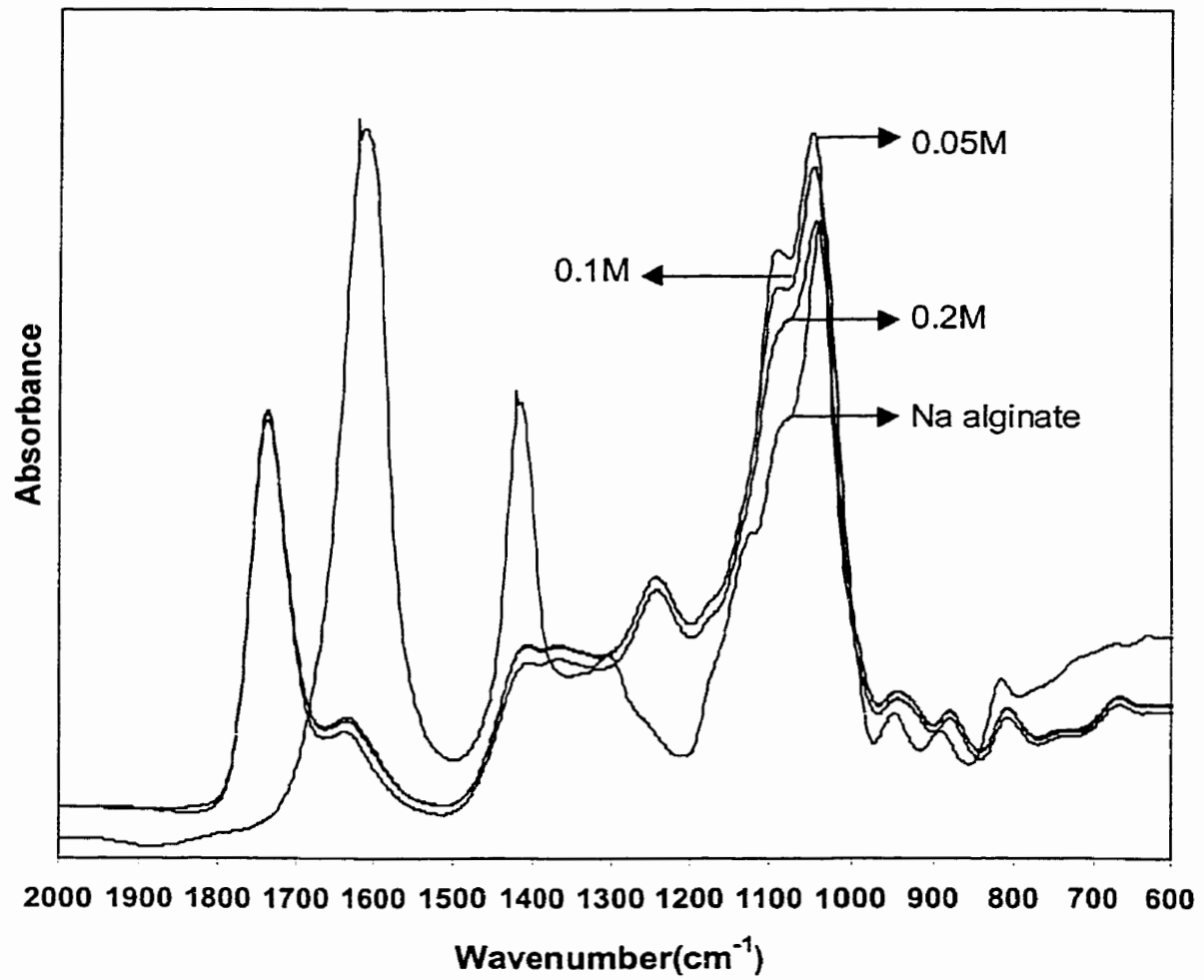


**Figure 6.3 FT-IR spectra of alginic acid membranes converted from sodium alginate membranes in H<sub>2</sub>SO<sub>4</sub> solutions of various concentrations**

group [Huang et al., 1999b]. Of special interest are the characteristic bands between 1100 and 1050  $\text{cm}^{-1}$  which could be attributed to the deformation (or bending) of  $-\text{OH}$  functional group [Perlin & Casu, 1982]. It is obvious that the band intensity between 1100 and 1050 is decreasing with the increase of the sulfuric acid concentration used to convert sodium alginate membrane into alginic acid membranes, while band broadening is observed with decrease in the concentration of sulfuric acid solution. In addition, the shoulder near the band of 1100  $\text{cm}^{-1}$  is getting more apparent with the decreasing sulfuric acid concentration, while the peak at 1050  $\text{cm}^{-1}$  slightly shifted to lower values with increasing sulfuric acid concentration. It is believed that all these phenomena in the intensity, band frequency, and shape are strongly affected by the inter or intramolecular hydrogen bonding of  $-\text{OH}$  groups. Since hydrogen bonds act as constraints to deformation vibrations, force constants for these vibrations are increased and wavenumber shifts to larger values are observed [Vinogradov & Linnell, 1971], while the band shifting to lower wave number are due to the O-H stretching [Hadzi & Bratos, 1976]. Michell and Higgins [1965] studied the nature of intramolecular hydrogen bonding (hydroxyl stretching) in glucose and xylose by IR spectra, and revealed that the band near 3530  $\text{cm}^{-1}$  is shifted to lower frequency. In Figure 6.3, the peak of sodium alginate at 1050  $\text{cm}^{-1}$  shifts to larger values due to the conversion to free acid forms. Alginic acid membrane converted in 0.05M sulfuric acid shows the largest hydrogen bonding based on this band shift analysis. This analysis is partially supported by the swelling degree results shown in Figure 6.2. The swelling degrees of alginic acid membranes are considerably lower than those of sodium alginate due to the higher hydrogen bonding. The swelling degrees of alginic acid membrane increase with the

exception of the alginic acid membrane converted in 0.1M for isopropanol mixture (Figure 6.2(b)) due to the shifting of the  $1050\text{ cm}^{-1}$  peak to a slightly lower wavenumber which signifies lower hydrogen bonding. It was also observed that the higher the hydrogen bonding results in larger peak intensity and a broader band. In summary, the hydrogen bonding of alginic acid membrane gets larger with the decreasing concentration of conversion solution from 0.2M to 0.05M. The band broadening, peak shifts at  $1050\text{ cm}^{-1}$  to larger frequency values and the increased peak intensity results from the hydrogen bonding. Thus the swelling degree of 0.05M alginic acid membrane is the lowest while sodium alginate membrane was found to have the highest swelling degree due to the low hydrogen bonding.

#### **6.4.4 Pervaporation experiments of aqueous ethanol mixtures**

Pervaporation experiments were carried out at  $50\text{ }^{\circ}\text{C}$  to study the feed concentration effects on various types of alginate composite membranes. Feed concentration ranges tested were 95 wt% to 50 wt% for ethanol mixtures and 90 wt% to 50 wt% for the isopropanol mixtures. In Figure 6.4(a), alginic acid composite membrane converted from sodium alginate by the solution technique in 0.1M  $\text{H}_2\text{SO}_4$  solution were tested for various ethanol mixtures and compared with the sodium alginate composite membrane. The flux increases with the increase of water content in the feed because of the increased plasticization action of water molecules in the membrane. The permeation flux of the alginic acid composite membrane is larger than that of the sodium alginate composite membrane over the whole feed concentration range. The hydrogen bonding in the current

membranes can explain this change in flux. From the sorption and the IR experiments, it was observed that the hydrogen bonding of the alginic acid membrane is larger than that of the sodium alginate membrane. In sorption experiments, the existence of stronger hydrogen bonding suppressed the swelling of membrane, thus the swelling degrees of sodium alginate membrane were found to be much higher than those of the alginic acid membranes. It is thus believed that the nature of the membrane and the interactions between feed component and membrane governs the swelling degrees of the tested membrane. However in the dynamic permeation experiments, the diffusion process due to the chemical potential difference becomes part of the separation process. This is the reason why the permeation flux and swelling degree do not necessarily correlate well. Relatively larger hydrogen bonding networks in the alginic acid membrane function as hydrophilic permeation pathways for the feed components. Figure 6.4(b) shows the permeation fluxes of cobalt ion crosslinked alginate membrane compared with the sodium alginate. The permeation flux of the cobalt crosslinked membrane is much lower than that of the sodium alginate membrane. It is well known that the structure of a crosslinked polymer is more packed than that of uncrosslinked polymer and chain mobility in a crosslinked polymer is a lot more restricted. Thus, the permeation flux is reduced. The separation factor plot in Figure 6.4(c) shows the characteristic convex trend. The sodium alginate composite membrane has a maximum value at 90% ethanol, while the others have maximum separation factors at the feed concentration of 20 wt% water. It was found that the separation factors obtained for alginate composite membrane did not follow the typical trade-off phenomenon which has been widely used to explain the high flux and low separation efficiency frequently encountered in pervaporation experiments

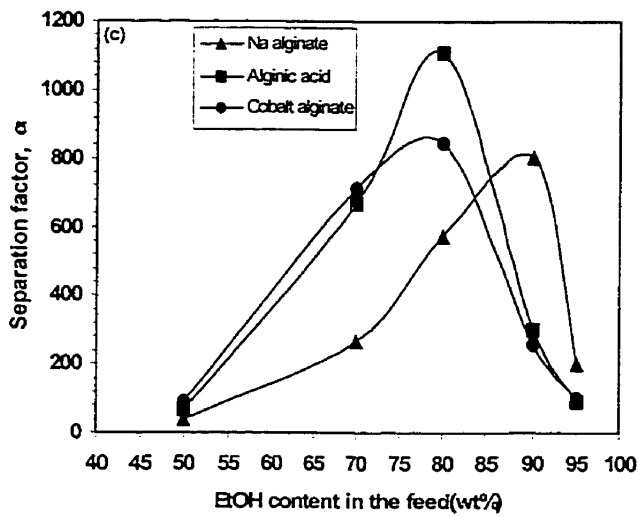
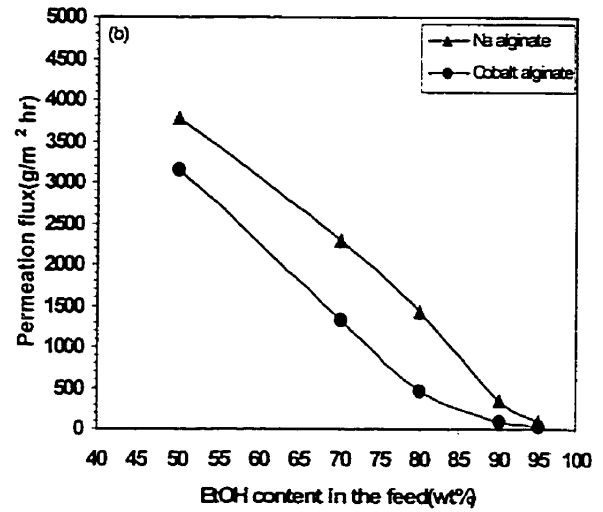
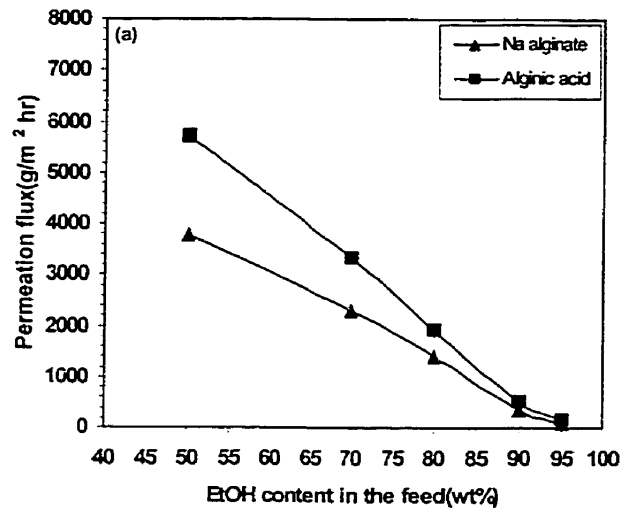


Figure 6.4 Effect of ethanol feed concentration on the flux through [(a) sodium alginate and alginic acid membranes, (b) sodium and cobalt alginate membranes] and (c) on the separation factor at 50 °C

[Feng & Huang, 1993]. In pervaporation study, the trade off phenomenon is not necessarily found for all kinds of membrane but generally observed for membrane separation systems in which polar interaction is not so strong. Many aspects contribute to the separation characteristics of a specific membrane such as the interaction between the permeants, the interaction between the permeant and membrane, and molecular sizes of the feed components etc. As shown in the pervaporation results of Fig. 6.4, sodium alginate membrane among three different membranes tested shows the highest separation factor at feed concentrations of 95 wt% and 90 wt% ethanol. The fluxes and separation factors at 95% azeotropic mixture are 95 g/m<sup>2</sup> hr and 202, 172 g/m<sup>2</sup> hr and 90, and 46 g/m<sup>2</sup> hr and 99 for Na alginate, alginic acid and cobalt alginate, respectively.

#### **6.4.5 Pervaporation experiments of aqueous isopropanol mixtures**

The same composite membranes were investigated for the pervaporation dehydration of isopropanol and the results are presented in Figure 6.5. In general, it is believed that the pervaporation dehydration of aqueous isopropanol mixtures proceeds more easily than that of aqueous ethanol mixtures due to the larger molecular size of isopropanol and relatively weak coupling phenomenon (less polar than ethanol) with water molecules and hydrophilic membranes. The higher permeation fluxes observed for isopropanol mixtures compared to ethanol mixtures can be attributed to less polarity, higher water activity and less coupling in the isopropanol mixtures. Unlike the case of ethanol mixture, permeation fluxes for 90 and 85% isopropanol mixture are larger than those of the alginic acid composite membrane. However, the flux trend for over 20 wt% water feed mixture is

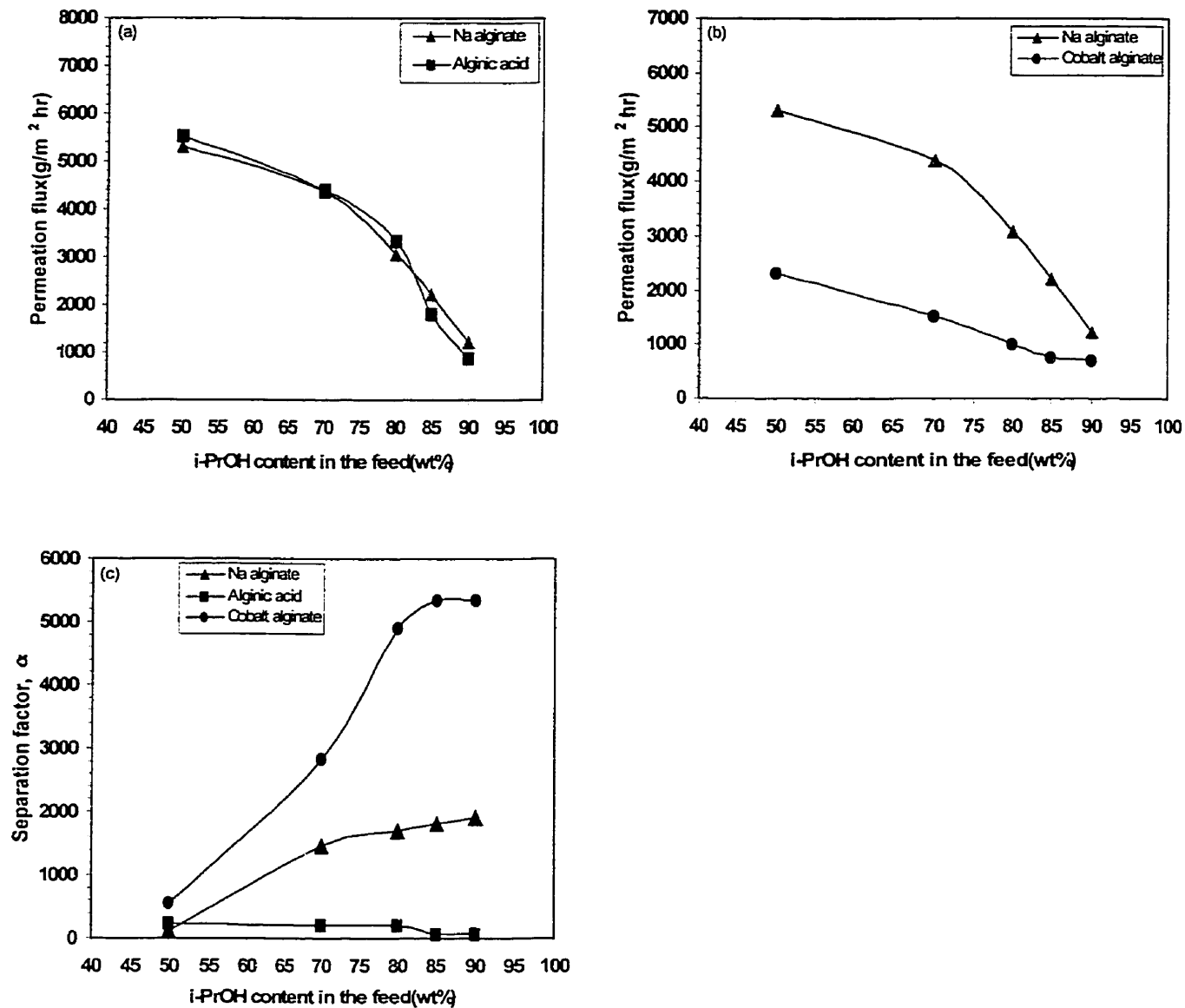


Figure 6.5 Effect of isopropanol feed concentration on the flux through [(a) sodium alginate and alginic acid membranes, (b) sodium and cobalt alginate membranes] and (c) on the separation factor at 50 °C

similar to that of ethanol mixtures. As expected for the crosslinked alginate membranes, the flux of alginate membrane crosslinked with cobalt ion was significantly reduced compared to sodium alginate composite membrane as shown in Fig. 6.5(b). The separation results are plotted in Fig. 6.5(c). The cobalt ion crosslinked membrane achieved high separation factor and low flux since the chain mobility and free volume of the membrane are substantially reduced after the three dimensional crosslinking. This figure shows that the separation performance of the alginic acid membrane for isopropanol mixture is quite low. Although the separation factor of alginic acid membrane for the ethanol mixtures is higher than that for isopropanol mixtures, the overall conversion from sodium alginate to alginic acid form sacrifices its selectivity and moderates its affinity to water. However, it must be emphasized that the alginic acid membrane has several benefits such as insolubility in water and relatively improved mechanical strength compared to the sodium alginate form.

#### **6.4.6 Temperature effects on the permeation flux**

For most of the polymeric pervaporation membranes, the increase of feed temperature results in linear increase of the permeation flux. It is well accepted that increased feed temperature enhances the thermal mobility of the polymeric chain, thus the diffusion rate of the permeating molecules is significantly increased. In other words, considering the driving force of the pervaporation process, the increase of the chemical potential difference in terms of the temperature difference leads to the flux increase.

The Arrhenius relationship represents the empirical linear relationship between the temperature and the permeation flux as shown below.

$$J = J_o \exp(-E_p/RT) \quad (1)$$

where  $J_o$  and  $E_p$  are the frequency factor and the apparent activation energy of permeation, respectively. Based on the solution-diffusion model, the activation energy of permeation can be expressed as follow [Feng & Huang, 1996c].

$$E_p = E_J - \Delta H_v \quad (2)$$

$$E_p = E_D + \Delta H \quad (3)$$

where  $\Delta H_v$  is the heat of vaporization,  $E_D$  and  $\Delta H$  are the activation energy of diffusion and the enthalpy of sorption of the permeant in the membrane, respectively. The activation energy of permeation can be equated with the minimum energy that must be possessed by the permeating components before the permeation will take place. In Figure 6.6, temperature dependence of the various alginate membranes on the flux is plotted for 90 wt% ethanol and isopropanol mixtures. For both mixtures, the activation energy increases in the following order, Na alginate>Co alginate>alginic acid membranes. This is because the membrane structure of alginic acid and cobalt alginate is loosened when they are prepared in the solution state (as stated in the membrane preparation section). Obviously for the alginate membrane crosslinked with cobalt ions it is more difficult for the diffusion process to take place compared to the alginic acid membranes.

The temperature effect on the flux according to the water content in the feed is shown for alginic acid membranes in Figures 6.7 and 6.8. It is apparent that the higher water content in the feed facilitates the mass transport caused by swelling in the membranes. It is interesting to note that the activation energy due to higher water content

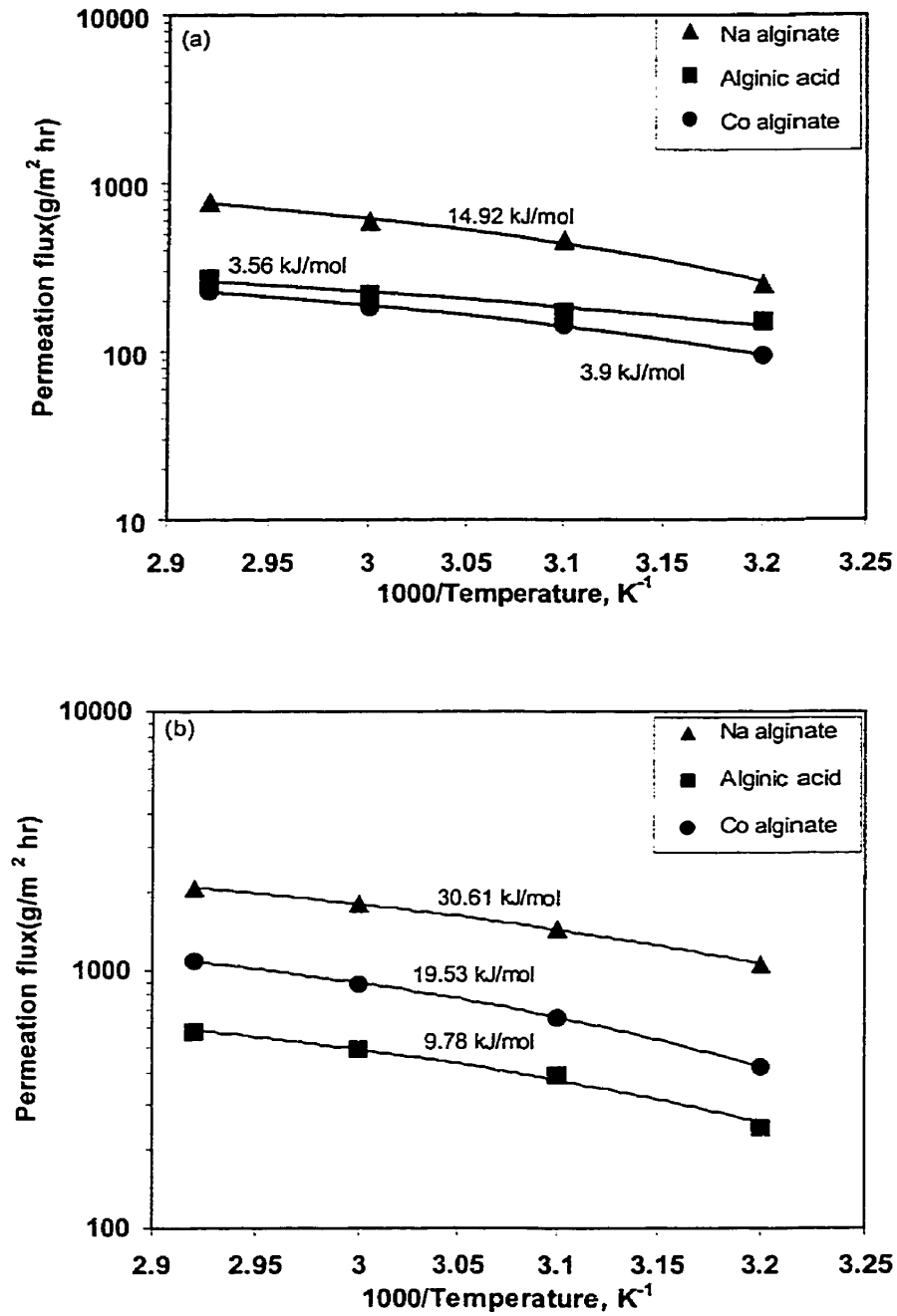


Figure 6.6 Temperature effect on the flux through various alginate membranes (a) at 90% ethanol mixture (b) at 90% isopropanol mixture

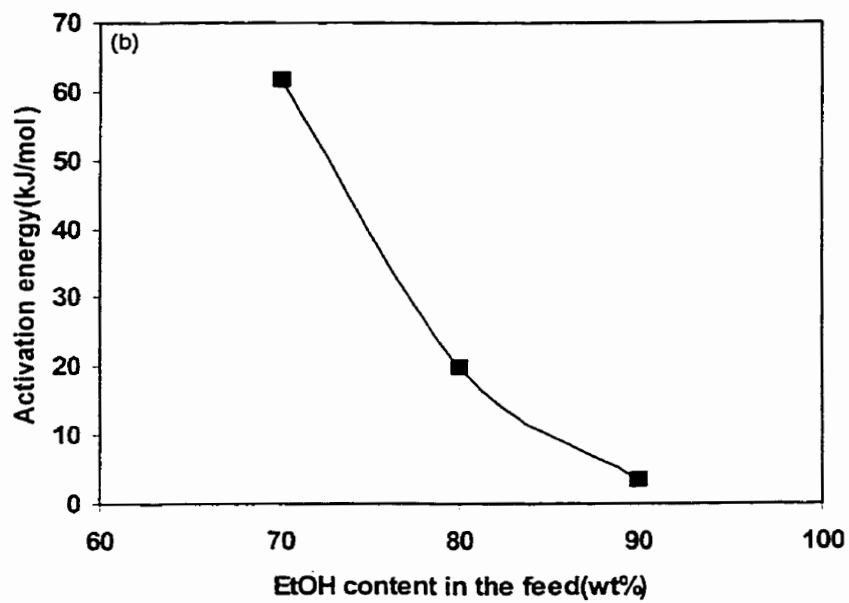
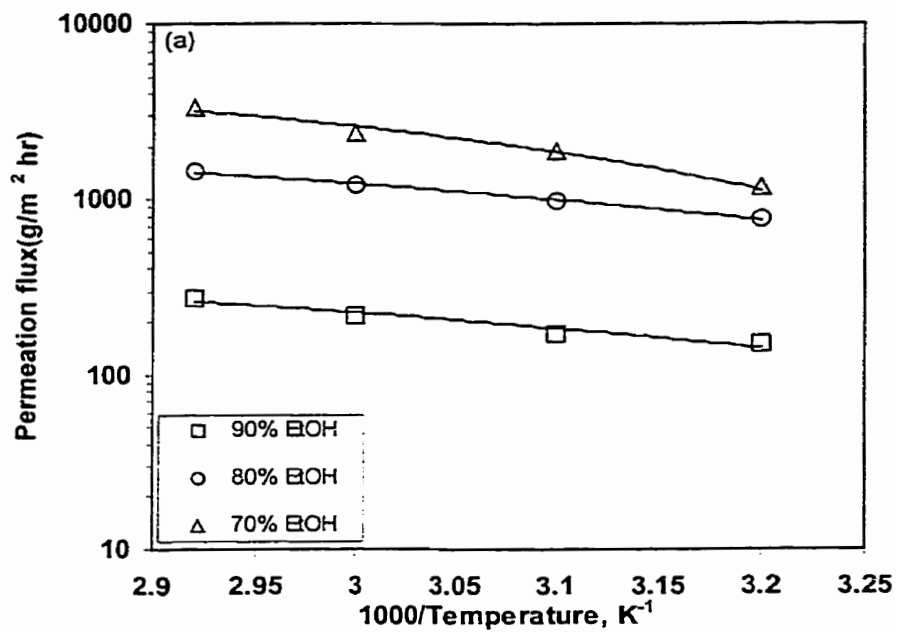


Figure 6.7 Temperature effect (a) on the flux through alginate membrane (0.1M), (b) permeation activation energies according to the ethanol feed concentration

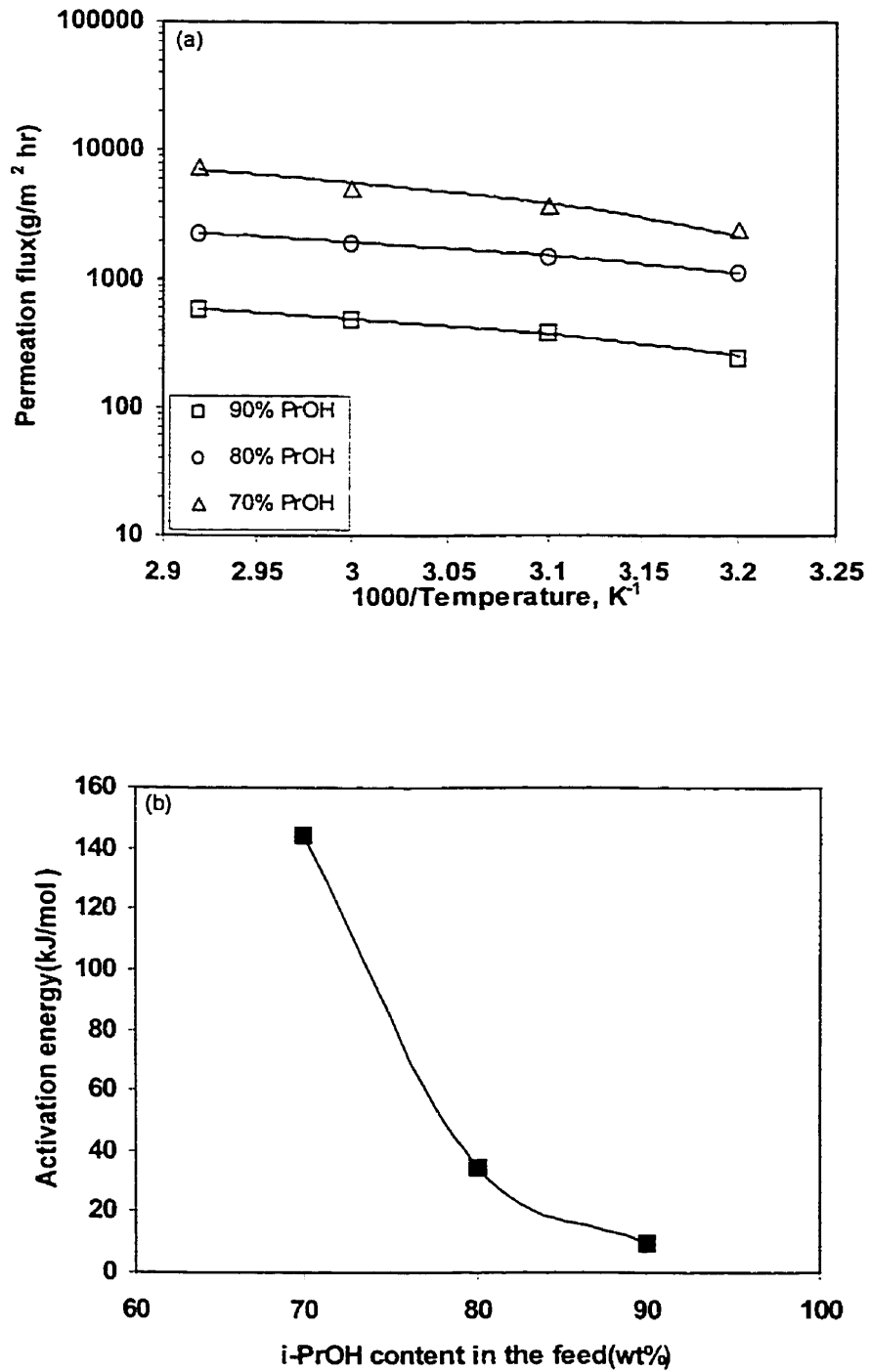


Figure 6.8 Temperature effect (a) on the flux through alginate membrane (0.1M), (b) permeation activation energies according to the isopropanol feed concentration

in the feed is higher than that for lower water content, because the diffusion through higher swollen membranes is expected to be easier than through less swollen membranes. This interesting phenomenon which also has been observed by other researchers [Yeom & Lee, 1998a] can be explained by the intensity of interaction of the polar alginic acid membrane with water molecules. There seems to be a trend that the interaction between the water molecules in the feed and the membrane increases with the increase of water content in the feed from 10% to 30% and thus much more energy is needed to permeate an unit mol of the feed mixture. This concept can be used to explain higher activation energy of the isopropanol mixture compared to that of the ethanol mixture at the same water content. Ethanol is relatively polar compared to isopropanol though it is less polar than water. Thus it can be summarized that the interaction (or affinity) of the aqueous ethanol mixture with the hydrophilic alginic acid membrane is weaker compared to that of aqueous isopropanol. This explains why the activation energy of the isopropanol mixture is higher than that of ethanol mixture at the same feed concentration.

## 6.5 CONCLUSIONS

Composite membranes consisting of alginate and chitosan top layers and porous polyvinylidene fluoride membrane were successfully prepared and they showed promising permselectivity for the dehydration of ethanol and isopropanol mixtures. The hydrophilicity of PVDF membrane by blending poly(vinylidene fluoride) with 1% PMMA was shown to be useful in giving better surface properties for adhesion of the alginate and chitosan top layers. FT-IR and contact angle measurements revealed the

differences in hydrogen bonding between alginate and alginic acid membranes. The optimization of membrane performance is needed for further improvement of current composite membrane.

## CHAPTER 7

# N-ACETYLATED CHITOSAN MEMBRANES FOR THE PERVAPORATION SEPARATION OF ALCOHOL/TOLUENE MIXTURES\*

---

### 7.1 SUMMARY

Composite chitin membranes supported by porous polyetherimide substrate were prepared for the pervaporation separation of ethanol/toluene and methanol/toluene mixtures. The chitin was obtained by modifying chitosan to its original form chitin by the N-acetylation reaction. It was found that the incorporation of additional acetyl groups into the chitosan structure decreased the total flux and increased separation factor from 401 g/m<sup>2</sup> hr;  $\alpha=34$  (pure chitosan) to 282 g/m<sup>2</sup> hr;  $\alpha=126$  (4 mol acetylated chitosan) for 10 % EtOH feed mixture and from 681 g/m<sup>2</sup> hr;  $\alpha=159$  (pure chitosan) to 484 g/m<sup>2</sup> hr;  $\alpha=607$  for 10 % MeOH feed mixture. It was concluded that chitin composite membranes could be a good candidate for this pervaporation system. Scanning electron microscopy and Fourier Transform Infrared determinations of the acetylated chitosan membranes were carried out and are reported. It was further shown that the chitin/polyetherimide

---

\* Part of this study has been published in Journal of Membrane Science, 176(2000), 223-231

composite membranes prepared had good pervaporation characteristics and were also found to be mechanically robust and stable to withstand the corrosive nature of the ethanol/toluene mixture during the pervaporation runs. This is the first reported successful application of chitin in the form of composite membranes for the pervaporation separation of organic/organic liquid systems.

## 7.2 INTRODUCTION

Pervaporation membrane processes are finding their application niches in the chemical industries as a process for breaking azeotropic concentration after distillation or as an intermediate between distillation processes. Most of the pervaporation studies published in journals have focussed on the discovery and the modification of new membrane materials for specific mixture separation. After the successful industrialization of plasma-polymerized and crosslinked PVA membranes for alcohol dehydration systems, much research attention has been paid to the polysaccharide natural polymers such as chitosan [Nawawi & Huang, 1997; Shieh & Huang, 1997; Feng & Huang, 1996b; Huang et al., 1999a; Lee et al., 1998a; Nam & Lee, 1999a; Uragami et al., 1994; Uragami et al., 1997] and alginate [Yeom et al., 1996b; Yeom & Lee 1998a; Huang et al., 1999b] because of their reasonably good hydrophilicities.

Chitin, poly-(1→4)-β-N-acetyl-D-glucosamine, the most abundant natural polymer next to cellulose is widely found in skeletons of crustaceans such as shrimps, crabs and lobsters, and in cell walls of microorganisms. Seafood waste from shrimps, lobsters and crabs generally contains 10-15% chitin. Chitin and its deacetylated derivative, chitosan

are finding applications in pharmaceutical system such as surgical suture and drug delivery, enzyme immobilization, and metal ion chelation [Muzzarelli, 1985]. Studies of chitin as a membrane material have been limited compared to chitosan because of difficulty of dissolution in most organic solvents. Strong intermolecular bonding between the acetylamino groups in its structural backbone resists solution by potential solvent systems. Various solvent systems such as N-methylpyrrolidone/dimethylacetamide/LiCl [Austin, 1977; Uragami et al., 1981], chloroacetic acid systems [Austin, 1975; Austin & Brine, 1977; Kifune et al., 1990], and dimethylacetamide/LiCl [Hirano et al., 1991] have been recognized and comprehensive reviews for the chitin solvent systems based on the solubility parameter have been reported [Austin, 1984]. However, none of them were completely successful for dissolving chitin because of strong intermolecular and intramolecular hydrogen bonding.

To achieve chemically resistant and mechanically stronger membrane, chitosan was modified to chitin membrane using acetic anhydride. Chitin is the skeletal material of the crustaceans widely distributed in nature. Also chitin is solid and strong, which is the positive properties in light of its application for organic-organic separation. The chemical versatility of chitosan offered by its reactive moieties came to the notice of several research groups [Hirano & Takeuji, 1983; Hirano et al., 1976; Hirano et al., 1994; Moore & Roberts, 1981a, 1981b, 1982]. Among many reactions involved in chitosan modification, the acylation of chitosan has gained special interest. Hirano et al. [Hirano et al., 1991] obtained chitin (N-Acetylchitosan) gel from chitosan gel by treating chitosan gel with acetic anhydride (about 10 mols/GlcN) in 70% aqueous methanol solution at room temperature for 18 hours. It was reported in this study that N-acetylchitosan

produced was not distinguishable from naturally occurring chitin in component analysis and IR spectra, but apparently differed in the physical properties (N-Acetylchitosan is soluble in formic acid, but natural chitin is insoluble) due to its modified molecular conformation and molecular weight [Hirano & Yamaguchi, 1976]. An interesting approach to increase the solubility of natural chitin is to convert chitin into diacetylchitin form in acetic anhydride/methanesulfonic acid at 0 °C for 3 hr. [Nishi et al., 1979]. Ruchenstein and Zeng [1996] successfully prepared porosity-controllable chitin membranes, and demonstrated that chitin membranes have strong affinity to lysozyme against ovalbumin [1997]. The same macroporous chitin membrane was adopted to efficiently extract a valuable protein, wheat germ agglutinin from wheat germ by using the strong binding ability of N-acetyl-D-glucosamine moieties of chitin to wheat germ agglutinin [Zeng & Ruchenstein, 1999]. In this study, chitin membranes for the pervaporation application were prepared by acylating chitosan membranes in various anhydrous solutions and compared with natural chitin membrane. A typical acylation reaction which acetyl chloride and acetic anhydride transfer acyl groups (acetyl groups) to the amine groups of chitosan is depicted in Figure 7.1.

In the only work investigating natural chitin, Uragami et al. [1981] studied the permeation characteristics of chitin ultrafiltration membranes investigating the change of the evaporation temperature of the NMP/DMAc/LiCl solvent system and the operating pressure. However to the best of our knowledge, no chitin membrane for the pervaporation application has been studied before. The strong solvent resistance of chitin is of particular interest for the separation of corrosive systems such as toluene. An interesting experiment in which hydrophilic chitosan membrane blended with

polyethylene oxide was used for the separation of ethanol/water system [Wang et al., 1999].

The goal of the present study is to investigate the pervaporation features of acetylated chitosan membranes for the separation of alcohol/toluene mixtures. The preparation of natural chitin membrane was extremely difficult due to its insolubility in most conventional solvents, unlike the case for chitosan membranes. We chose the alcohol/toluene mixture because this mixture has rarely been studied previously, but has growing industrial potential. Previous works for the pervaporation separation of this system include PAA/PVA blend [Park et al., 1994], polypyrrole [Zhou et al., 1996], and cellulose derivative [Bhat & Pangarkar, 2000] membranes. Modified chitosan membranes were studied for the separation of benzene/cyclohexane [Inui et al., 1998] and methanol/MTBE [Nam & Lee, 1999b] mixtures in the past. In this study, chitosan membranes were acetylated in various concentrations of acetic anhydride solutions and tested for the pervaporation separation of ethanol/toluene and methanol/toluene mixtures.

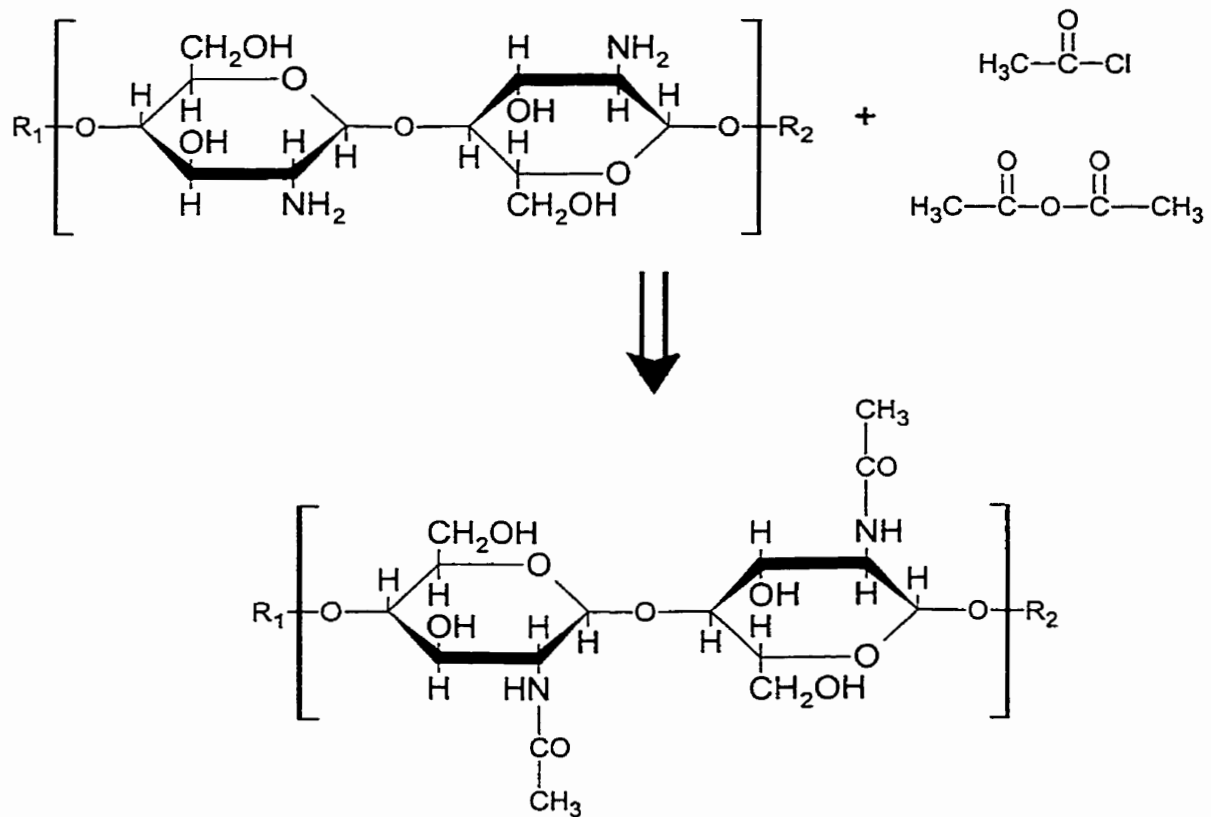


**Figure 7.1 N-acetylation reaction of chitosan membrane to chitin membrane**

## **7.3 EXPERIMENTAL**

### **7.3.1 Materials**

Chitosan flakes (Flonac-N) with MW 100,000 and 99% N-deacetylation degree were donated by Kyowa Technos Inc, Japan. Chitin flakes, aromatic polyetherimide and polyacrylonitrile (MW 150,000) were obtained from Polysciences, Inc., USA. Toluene, methanol, ethanol, HCl and N,N-dimethylformamide (DMF) were obtained from BDH Inc., Toronto, ON. Sigma chemical, USA supplied the acetic anhydride, N-methyl-2-pyrrolidinone (NMP), LiCl, glutaraldehyde (25%), and ethylene glycol (monomethyl ether). EM Science, NJ, USA supplied N-dimethyl-acetamide (DMAc). A non-woven polyester fabric donated by BBA nonwovens (Veratec) of International Paper Co., USA was used as the backing material for the composite membrane. Water was de-ionized and distilled before use.

### **7.3.2 Membrane preparation and N-acetylation reaction**

Porous polyetherimide (PEI) membranes were prepared via the wet phase inversion technique from the casting solutions containing 18 wt% PEI, 77 wt% DMAc, and 5% ethylene glycol. The casting solution was cast onto a polyester non-woven fabric held on a glass plate with the aid of a casting knife made in this laboratory. The cast film was immediately immersed into a coagulation bath. The resulting membrane was washed in de-ionized water thoroughly and air-dried completely at ambient temperature. The initial

microporous PEI membranes showed a pure water permeation rate of 115.8 kg/m<sup>2</sup> hr at transmembrane pressure of 100 psi and operating temperature 22 °C. Most of the water flux tests were performed in replicate to achieve precision in the flux. The PEI membrane was soaked in 0.1 wt% PVA binding solution for 1 hr. and crosslinked in 80 wt% aqueous acetone solution containing 1.6 wt% glutaraldehyde and 0.05 wt% HCl for 1 hour in order to enhance the wettability of the membrane surface. For the preparation of composite membranes, the dip coating technique was applied to prepare thin film composite membrane in which PEI porous membranes were immersed into 0.5% chitosan solution consisting of 4 wt% acetic acid and dried in the oven of 60 °C for 100 minutes. Chitin flake of 1.8 g dried overnight at 70 °C was dissolved in the solvent mixture of 320 g (50 wt% NMP/50 wt% DMAc) in the presence of 4% LiCl. LiCl and DMAc were first well mixed to dissolve LiCl completely and then the designated amount of chitin flake was added, and stirred for 1hr. Finally NMP solvent was added, the solution was stirred for several days in order to get a satisfactory viscous solution. Chitin solution was filtered to remove the undissolved portion and impurities before use. It was found that complete dissolved solution was rarely obtained and thus the small amount of water which is detrimental for the dissolution had to be removed. Before casting the chitin membrane, chitin solution was filtered to remove coarse undissolved flakes and impurities. The chitin film obtained was only used for the FT-IR measurement. Chitosan solutions consisting of 0.5 wt% chitosan in 4 wt% aqueous acetic acid solutions was filtered to remove any possible undissolved solids and impurities. Dense membranes were prepared by casting the chitosan or chitin solution onto a clean glass plate using a casting knife designed in this laboratory. Pure chitin membrane was evaporated for the fixed time,

coagulated in acetone, and then washed thoroughly to remove the trapped solvent for 24 hours. Chitosan membranes were treated in 0.8M NaOH solution containing 50 vol% ethanol solution for 24 hours at room temperature, washed thoroughly to completely remove NaOH, dried at room temperature. N-acylated chitosan membranes were prepared by immersing chitosan composite membranes into the acetic anhydride in methanol/ethanol solution for 24 hours. Then, membranes are washed thoroughly in deionized water for 1 day, and dried for further use.

### **7.3.3 Pervaporation experiment**

The pervaporation experiment was carried out using the apparatus and method described in chapter 3.

### **7.3.4 FT-IR measurement**

A BOMEM Michelson series 100 FT-IR spectrometer was used to identify and characterize structural changes in various chitin membranes and to determine the degree of N-acetylation of chitin and chitosan membranes. The experiments were run with air as the background, and the resolution and number of scans were  $4.0\text{ cm}^{-1}$  and 16, respectively. Films were sandwiched between rectangular holders, whose insides were circularly out. The sample thickness was about  $10\ \mu\text{m}$ . The absorbance band of  $1650\text{ cm}^{-1}$  which represents amid I band was split into two components: one centered around  $1650\text{ cm}^{-1}$  due to single hydrogen bonded amid groups and one centered around  $1630\text{ cm}^{-1}$  due

to amid groups involved in two hydrogen bonds. The degree of N-acetylation was calculated using the following equation [Roberts, 1997].

$$\text{Degree of } N\text{-acetylation}(\%) = \left[ \left( A_{1650} / A_{3450} \right) + \left( A_{1630} / A_{3450} \right) - 0.13 \right] \times 85.5 \quad (1)$$

### 7.3.5 Scanning electron microscopy

Scanning electron microscopy was used to study the cross section morphology of the various composite membranes and to measure the thickness of the membrane. Cryogenic fracturing of the membrane was done after freezing the samples in liquid nitrogen. All specimens were coated with a conductive layer (400Å) of sputtered gold. A Jeol JSM 805 scanning electron microscopy was used for the specimens at 20kV.

## 7.4 RESULTS AND DISCUSSION

### 7.4.1 SEM and FT-IR measurement

Scanning electron micrographs of the typical composite membranes are presented in Figure 7.2. It is obvious from the pictures that chitosan thin layer was properly cast on the top of the polyetherimide substrate. The pictures also show the morphology of PEI porous membrane prepared by wet phase inversion technique. PEI substrate consists of microvoids in the form of honeycomb as well as fingerlike macrovoids that is frequently found in the process of instantaneous demixing in wet phase inversion. However the macrovoids do not span the entire width of the membrane. Change of the chemical

bonding of chitosan membrane after N-acetylation reaction has been studied using FT-IR as presented in Figure 7.3. N-acetylated chitosan membranes show similar chemical bonding with the reference chitin. Degrees of acetylation (DA) measured using equation 1 were 70% DA and 90% DA for 4 mol acetic anhydride and 7 mol acetic anhydride in methanol/ethanol reaction medium, respectively. Thus the chemical reaction method was found to be feasible. However due to different chain conformations, a difference in transmittance for the specific wavenumber is noticed.

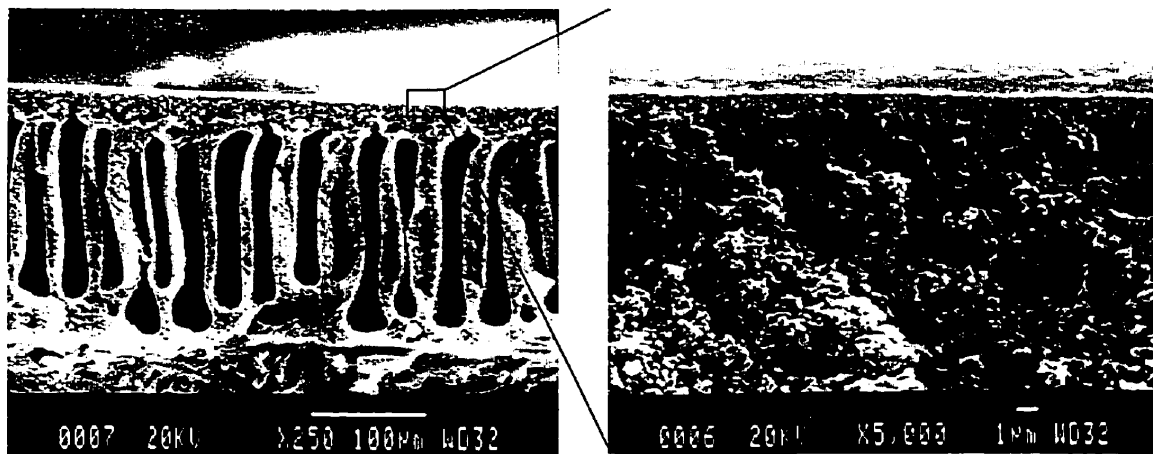


**Figure 7.2 SEM pictures of the chitosan/polyetherimide (PEI) composite membranes**

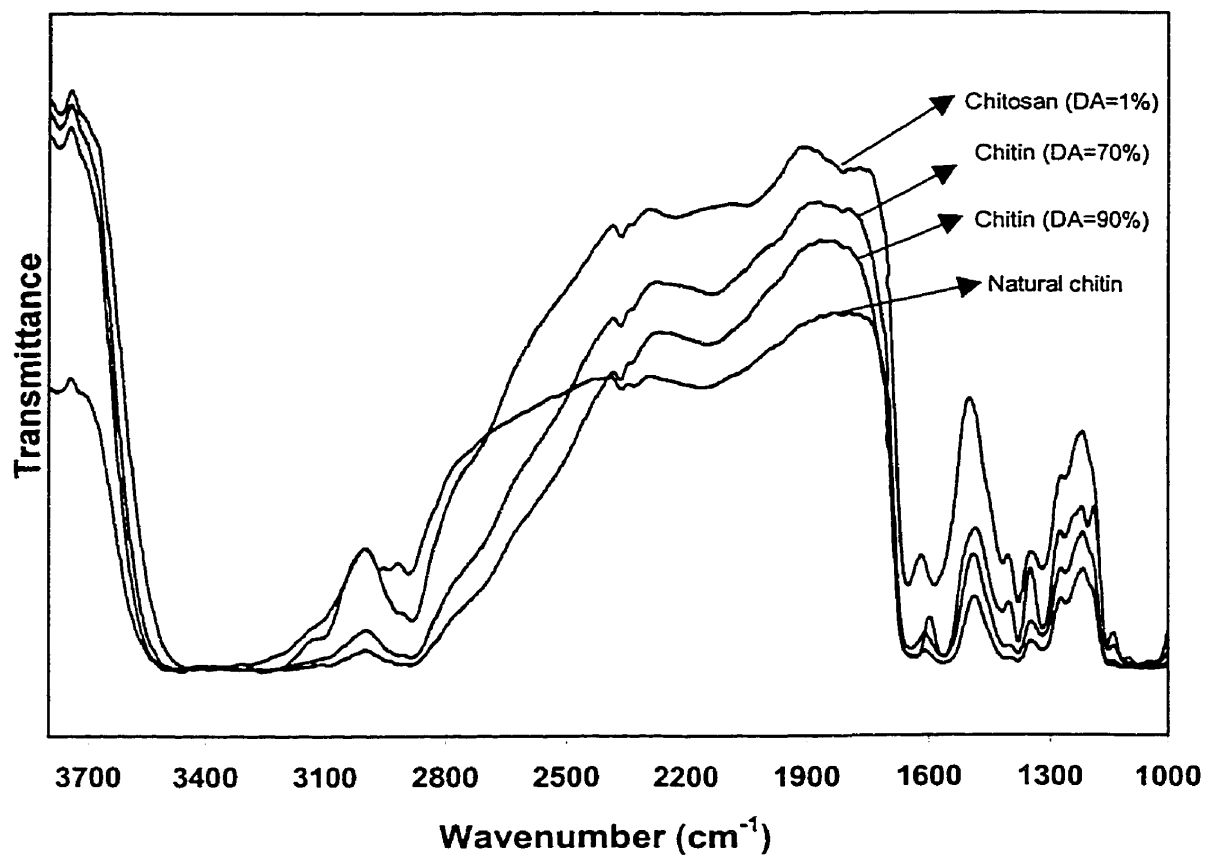


**Figure 7.3 FT-IR diagram of chitosan, natural chitin and acetylated chitosan membranes**

### 7.4.2 Swelling behavior in water

Figure 7.4 presents the swelling properties of various chitosan membranes acetylated in different concentrations of acetic anhydride solutions that ranged from 0 mole acetic anhydride/GlcN to 7 mole. It is apparent that the amount of water sorption increased with the increase of the concentration of acetic anhydride, in other expression, with the decrease of deacetylation degree. This phenomenon explains that the more acetylated chitosan membranes accommodate more water within the membranes because of the bulkier structure after the incorporation of acetyl groups. Upon the addition of acetic anhydride,  $\text{NH}_2$  amino group that contributes to external hydrogen bonding is converted to  $\text{NHCOCH}_3$  acetyl group which gives inter or intra molecular hydrogen bonding with the water molecules. It is widely recognized that the difficulty of dissolving natural chitin even in the mixture of various solvents arises from the strong internal molecular bonding. That is, the more acetylated chitosan membrane offers a loosened matrix and accommodates more water molecule through hydrogen bonding and geometrical trapping. In case of chitosan membrane acetylated in 10 M acetic anhydride solution water sorption data and further pervaporation test was omitted from Figure 7.4 and relevant figures because of the brittleness, however its sorption amount was relatively high (6.027g/g polymer) compared to those of membranes treated in less acetic anhydride solutions. In appearance, this membrane was extremely swollen like a gel absorbing a lot of liquid as well as maintaining its dimension. Also water capsules of various sizes were noticed within this interesting membrane. With the excess amount of acetic anhydride, acetylation reaction further progresses and the results may be diacetylated or triacetylated

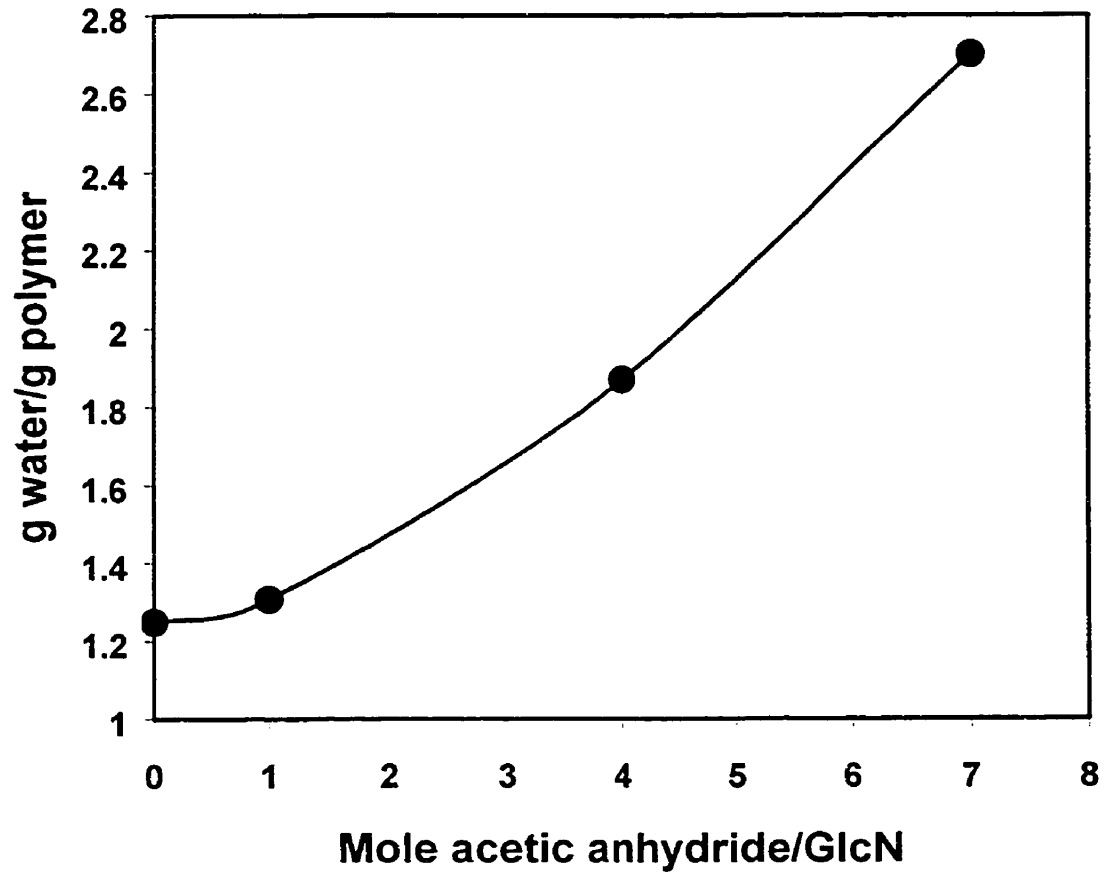


**Figure 7.4** Water sorption behaviors of N-acetylated chitosan membranes according to the degree of acetylation

structure which can behave like a gel. This is why the sorption amount of water of this membrane for 10 M acetic anhydride is considerably high.

### 7.4.3 Pervaporation of ethanol/toluene mixtures

In our previous study [Huang et al., 1999a], it was revealed that the binding of porous polysulfone support in the preparation of thin film composite membrane made a positive effect on the permeation flux. This is attributed to the reduction of the interface resistance between the top layer and support layer. Binding polymer molecules narrowed the pore diameter and continuously on casting top layer the penetration of the solution into the pores was prohibited to a certain extent, which can be understood to be the reduction of membrane resistance in the well-known resistance in series model. Since the pervaporation was run for 2 hours to achieve the equilibrium performance before collecting the permeate during continuous 2 hours, the pervaporation reliability of the pure chitosan membrane was studied for 50 wt% ethanol/50% toluene mixture at 35 °C in Figure 7.5. The permeation flux of chitosan membrane decreased very slightly over the explored operating time range, so it is assumed that the pervaporation experiment represents reliable data at least for the experimental condition in this study. Chitosan has been known as a good dehydration membrane rather than as a good organic/organic separation membrane. Thus it might be worthwhile to compare ethanol separation performance with its flux performance in the dehydration of water/ethanol mixture. As clearly shown in Figure 7.6, flux in the dehydration application increases with the increase in water content in the feed mixture due to the strong swelling property of

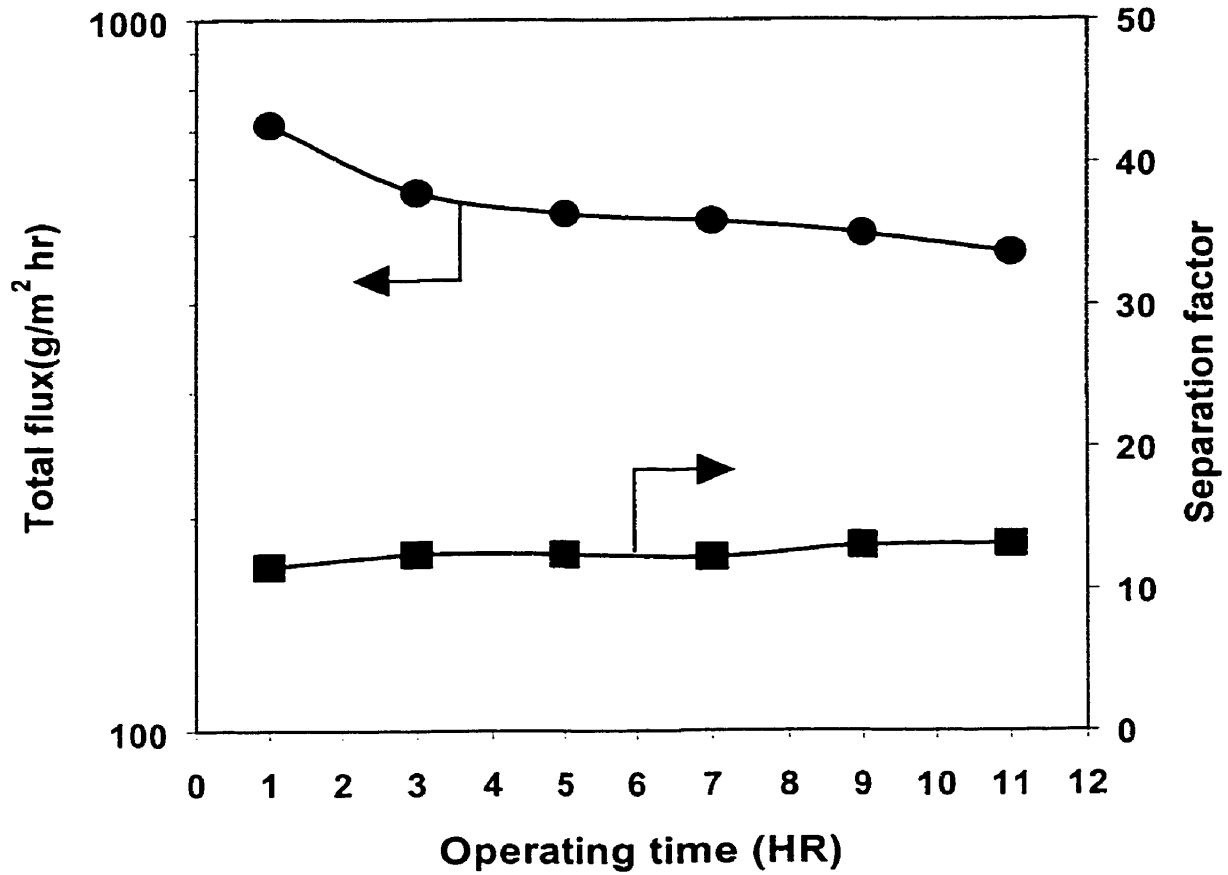


Figure 7.5 Pervaporation performance of pure chitosan membrane for 50% ethanol/50% toluene mixture at 50 °C

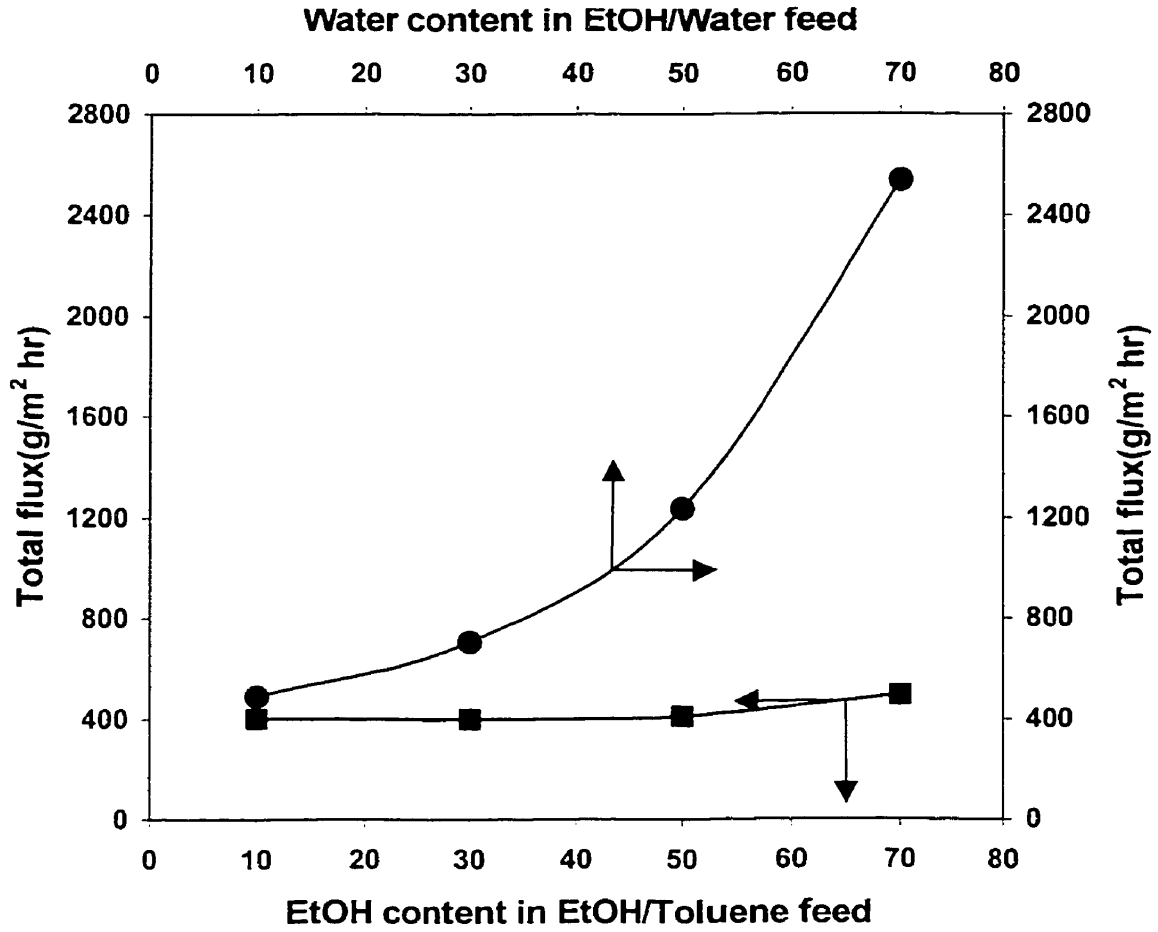


Figure 7.6 Comparison of the membrane performance between the dehydration application and organic-organic separation application of the chitosan membrane at 35 °C

chitosan in water. However for ethanol/toluene flux hardly increases even with the increase of ethanol content in the feed mixture. It must be noted that chitosan is a hydrophilic material more swellable in water/ethanol mixture rather than in ethanol/toluene mixture. The flux difference for water/ethanol and ethanol/toluene mixtures is much pronounced with the increase of water content in the feed mixture.

Figure 7.7 shows the pervaporation characteristics of pure and N-acetylated chitosan membranes for ethanol/toluene mixtures. Permeation flux of pure chitosan membrane does not change much from 10% ethanol to 50% ethanol mixture because chitosan membrane is not much swollen in ethanol. Pure chitosan membrane showed the highest permeation fluxes through the feed concentration range compared to those of the N-acetylated membranes. Decreased fluxes of N-acetylated membranes are attributed to the strong inter or intramolecular bonding among acetyl functional groups resulted in less swelling of the membrane in ethanol/toluene mixtures, that is less interaction between the feed mixture and membrane. With the introduction of acetyl groups into the matrix of chitosan the chemical structure of the chitosan membrane becomes bulky and stiff, and then the acetylated chitosan is mechanically brittle. Thus the chain mobility of the membrane was substantially hindered due to the bulky acetyl groups and also the free volume which continuously accommodate the permeating component decreased. In case of acetylated membrane in 7 mol acetic anhydride (90% degree of acetylation), permeation flux increases to the minimal extent through the whole feed concentration range probably due to its rigid structure which is hardly swollen in the feed mixtures. In fact, 7 mol of acetic anhydride was the maximum content which acetylated membrane can function for the separation of ethanol/toluene mixture. 10 mol of acetic anhydride

that was tried was proven to be excessive because the membrane acetylated with 10 mol was so rigid and brittle. In addition, there was almost no transport through this membrane. It is apparent that separation factor decreases with the increase of N-acetylation degree from Figure 7.7(b). Since the permeation of ethanol and toluene is greatly hindered with the introduction of acetyl groups into the chitosan structure, the transport of ethanol and toluene becomes slow, especially the transport of toluene which has large molecular size and is less polar than ethanol. From the N-acetylated membranes, the following advantage can be derived. N-acetylation reaction is a good strategy to make chitosan stronger, chemical resistant and efficient for the separation of alcohol/toluene mixtures. The N-acetylation reaction for chitosan membrane with the application of alcohol/toluene separation reveals a similarity to the general crosslinking reaction for that with the application of dehydration in light of the decrease of the permeation flux and the increase of separation efficiency. Note that the chemical crosslinking of the dehydration membrane commonly results in reduced permeation fluxes and increased separation factors, so called trade-off phenomenon although the mild crosslinking can result in the membrane having high flux and separation factor.

Figure 7.8 presents the relationship between the total flux and temperature. As expected, fluxes increase with increasing feed temperature for all membranes tested. It is interesting that flux increase of the membrane acetylated in 7 mol acetic anhydride is less pronounced than those of the pure chitosan and the membrane acetylated in 4 mol acetic anhydride (70% degree of acetylation). It is believed that large portion of acetyl group of 7 mol acetic anhydride incorporated into chitosan backbone restricts the thermal mobility of membrane more than that of 4 mol acetic anhydride and pure CS. Also it was

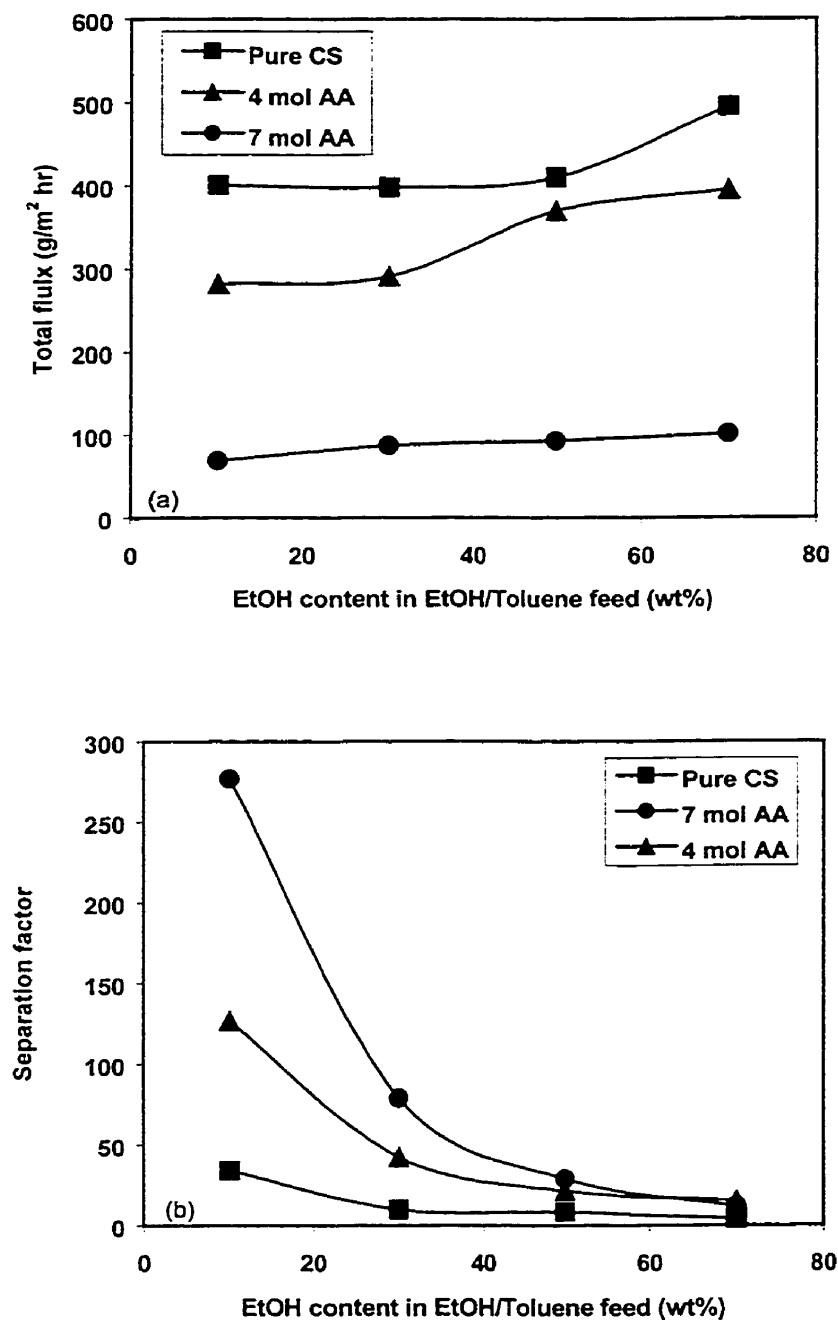


Figure 7.7 Feed concentration effect on (a) total flux and (b) separation factor of N-acetylated membranes and pure chitosan membrane for ethanol/toluene feed mixture at 35 °C (AA : Acetic Anhydride)

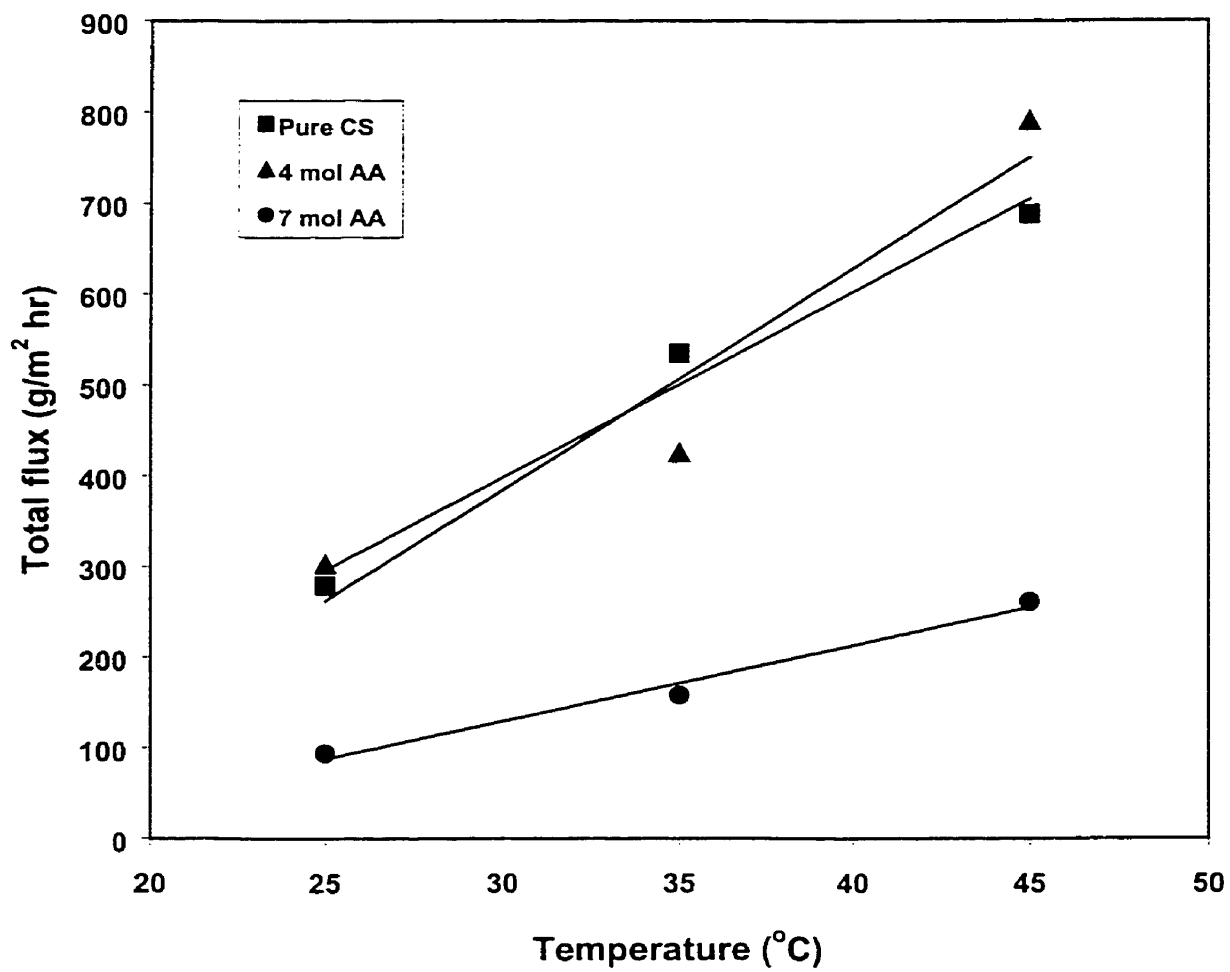


Figure 7.8 Temperature effect on the total flux of 70% ethanol/30% toluene mixture

recognized that there is no large difference of flux between 70% acetylated membrane (acetylated in 4 mol acetic anhydride) and pure chitosan membrane. This interesting phenomenon can be postulated that as a result of the loosened membrane structure caused by the introduction of the acetyl groups at 4 mol acetic anhydride although the reason is not clear.

#### **7.4.4 Pervaporation of methanol/toluene mixtures**

Toluene has been used as a reaction medium in the solution polymerization process and methanol is added into the process to isolate the polymer. This mixture is known to be difficult to separate each other. Pervaporation results of N-acetylated membrane for methanol/toluene mixture are shown in Figure 7.9. Methanol/toluene mixture can be found in the polymerization process of certain polymers. The total flux of methanol/toluene mixture in Figure 7.9 is much larger than that of ethanol/toluene mixture shown in Figure 7.7. The smaller molecular size of methanol compared to ethanol played a positive role in the increased flux. However it must be pointed out that methanol is a relatively polar solvent among most of solvents although the polarity of methanol is less than that of water. Therefore, it is believed that methanol in the feed mixture swells the membrane much more than ethanol in the feed mixture due to its larger polarity. The total flux of methanol/toluene mixture increases with the methanol content in the feed proportionally. In case of the acetylated membrane in 4 mol acetic anhydride, trend of flux increase is somewhat similar to that of pure chitosan. However, the total flux is still lower than that of the pure chitosan membrane due to the introduction

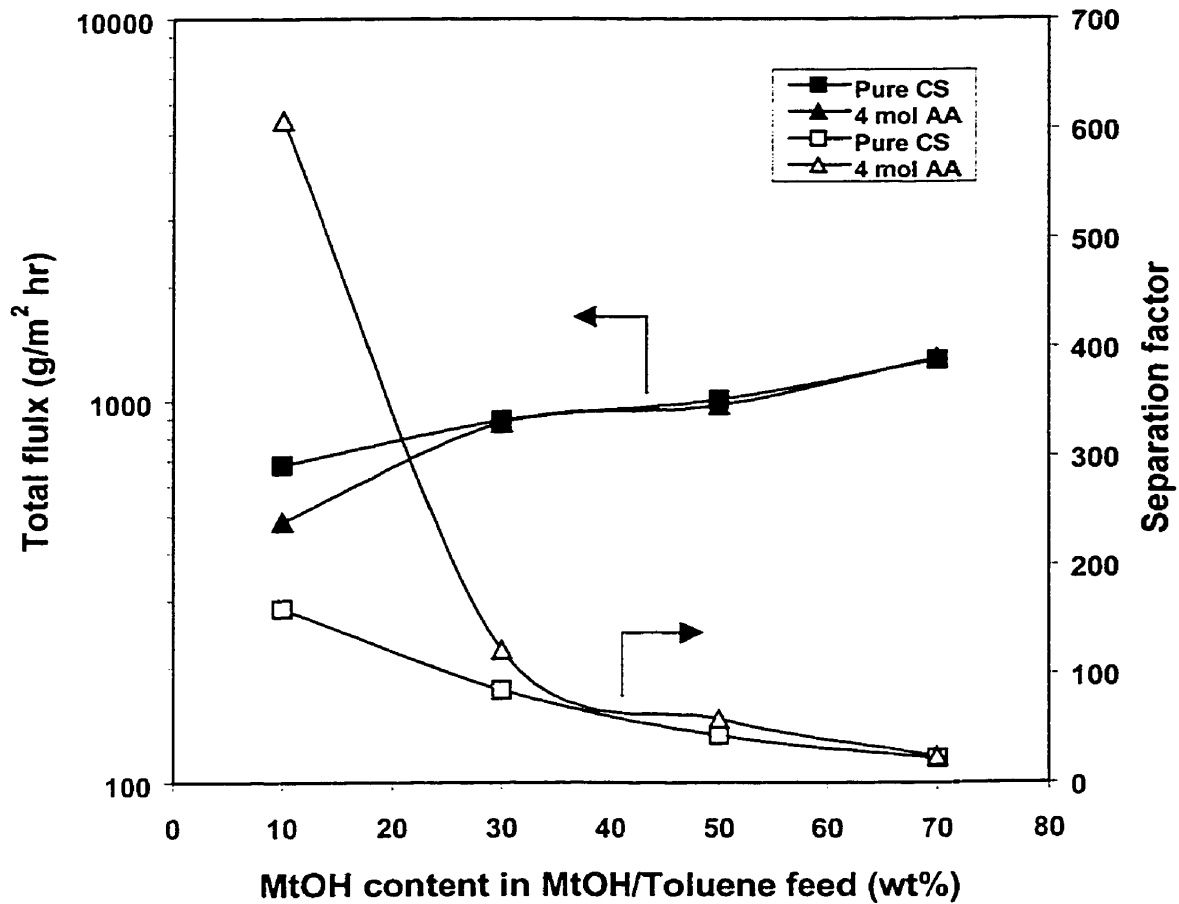


Figure 7.9 Feed concentration effect on total flux and separation factor of N-acetylated membrane and pure chitosan membrane for methanol/toluene mixtures at 35 °C (AA : Acetic Anhydride)

of rigid acetyl functional group although the flux difference is less pronounced compared to that of ethanol/toluene mixture. Good separation factor is achieved with the modified and unmodified chitosan membranes in Figure 7.9.

## 7.5 CONCLUSIONS

Composite chitosan membranes supported by porous polyetherimide membranes were prepared, N-acetylated and applied for the separation of alcohol/toluene mixture. Promising performance was obtained in terms of the flux and alcohol content in the permeate. Chitosan was reconverted to its origin, chitin which is expected to be mechanically strong and resistant for most of solvents. Total flux was decreased with the incorporation of acetyl functional group due to the large inter or intramolecular bonding among the acetyl groups. It is concluded that N-acetylated chitosan can be a good candidate not only for the dehydration application but also for the separation of alcohol from other organics such as alcohol/toluene and methanol/MTBE with the chemical modification. In continuous chapter the pervaporation application of chitosan membrane for the separation of methanol/MTBE was studied.

## CHAPTER 8

# CHITOSAN/ANIONIC SURFACTANT COMPLEX MEMBRANES FOR THE PERVAPORATION SEPARATION OF METHANOL/MTBE AND CHARACTERIZATION OF THE POLYMER/SURFACTANT SYSTEM\*

---

### 8.1 SUMMARY

For the separation of methanol/MTBE mixtures, methanol selective chitosan composite membranes were prepared and tested for pervaporation experiments. When anionic surfactants are added into the cationic chitosan solution, the solution viscosity was drastically decreased due to the collapsed chain conformation. Pervaporation characteristics of surfactant modified chitosan membrane were substantially improved due to the decreased membrane thickness and possible enhanced affinity to methanol. Rheological data of the casting solution was measured using viscometer and the surface morphology of the surfactant complexed chitosan membrane was investigated by atomic force microscopy (AFM).

---

\* Part of this study has been accepted for the publication in Journal of Membrane Science in August, 2000

## 8.2 INTRODUCTION

Pervaporation membrane separation process is a membrane process to separate the liquid/liquid mixture by using the difference of chemical potential of the component intended to be separated across the membrane. The performance of the pervaporation membrane largely relies on the physical and chemical properties of the membrane material.

The choice of material for the pervaporation separation of organic/organic separation process is difficult mainly because of the lack of polymer material sustainable in harsh operating conditions and the difficulty of controlling the membrane affinity to the separated component. Considerable effort has been made to separate MtOH/MTBE [Chen & Martin, 1995a; Yang et al., 1998; Cao et al., 1999a, 1999b, 2000; Nam & Lee, 1999b; Rhim & Kim, 2000], EtOH/MTBE [Nguyen et al., 1997, 1998; Lao et al., 1997], alcohol/toluene [Park et al., 1994, 1998; Huang et al., 2000], and benzene/cyclohexane [Park & Oh et al., 1994; Sun et al., 1999; Inui et al., 1998; Wang et al., 1999] mixtures. Chitosan is the deacetylated form of chitin, which is the second most abundant biopolymer in nature. Chitosan has both reactive amino and hydroxyl groups that can be used for chemical reactions and salt formation. These hydrophilic groups are considered to play an important role in preferential water sorption and diffusion through the chitosan membrane. Chitosan membranes have been studied mostly for the dehydration of alcohols. From previous researches in this laboratory [Huang et al., 1999a; Moon et al., 1999], chitosan has been shown to have good film forming properties, chemical resistance, and high permselectivity for water. Cationic chitosan can form polyelectrolyte

complexes with the oppositely charged polymers such as sodium alginate, carboxymethyl cellulose and anionic surfactants. In early work polyelectrolyte complex membranes [Michaels, 1965] have attracted interest for use as pervaporation dehydration applications due to its large hydrophilicity and unique properties. Nam and Lee [1999b] have carried out an interesting study regarding the chitosan/surfactant system for the separation of methanol/MTBE. It was stated that the flux and separation factor of chitosan-surfactant complex membrane was greatly increased because the membrane structure was loosened with the incorporation of surfactant molecules and thus the membrane nature was modified.

For the separation of methanol from methanol/MTBE mixtures, hydrophilic polar polymers are preferred. In this sense, chitosan is a good candidate for methanol/MTBE separation together with good physical properties. Very recently, Yoshikawa et al. [2000] studied the methanol/MTBE separation using agarose which is a natural polymer like chitosan. They observed the good permselectivity to methanol.

It is well known that ionic surfactants can be ionically bound to the polymers having opposite, strong and cooperative charges. Surfactant ion binding to a polymer with the opposite charge is a discharging process, and is more favorable than its binding to a neutral polymer [Shirahama, 1998]. The structure of polymer-surfactant complex membranes relies on the charge, hydrophobicity and molecular weight of the polymer as well as the charge and shape of the surfactant. Figure 8.1 is the presumed depiction of the reaction mechanism of chitosan and anionic surfactants. Four anionic surfactants and an amphoteric were used to make the chitosan/surfactant complex and their chemical structures are presented in Figure 8.2. The reason why we investigated the various

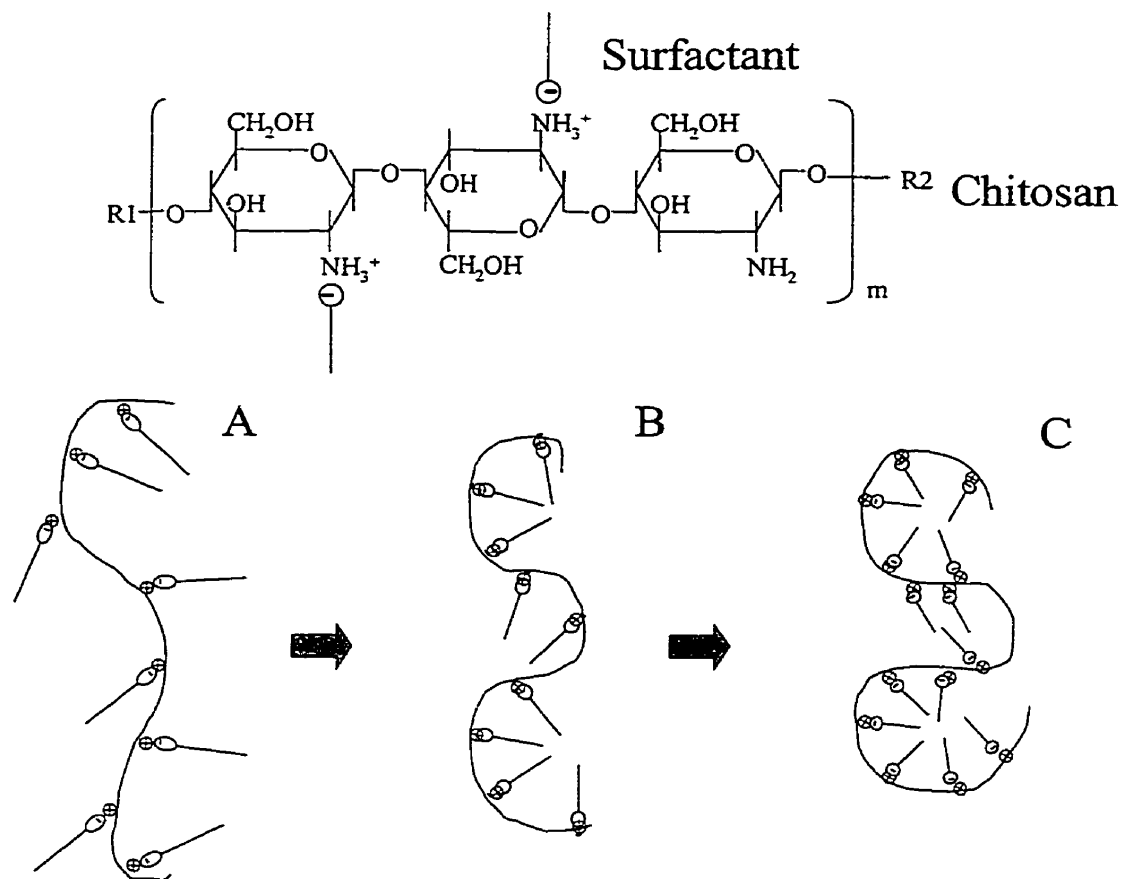


**Figure 8.1** Tentative model of the formation of the chitosan-anionic surfactant complex in the solution. Surfactant molecules binding to chitosan chain according to the increase of the amount of surfactant from A (initiation of binding) to C (shrunk coil)

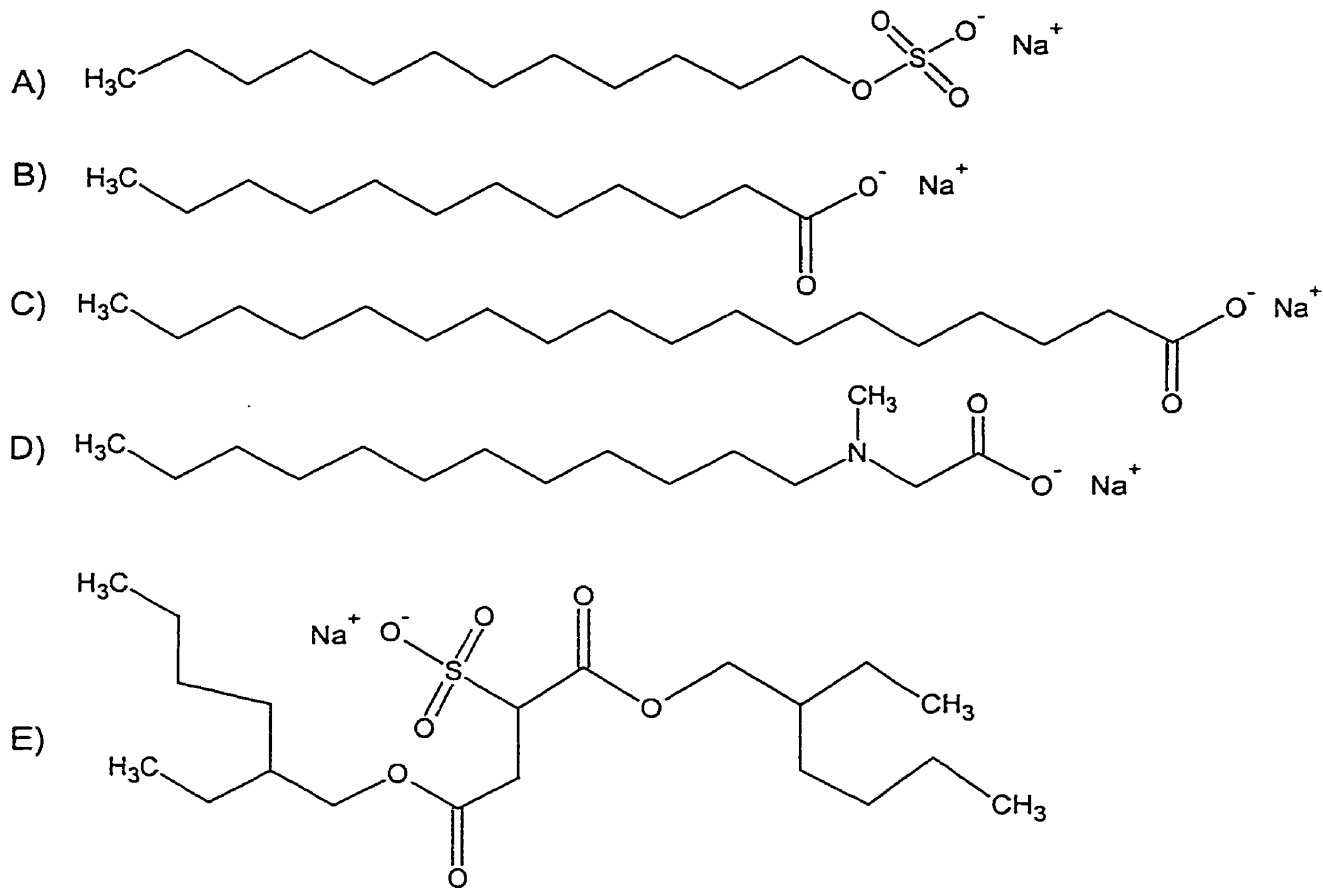


**Figure 8.2** Chemical structures of anionic surfactants; A) sodium dodecyl sulfate (SDS)-C<sub>12</sub>H<sub>25</sub>NaO<sub>4</sub>S, B) sodium laurate (SL)-C<sub>12</sub>H<sub>23</sub>NaO<sub>2</sub>, C) sodium stearate (SS)-C<sub>18</sub>H<sub>35</sub>NaO<sub>2</sub>, D) amphoteric sodium N-lauroyl sarcosinate (SLS)-C<sub>15</sub>H<sub>28</sub>NNaO<sub>3</sub>, and E) dioctyl sodium sulfosuccinate (DSS)-C<sub>20</sub>H<sub>37</sub>NaO<sub>7</sub>S

surfactants/chitosan systems is to elucidate the nature of the binding behavior of the different surfactants in terms of the surface characteristics and to study the alteration of membrane performance for the separation of MtOH/MTBE mixtures. Methyl tert-butyl Ether (MTBE) is a primary component of modern oxygenated California reformulated gasoline, and is currently being used as an octane enhancing fuel additive despite concerns about its contamination of drinking water. During the manufacturing process of MTBE, excessive methanol is used to increase the yield and the separation of methanol/MTBE becomes difficult at the azeotropic concentration.

The aim of this study is to investigate the pervaporation characteristics of chitosan membranes bound with various anionic surfactants having different chain length or hydrophilic head groups, and rationalize their performance in the light of the interfacial phenomena between the polymer and surfactant. The physicochemical changes in the membranes upon the addition of surfactants were illuminated by means of instrumental investigations and the pervaporation experiments.

### **8.3 THEORY OF SURFACTANT/POLYMER BINDING**

It was stated that the strong binding of surfactant molecules to polymer of opposite charge started at even much lower concentration than the critical micelle concentration (cmc) of surfactant because the strong electrostatic potential around the polymer chain attracts the surfactant molecules into the surroundings of the polymer chain. Hydrophobic interaction between the alkyl chain of the surfactant and possible the hydrophobic portion of polymer is considered another driving force of polymer/surfactant complex formation.

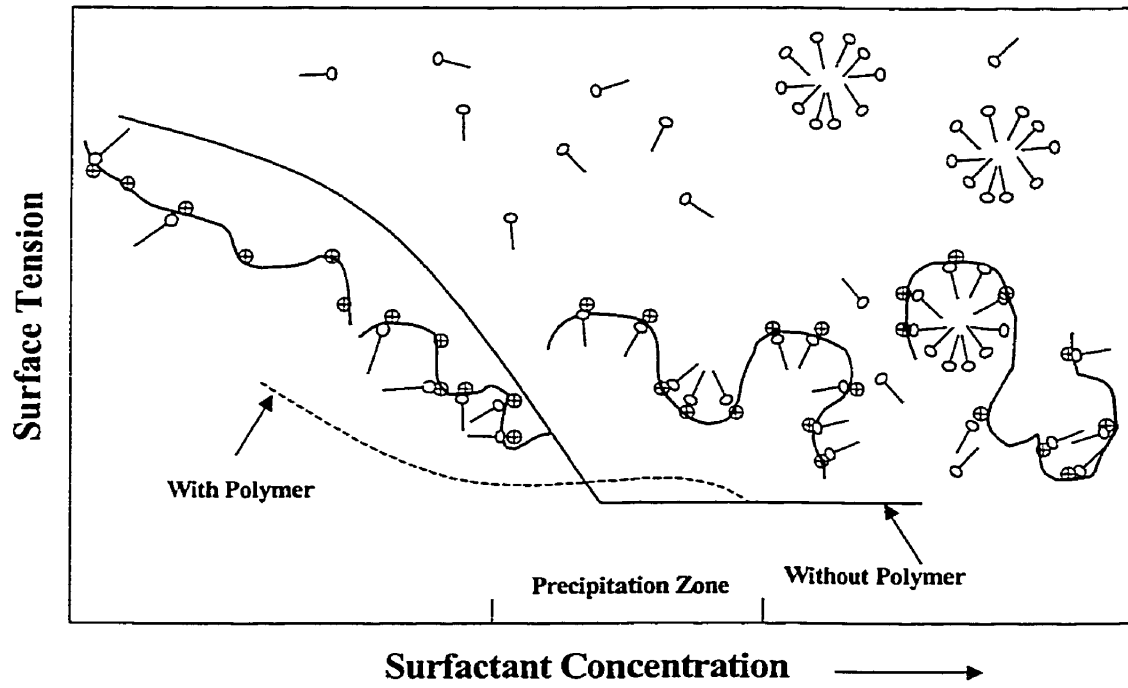


**Figure 8.3 Model to describe the polymer and surfactants association behavior in aqueous solution**

Also the binding phenomena strongly depends on the chain length and charge of surfactant, the temperature, and the salt in the solution as well as the molecular weight of polymer, the polymer properties (e.g. hydrophilicity or hydrophobicity), charge density, and structure of the polymer. The detailed effects concerning the change of the binding conditions can be found in review papers [Wei & Hudson, 1995; Bekturov & Bimendina, 1997]. The binding isotherms to describe the interaction of surfactant with the oppositely charged polymer are varied according to the nature of binding sites. One of the simple models is the closed association (CA) model [Linse et al., 1998].

$$\beta = \frac{K_0 K C_s}{1 + K_0 K C_s}$$

where  $\beta$  is the degree of binding,  $K_0 K$  is the cooperative binding constant and  $C_s$  is the concentration of free surfactant molecule in the solution. The binding isotherm illustrates the following aspects. At low surfactant concentration there is no significant interaction. At the critical association concentration (CAC) a strong binding occurs cooperatively. At higher concentration a plateau region which represents further increase of the free surfactant concentration like the case in the absence of the polymer emerge [Jönsson et al., 1998]. This simple model to describe the polymer and surfactant association behavior in aqueous solution is presented in Figure 8.3 [Ober & Wegner, 1997].

## 8.4 EXPERIMENTAL

### 8.4.1 Materials

Chitosan flakes (Flonac-N) with MW 100,000 and 99% N-deacetylation degree were donated by Kyowa Technos Inc, Japan. EM Science, NJ, USA supplied N-dimethylacetamide (DMAc). Sigma Chemical, USA supplied ethylene glycol (monomethyl ether). Aromatic polyetherimide (MW 30,000) was from Polysciences, Inc., PA, USA. Acetic acid (glacial) and methanol were supplied by BDH Chemicals Co., Toronto, Canada. Methyl tert-butyl Ether ( $C_5H_{12}O$ ) from Aldrich Chemical Co. was used as received.

Anionic surfactants, sodium dodecyl sulfate (SDS), sodium laurate (SL), sodium stearate (SS), dioctyl sodium sulfosuccinate (DSS) and amphoteric sodium N-lauroyl sarcosinate (SLS) were purchased from Sigma Chemical, USA. Water was de-ionized and distilled before use.

#### **8.4.2 Membrane preparation**

Chitosan solutions consisting of 0.8 wt% chitosan in 2 wt% aqueous acetic acid solutions were filtered to remove any undissolved solids and impurities. Then surfactant dissolved in water was added into the prepared chitosan solution and blended for several hours to obtain homogeneous chitosan/surfactant complex solution. Porous polyetherimide (PEI) membranes were prepared via the wet phase inversion technique from the casting solutions containing 18 wt% PEI, 77 wt% DMAc, and 5% ethylene glycol. The casting solution was cast onto a polyester non-woven fabric held on a glass plate with the aid of a casting knife made in this laboratory. The cast film was immediately immersed into a coagulation bath. The resulting membrane was washed in de-ionized water thoroughly and air-dried completely at ambient temperature. Initial microporous PEI membranes

showed a pure water permeation rate of 115.8 kg/m<sup>2</sup> hr at transmembrane pressure of 100 psi and operating temperature 22 °C. Most of the water flux tests were performed in replicate to achieve precision in the flux. Composite membrane supported by porous poly (etherimide) (PEI) membrane was prepared by casting the chitosan/surfactant solution onto the porous support and dried for 24 hours at ambient temperature. In order to clarify the effect of surfactant addition for the chitosan top layer thickness the same amounts of chitosan solutions were cast on the porous substrates. Composite membranes prepared were used for the pervaporation separation experiment without any further post treatment.

### 8.4.3 Pervaporation experiment

The pervaporation experiment was carried out using the apparatus and method described in chapter 3. Pervaporation separation performances are characterized in terms of the permeation flux (kg/m<sup>2</sup> hr) and MeOH content in the permeate

$$J = \frac{Q}{At}$$

where  $Q$  is the amount of the permeate (kg),  $A$  is the membrane area (m<sup>2</sup>) and  $t$  is the operating time (hr).

Analysis of the permeate composition was carried out by using a HP 5890 Gas Chromatography with a TCD detector. The column used in GC analysis was 6' × 0.125" packed with Porapak Q.

### 8.4.4 Rheological properties of chitosan/surfactant solutions

The rheological data were collected using a Fann coaxial cylinder viscometer at room temperature. This instrument consists of a stationary inner cylinder surrounded by a rotating outer (concentric) cylinder. The outer cylinder rotated at a known speed and the torque (dial reading) on the inner cylinder was measured. The rotor of this viscometer had an internal radius of 1.8415 cm. The bob had a radius of 1.7245 cm. In order to make sure that wall effects were absent, the rheological data of chitosan/surfactant solutions were collected with a larger gap-width bob/rotor system as well. It was found that there were no wall effects present in these measurements.

#### **8.4.5 Scanning electron microscopy**

Scanning electron microscopy was used to study the cross section morphology of the various composite membranes and to measure the thickness of the membrane. Cryogenic fracturing of the membrane was done after freezing the samples in liquid nitrogen. All specimens were coated with a conductive layer (400Å) of sputtered gold. A Jeol JSM 805 scanning electron microscopy was used for the specimens at 20kV.

#### **8.4.6 Atomic force microscopy**

AFM of Molecular Imaging, Phoenix, AZ, USA was used. The AFM images are taken in the tapping mode based on the optical lever cantilever detection design. The images presented in this study contain 256×256 data points. The Si single crystal cantilevers used for imaging were between 1 μm in length and possessed a spring constant in the 31-71 N/m range. The force applied for imaging ranged from 1.0 to 100 nN.

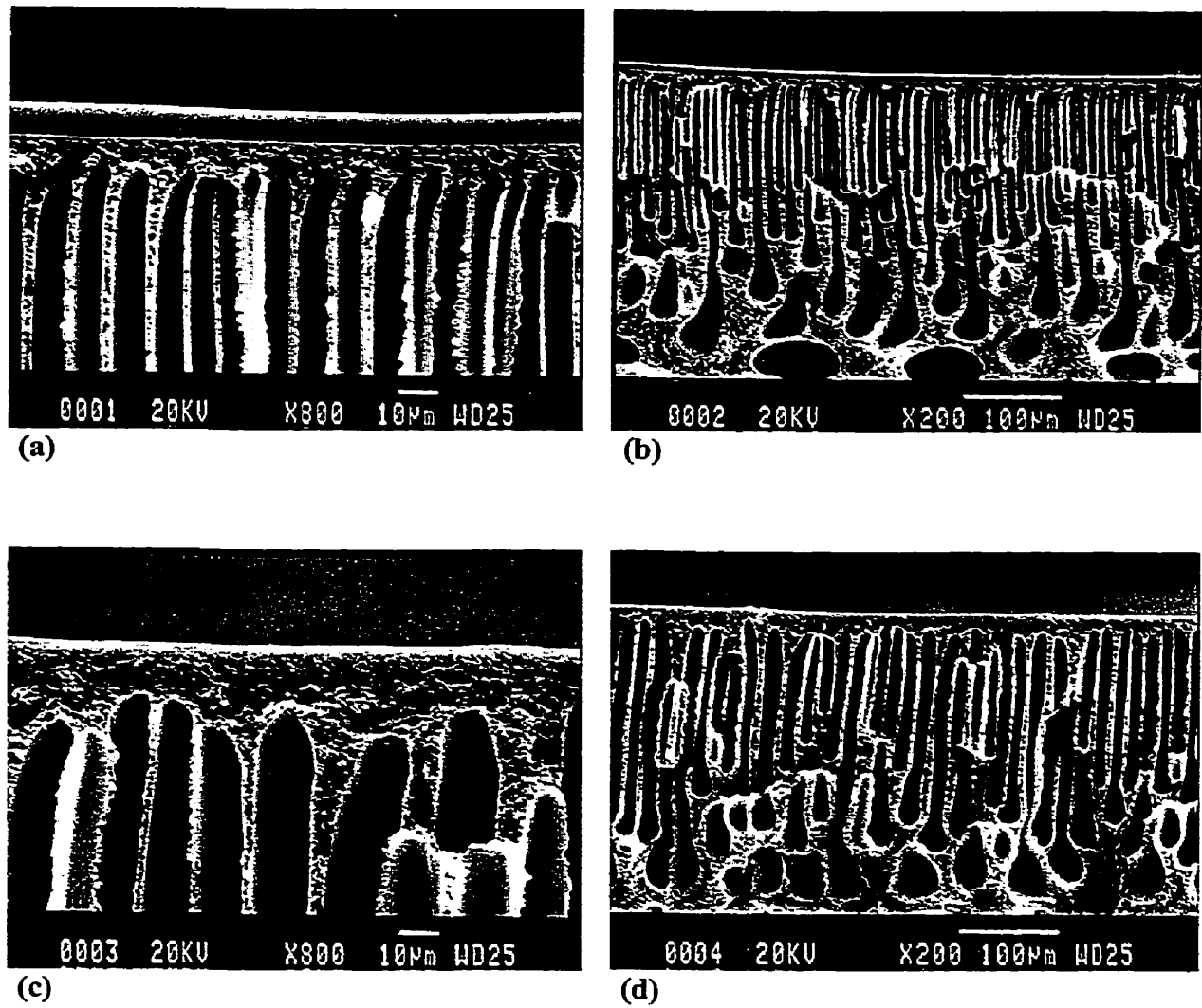


**Figure 8.4 SEM picture of the composite membrane. (a) and (b) are the adjacent view and overview of the membrane cross-section without the addition of surfactant, respectively; (c) and (d) are the adjacent view and overview of the membrane cross-section with the addition of DSS surfactant, respectively**

## **8.5 RESULTS AND DISCUSSIONS**

### **8.5.1 Scanning electron microscopy**

The morphology of the composite membrane prepared in this study is shown in Figure 8.4. It is apparent that dense chitosan top layer is coated on the top of finger like microporous PEI membrane. Note that top layer thickness of pure chitosan is about 10  $\mu\text{m}$  in Figure 8.4(a) and (b). However, when the casting solution is complexed with anionic surfactant the top layer thickness of the composite membrane was drastically decreased. The thickness of complexed chitosan layer was about 2  $\mu\text{m}$  as shown in Figure 8.4(c) and (d) and is the direct result of chitosan/surfactant association behavior. Detailed justification for this phenomenon will be given with the analysis of solution viscosity data in the next section.

### **8.5.2 Rheological properties of the polymer/surfactant solution**

In order to identify the effects of anionic surfactants on the chitosan chains, that is, the conformation change of the chitosan chains, the solution viscosities were measured using a cylinder viscometer and the results are plotted in Figure 8.5. Upon the addition of oppositely charged surfactant (0.005 wt% based on chitosan solution) to the polymer solution, immediate interaction takes place in the solution largely because of the electrostatic attraction among many possible forces such as van der Waals, hydrogen bonding and hydrophobic interaction between the polymer electrolyte and the surfactant molecules. First this binding phenomenon will neutralize the ionic charge of the system

and cause change in the polymer conformation. As a result, the physical and chemical properties of the polymer solution will be greatly altered. One of the well-defined phenomena upon the increased addition of the surfactant is that the size of polymer chain collapses or reduces. This can be explained by the hydrophobic interaction among the hydrophobic tails of the surfactant molecules attached on the polymer chain. The hydrophobic tails of the surfactant molecules can interact with the hydrophobic portion of polymer chain, which increases the solution viscosity rapidly [Jönsson et al., 1998], however this was not observed in this study because chitosan does not have a hydrophobic alkyl portion on it. There was also a report that the volume of polymer gel rapidly decreased or collapsed with the addition of the oppositely charged surfactant resulting from the hydrophobic aggregation of surfactant molecules in the gel with decrease in the osmotic pressure of counter-ion released to the solution [Ryabina et al., 1990]. Upon the addition of surfactants, the chitosan solution viscosities decreased drastically for all cases. Newtonian behavior was observed for all DSS, SDS and SS surfactants. This can be rationalized by the following. As depicted in Figure 8.1A the situation that surfactant bound to chitosan chain is not stable thermodynamically because the alkyl portion faces toward the solution. Thus, surfactants will attract other hydrophobic portions in the solution which can be offered only by other hydrophobic tails of surfactants. As a result, the thermodynamically stable environment that means the conformational rearrangement of chitosan chain into a much reduced size occurs as depicted in Figure 8.1C. Apparently, the size reduction results in the reduction of viscosity. Another proof of the size reduction of chitosan molecule is the SEM pictures of Figure 8.4(a) and (c) representing the top layer thickness of chitosan. As described

before, the top layer thickness was developed upon the addition of surfactants to the casting solution because the size reduction of polymer chains decreased the degree of overlapping significantly providing mutually shared framework. The effect of surfactant concentration on the solution viscosity is shown in Figure 8.6 and 8.7. Concentrations of DSS and SDS surfactants were increased from 0.002% to 0.008% and 0.002% to 0.01%, respectively. Solution viscosities generally decrease with increasing the concentration of surfactants. During the preparation of the solutions the turbidity of the solutions that is the typical phenomenon of cmc was not observed over the explored concentration range. However in case of SDS, solution viscosity with added 0.01% SDS is not lower than that of added 0.006% SDS. It was found that the precipitates occurred at 0.01% SDS, which might suggest that 0.01% was already over the cmc. Thus the precipitate might affect the solution viscosity.

The size of polymer chain decreased according to the increase of surfactant concentration due to the increased hydrophobic interaction among the hydrophobic tails of surfactants. Our interest is how the altered conformation of chitosan chains affects the membrane performance for the separation of the methanol/MTBE mixture. This will be discussed in the pervaporation section.

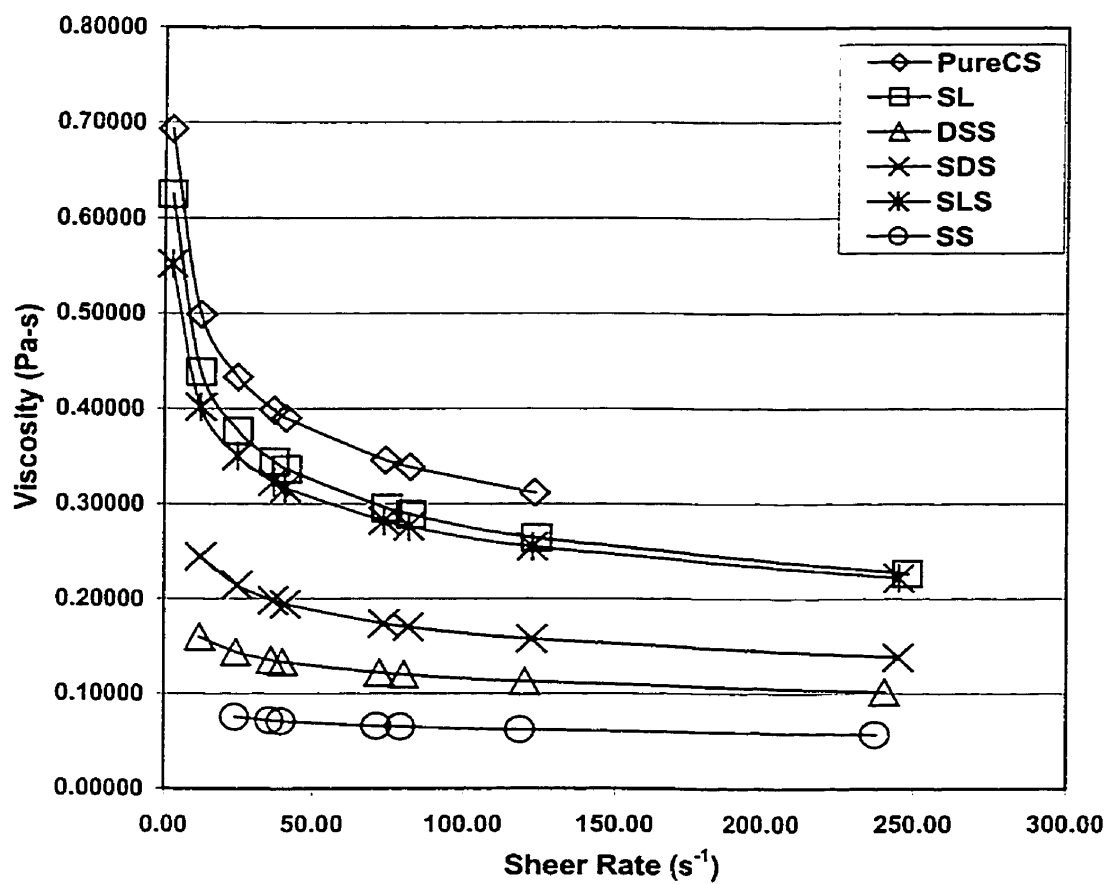


**Figure 8.5** Apparent viscosities of polymer solution with the addition of various surfactants at ambient temperature

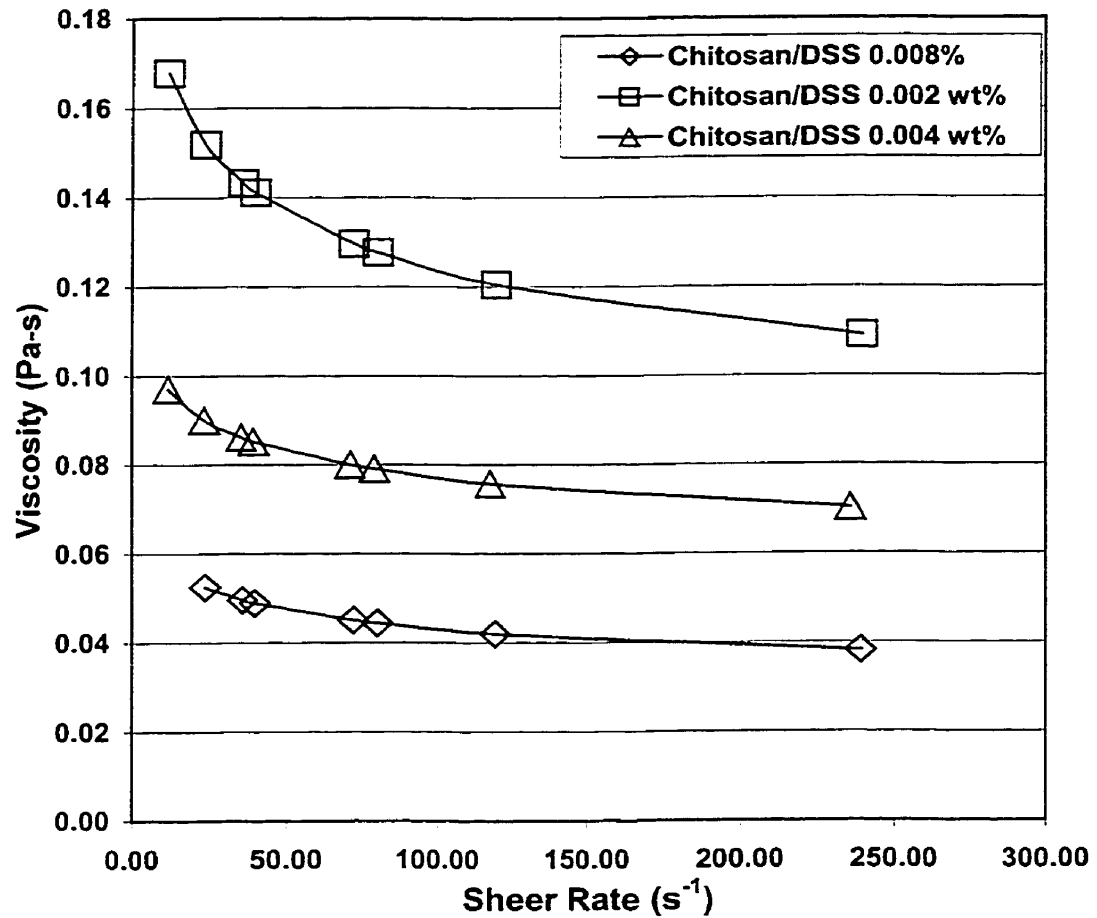


**Figure 8.6** Surfactant (DSS) concentration effect on apparent viscosities of polymer solutions at ambient temperature

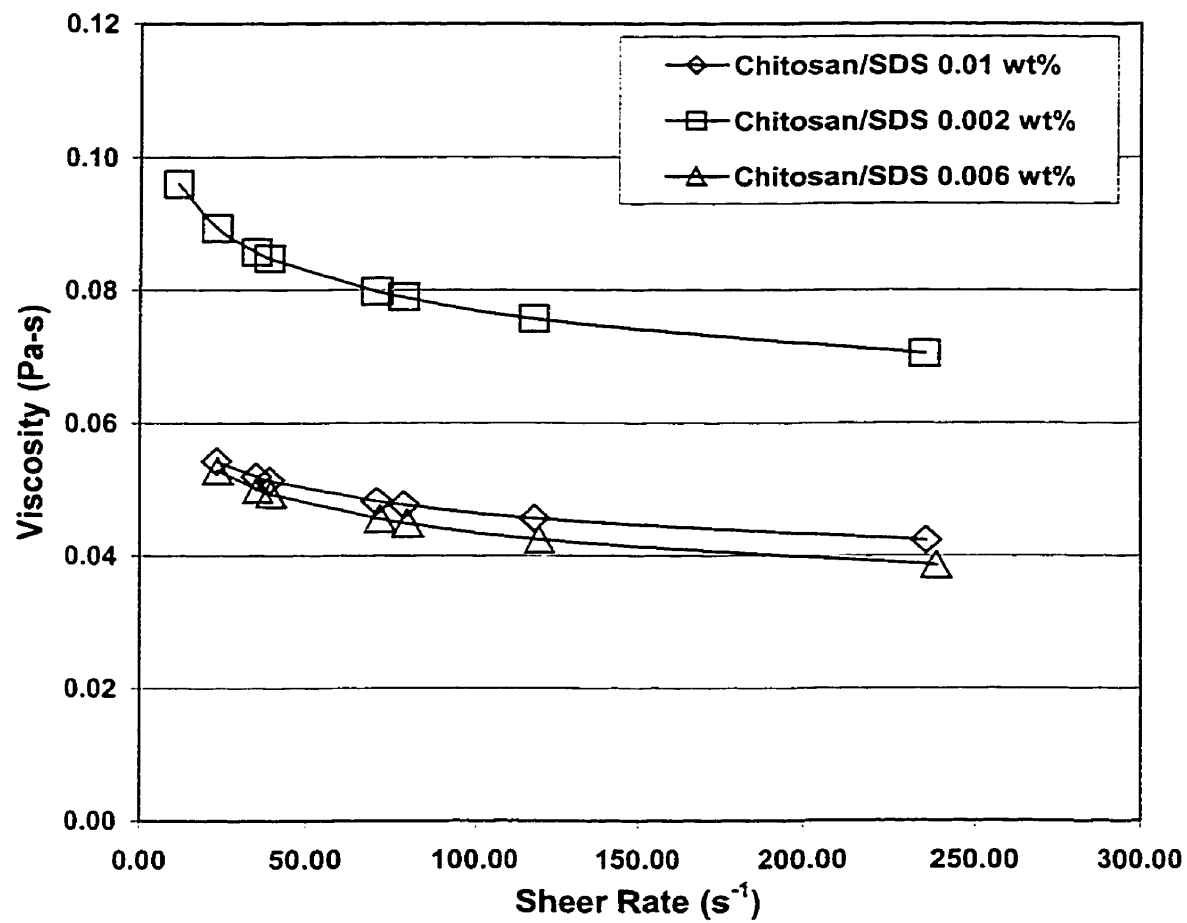


**Figure 8.7 Surfactant (SDS) concentration effect on apparent viscosities of polymer solutions at ambient temperature**

### 8.5.3 Atomic force microscopy (AFM) study of membrane surface

Possible change of membrane surface morphology due to the addition of surfactant was studied by means of AFM. Three membranes were prepared with the solutions of pure chitosan, 0.002% SDS added chitosan, and 0.008% DSS added chitosan. Figure 8.8 presents the AFM topography and amplitude images of membranes without surfactant (a), (b), with SDS addition (c), (d) and with DSS addition (e), (f). From the AFM pictures it is clear that the surfaces of modified membranes with surfactant are generally more level than that of non-surfactant membrane. As explained in the rheological experiment section, upon the addition of surfactant the chitosan chain experienced chain shrinkage or chain agglomerate arising from the attraction among surfactant tails. Thus it was expected that the surface of surfactant added membrane was less rough than before. Membrane surfaces can be characterized more clearly in AFM 3D views of Fig. 8.9. Surfaces of surfactant added membranes, (b) and (c), is less rough than that of pure CS (a) and show larger rumps caused by the agglomeration of the polymer chains. However, in this experiment I did not intend to analyze the relationship between the surface morphology and the pervaporation characteristics.

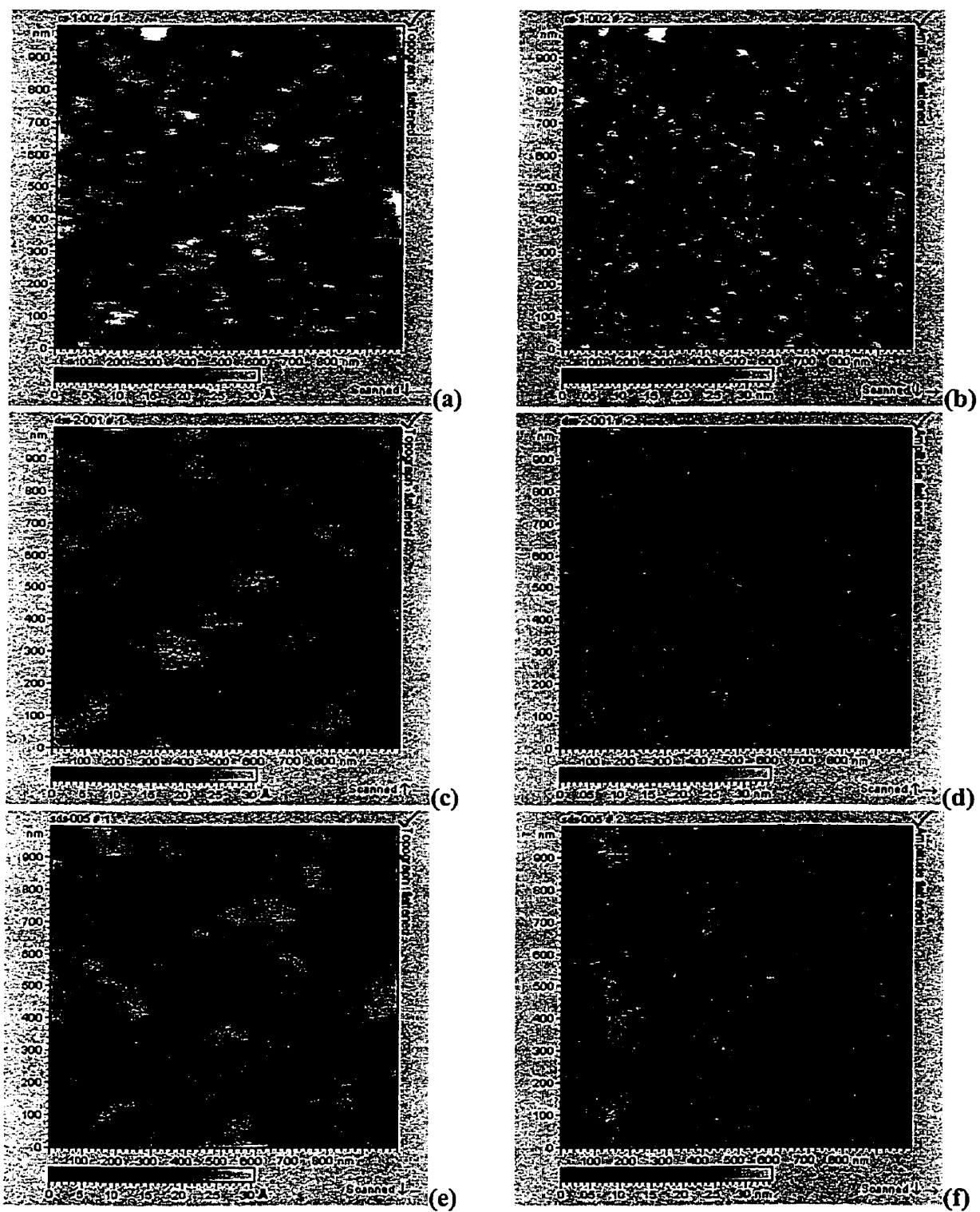


**Figure 8.8** AFM topography [(a), (c) and (e)] and amplitude [(b), (d) and (f)] views of pure CS, modified CS with DSS 0.008% and modified CS with SDS 0.02%

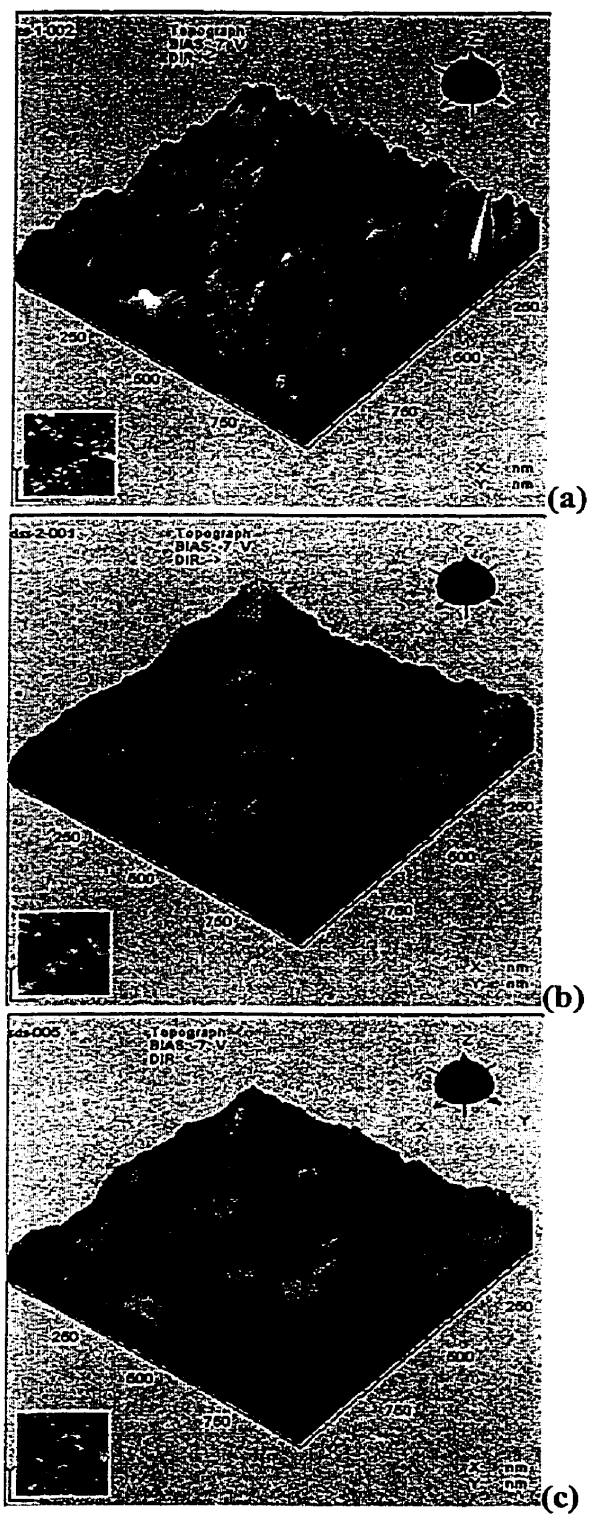


**Figure 8.9** AFM 3D views of pure CS membrane (a), DSS (0.008%) modified CS (b), and SDS (0.002%) modified CS (c)

#### 8.5.4 Pervaporation of methanol/MTBE mixture

It must be pointed out that chitosan membrane is a hydrophilic membrane and methanol is to be selectively separated against less polar MTBE. Upon the addition of surfactants, it was found that there were conformational changes of polymer chains as noted in the previous section. This conformational change can affect the permeation flux positively or negatively, depending on the binding geometry of surfactant on the polymer chain. That is, the separation performance of the surfactant complexed membranes is largely affected by the surfactant type, the extent of binding, and the quantity of surfactant etc.

In order to recognize the effect of varying aspects such as the type of the head group, the length of hydrophobic tail, and the morphology of surfactant for the characteristics of pervaporation separation, pervaporation experiments were carried out with the composite membranes complexed with 0.005% surfactants. From Figure 8.9, it is obvious that methanol is the component separated selectively through the chitosan composite membranes because of the high MeOH content in the permeate. This implies that the existence of surfactant does not substantially alter the chemical nature of chitosan complex membranes. It is interesting to note that the fluxes of SL and SS complexed membrane are less than that of pure CS. Note that they have carboxyl ( $\text{RCOO}^-$ ) head groups and linear alkyl groups. Among the surfactants tested, DSS is of special interest due to its high flux and reasonable separation efficiency. This can be attributed to its unique chemical structure as depicted in Figure 8.2(E). The nonlinear morphology of the DSS molecule creates more loose or less a packed matrix by hindering the close packing

and intermolecular bonding of chitosan polymer chain. Thus more space to accommodate the permeant was created, resulting in the high permeation flux.

Surfactant concentration in the chitosan solution might affect the separation characteristics by altering the matrix membrane properties. 3 different surfactant concentrations for DSS and SDS surfactants were studied in terms of the flux and separation efficiency (MeOH content in the permeate). First as shown in Figure 8.10 for DSS surfactant, it is difficult to rationalize the trend. However it was noted that flux was drastically decreasing with the increase of DSS surfactant from 0.002% to 0.004%. There are two possible explanations for this phenomenon. First more surfactant molecules are bound onto the chitosan polymer chain upon the increase of surfactant amount and surfactants block the possible passage between the chains. That is, the membrane matrix is more entangled. Second, surfactants binding the polymer chain will mitigate the gyrosopic movement of polymer chains by offering geometrical hindrance, which results in the lessened permeation flux. However, with the further increase of surfactant from 0.004% to 0.008% there is no significant variation for the permeation flux. It is believed that 0.008% is already over or around the critical micelle concentration which does not change the conformation of the polymer chains. It was found that complete dissolution of 0.008% DSS into chitosan solution was extremely difficult and so was that of 0.01% SDS as shown in Figure 8.11. A slight increase of the flux is shown at 0.01% SDS in Figure 8.11. It is postulated that the cores of micelles substantially formed over 0.006% SDS offer the passages for methanol. This postulate can also explain the increase of separation efficiency (MeOH content in the permeate) from 0.006% SDS to 0.01% SDS as shown in Figure 8.11 and from 0.004% to 0.008% DSS in Figure 8.10.

The feed concentration effect was investigated for DSS modified (CS-DSS) and pure chitosan membranes at 25 °C operating temperature and is presented in Figure 8.12. The flux for CS-DSS is larger than that of the pure CS membrane. Flux difference is increasing according to the increase of MeOH content in the feed mixture from 10% to 30%. The larger flux of the CS-DSS membrane can be explained as follows. As mentioned earlier, top layer thickness of CS-DSS is thinner than that of pure CS membrane. Thus mass transport through this thinner membrane is easier than through the thick pure CS membrane and in higher methanol feed concentration the swelling action of methanol facilitates mass transport through the thinner membrane. In Figure 8.13 it is shown that the MeOH content in the permeate for CS-DSS membrane is still larger than that of pure CS membrane without a common trade off phenomenon occurring between the flux and separation efficiency. This is attributed to the enhanced affinity to methanol after the incorporation of surfactant molecules on the chitosan chain. It is postulated that surfactant molecules control the hydrophilic-hydrophobic balance of the composite membrane which is of importance for organic-organic separation membranes.

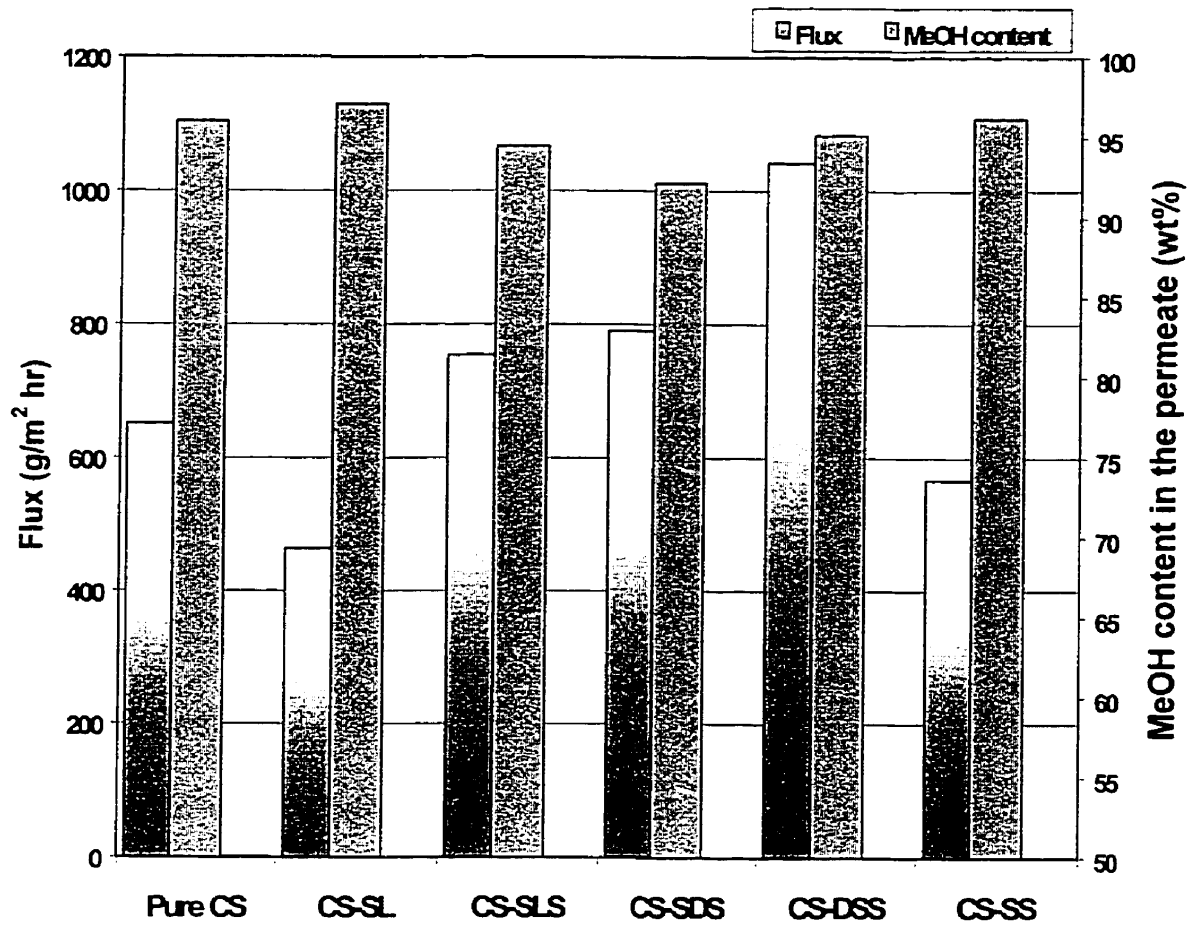


Figure 8.10 Pervaporation performance of chitosan composite membranes complexed with various surfactants for 20% MeOH/80% MTBE at 25 °C

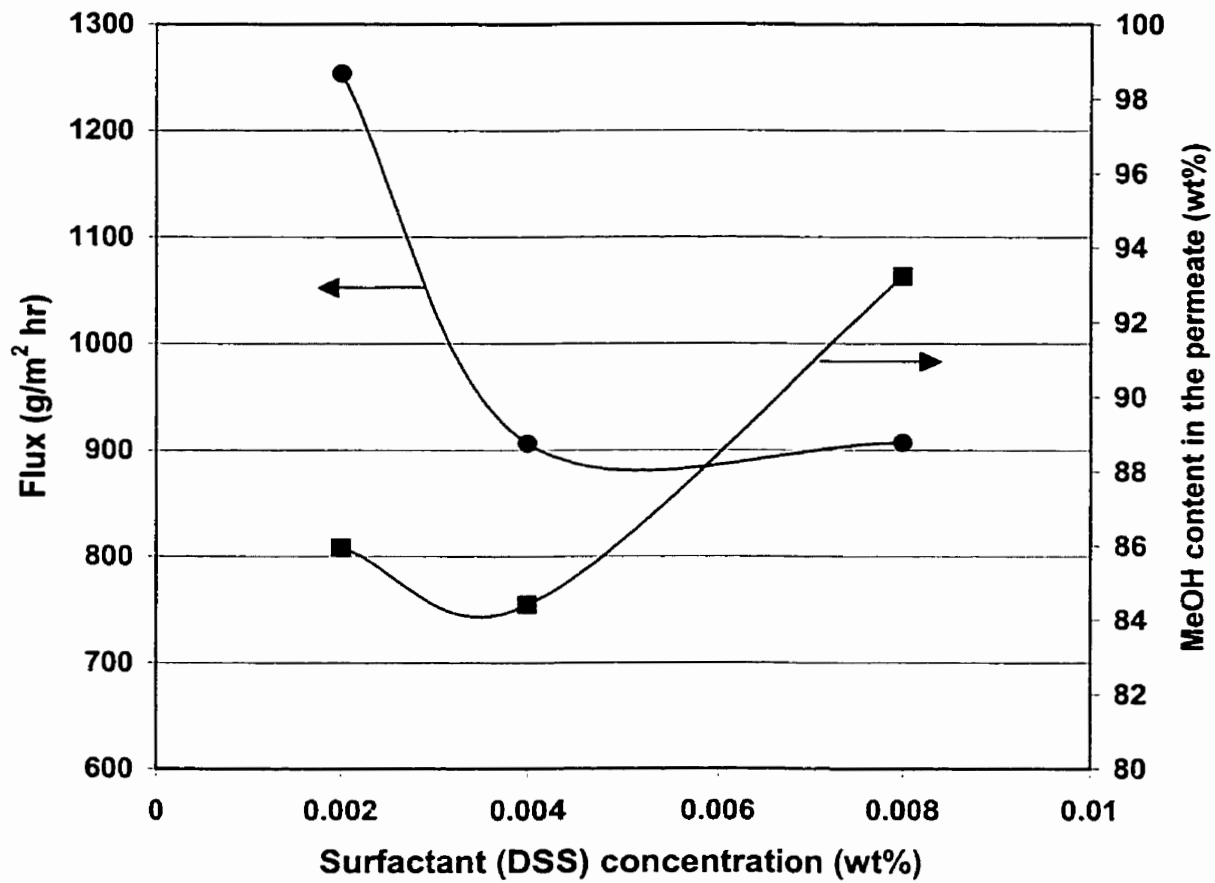


Figure 8.11 Surfactant (DSS) concentration effect on pervaporation performance at 25 °C

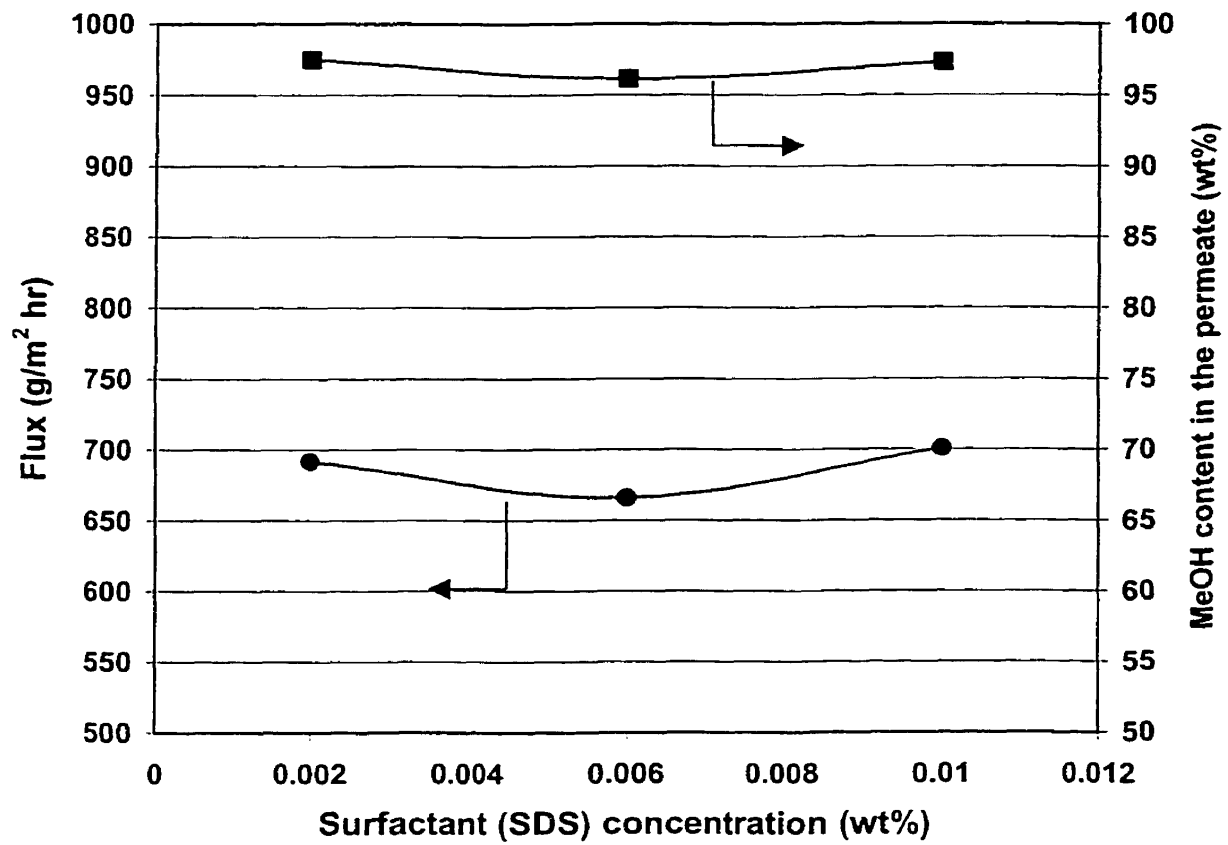
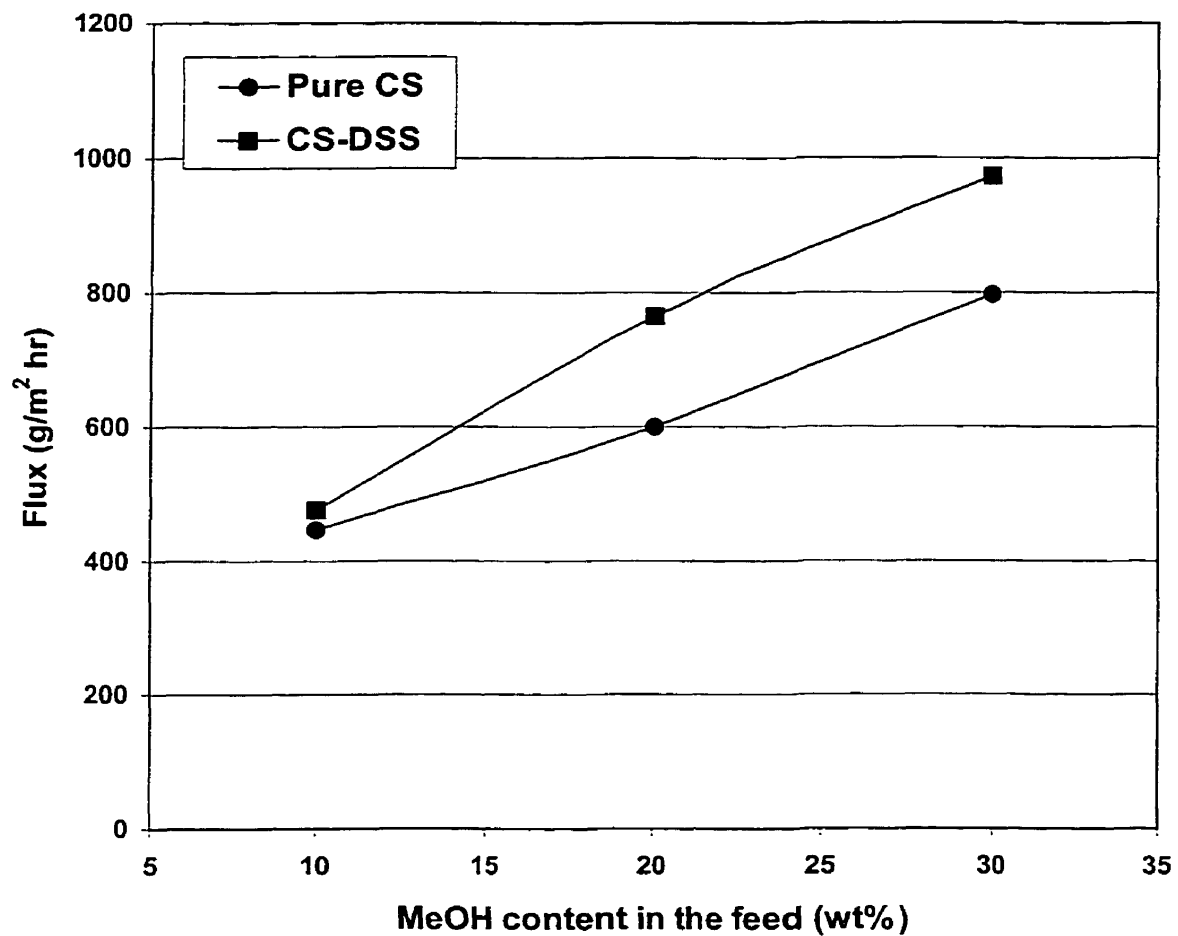
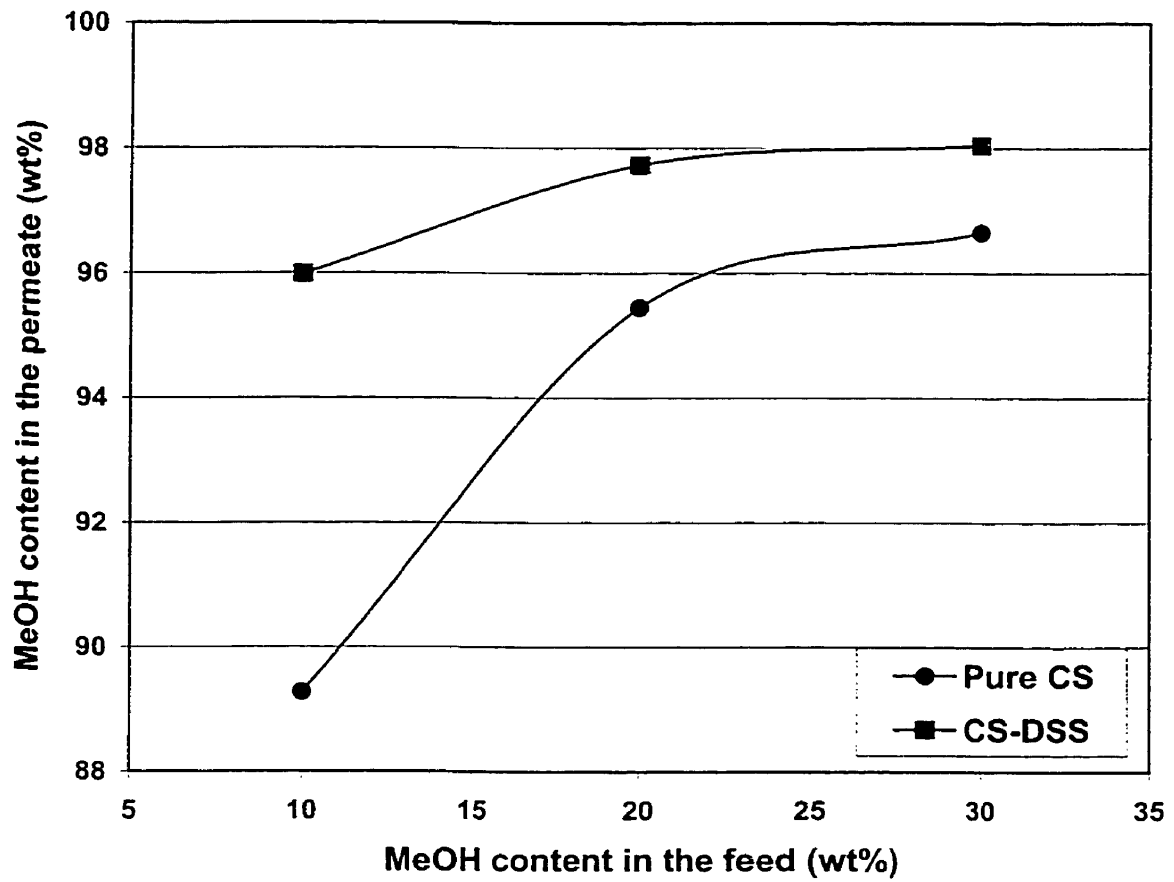


Figure 8.12 Surfactant (SDS) concentration effect on pervaporation performance at 25 °C



**Figure 8.13** Feed concentration effect on permeation flux of pure chitosan and DSS complexed chitosan (CS-DSS) composite membrane at 25 °C



**Figure 8.14** Feed concentration effect on MeOH concentration in the permeate of pure chitosan and DSS complexed chitosan (CS-DSS) composite membranes at 25 °C

### 8.5.5 Temperature effect on the pervaporation performance

Experimental data of temperature dependence of total permeation flux generally exhibits an Arrhenius relationship.

$$J = J_0 \exp(-E_p/RT)$$

where  $J_0$  and  $E_p$  are the pre-exponential factor and the apparent activation energy of permeation, respectively. Based on the solution-diffusion model, the activation energy of permeation can be expressed as follows.

$$E_p = E_D + \Delta H$$

where  $E_D$  and  $\Delta H$  are the activation energy of diffusion and the enthalpy of sorption of the permeant in the membrane, respectively.

Figures 8.14 and 8.15 show the temperature effect on the flux and separation efficiency, respectively for various composite membranes at 20% MeOH/80% MTBE mixture of the feed. In the figures, the effect of temperature on the flux is positive and justified based on the solution-diffusion model. As stated in the transport model rate determining process, diffusion process is facilitated at higher temperature due to the increased thermal motion of the polymeric chain. The other factor affecting the increase of the permeation flux upon the increase of the feed temperature is the partial vapor pressure of the permeant.

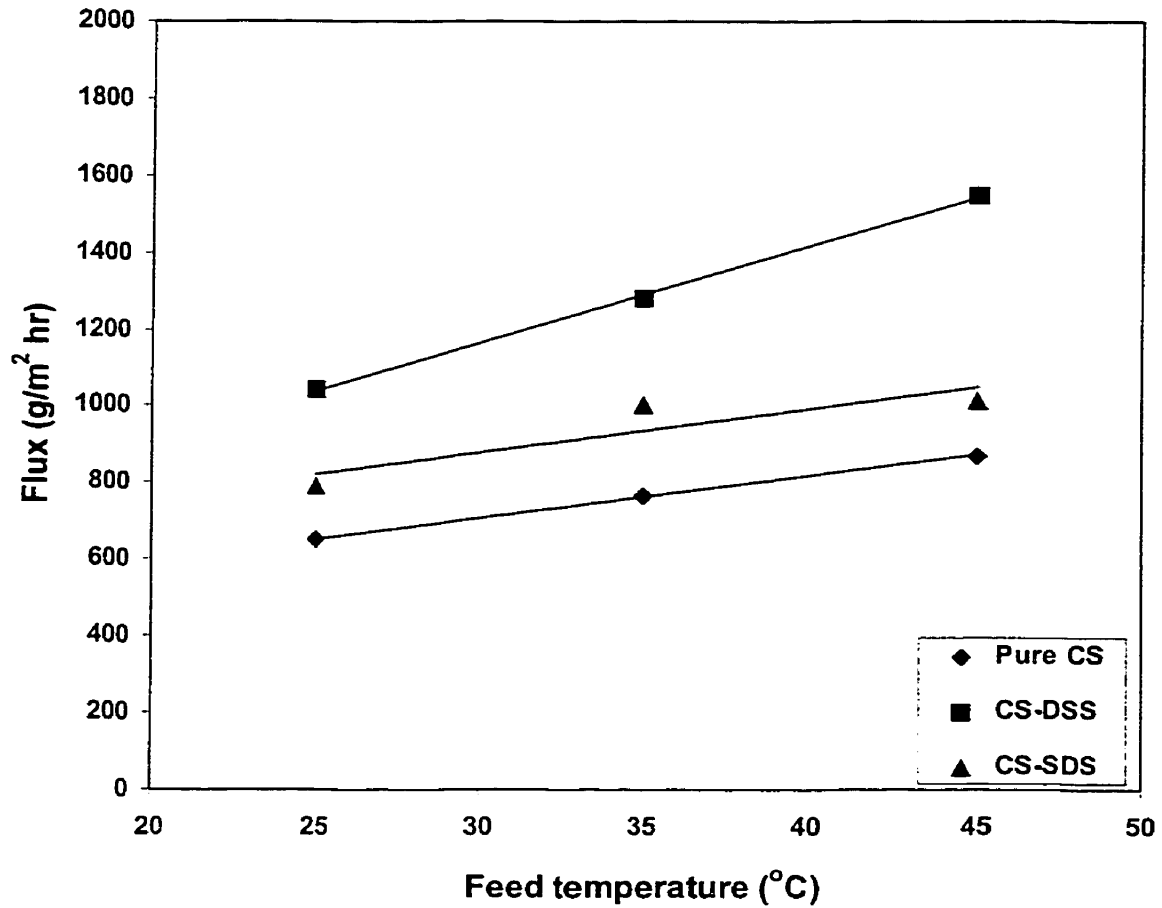


**Figure 8.15 Temperature effect on the permeation fluxes of pure, DSS modified, and SDS modified chitosan composite membranes for 20% MeOH/80% MTBE**

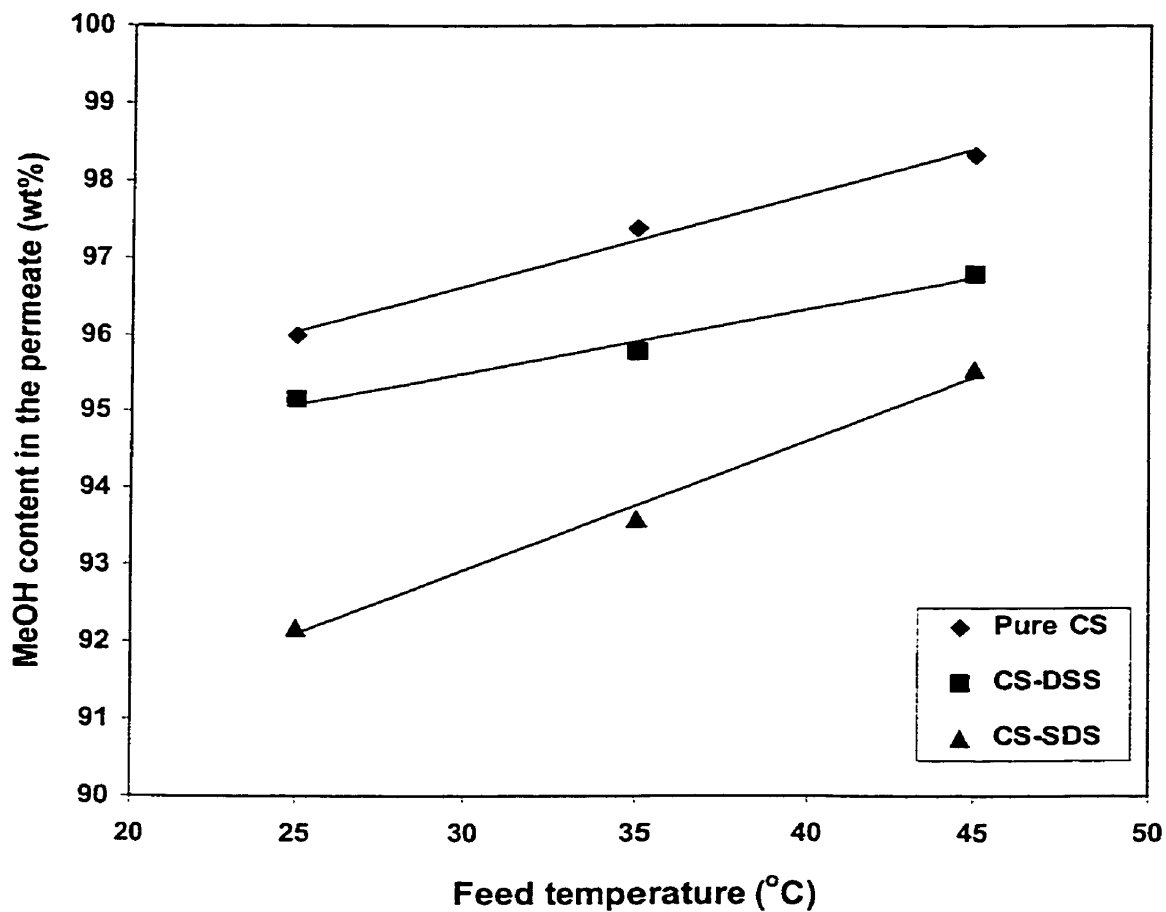


**Figure 8.16** Temperature effect on MeOH content in the permeate of pure, DSS modified, and SDS modified chitosan composite membranes for 20% MeOH/80% MTBE

## 8.6 CONCLUSIONS

Cationic polymer, chitosan, was complexed with oppositely charged surfactants. It was observed that surfactants are bound onto polymer chain strongly and cooperatively upon addition. One of characteristics of polymer/surfactant interaction is the size reduction of the polymer chain. This behavior was revealed by measurement of viscosity of chitosan solution. The advantage of size reduction of polymer chain for the membrane preparation is to reduce the membrane thickness. When the size of the unit polymer chain decreases due to the hydrophobic interaction of the surfactant tail, the possibility to form the polymer chain mesh on drying becomes difficult, and the membrane thickness is getting thinner. In this study, reduced thickness with the addition of DSS surfactant positively affected the permeation flux and achieved high MeOH content in the permeate because of the mitigated transport resistance of the permeant and enhanced affinity to methanol. High flux and good separation efficiency were achieved for the chitosan-surfactant complex membrane. Its potential application as a pervaporation membrane for separating alcohol/organic mixtures is quite promising.

## **CHAPTER 9**

# **ETHYLENE PROPYLENE DIENE MONOMER (EPDM) MEMBRANES FOR THE PERVAPORATION SEPARATION OF AROMA COMPOUND**

---

### **9.1 SUMMARY**

Ethylene propylene diene monomer (EPDM) rubber membranes were fabricated in thin film composite form to separate an aroma compound, ethyl butyrate, from water and to study the effect of operating parameters on the pervaporation performance. The resistance-in-series model was applied for the pervaporation results in order to estimate the transport phenomenon of the permeant. The partial flux of ethyl butyrate increased with the feed concentration. It was found that total flux decreased with the increase of the permeate pressure while organic flux increased. The effect of concentration polarization phenomenon on the pervaporation performance was observed with the change of the feed flow rate and the trend of concentration polarization was investigated. It was found that the overall mass transfer coefficient was a function of the feed flow rate at the fixed feed concentration.

## 9.2 INTRODUCTION

Among the major applications of pervaporation membrane processes, there has been a proliferation of papers dealing with dehydration application. However, organic separation from organic/water mixtures as an application area is relatively less addressed. Specifically organic separation from water is important in the following two areas; alcohol or aroma compound separation and volatile organic compound (VOC) separation. Traditional separation methods include packed tower air stripping, adsorption, distillation and oxidation as well as the relatively new membrane distillation process [Zander et al., 1989]. VOC removal from wastewater stream is becoming an important application of the pervaporation process in environmental treatment. However there exists a major hurdle limiting its commercialization, which is the lack of proper membrane materials for this application. There has also been growing research interest for the pervaporation application to biotechnology such as the aroma separation and the fruit juice concentration.

Generally hydrophobic elastomers such as polydimethylsiloxane (PDMS) [Almquist and Hwang, 1999; Yeom et al., 1999] and polyurethane [Hoshi et al., 1999a, 2000] as well as block copolymers such as S-B-S [Dutta and Sikdar, 1999] and acrylate [Hoshi et al., 1999b] have been extensively investigated for VOC removal application. Since pervaporation separation occurs based on sorption and diffusion processes, it was natural that researchers tried to increase the sorption selectivity of PDMS to organic compounds, by means of the incorporation of hydrophobic fillers (such as zeolite, silicas,

carbon blacks) [Vankelecom et al. 1997a, 1997b] and grafting of fluoroalkyl methacrylate onto PDMS [Mishima and Nakagawa, 1999, 2000].

For alcohol or aroma separation from water, many hydrophobic materials used for the VOC removal were studied. Among them PEBA [Djebbar et al., 1998; Baudot and Marin, 1996; Sampranpiboon et al., 2000] and polyoctylmethylsiloxane (POMS) [Schäfer et al., 1999] as well as zeolite filled PDMS [Adnadjevic et al., 1997] were the materials which showed promise. However in case of alcohol separation it was recognized that PDMS is not sufficiently permselective because alcohol compounds are generally not so hydrophobic compared to aroma compounds or VOCs.

Lu et al. [2000] found in the study of acetic acid/water separation that the advantage of silicalite addition into PDMS could be pronounced when the operating temperature is increased because the enhanced thermal energy lessens the kinetic limitation of silicalite in the membrane matrix. Effects of incorporated fillers on the sorption and the diffusion of aroma compounds were studied by Vankelecom et al. [1997b].

Ethyl butyrate is a colorless liquid with pineapple odor mostly found in fruit juices and is used as a model compound of aroma due to its popularity and moderate hydrophobicity.

Ethylene-propylene-diene-monomer (EPDM) rubber contains ethylidene norbornene (ENB) as inserted diene comonomer in the chains.

In the current study, we investigated EPDM rubber as a membrane material for the separation of an aroma compound using ethyl butyrate (EB) as a model compound. In addition the mass transport phenomena of aroma compound through EPDM membrane was investigated and correlated using a resistance-in-series model. In previous studies

[Nijhuis et al., 1991; Meuleman et al., 1999; Pereira et al., 1998], EPDM was mainly used to separate volatile organic compounds from aqueous solution.

### 9.3 RESISTANCE-IN-SERIES MODEL FOR THE ESTIMATION OF TRANSPORT PHENOMENON

A convenient model to describe the mass transport of a component is the resistance-in-series model (Figure 9.1), in which the overall resistance to mass transport ( $R_o$ ,  $s/m$ ) is written in the sum of the boundary layer resistance ( $R_{Li}$ ), the membrane resistance ( $R_{mi}$ ), and the permeate resistance ( $R_{pi} \approx 0$ ) as follows.

$$R_o = R_{Li} + R_{mi} = \frac{1}{K_i} = \frac{1}{k_{Li}} + \frac{1}{k_{mi}}$$

where  $K_i$  is the overall mass transfer coefficient (m/s).

Previously several research groups used the resistance-in-series model to interpret the pervaporation data [Nijhuis et al., 1991; Ji et al., 1994, 1995; Wijmans et al., 1996; Cote and Lipski, 1988; Raghunath and Hwang, 1992; Meuleman et al., 1999; Dutta and Sikdar, 1999].

The permeation flux of a component  $i$  through the diffusion boundary layer on the feed stream can be expressed as

$$J_i = k_{Li}(C_{bi} - C_i^*) \quad (1)$$

where  $J_i$  is the permeation flux ( $kmol/m^2 \cdot s$ ) of the component  $i$ ,  $k_{Li}$  is the boundary layer mass transfer coefficient (m/s) and  $C_{bi}$  and  $C_i^*$  are the concentrations of component  $i$  at feed bulk and interface with the membrane, respectively.

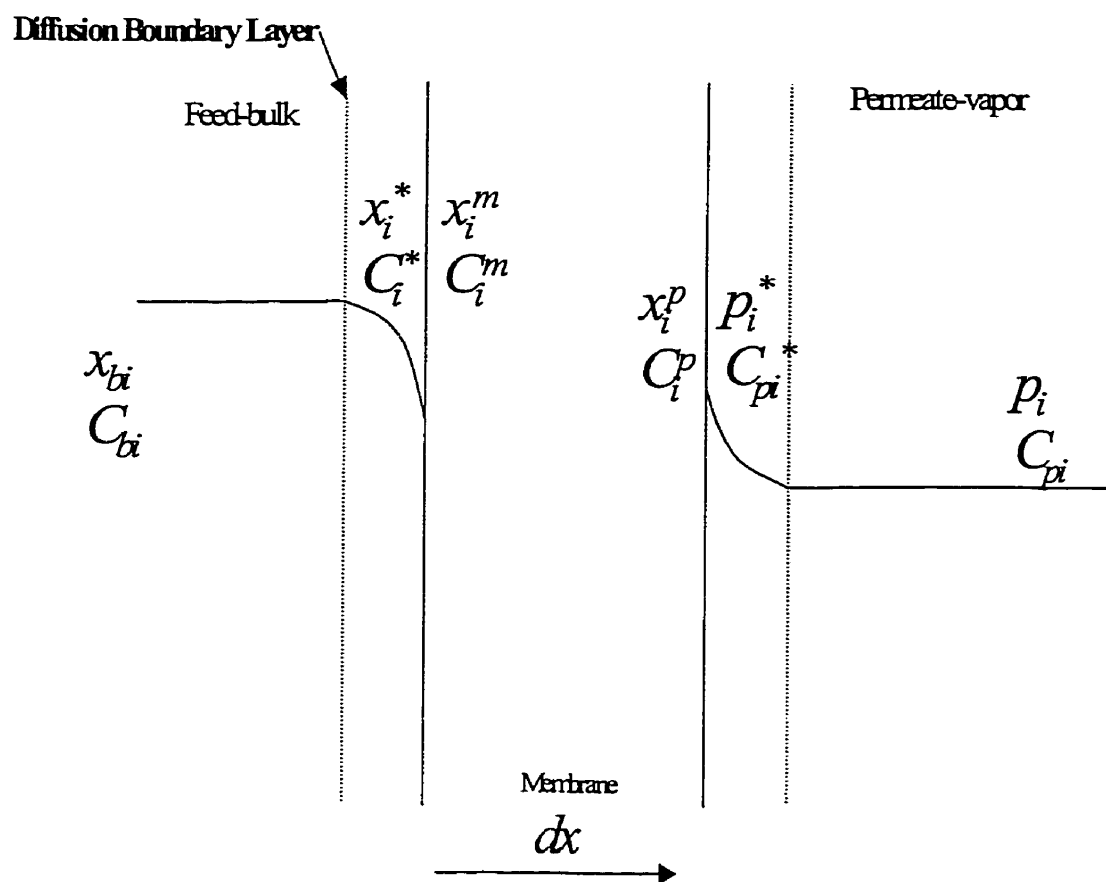


Figure 9.1 Diagram of resistance-in-series model

Equation (1) can be written in the mole fraction form instead of the concentration. Note that  $C_{bi}$  equals to the product of  $\rho_L$  and  $x_{bi}$ .

$$J_i = k_{Li} \cdot \rho_L (x_{bi} - x_i^*) \quad (2)$$

where  $x$  is the mole fraction,  $\rho_L$  is the density of water since the concentration of component  $i$  is very low in this derivation.

The permeation flux of the component  $i$  through the membrane can be expressed based on Fick's first law.

$$J = -D \frac{dC}{dx}$$

*Boundary condition*

$$x = 0, C = C_i^m$$

$$x = \delta, C = C_i^p$$

$$J_i = D_i \frac{(C_i^m - C_i^p)}{\delta} \quad (3)$$

The permeation flux in terms of overall mass transfer coefficient can be expressed as

$$J_i = K_i (C_{bi} - C_i^p) \quad (4)$$

Equation (3) and (4) can be simplified into (5) and (6), respectively when  $C_i^p \cong 0$  at low permeate pressure.

$$J_i = \frac{D_i C_i^m}{\delta} \quad (5)$$

$$J_i = K_i \cdot C_{bi} \quad (6)$$

where  $K_i$  is the overall mass transfer coefficient.

From equations (1) and (6) the following equation was derived.

$$J_i = K_i \left( \frac{J_i}{k_{Li}} + C_i^* \right) \quad (7)$$

When the equilibrium sorption is assumed to be linear between the concentrations of the component  $i$  in the interface and that in the membrane, the partition coefficient is defined as follows, which is commonly obtained by the sorption experiments.

$$H = \frac{C_i^m}{C_i} \quad (8)$$

From equations (5) and (8) the following intermediate equation can be written.

$$C_i^* = \frac{J_i \delta}{H \cdot D_i} \quad (9)$$

Substituting equation (9) into (7), gives equation (10).

$$\frac{1}{K_i} = \frac{1}{k_{Li}} + \frac{\delta}{D_i \cdot H} \quad (10)$$

or  $\frac{1}{K_i} = \frac{1}{k_{Li}} + \frac{\delta}{P_i}$

where  $k_{Li}$  is the liquid boundary layer mass transfer coefficient ( $=D_{Li}/t$ ) and  $P_i$  is the permeability of the permeant  $i$  ( $=D_i \cdot H$ ).

This is the overall mass transfer coefficient derived from the resistance-in-series model.

Hence the boundary layer mass transfer resistance (the intercept of the plot) and the permeability (reciprocal slope) of the permeant in addition to the membrane resistance can be obtained from the permeation flux data vs. the various membrane thicknesses.

Sometimes it is convenient to use partial vapor pressure difference in expressing the permeation fluxes. The flux in the permeate stream is written as follows

$$J_i = k_v (p_i^* - p_i)$$

The resistance-in-series model derived in terms of the pressure difference can be found in the work of Ji et al. [1994].

However in this study, equation (10) was used to estimate the experimental results.

## 9.4 EXPERIMENTAL

### 9.4.1 Materials

The EPDMs used in this experiment are listed in Table 1. Polyacrylonitrile (MW 150,000) was obtained from Polysciences, Inc., USA. N,N-Dimethylformamide was purchased from Aldrich Chemical Co. Inc., USA. Ethyl butyrate (or ethyl butanoate) was the product of Aldrich Chemical Company, Inc. Ethylene glycol (monomethyl ether) from Sigma Chemical Co. was used as such. A non-woven polyester fabric donated by BBA nonwovens (Veratec), USA was used as the backing material for the composite membrane. PVDF UF membranes from Millipore were utilized as porous substrates in most of experiments. Water was de-ionized and distilled before use.

	wt % of ethylene in ethylene/propylene	wt % of ENB (diene)	M <sub>w</sub> (g/mol)
Vistalon 8800	54	10	113,373
Vistalon 8609	62	8	94,944
Kelton 514	52	8	84,168

**Table 9.1 Analysis of EPDMs used in this study**

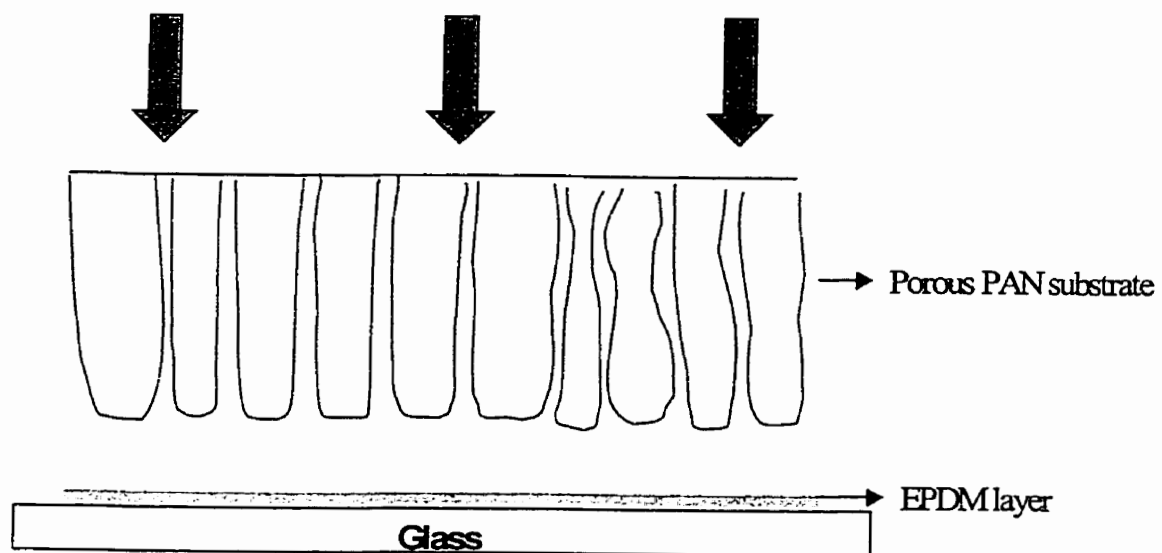


**Figure 9.2 Fabrication of EPDM thin film composite membranes**

### 9.4.2 Membrane preparation

Porous polyacrylonitrile (PAN) membranes were prepared via the wet phase inversion technique from the casting solutions containing 12 wt% PAN, 83 wt% DMF, and 5% ethylene glycol. The initial microporous PAN membranes showed a pure water permeation rate of  $261\text{-kg/m}^2\text{ hr}$  at transmembrane pressure of 100 psi and operating temperature  $22\text{ }^\circ\text{C}$ . Most of the water flux tests were performed in replicate to achieve precision in the flux. For the preparation of composite membranes with different thickness, two EPDM solutions of 9% and 11% in toluene were prepared. EPDM solution was cast onto a glass and then solution was allowed to evaporate for a certain time at room temperature. Before complete evaporation of EPDM thin film the porous PVDF substrates were laid over the partially evaporated EPDM thin film (Figure 9.2) and then the composite membrane was kept in the oven for 12 hrs at  $60\text{ }^\circ\text{C}$  to remove the residual toluene. With this technique, mass transfer resistance due to the intrusion of top layer solution into the porous substrate [Vankelecom et al., 1999] during the fabrication of composite membrane can be mitigated. Since EPDM films were sticky after drying, it was hard to handle the thin dense membranes. Thicknesses of the membrane used were Mem 1 ( $32\text{ }\mu\text{m}$ ), Mem 2 ( $76\text{ }\mu\text{m}$ ), and Mem 3 ( $95\text{ }\mu\text{m}$ ).

### 9.4.3 Pervaporation

The pervaporation experiment was carried out using the apparatus and method described in a previous publication [Huang et al., 1999]. The permeate was analyzed using total organic carbon analyzer (TOC) of Shimadzu (TOC-500), Japan.

Sorption amount of EPDM membranes for aroma was calculated using the following equation, which was used to estimate the partition coefficient  $H$  in this manuscript.

$$\text{Sorbed amount} = \frac{\text{total phenol amount sorbed (g)}}{\text{weight of dry membrane (g)}}$$

The permeation flux of aroma and the separation factor were calculated by the following equations;

$$J_a (\text{g} / \text{m}^2 \cdot \text{hr}) = \frac{Q_a (\text{g})}{A(\text{m}^2) \times t(\text{hr})}$$

$$\alpha_{\text{aroma/water}} = [Y_A / Y_W] / [X_A / X_W]$$

where  $J_p$  is the partial flux of aroma,  $Q_a$  is the amount of aroma compound in the permeate,  $A$  is the membrane area,  $t$  is the operating time which was generally more than 3 hours,  $X$  and  $Y$  are the weight fractions of the feed and permeate, respectively.

#### 9.4.4 Scanning electron microscopy

Scanning electron microscopy was used to study the cross section morphology of the various composite membranes and to measure the thickness of the membrane. Cryogenic fracturing of the membrane was done after freezing the samples in liquid nitrogen. All specimens were coated with a conductive layer (400Å) of sputtered gold. A Hitachi S-3000N scanning electron microscopy was used for the specimens at 20kV.

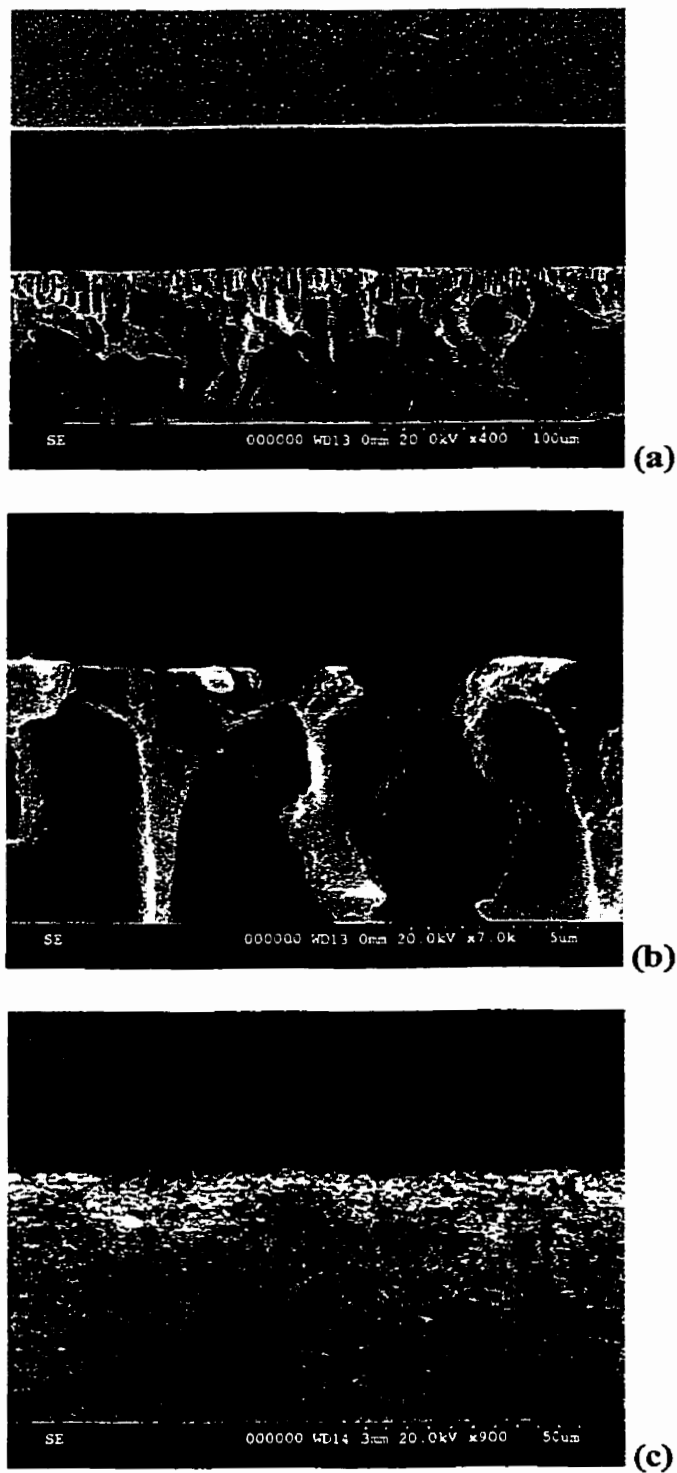


**Figure 9.3 SEM pictures of the composite membranes (a) PAN supported membrane, (b) close view of PAN supported membrane and (c) PVDF supported membrane**

## 9.5 RESULTS AND DISCUSSION

The morphology of the composite membranes used in this study is presented in Figure 9.3. It is obvious from the pictures that EPDM thin layer was properly cast on the top of the PAN and PVDF substrates. Close view of PAN supported membrane (Figure 9.3b) revealed that there was no penetration of EPDM solution into the micro pores of the substrates by the fabrication method used in this study.

In order to find out the effect of porous substrates on the pervaporation performance composite membranes consisting of top layer of about 76 micron thickness and four different substrates were prepared and tested for aqueous aroma solution ranging from EB feed concentration of 100 ppm to 400 ppm. Porous PMMA and PVDF substrates were commercial products having 0.22  $\mu\text{m}$  and 0.45  $\mu\text{m}$  pore diameters, respectively. PAN and PSf substrates were prepared in the lab by wet phase inversion techniques and showed 261 and 154  $\text{kg/m}^2 \text{ hr}$  water flux at transmembrane pressure of 100 psi and operating temperature 22  $^{\circ}\text{C}$ . The apparent difference in pore size and surface porosity was expected among four different substrates. In Figure 9.4, EB flux of membrane supported by PMMA substrate revealed the lowest EB flux followed by membrane supported by PSf substrate. This result suggests that EB flux is the function of substrate porosity since EB fluxes of the membranes supported by high water flux and pore diameter substrates are generally higher than those of the opposites. General trade off phenomena between EB flux and separation factor are observed in Figures 9.4 and 9.5. With this experiment it was concluded that substrates affect the pervaporation performance of EPDM composite membranes based on their surface porosity rather than

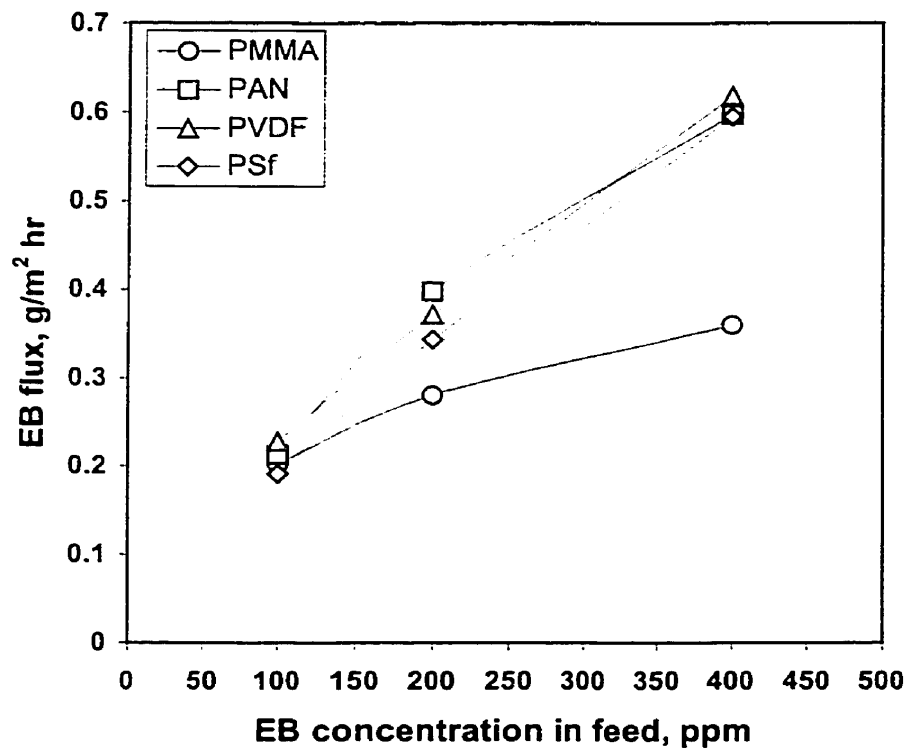


**Figure 9.4** Effect of substrates on the partial flux of ethyl butyrate (Mem 2 and Vistalon 8609)

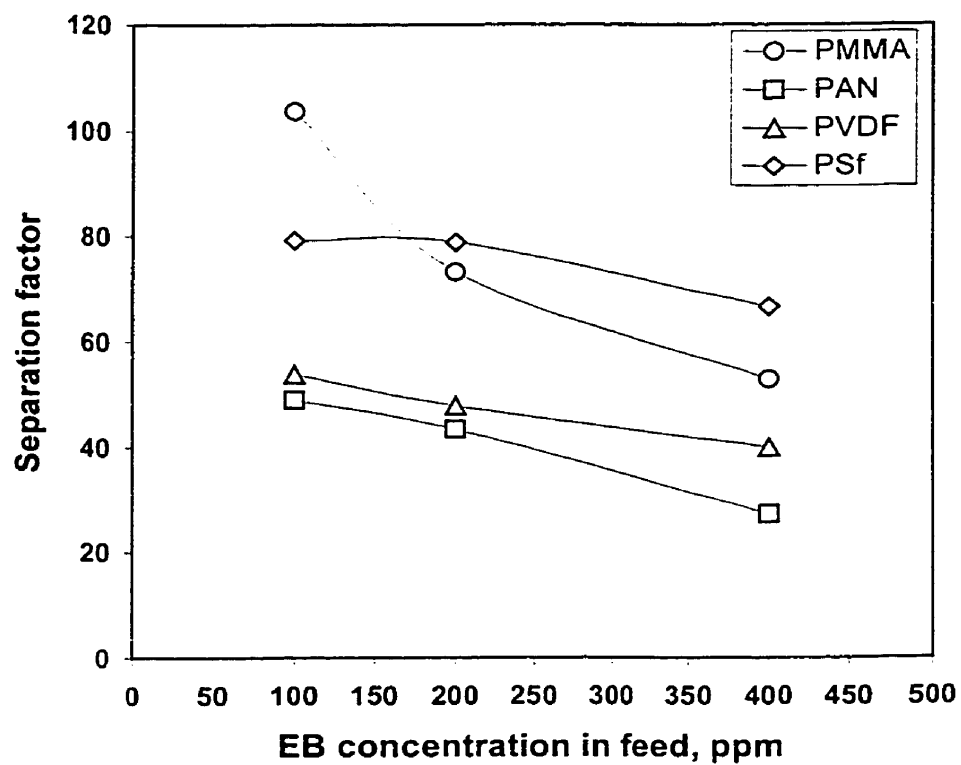


Figure 9.5 Effect of substrates on separation factor (Mem 2 and Vistalon 8609)

the types of materials. Note that PMMA and PAN are relatively hydrophilic, whereas PVDF and PSf are relatively hydrophobic. It should be pointed out that substrates were porous PVDF membranes throughout the whole experiments hereafter although PAN substrate showed comparable performance.

From this experiment, it was also found that the EPDM rubber was reasonably selective for the aroma compound, ethyl butyrate although the organic flux of EPDM membrane was slightly lower than those of PEBA and PDMS membranes reported in our lab [Sampranpiboon et al., 2000] and that of EPDM membrane for VOC separation [Pereira et al., 1998]. Note that the membrane studied in this work is relatively less hydrophobic than PEBA and PDMS, in addition, EB is relatively more hydrophilic than VOCs.

Figure 9.6 shows ethyl butyrate (EB) fluxes of three different composite membranes supported by porous PVDF substrates as a function of feed concentration. EB fluxes increase linearly with the increase of feed concentration. Overall mass transfer coefficients for different thicknesses,  $K_i$ , were obtained from the slopes based on the equation (6). It was observed that EB flux becomes larger with the reduction of membrane thickness because the diffusion resistance of EB through the membrane is mitigated with the reduction of the membrane thickness. Water and organic fluxes as a function of reciprocal membrane thickness are presented in Figure 9.7. Water flux that was independent of the feed concentration increases with decreasing membrane thickness.

Independency of water flux with the feed concentration suggests that water permeation is not affected by the concentration polarization in case of the removal of small amounts of organic from water stream. EB flux for EPDM membranes with the thickness range of 32-96  $\mu\text{m}$  is shown to be almost linearly increasing with reciprocal membrane thickness. The overall mass transfer resistance calculated from the plot of organic flux vs. the feed concentration is given in Figure 9.8 as a function of membrane thickness. The permeabilities of aroma compound obtained from the inverse slopes are slightly larger for Kelton 514 EPDM membrane than for Vistalon-8609 EPDM membrane. This can be attributed to the higher propylene content in Kelton 514 copolymer than that in Vistalon-8609. Note that polypropylene is more hydrophobic than polyethylene. Mass transfer resistance values are listed in Table 9.2. From the table, it is found that with the increase of membrane thickness the membrane resistance increases. The ratio of membrane mass transfer coefficient to liquid boundary layer mass transfer coefficient,  $k_m/k_{Li}$ , which represents the relative importance of hydrodynamic operation in small amount organic separation, increases with the decrease of membrane thickness. From this result, it is concluded that proper strategies to avoid any concentration polarization phenomenon have to be taken into consideration in order to achieve the maximum performance with given membrane material and membrane thickness in case of separation of small amount of organic compound.

Effect of feed flow rate on organic flux is shown in Figures 9.9 and 9.10. Organic flux increases with the feed flow rate. This suggests that the concentration polarization plays an important role in the application involving separation of small amounts of organic compounds.

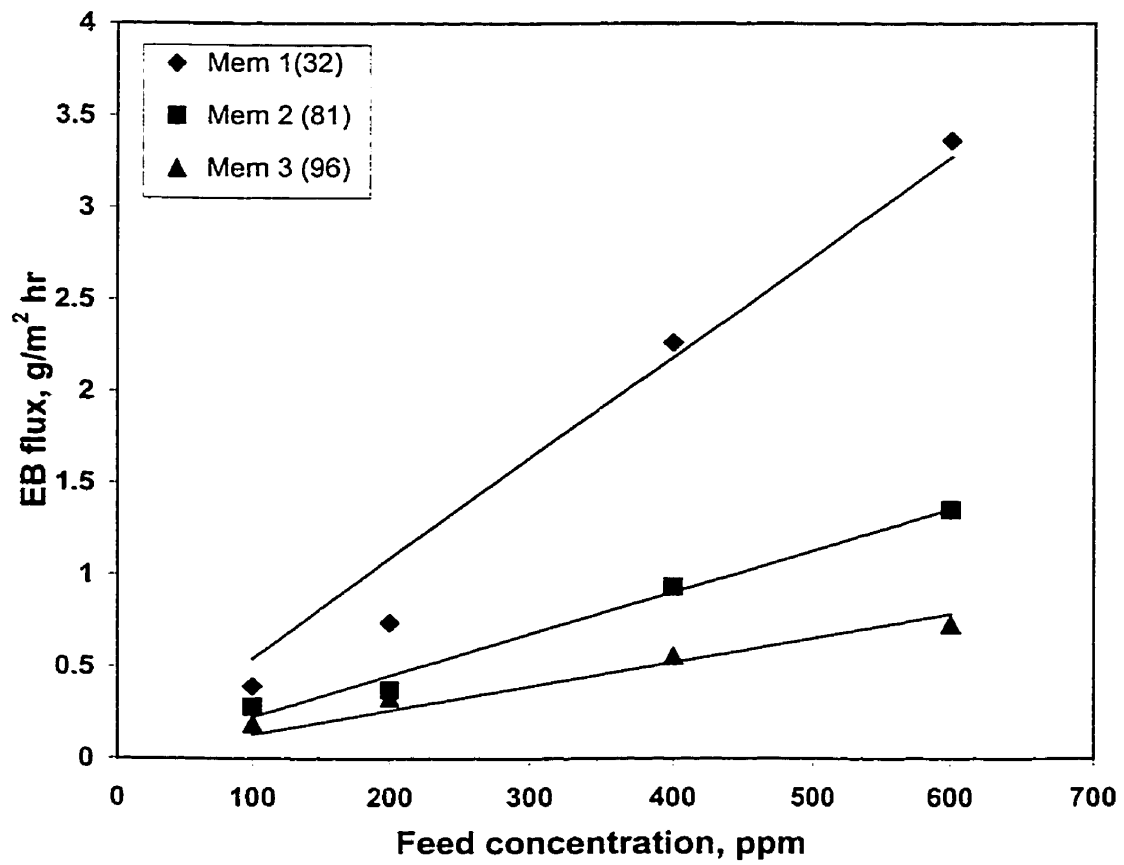


Figure 9.6 Effect of feed concentration on the aroma flux in EPDM membranes (Kelton 514) at 30 °C

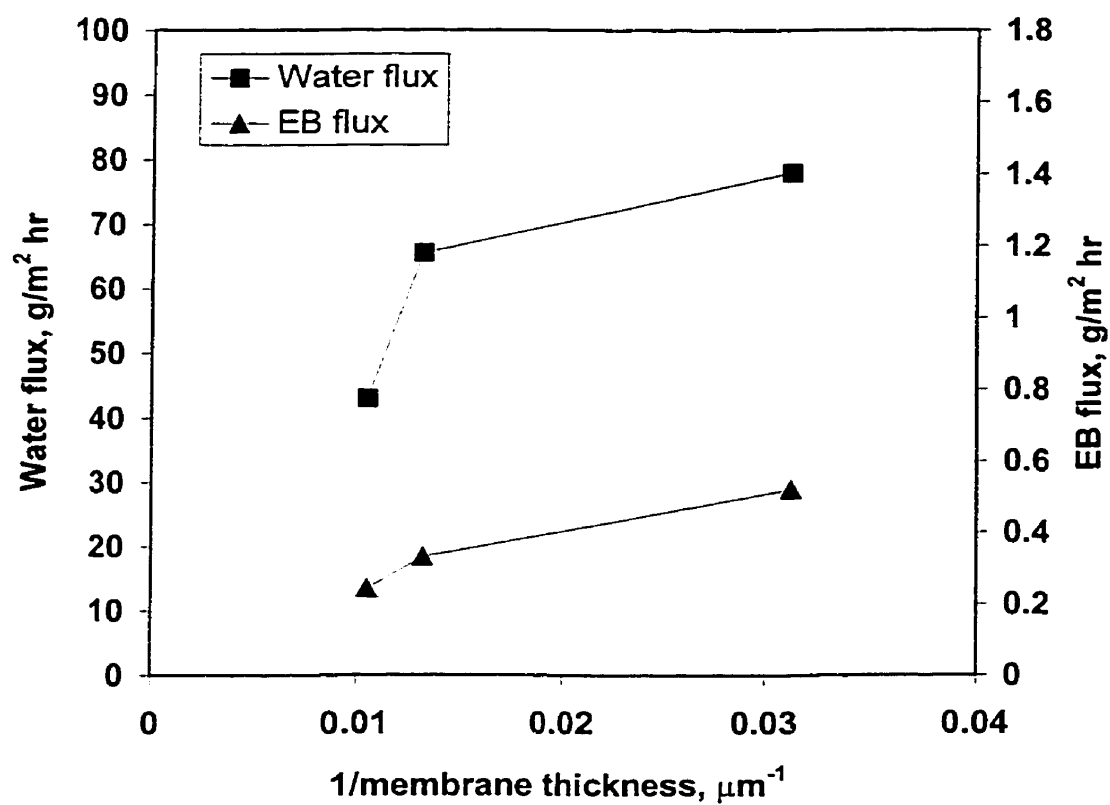


Figure 9.7 Water and organic flux for V-8609 EPDM membranes at feed concentration 600 ppm and 30 °C

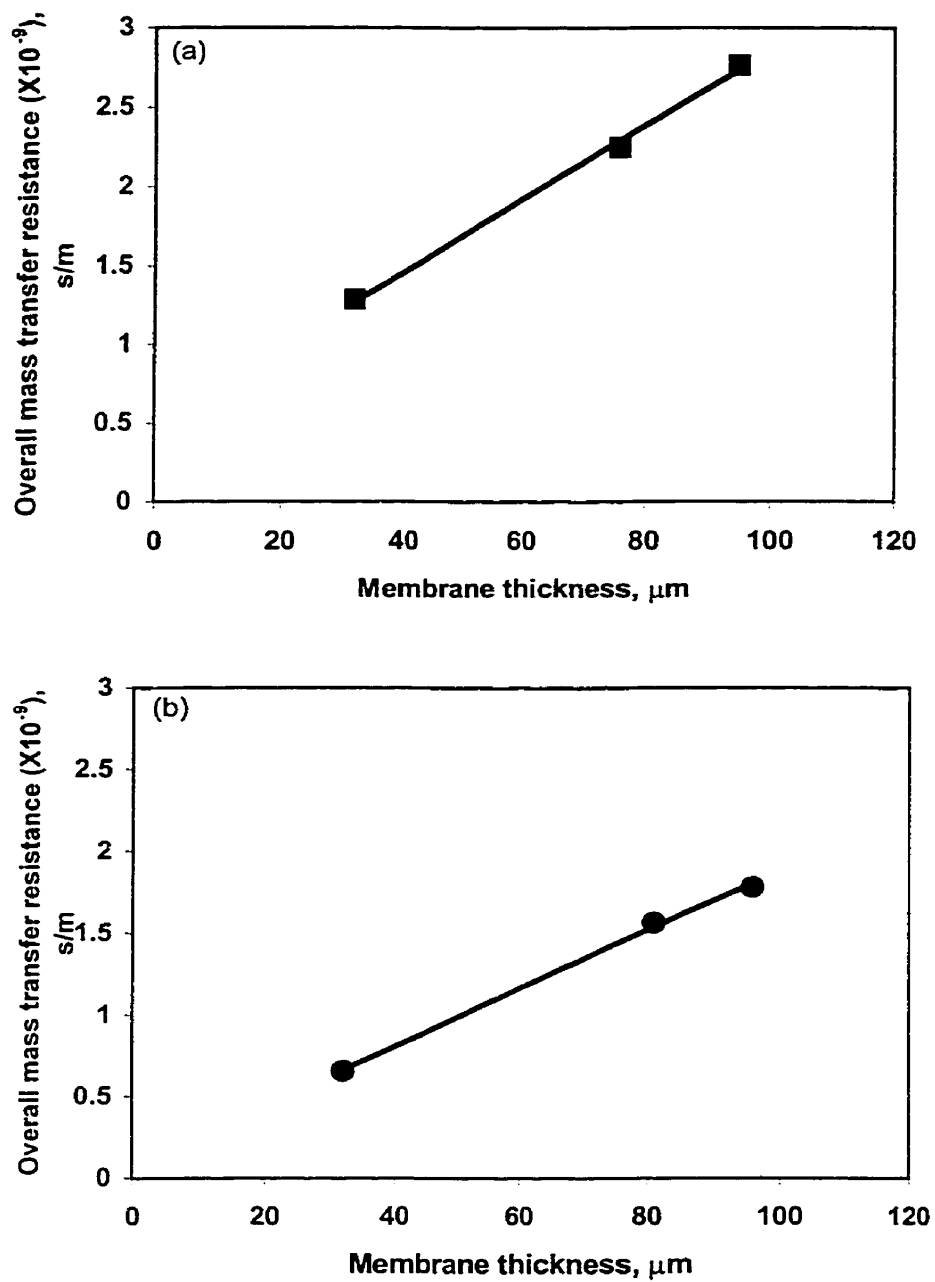


Figure 9.8 Mass transfer resistances as a function of EPDM membrane thickness for Vistalon-8609 (a) and Kelton-514 (b)

	Thickness	$K_i$ (m/s)	$1/K_i$ (s/m)	$1/k_L$ (s/m)	$1/k_m$ (s/m)	$k_m/k_L$
V-8609	32 $\mu\text{m}$	7.78E-10	1.29E+09	5.28E+08	745600	7.08E+02
	76 $\mu\text{m}$	4.44E-10	2.25E+09	5.28E+08	1770800	2.98E+02
	95 $\mu\text{m}$	3.61E-10	2.77E+09	5.28E+08	2213500	2.38E+02
Kelton-514	32 $\mu\text{m}$	1.53E-09	6.54E+08	8.97E+07	572800	1.57E+02
	81 $\mu\text{m}$	6.39E-10	1.57E+09	8.97E+07	1449900	6.19E+01
	96 $\mu\text{m}$	5.61E-10	1.78E+09	8.97E+07	1718400	5.22E+01

**Table 9.2 Overall mass transfer resistance, boundary layer resistance and membrane resistance for EPDM membranes at 30 °C**

From Figure 9.9 it can be concluded that the concentration polarization depends on the feed concentration. When the feed concentration is 100 ppm, the change of EB flux is not significant with the flow rate compared to other feed concentrations. However the EB flux changes significantly with the increase of feed concentration when the feed concentration is above 100 ppm. For the feed concentration ranging from 200 to 600 ppm, EB flux is almost constant above the flow rate of 1.4 l/min. Separation factors increase with the feed flow rate as shown in Figure 9.10. This is due to the reduced concentration polarization at higher flow rate operation. Overall mass transfer resistance was calculated from the experimental data and was plotted with feed flow rate in Figure 9.11. In this experiment, it was assumed that the membrane resistance is constant over the explored feed flow rate range. From the linear decrease of overall mass transfer resistance, it can be concluded that liquid boundary layer resistance can be significantly mitigated with the increase of feed flow rate.

Figure 9.12 shows the effects of down stream pressure on the total flux and EB flux. Total permeation flux decreases with the increase of down stream pressure as

expected. Due to the reduced driving force, transport of the permeants was hindered. However, it is quite interesting that EB flux in Figure 9.12(b) and separation factor in Figure 9.13 increase with the increase of the permeate pressure. It is clear that only water transportation was greatly reduced upon the decrease of the driving force without affecting the transport of EB. When water molecules are excluded from the hydrophobic EPDM membrane, EB molecules with higher affinity to EPDM replace the transport channel for water molecules and swell the membrane. Based on this mechanism, the larger EB flux and the better separation factor can be rationalized. In addition, higher EB content in the feed solution makes the membranes more swollen and facilitates the transport of EB component. However, concurrent fast transport of water molecules lowers the separation factor with the increase of EB content in the feed solution.

Feed temperature effect on EB flux was investigated as shown in Figure 9.14. Temperature was increased from 15 °C to 35 °C. The reason that the feed temperature of 15 °C is explored is because odor of aroma compound can be preserved at lower operating temperature in pervaporation separation of aroma. EB flux increases with the temperature because of fast thermal motion of polymer chain resulting in more available free volume at unit time. Larger flux of Vistalon-8609 membrane than that of Kelton-514 can be attributed to the larger portion of ethylene which makes the membrane less stiff.

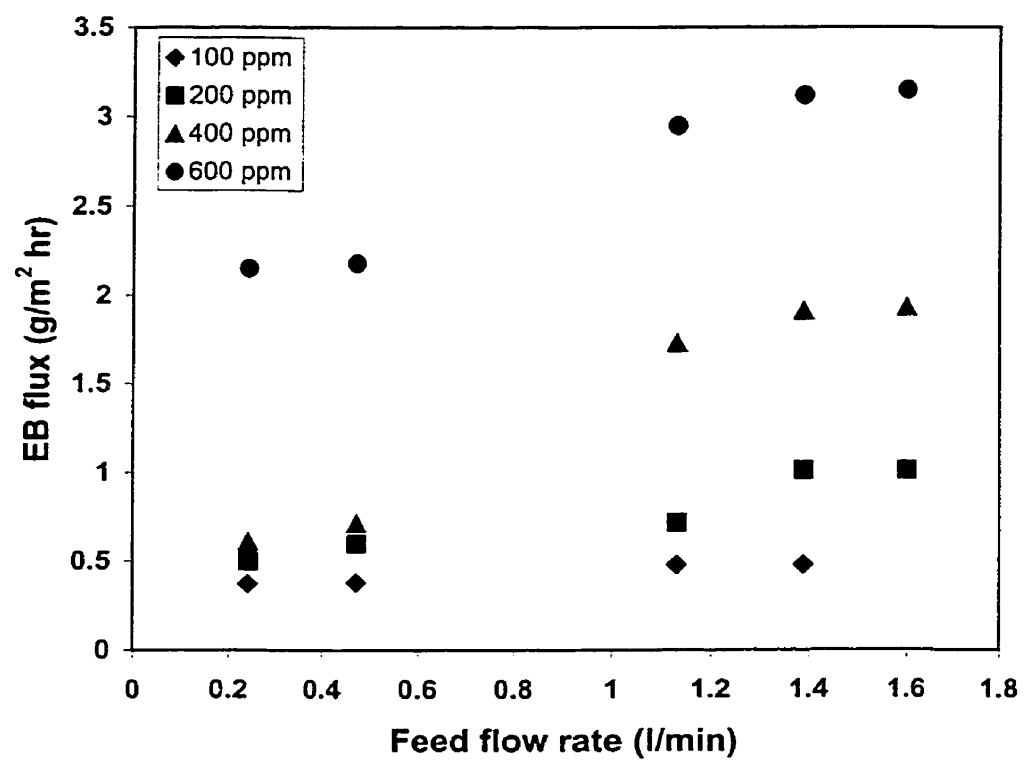
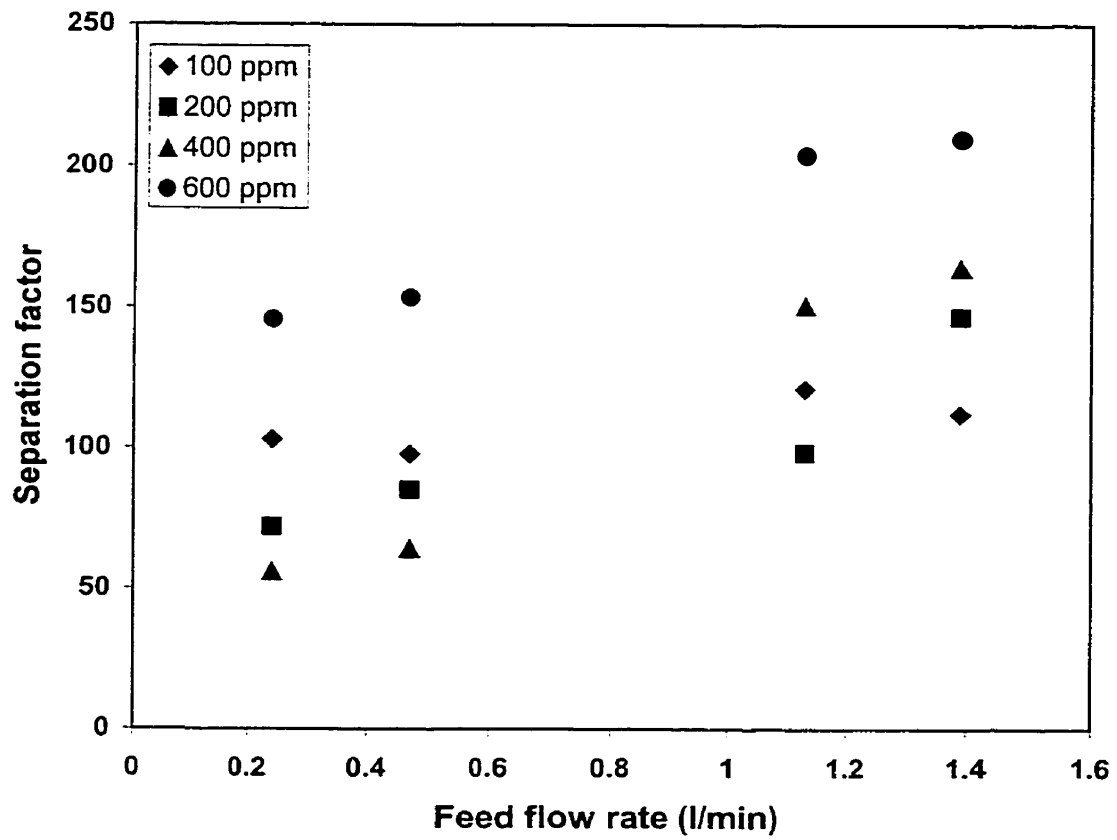


Figure 9.9 Effect of feed flow rate on EB flux (V-8609 EPDM membranes at 30 °C)



**Figure 9.10** Effect of feed flow rate on separation factor (V-8609 EPDM membranes at 30 °C)

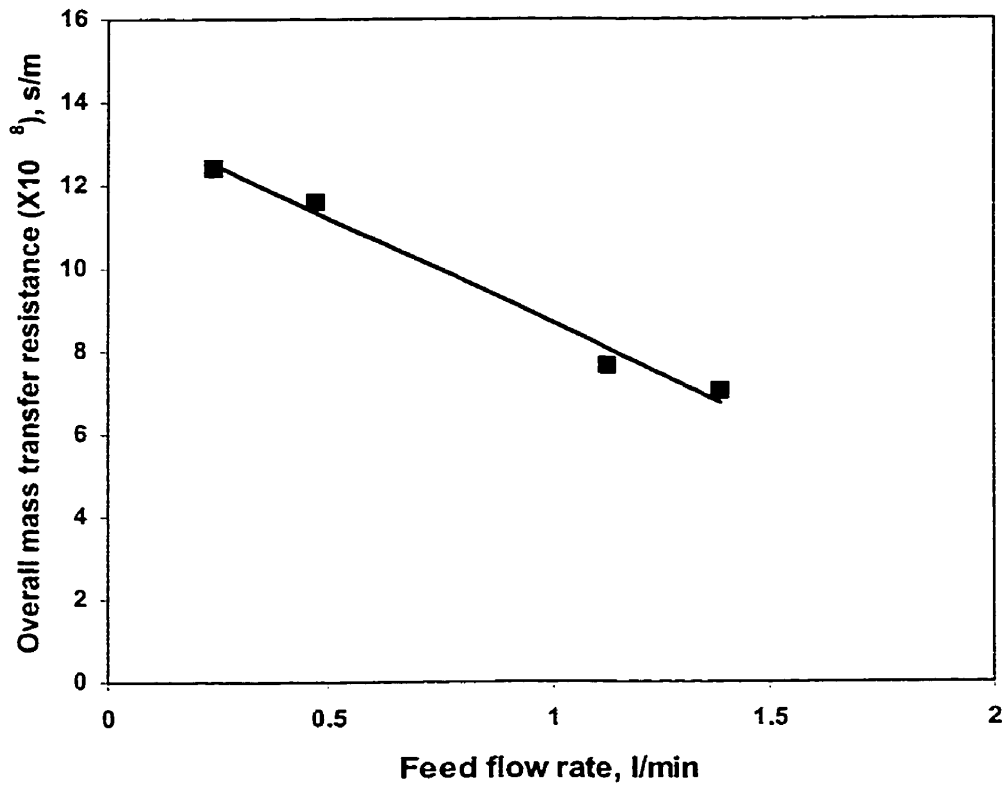


Figure 9.11 Overall mass transfer resistance as a function of feed flow rate for K-514 EPDM membranes at 30 °C)

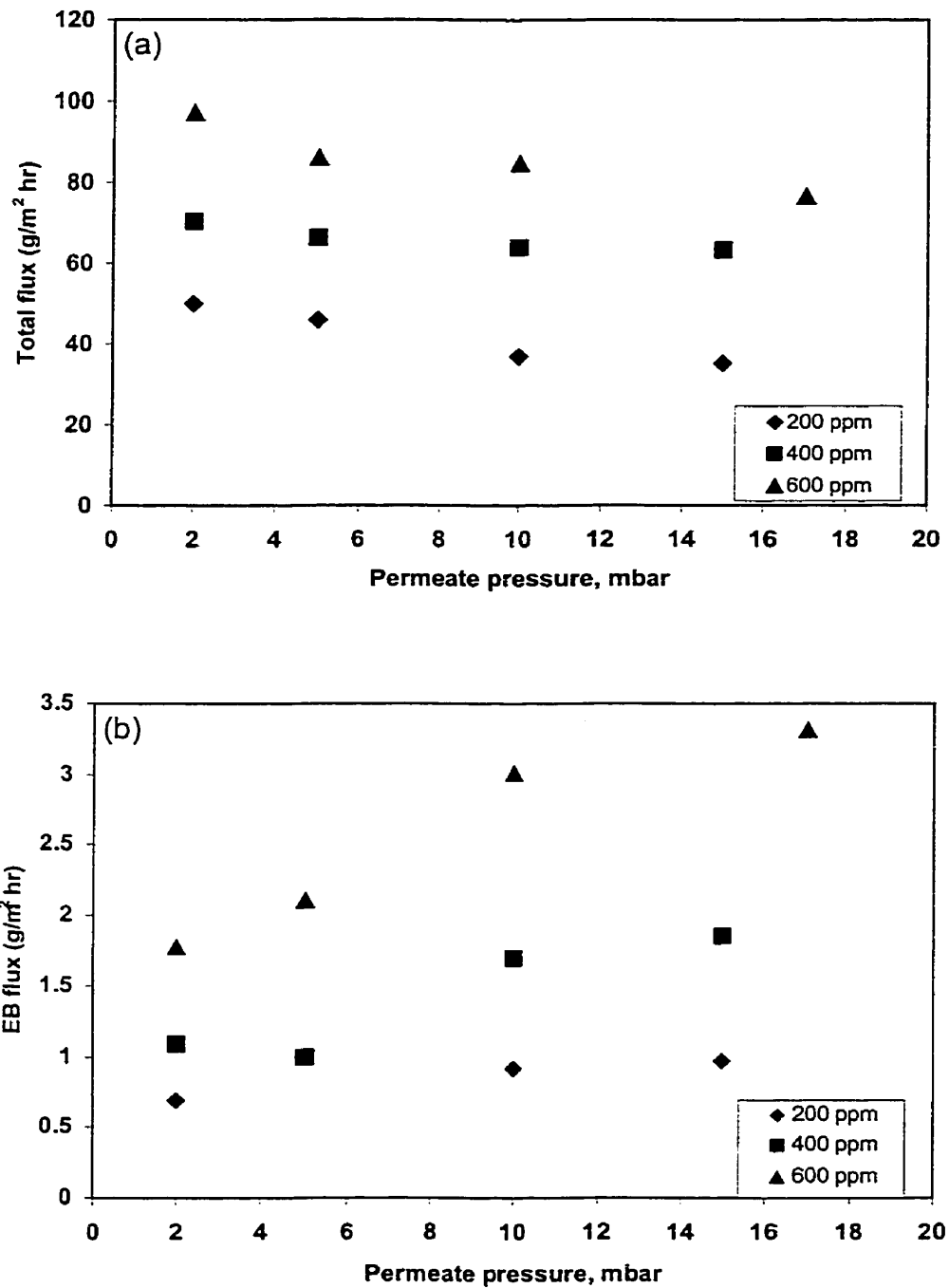


Figure 9.12 Effect of permeate pressure on the total flux (a) and on EB (ethyl butyrate) flux through EPDM membranes (Vistalon 8800) at 30 °C

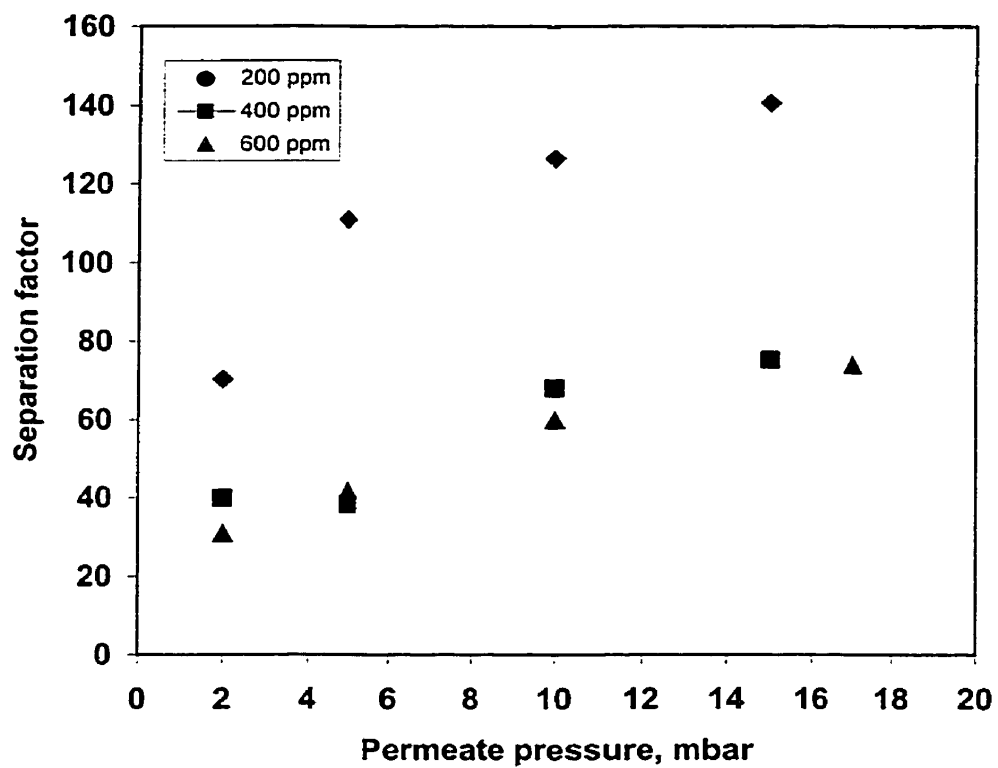
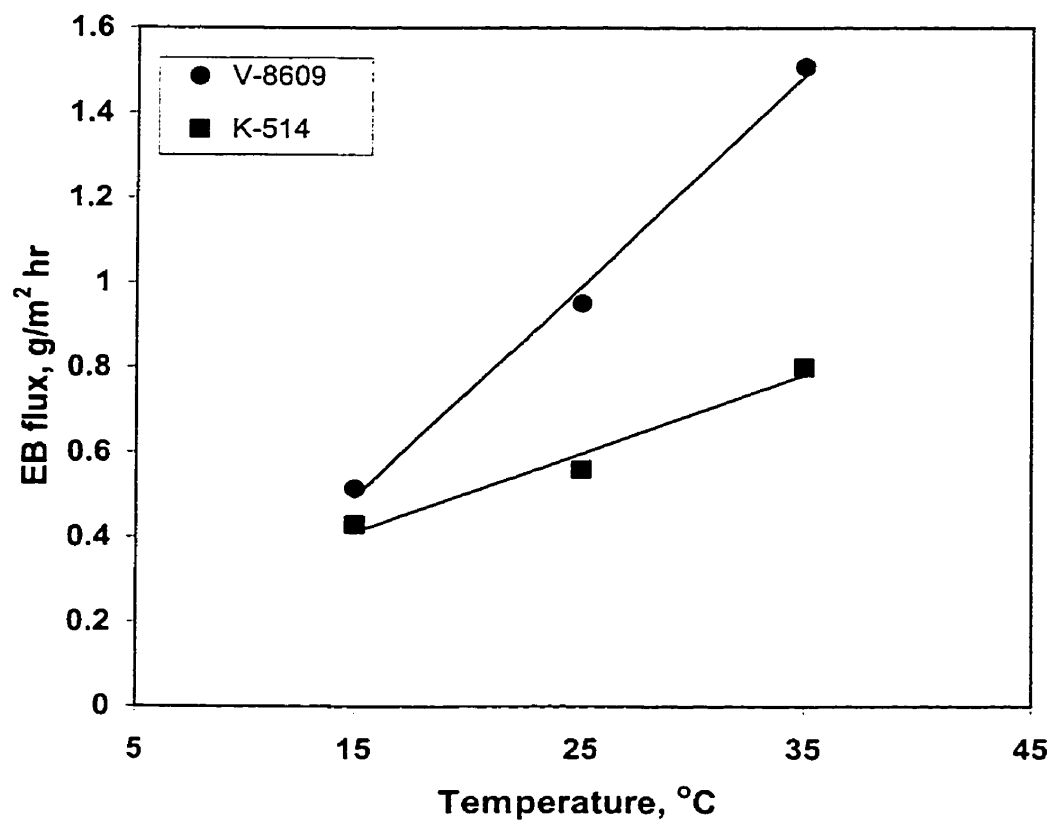


Figure 9.13 Effect of permeate pressure on separation factor through EPDM membranes (Vistalon 8800) at 30 °C



**Figure 9.14 Feed temperature effects on EB flux through two different EPDM membranes (membrane thickness 76  $\mu\text{m}$ )**

## 9.6 CONCLUSIONS

Various EPDM membranes having thin film composite form were studied for the separation of ethyl butyrate, aroma compound, from water stream and were shown to be selective for aroma compound. EPDM membrane having more propylene content (Kelton 514) is more permselective to ethyl butyrate. However due to the more rigid property of propylene the total flux of membrane was lower than that of Vistalon-8609 EPDM membrane.

A resistance-in-series model was used to calculate the mass transfer coefficient in the separation of aroma compound from water. It was observed that the existence of liquid boundary layer resistance in small amount of ethyl butyrate separation was important together with the membrane layer resistance. In addition, the effect of various operating parameters such as feed flow rate, down stream pressure, and operating temperature were also investigated in terms of organic flux and were proven to be significant in the separation performance of EPDM membranes.

## CHAPTER 10

# ORIGINAL CONTRIBUTIONS TO RESEARCH AND RECOMMENDATIONS

---

### 10.1 ORIGINAL CONTRIBUTIONS TO RESEARCH

In this thesis, various promising pervaporation membranes were prepared in the forms of dense and thin film composite membranes and investigated for the pervaporation separation of liquid/liquid mixtures such as water/alcohol, alcohol/toluene, methanol/MTBE and aqueous aroma solutions.

1. Sodium alginate membranes that were not well studied in the past were prepared and applied for the pervaporation dehydration of aqueous alcohol mixtures. It was revealed that the permeation flux and separation factor strongly depend on the ionic crosslinking system used. Among the evaluated metal ions, calcium ion ( $\text{Ca}^{2+}$ ) was the best crosslinker in terms of the flux and separation factor.
2. Novel two ply dense composite membranes were prepared using successive castings of sodium alginate and chitosan solutions for the pervaporation dehydration of isopropanol and ethanol. Preparation and operating parameters namely polymers type facing to the feed stream, NaOH treatment for the regeneration of chitosan, and crosslinking system types were investigated using

the factorial design method. It was observed that these parameters were all critical to the performance of the membranes in terms of the main and interaction effects.

3. Efforts to enhance the stability of the composite membrane consisting of chitosan dense layer and polysulfone support have been made by pretreating the porous support in hydrophilic polymer solution before the casting of top layer. The increase of the flux after the pretreatment was attributed to the reduced intrusion of chitosan solution into micropores, which mitigated the resistance of a permeate transport.
4. Double top layer composite membranes consisting of alginate, chitosan, and porous polyvinylidene fluoride (PVDF) consecutively were prepared. This is the first reported research to overcome the mechanical weakness of alginate layer in the composite membrane. By blending with hydrophilic PMMA polymer the hydrophobic surface property of porous PVDF was changed to be less hydrophobic, which resulted in enhancing the stability of composite membranes.
5. N-acetylated chitosan (chitin) membranes were fabricated for the first time for alcohol separations. Chitin membranes were mechanically robust and stable to withstand the corrosive nature of the ethanol/toluene mixture during the pervaporation runs. This is the first reported successful application of chitin in the form of composite membranes for the pervaporation separation of organic/organic liquid systems.
6. Polyelectrolyte complex membranes were prepared using chitosan and surfactants and the rheological properties of the casting solutions were extensively investigated for the first time. When anionic surfactants are added into the

cationic chitosan solution, the solution viscosity was drastically decreased due to the collapsed chain conformation. Pervaporation characteristics of surfactant modified chitosan membrane were substantially improved due to the decreased membrane thickness and possible enhanced affinity to methanol.

7. EPDM rubber membranes were fabricated and tested for the pervaporation separation of a model aroma compound for the first time. Transport phenomena of aroma compound were investigated and modeled using the resistance-in-series model.

## 10.2 RECOMMENDATIONS FOR FUTURE WORK

There is no lack of topics for future research on pervaporation membranes. Some examples of future research topics are the development of novel membrane materials and their applications in terms of engineering aspects, and the exploration of new application areas.

*Material considerations.* Because of the importance of suitable membrane materials for specific applications, identification of new membrane materials and modification of the existing materials should be addressed in pervaporation studies. For example, polyelectrolyte complex membrane consisting of chitosan and certain anionic polymers may be good candidates for the dehydration and alcohol separations. Sodium carboxy methyl cellulose and poly (styrene sulfonic acid) can be possible candidates as anionic polymers.

*Feed mixture considerations.* Binary feed mixtures are widely used in pervaporation research. However, in reality truly binary feed mixtures are rarely found especially in processes such as industrial wastewater treatment. It is now time to look at ternary or complex feed mixtures which are commonly encountered as industrial liquid mixtures.

*Application considerations.* Among three major applications of the pervaporation membrane processes, the dehydration application is quite mature whereas the organic/organic separation and organic removal from water are relatively less studied in academia and industry mainly because of the difficulties in finding suitable membrane materials and module design sustainable in harsh operating conditions. Pervaporation studies should focus on the separation of organic/organic mixtures which are often encountered in the petrochemical processes.

*Engineering considerations.* Among various membrane modules, plate and frame module is used in laboratory scale experiments because of the convenience. However, when industrial applications are involved, one has to think in terms of engineering aspects such as module type and size, although the membrane material is also critical in the pervaporation performance. In this sense, spiral wound module may play an important role for future pervaporation processes. It is strongly recommended that the investigation of the spiral wound modules be carried out in the future. With this industry friendly module, one can study various engineering issues relevant to the scale up, such as the flow pattern in the module, concentration polarization effect and heat and mass transfer issues etc.

## NOMENCLATURE

---

A	The membrane area in Chapter 1
$A_d$	Proportionality factor
C	Concentration or accounting for peak broadening in Chapter 2
$C_i$	Weight fraction of the permeate in Chapter 4
$C^m$	Total molar concentration in the membrane, mol/m <sup>3</sup>
D	Diffusion coefficient, m <sup>2</sup> /s
E	Activation energy, J/mol
$E_p$	Apparent activation energy of the permeation
$E_D$	Activation energy of diffusion
$\Delta F$	Surface free energy difference
$f$	Fractional free volume
H	Partition coefficient in Chapter 9
$\Delta H$	Enthalpy of sorption
J	The permeation flux, kg/m <sup>2</sup> hr
$J_o$	Coefficient of exponential term
K	Partition coefficient in Chapter 2
$K_{o \text{ or } i}$	Overall mass transfer coefficient in Chapter 9, m/s
$k_i$	Mass transfer coefficient, m/s
L	Column length
P	Permeability or pressure, Pa
$P_v$	Saturation vapor pressure, Pa

$p$	Partial pressure
$Q$	The amount of the permeate
$q$	Shape factor
$R_i$	Resistance to mass transport, s/m
$R$	Gas constant
$r$	Pore radius in Chapter 2
$S$	Solubility
$T$	Feed temperature
$t$	Operating time
$t_r$	Retention time
$V$	Linear velocity of carrier gas
$W_{1/2}$	Peak width at half of the maximum height
$w$	Mass fraction
$X$	Weight fraction of the feed
$x_1$	Mole fraction in the feed and in the permeate side, subscript 2
$Y$	Weight fraction of the permeate

### Greek Letters

$\alpha$	Separation factor
$\beta$	Enrichment factor in Chapter 2 or degree of binding in Chapter 8
$\gamma$	Interfacial tension or liquid surface tension ( $J/m^2$ ) in Chapter 2
$\gamma^m$	Activity coefficient inside the membrane

$\lambda$	Jump length, m
$\tau$	Adsorption dwell time, sec
$\delta$	Solubility parameter or membrane thickness in Chapter 2
$\Delta$	The difference in solubility parameters
$\theta$	Contact angle in Chapter 2
$\Phi$	Volume fraction of the solvent
$\chi$	Flory-Huggins parameter
$\sigma_i^2$	Peak variance

## REFERENCES

---

- Adnadjevic, B., J. Jovanovic, and S. Gajinovic, **Effect of different physicochemical properties of hydrophobic zeolites on the pervaporation properties of PDMS-membranes**, *J. Mem. Sci.*, 136(1997), 173-179
- Allan, G.G. and M. Peyron, **The kinetics of the depolymerization of chitosan by nitrous acid** in *Chitin and Chitosan* edited by G. Skjak-Bræk et al., Elsevier Application Sciences, 1988
- Almquist, C.B. and S.-T. Hwang, **The permeation of organophosphorus compounds in silicone rubber membranes**, *J. Mem. Sci.*, 153(1999), 57-69
- Aptel, P., J. Cuny, J. Jozefonvicz, G. Morel, and J. Neel, **Liquid transport through membranes prepared by grafting of polar monomers onto poly(tetrafluoroethylene) films. II. Some factors determining pervaporation rate and selectivity**, *J. Appl. Polym. Sci.*, 18(1974), 351-364
- Arnold, D. and R.L. Laurence, **Chapter 8. Solute diffusion in polymers by capillary column inverse gas chromatography**, in *Inverse gas chromatography* edited by Lloyd et al., ACS series, Washington, 1989
- Arnold, D. and R.L. Laurence, **Size effects on solvent diffusion in polymers**, *Ind. Eng. Chem. Res.*, 31(1992), 218-228
- Aspinall, G.O. (edited), **The polysaccharides**. Vol.1, Academic press, 1982
- Austin, P.R., **Solvents for and purification of chitin**, US patent 3,892,731, 1975
- Austin, P.R., **Chitin solution**, US patent 4,059,457, 1977
- Austin, P.R. and C.J. Brine, **Chitin films and fibers**, US patent 4,029,727, 1977
- Austin, P.R., **Chitin solvents and solubility parameters** in *Chitin, chitosan and related enzymes* edited by J.P. Zikakis, Academic press, Inc., 1984
- Bai, J., A.E. Fouda, T. Matsuura, and J.D. Hazlett, **Study on the preparation and performance of polydimethylsiloxane-coated polyetherimide membranes in pervaporation**, *J. Appl. Polym. Sci.*, 48(1993), 999-1008
- Balik, C.M., **On the extraction of diffusion coefficients from gravimetric data for sorption of small molecules by polymer thin films**, *Macromol.*, 29(1996), 3025-3029

- Balint, T., E. Nagy, and M. Kraxner, **Study of interaction between butyl alcohols and cellulose acetate polymers with reverse osmosis, high pressure liquid chromatography, and pervaporation methods**, *J. Mem. Sci.*, 78(1993), 101-114
- Baltus, R.E., M.M. Alger, and T.J. Stanley, **Solubility and diffusivity of cyclic oligomers in poly(dimethylsiloxane) using capillary column inverse gas chromatography**, *Macrom.*, 26(1993), 5651-5656
- Baudot, A., M. Marin, **Dairy aroma compounds recovery by pervaporation**, *J. Mem. Sci.*, 120(1996), 207-220
- Baudot, A. and M. Martin, **Improved recovery of an ester flavor compound by pervaporation coupled with a flash condensation**, *Ind. Eng. Chem. Res.*, 38(1999), 4458-4469
- Baudot, A., I. Souchon, and M. Martin, **Total permeate pressure influence on the selectivity of the pervaporation of aroma compounds**, *J. Mem. Sci.*, 158(1999), 167-185
- Bekturov, E.A. and L.A. Bimendina, **Complexes of water-soluble polymers**, *Rev. Macromol. Chem. Phys.*, C37(1997), 501-518
- Bhat, A.A. and V.G. Pangarkar, **Methanol-selective membranes for the pervaporative separation of methanol-toluene mixtures**, *J. Mem. Sci.*, 167(2000), 187-201
- Bhattacharya, S. and S.-T. Hwang, **Concentration polarization, separation factor, and Peclet number in membrane processes**, *J. Mem. Sci.*, 132(1997), 73-90
- Binning, R.C. and F.E. James, **Permeation, a new way to separate mixtures**, *The oil and Gas J.*, May 26(1958a), 104-105
- Binning, R.C. and F.E. James, **Now separate by membrane permeation**, *Petroleum Refiner*, 37, 5(1958b), 214-215
- Binning, R.C., R.J. Lee, J.F. Jennings, and E.C. Martin, **Separation of liquid mixtures by permeation**, *Ind. Eng. Chem.*, 53(1961), 45-50
- Bitter, J.G.A., **Chapter 8 in Transport mechanisms in membrane separation processes**, Plenum Press, 1991
- Blume, I., J.G. Wijmans, and R.W. Baker, **The separation of dissolved organics from water by pervaporation**, *J. Mem. Sci.*, 49(1990), 253-286
- Bonifaci, L., L. Carnelli, and L. Cori, **Determination of infinite dilution diffusion and activity coefficients of solvents in polystyrene by inverse gas chromatography on a capillary column**, *J. Appl. Polym. Sci.*, 59(1994), 1923-1930

Boom, R.M., I.M. Wienk, V.D. Boomgaard, and C.A. Smolders, **Microstructures in phase inversion membranes. Part 2. The role of a polymeric additive**, *J. Mem. Sci.*, 73(1992), 277-292

Box, G.E.P., W.G. Hunter, and J.S. Hunter, **Chapter 10 in Statistics for experimenters**, John Wiley & Sons, Inc., 1978

Boucher-Sharma, A., G. Chowdhury, T. Matsuura, **Removal of n-butanol from aqueous solutions by ion-exchange membranes containing organic counterions**, *J. Appl. Polym. Sci.*, 74(1999), 47-58

Bunn, A., and J.B. Rose, **Sulphonation of polyphenylene ether sulphone containing hydroquinone residues**, *Polymer*, 34(1993), 1114-1116

Brink, L.E.S. and D.J. Romijn, **Reducing the protein fouling of polysulfone surfaces and polysulfone ultrafiltration membranes: optimization of the type of presorbed layer**, *Desal.*, 78(1990), 209-233

Brookes, P.R. and A.G. Livingston, **Aqueous-aqueous extraction of organic pollutants through tubular silicone rubber membranes**, *J. Mem. Sci.*, 104(1995), 119-137

Brun, J-P., C. Larchet, R. Melet, and G. Bulvestre, **Modeling of the pervaporation of binary mixtures through moderately swelling, non-reacting membranes**, *J. Mem. Sci.*, 23(1985a), 257-283

Brun, J-P., C. Larchet, G. Bulvestre, and B. Auclair, **Sorption and pervaporation of dilute aqueous solutions of organic compounds through polymer membranes**, *J. Mem. Sci.*, 25(1985b), 55-100

Bruschke, H.E.A., **Removal of ethanol from aqueous streams by pervaporation**, *Desal.*, 77(1990), 323-330

Cabasso, I., E. Klein, and J.K. Smith, **Polysulfone hollow fibers. II. Morphology**, *J. Appl. Polym. Sci.*, 21(1977), 165-180

Cabasso, I., and Z.-Z. Liu, **The permselectivity of ion-exchange membranes for non-electrolyte liquid mixtures I. Separation of alcohol/water mixtures with Nafion hollow fibers**, *J. Mem. Sci.*, 24(1985), 101-109

Cao, S., Y. Shi, and G. Chen, **Pervaporation separation of MeOH/MTBE through CTA membrane**, *J. Appl. Polym. Sci.*, 71(1999a), 377-386

Cao, S., Y. Shi, and G. Chen, **Properties and pervaporation characteristics of chitosan-poly(N-vinyl-2-pyrrolidone) blend membranes for MeOH-MTBE**, *J. Appl. Polym. Sci.*, 74(1999b), 1452-1458

- Cao, S., Y. Shi, and G. Chen, **Influence of acetylation degree of cellulose acetate on pervaporation properties for MeOH/MTBE mixture**, *J. Mem. Sci.*, 165(2000), 89-97
- Cao, B. and T. Kajiuchi, **Pervaporation separation of styrene-ethylbenzene mixture using poly(hexamethylene sebacate)-based polyurethane membranes**, *J. Appl. Polym. Sci.*, 74(1999), 753-761
- Cao, B., H. Hinode, and T. Kajiuchi, **Permeation and separation of styrene/ethylbenzene mixtures through cross-linked poly(hexamethylene sebacate) membranes**, *J. Mem. Sci.*, 156(1999), 43-47
- Chandak, M.V., Y.S. Lin, W. Ji, and R.J. Higgins, **Sorption and diffusion of volatile organic compounds in polydimethylsiloxane membranes**, *J. Appl. Polym. Sci.*, 67(1998), 165-175
- Chandy, D., D.L. Mooradian, and G.H. Rao, **Chitosan/polyethylene glycol-alginate microcapsules for oral delivery of hirudin**, *J. Appl. Polym. Sci.*, 51(1994), 1427-1432
- Chang, Y.-H., J.-H. Kim, S.-B. Lee, H.-W. Rhee, **Polysiloxaneimide membranes for removal of VOCs from water by pervaporation**, *J. Appl. Polym. Sci.*, 77(2000), 2691-2702
- Chavasit, V., C. Kienzle-Sterzer, and J.A. Torres, **Formation and characterization of an insoluble polyelectrolyte complex**, *Polym. Bull.*, 19(1988), 223-230
- Chen, W.-J. and C.R. Martin, **Highly methanol-selective membranes for the pervaporation separation of methyl t-butyl ether/methanol mixtures**, *J. Mem. Sci.*, 104(1995a), 101-108
- Chen, W.-J., P. Aranda, and C.R. Martin, **Pervaporation separation of ethanol/water mixtures by polystyrenesulfonate / alumina composite membranes**, *J. Mem. Sci.*, 107(1995b), 199-207
- Chen, M.-H., T.-C. Chiao, and T.-W. Tseng, **Preparation of sulfonated polysulfone/polysulfone and aminated polysulfone/polysulfone blend membranes**, *J. Appl. Polym. Sci.*, 61(1996), 1205-1209
- Chen, X., Z. Ping, and Y. Long, **Separation properties of alcohol-water mixture through silicalite-I-filled silicone rubber membranes by pervaporation**, *J. Appl. Polym. Sci.*, 67(1998), 629-636
- Chen, F.R. and H.F. Chen, **Diffusion model of the pervaporation separation of ethylene glycol-water mixtures through crosslinked poly(vinyl alcohol) membrane**, *J. Mem. Sci.*, 139(1998), 201-209

- Chian, E.S.K. and H.H.P. Fang, **Constrained optimization of cellulose acetate membrane using two-level factorial design**, *J. Appl. Polym. Sci.*, 19(1975), 251-263
- Chiang, W.-Y. and C.-C. Huang, **Separation of liquid mixtures by using polymer membranes. IV. Water-alcohol separation by pervaporation through modified acrylonitrile grafted polyvinyl alcohol copolymer(PVA-g-AN) membranes**, *J. Appl. Polym. Sci.*, 48(1993), 199-203
- Chiang, W.-Y. and C.-M. Hu, **Separation of liquid mixtures by using polymer membranes. I. Water-alcohol separation by pervaporation through PVA-g-MMA/MA membrane**, *J. Appl. Polym. Sci.*, 43(1991), 2005-2012
- Chiang, W.-Y. and C.-L. Chen, **Separation of water-alcohol mixture by using polymer membranes-6. Water-alcohol pervaporation through terpolymer of PVA grafted with hydrazine reacted SMA**, *Polymer*, 39(1998), 2227-2233
- Cohen, M.H. and D. Turnbull, **Molecular transport in liquids and gases**, *J. Chem. Phys.*, 31(1959), 1164-1169
- Colman, D., T. Naylor, and G. Pearce, **Alcohol dehydration by pervaporation in The membrane alternative** edited by Howell, Elsevier, New York, 1990, 99-104
- Conder, J.R. and C.L. Young, **Physicochemical measurement by gas chromatography**, John Wiley & Sons, 1979
- Côté, P. and C. Lipski, **Mass transfer limitations in pervaporation for water and wastewater treatment**, Proc. of 3rd Int. Conf. on Pervaporation Processes in the Chemical Industry, Nancy, France, Sept. 19-22, 1988
- Crank, J. and G.S. Park, **Diffusion in polymers**, Academic Press, London, 1968
- Dagaonkar, M.V., S.B. Sawant, J.B. Joshi, and V.G. Pangarkar, **Sorption and permeation of aqueous alkyl piperazines through hydrophilic and organophilic membranes: A transport analysis**, *Sep. Sci. Tech.*, 33(1998), 311-331
- Deng, S., B. Shiyao, S. Sourirajan, and T. Matsuura, **Study of the pervaporation of isopropyl alcohol/water mixtures by cellulose acetate membranes**, *J. Coll. Interf. Sci.*, 136(1990), 283-291
- Deng, S., S. Sourirajan, and T. Matsuura, **Study of polydimethylsiloxane/aromatic polyamide laminated membrane for separation of acetic acid/water mixtures by pervaporation process**, *Sep. Sci. Tech.*, 29(1994), 1209-1216

- Djebbar, M.K., Q.T. Nguyen, R. Clément, Y. Germain, **Pervaporation of aqueous ester solutions through hydrophobic poly(ether-block-amide) copolymer membranes**, J. Mem. Sci., 146(1998), 125-133
- Dotremont, C., B. Brabants, K. Geeroms, J. Mewis, and C. Vandecasteele, **Sorption and diffusion of chlorinated hydrocarbons in silicalite-filled PDMS membranes**, J. Mem. Sci., 104(1995), 109-117
- Dotremont, C., S. Van den Ende, H. Vandommele, and C. Vandecasteele, **Concentration polarization and other boundary layer effects in the pervaporation of chlorinated hydrocarbons**, Desal., 95(1994), 91-113
- Drioli, E., S. Zhang, and A. Basile, **Recovery of pyridine from aqueous solution by membrane pervaporation**, J. Mem. Sci., 80(1993), 309-318
- Dutta, B.K. and S.K. Sikdar, **Separation of volatile organic compounds from aqueous solutions by pervaporation using S-B-S block copolymer membranes**, Environ. Sci. Technol., 33(1999), 1709-1716
- Feng, X., **Studies on pervaporation membranes and pervaporation processes**, Ph.D. dissertation, University of Waterloo, On, Canada, 1994
- Feng, X. and R.Y.M. Huang, **Dehydration of isopropanol by pervaporation using aromatic polyetherimide membranes**, Sep. Sci. Tech., 28(1993), 2035-2048
- Feng, X. and R.Y.M. Huang, **Concentration polarization in pervaporation separation processes**, J. Mem. Sci., 92(1994), 201-208
- Feng, X. and R.Y.M. Huang, **Permeate pressure build-up in shellside-fed hollow fiber pervaporation membranes**, Canadian J. Chem. Eng. 73(1995), 833-843
- Feng, X. and R.Y.M. Huang, **Preparation and performance of asymmetric polyetherimide membranes for isopropanol dehydration by pervaporation**, J. Mem. Sci., 109(1996a), 165-172
- Feng, X. and R.Y.M. Huang, **Pervaporation with chitosan membranes. I. Separation of water from ethylene glycol by a chitosan/polysulfone composite membrane**, J. Mem. Sci., 116(1996b), 67-76
- Feng, X. and R.Y.M. Huang, **Estimation of activation energy for permeation in pervaporation processes**, J. Mem. Sci., 118(1996c), 127-131
- Feng, X. and R.Y.M. Huang, **Liquid separation by membrane pervaporation : A review**, Ind. Eng. Chem. Res., 36(1997), 1048-1066
- Felder, R.M., **Estimation of gas transport coefficients from differential permeation, integral permeation, and sorption rate data**, J. Mem. Sci., 3(1978), 15-27

- Fels, M. and R.Y.M. Huang, **Theoretical interpretation of the effect of mixture composition on separation of liquids in polymers**, *J. Macromol. Sci.-Phys.*, B5(1971), 89-110
- Frisch, H.C. and S.A. Stern, **Diffusion of small molecules in polymers**, *Crit. Rev. Solid state Mat. Sci.*, 11(1983-1984), 123-187
- Fujita, H., **Diffusion in polymer-diluent systems**, *Adv. Polym. Sci.*, 3(1961), 1-47
- Ganesh, K., R. Nagarajan, and J.L. Duda, **Rate of gas transport in glassy polymers: A free volume based predictive model.**, *Ind. Eng. Chem. Res.*, 31(1992), 746-755
- Gao, S. and Q. Bao, **Determination of interfacial parameters of cellulose acetate membrane materials by HPLC**, *J. Liquid Chrom.* 12(1989), 2083-2092
- Ge, J., Y. Cui, Y. Yan, and W. Jiang, **The effect of structure on pervaporation of chitosan membrane**, *J. Mem. Sci.*, 165(2000), 75-81
- George, S.C., K.N. Ninan, S. Thomas, **Pervaporation separation of chlorinated hydrocarbon and acetone mixtures with crosslinked styrene-butadiene rubber and natural rubber blend membranes**, *J. Mem. Sci.*, 176(2000), 131-142
- Giddings, J.C., **Dynamics of chromatography**, Marcel Dekker, NY, 1965
- Goto, M., A. Shiosaki, and T. Hirose, **Separation of water/ethanol vapor mixtures through chitosan and crosslinked chitosan membranes**, *Sep. Sci. Tech.*, 29 (1994), 1915-1923
- Gray, D.G. and J.E. Guillet, **The application of the molecular probe technique to a study of polymer crystallization rates**, *Macrom.*, 4(1971), 129-133
- Gray, D.G. and J.E. Guillet, **Studies of diffusion in polymers by gas chromatography**, *Macrom.*, 6(1973), 223-227
- Gref, R., Q.T. Nguyen, P. Schaetzel, J. Neel, **Transport properties of poly(vinyl alcohol) membranes of different degrees of crystallinity. I. Pervaporation results**, *J. Appl. Polym. Sci.*, 49(1993), 209-218
- Greenlaw, F.W., R.A. Shelden, and E.V. Thompson, **Dependence of diffusive permeation rates on upstream and downstream pressures. I. Single component permeant**, *J. Mem. Sci.*, 2(1977a), 141-151
- Greenlaw, F.W., R.A. Shelden, and E.V. Thompson, **Dependence of diffusive permeation rates on upstream and downstream pressures. II. Two component permeant**, *J. Mem. Sci.*, 2(1977b), 333-348

Guiver, M.D., A.Y. Tremblay, and C.M. Tam, **Reverse osmosis membranes from novel hydrophilic polysulfones**, in *Advances in reverse osmosis and ultrafiltration* edited by Matsuura and Sourirajan, National Research Council of Canada, Ottawa, 1989, 53-70

Guillet, J.E. and A.N. Stein, **Study of crystallinity in polymers by the use of "Molecular probes"**, *Macrom.*, 3(1970), 102-105

Habert, A.C., R.Y.M. Huang, and C.M. Burns, **Ionicly crosslinked polyacrylic acid membranes. I Wet Technique**, *J. Appl. Polym. Sci.*, 24(1979a), 489-501

Habert, A.C., C.M. Burns, and R.Y.M. Huang, **Ionicly crosslinked polyacrylic acid membranes. II Dry Technique**, *J. Appl. Polym. Sci.*, 24(1979b), 801-809

Hadzi, D. and S. Bratos, **Chapter 12. Vibrational spectroscopy of the hydrogen bond in The hydrogen bond**, Vol II. *Structure and spectroscopy* edited by P. Schuster, G. Zundel and C. Sandorfy, North-Holland Publishing Company, 1976

Hao, J., K. Tanaka, H. Kita, and K. Okamoto, **The pervaporation properties of sulfonyl-containing polyimide membranes to aromatic/aliphatic hydrocarbon mixtures**, *J. Mem. Sci.*, 132(1997), 97-108

Hari, P.R., T. Chandy, and C.P. Sharma, **Chitosan/calcium-alginate beads for oral delivery of insulin**, *J. Appl. Polym. Sci.*, 59(1996), 1795-1801

Hawkes, S.J., **Modernization of the van Deemter equation for chromatographic zone dispersion**, *J. Chem. Ed.*, 60(1983), 393-398

Heintz, A., H. Funke, and R.N. Lichtenthaler, **Chapter 6. Sorption and diffusion in pervaporation membranes** in *Pervaporation membrane separation processes* edited by Huang, Elsevier, New York, 1991

Heintz, A. and W. Stephan, **A generalized solution-diffusion model of the pervaporation process through composite membranes. Part I. Prediction of mixture solubilities in the dense active layer using the UNIQUAC model**, *J. Mem. Sci.*, 89(1994a), 143-151

Heintz, A., and W. Stephan, **A generalized solution-diffusion model of the pervaporation process through composite membranes. Part II. Concentration polarization, coupled diffusion and the influence of the porous support layer**, *J. Mem. Sci.*, 89(1994b), 153-169

Hennepe, H.J.C. te, D. Bargeman, M.H.V. Mulder, and Smolders, C.A., **Zeolite-filled silicone rubber membranes Part I. Membrane preparation and pervaporation results**, *J. Mem. Sci.*, 35(1987), 39-55

Hernandez-Muñoz, P., R. Gavara, R. J. Hernandez, **Evaluation of solubility and diffusion coefficients in polymer film-vapor systems by sorption experiments**, J. Mem. Sci., 154(1999), 195-204

Hester, J.F., P. Banerjee, and A.M. Mayers, **Preparation of protein-resistant surfaces on poly(vinylidene fluoride) membranes via surface segregation**, Macromol. 32(1999), 1643-1650

Hirai, A. and H. Odani, **Sorption and transport of water vapor in alginic acid, sodium alginate, and alginate-cobalt complex films**, J. Polym. Sci.: Part B: Polym. Phys., 32(1994), 2329-2337

Hirano, S., Y. Ohe, and H. Ono, **Selective N-acylation of chitosan**, Carbohydr. Res., 47(1976), 315-320

Hirano, S. and R. Yamaguchi, **N-acetylchitosan gel: A polyhydrate of chitin**, Biopolymers, 15(1976), 1685-1691

Hirano, S. and M. Takeuji, **Structural analysis of the reaction products of chitosan with o-, m- and p-phthalaldehydes**, Int. J. Bio. Macromol., 5(1983), 373-376

Hirano, S., R. Yamaguchi, N. Fukui, and M. Iwata, **Biological gels: The gelation of chitosan and chitin** in Biotechnology and polymers edited by Gebelein, C.G., Plenum press, NY, 1991

Hirano, S., A. Usutani, and M. Zhang, **Chitin xanthate and some xanthate ester derivatives**, Carbohydr. Res., 256(1994), 331-336

Ho, W.S., G. Sartori, W.A. Thaler, and D.C. Dalrymple, **Polyimide aliphatic polyester copolymers**, US Patent 4,990,275, 1991

Ho, W.S. and K.K. Sirkar (ed.), **Membrane Handbook**, Van Nostrand Reinhold, New York, 1992

Ho, W.S. and D.C. Dalrymple, **Facilitated transport of olefins in Ag<sup>+</sup>-containing polymer membranes**, J. Membr. Sci., 91(1994), 13-25

Ho, W.S., G. Sartori, W.A. Thaler, D.C. Dalrymple, R.P. Mastondrea and D.W. Savage, **Hard/soft segment copolymer membranes for aromatics/saturates separation**, ICOM 96, Yokohama, Japan, 1996

Hoshi, M., M. Ieshige, T. Saitoh, T. Nakagawa, **Separation of aqueous phenol through polyurethane membranes by pervaporation. II. Influence of diisocyanate and diol compounds and crosslinker**, J. Appl. Polym. Sci., 71(1999a), 439-448

- Hoshi, M., T. Saitoh, C. Toshioka, A. Higuchi, and T. Nakagawa, **Pervaporation separation of 1,1,2-trichloroethane-water mixture through crosslinked acrylate copolymer composite membranes**, *J. Appl. Polym. Sci.*, 74(1999b), 983-994
- Hoshi, M., M. Ieshige, T. Saitoh, T. Nakagawa, **Separation of aqueous phenol through polyurethane membranes by pervaporation. III. Effect of the methylene group length in poly(alkylene glycols)**, *J. Appl. Polym. Sci.*, 76(2000), 654-664
- Howell, J., **The membrane alternatives**, Elsevier Applied Sci., 1990, 1-81
- Hu, D.S., C.D. Han, and L.I. Stiel, **Gas chromatographic measurements of infinite dilution diffusion coefficients of volatile liquids in amorphous polymers at elevated temperatures**, *J. Appl. Polym. Sci.*, 33(1987), 551-576
- Huang, R.Y.M. and V.J.C. Lin, **Separation of liquid mixtures by using polymer membranes. I. Permeation of binary organic liquid mixtures through polyethylene**, *J. Appl. Polym. Sci.*, 12(1968), 2615-2631
- Huang, R.Y.M. and N.R. Jarvis, **Separation of liquid mixtures by using polymer membranes. II. Permeation of aqueous-alcohol solutions through cellophane and poly(vinyl alcohol)**, *J. Appl. Polym. Sci.*, 14(1970), 2341-2356
- Huang, R.Y.M., C.J. Gao, and J.J. Kim, **Ionicly crosslinked polyacrylic acid membranes. IV Composite reverse osmosis membranes**, *J. Appl. Polym. Sci.*, 28(1983), 3063-3073
- Huang, R.Y.M. and J.-W. Rhim, **Theoretical estimates of diffusion coefficients**, *J. Appl. Polym. Sci.*, 41(1990), 535-546
- Huang, R.Y.M. (editor), **Pervaporation membrane separation processes**, Elsevier, New York, 1991
- Huang, R.Y.M. and C.K. Yeom, **Development of crosslinked poly(vinyl alcohol)(type II) and permeation of acetic acid-water mixtures**, *J. Mem. Sci.*, 62(1991), 59-73
- Huang, R.Y.M. and J.W. Rhim, **Separation characteristics of pervaporation membrane separation processes using modified polyvinylalcohol membranes**, *Polym. Inter.*, 30(1993a), 123-128
- Huang, R.Y.M. and J.W. Rhim, **Modification of polyvinylalcohol using maleic acid and its application to the separation of acetic acid-water mixtures by the pervaporation technique**, *Polym. Inter.*, 30(1993b), 129-135
- Huang, R.Y.M. and X. Feng, **Resistance model approach to asymmetric polyetherimide membranes for pervaporation of isopropanol/water mixtures**, *J. Mem. Sci.*, 84(1993), 15-27

- Huang, R.Y.M., R. Pal, and G.Y. Moon, **Crosslinked chitosan composite membrane for the pervaporation dehydration of alcohol mixtures and enhancement of structural stability of chitosan/polysulfone composite membranes**, *J. Mem. Sci.*, 160(1999a), 17-30
- Huang, R.Y.M., R. Pal, and G.Y. Moon, **Characteristics of sodium alginate membranes for the pervaporation dehydration of ethanol-water and isopropanol-water mixtures**, *J. Mem. Sci.*, 160(1999b), 101-113
- Huang, R.Y.M., G.Y. Moon, and R. Pal, **N-acetylated chitosan membranes for the pervaporation separation of alcohol/toluene mixtures**, *J. Membr. Sci.*, 176(2000), 223-231
- Huguet, M.L., A. Groboillot, R.J. Neufeld, D. Poncelet, and E. Dellacherie, **Hemoglobin encapsulation in chitosan/calcium alginate beads**, *J. Appl. Polym. Sci.*, 51(1994), 1427-1432
- Hwang, S.-T. and K. Kammermeyer, **Membranes in separations**, J. Wiley and Sons, 1975
- Inui, K., K. Tsukamoto, T. Miyata, and T. Uragami, **Permeation and separation of a benzene/cyclohexane mixture through benzoylchitosan membranes**, *J. Membr. Sci.*, 138(1998), 67-75
- Inui, K., T. Noguchi, T. Miyata, and T. Uragami, **Pervaporation characteristics of methyl methacrylate-methacrylic acid copolymer membranes ionically crosslinked with metal ions for a benzene/cyclohexane mixture**, *J. Appl. Polym. Sci.*, 71(1999), 233-241
- Ishihara, K., Y. Nagase, and K. Matsui, **Pervaporation of alcohol/water mixtures through poly[1-trimethylsilyl-1-propyne] membrane**, *Mak. Chem., Rapid Commun.*, 7(1986), 43-46
- Ito, A., Y. Feng, and H. Sasaki, **Temperature drop of feed liquid during pervaporation**, *J. Mem. Sci.*, 133(1997), 95-102
- Jegal, J. and K. H. Lee, **Pervaporation separation of water-ethanol mixtures through PVA-sodium alginate blend membranes**, *J. Appl. Polym. Sci.*, 61(1996), 389-392
- Jegal, J. and K. H. Lee, **Chitosan membranes crosslinked with sulfosuccinic acid for the pervaporation separation of water/alcohol mixtures**, *J. Appl. Polym. Sci.*, 71(1999), 671-675
- Ji, W., S.K. Sirkar, S.-T. Hwang, **Modeling of multicomponent pervaporation for removal of volatile organic compounds from water**, *J. Mem. Sci.*, 93(1994), 1-19

- Ji, W., S.K. Sirkar, S.-T. Hwang, **Sorption, diffusion and permeation of 1,1,1-trichloroethane through adsorbent-filled polymeric membranes**, J. Mem. Sci., 103(1995), 243-255
- Ji, W. and S.K. Sirkar, **Pervaporation using adsorbent-filled membranes**, Ind. Eng. Chem. Res., 35(1996), 1124-1132
- Jia, M.-D., K.-V. Peinemann, and R.-D. Behling, **Preparation and characterization of thin-film zeolite-PDMS composite membranes**, J. Mem. Sci., 73(1992), 119-128
- Jian, K. and P.N. Pintauro, **Integral asymmetric poly(vinylidene fluoride)(PVDF) pervaporation membranes**, J. Mem. Sci., 85(1993), 301-309
- Jian, K. and P.N. Pintauro, **Asymmetric PVDF hollow-fiber membranes for organic/water pervaporation separations**, J. Mem. Sci., 135(1997), 41-53
- Jonquieres, A., D. Roizard, J. Cuny, and P. Lochon, **Solubility and polarity parameters for assessing pervaporation and sorption properties. A critical comparison for ternary systems alcohol/ether/polyurethaneimide**, J. Mem. Sci., 121(1996), 117-133
- Jönsson, B., B. Lindmann, K. Holmberg, and B. Kronberg, **Chapter 11. Surfactant-polymer systems in Surfactants and polymers in aqueous solution**, Wiley & Sons, 1998
- Joscelyne, S.M. and G. Trägårdh, **Membrane emulsification-a literature review**, J. Mem. Sci., 169(2000), 107-117
- Juang, R.-S. and R.-C. Shiau, **Metal removal from aqueous solutions using chitosan-enhanced membrane filtration**, J. Mem. Sci., 165(2000), 159-167
- Kataoka, T., T. Tsuru, S. Nakao, and S. Kimura, **Permeation equations developed for prediction of membrane performance in pervaporation, vapor permeation, and reverse osmosis based on the solution-diffusion model**, J. Chem. Eng. Japan, 24(1991), 326-333
- Kataoka, T., T. Tsuru, S. Nakao, and S. Kimura, **Membrane transport properties of pervaporation and vapor permeation in ethanol-water system using polyacrylonitrile and cellulose acetate membranes**, J. Chem. Eng. Japan, 24(1991), 334-339
- Kang, Y.S., S.W. Lee, U.Y. Kim, and J.S. Shim, **Pervaporation of water-ethanol mixtures through crosslinked and surface-modified poly(vinyl alcohol) membrane**, J. Mem. Sci., 51(1990), 215-226

- Kerres, J., W. Cui, and S. Reichle, **New sulfonated engineering polymers via the metalation route. I. Sulfonated polyethersulfone PSU Udel via metalation-sulfination-oxidation**, *J. Polym. Sci.: Part A: Polym. Chem.*, 34(1996), 2421-2438
- Kifune, K., K. Inoue, and S. Mori, **Chitin fibers and process for the production of the same**, US patent 4,932,404, 1990
- Kim, J.-H. and K.-H. Lee, **Effect of PEG additive on membrane formation by phase inversion**, *J. Mem. Sci.*, 138(1998), 153-163
- Kim, K.J., A.G. Fane, and C.J.D. Fell, **The performance of ultrafiltration membranes pretreated by polymers**, *Desal.*, 70(1988), 229-249
- Kober, P.A., **Pervaporation, perstillation and percrystallization**, *J. Mem. Sci.*, 100(1995), 61-64
- Kontominas, M.G., R. Gavara, and J.R. Giacín, **The adsorption of hydrocarbons on polystyrene by inverse gas chromatography: Infinite dilution concentration region**, *Eur. Polym. J.*, 30(1994), 265-269
- Koops G.H., J.A.M. Nolten, M.H.V. Mulder, and C.A. Smolders, **Membrane development for the dehydration of acetic acid by pervaporation-PAN/PVC composite membrane and PSf integrally skinned membrane**, Proc. 6<sup>th</sup> Int. conf. on Pervaporation Proc. in the Chem. Ind., Ottawa, Canada, Bakish Materials Cop., Englewood, NJ, 1992
- Koops G.H., J.A.M. Nolten, M.H.V. Mulder, and C.A. Smolders, **Poly(vinyl alcohol) polyacrylonitrile composite membranes for the dehydration of acetic acid**, *J. Mem. Sci.*, 81(1993), 57-70
- Koops G.H., J.A.M. Nolten, M.H.V. Mulder, and C.A. Smolders, **Selectivity as a function of membrane thickness: gas separation and pervaporation**, *J. Appl. Polym. Sci.*, 53(1994), 1639-1651
- Koros, W.J. and G.K. Fleming, **Membrane-based gas separation; Review**, *J. Mem. Sci.*, 83(1993), 1-80
- Kujawski, W., **Pervaporative removal of organics from water using hydrophobic membranes. Binary mixtures**, *Sep. Sci. Tech.*, 35(2000), 89-108
- Kurokawa, Y., N. Shirakawa, M. Terada, and N. Yui, **Formation of polyelectrolyte complex and its adsorption properties**, *J. Appl. Polym. Sci.*, 25(1980), 1645-1653
- Kusumocahyo, S.P., K. Sano, M. Sudoh, and M. Kensaka, **Water permselectivity in the pervaporation of acetic acid-water mixture using crosslinked poly (vinyl alcohol) membranes**, *Sep. Purif. Tech.*, 18(2000), 141-150

- Lai, J.Y., S.-H. Li, K.-R. Lee, **Permselectivities of polysiloxaneimide membrane for aqueous ethanol mixture in pervaporation**, *J. Mem. Sci.*, 93(1994), 273-282
- Lai, J.-Y., Y.-H. Chu, S.-L. Huang, and Y.-L. Yin, **Separation of water-alcohol mixtures by pervaporation through asymmetric nylon 4 membrane**, *J. Appl. Polym. Sci.*, 53(1994), 999-1009
- Lang, K., G. Chowdhury, T. Tatsuura, and S. Sourirajan, **Reverse osmosis performance of modified polyvinyl alcohol thin-film composite membranes**, *J. Colloid & interf. Sci.*, 166(1994), 239-244
- Lao, G.S., M. Niang, and P. Schaetzel, **Pervaporation separation of ethyl tert-butyl ether and ethanol mixtures with a blended membrane**, *J. Mem. Sci.*, 125(1997), 237-244
- LaPack, M.A., J.C. Tou, V.L. McGuffin, and C.G. Enke, **The correlation of membrane permselectivity with Hildebrand solubility parameters**, *J. Mem. Sci.*, 86(1994), 263-280
- Lawson, K.W. and D.R. Lloyd, **Membrane distillation**, *J. Mem. Sci.*, 124(1997), 1-25
- Lee, K.-R., M.-J. Liu, and J.-Y. Lai, **Pervaporation separation of aqueous alcohol solution through asymmetric polycarbonate membrane**, *Sep. Sci. Tech.*, 29(1994), 119-134
- Lee, K.Y., W.H. Park, and W.S. Ha, **Polyelectrolyte complexes of sodium alginate with chitosan or its derivatives for microcapsules**, *J. Appl. Polym. Sci.*, 63(1997), 425-432
- Lee, Y.M., P. Bourgeois, and G. Belfort, **Sorption, diffusion, and pervaporation of organics in polymer membranes**, *J. Mem. Sci.*, 44(1989), 161-181
- Lee, Y.M., S.Y. Nam, and D.J. Woo, **Pervaporation of ionically surface crosslinked chitosan composite membranes for water-alcohol mixtures**, *J. Mem. Sci.*, 133(1997), 103-110
- Lee, Y.M., H.B. Park, S.Y. Nam, J.M. Won, and H. Kim, **Effect on deacetylation degree in chitosan composite membranes on pervaporation performance**, *Sep. Sci. Tech.*, 33(1998), 1255-1269
- Lee, Y.M., S.Y. Nam, and D.J. Woo, **Pervaporation performance of  $\beta$ -chitosan membrane for water/alcohol mixtures**, *J. Polym. Eng.*, 18(1998a), 131-146
- Linse, P., L. Piculell, and P. Hansson, **Chapter 5. Models of polymer-surfactant complexation** in *Polymer-surfactant systems* edited by J.C.T. Kwak, Marcel Dekker, 1998

- Lipnizki, F., S. Hausmanns, P.-K. Ten, R.W. Field, G. Laufenberg, **Organophilic pervaporation: prospects and performance**, Chem. Eng. J., 73(1999a), 113-129
- Lipnizki, F., R.W. Field, and P.-K. Ten, **Pervaporation-based hybrid process: a review of process design, applications and economics**, J. Mem. Sci., 153(1999b), 183-210
- Lloyd, D.R. and T.B. Meluch, **Selection and evaluation of membrane materials for liquid separations**, in Materials science of synthetic membranes edited by Lloyd, D.R., Amer. Chem. Soc., 1985, 47-79
- Loeb, S. and S. Sourirajan, **Sea water demineralization by means of an osmotic membrane**, Adv. Chem. Ser., 38(1962), 117-132
- Lu, S.-Y., C.-P. Chiu, H.-Y. Huang, **Pervaporation of acetic acid/water mixtures through silicalite filled polydimethylsiloxane membranes**, J. Mem. Sci., 176(2000), 159-167
- Ludtke, O., R.-D. Behling, and K. Ohlrogge, **Concentration polarization in gas permeation**, J. Mem. Sci., 146(1998), 145-157
- Lukas, J., K. Richau, H.-H. Schwart, and D. Paul, **Surface characterization of polyelectrolyte complex membranes based on sodium cellulose sulfate and poly(dimethyldiallylammonium chloride)**, J. Mem. Sci., 106(1995), 281-288
- Lukas, J., K. Richau, H.-H. Schwart, and D. Paul, **Surface characterization of polyelectrolyte complex membranes based on sodium cellulose sulfate and various cationic components**, J. Mem. Sci., 131(1997), 39-47
- Luo, G.S., M. Niang, and P. Schaetzl, **Pervaporation separation of ethyl tert-butyl ether and ethanol mixtures with a blended membrane**, J. Mem. Sci., 125(1997), 237-244
- Maeda, Y. and M. Kai, **Chapter 9. Recent progress in pervaporation membranes for water/ethanol separation** in Pervaporation membrane separation processes edited by Huang, Elsevier, NY, 1991, 391-435
- Matsuura, T., **Synthetic membranes and membrane separation processes**, CRC press, 1994
- Matsuura, T. and S. Sourirajan, **Properties of polymer-solution interfacial fluid from liquid chromatographic data**, J. Colloid Interface Sci., 66(1978), 589-592
- Matsuyama, H., H. Shiraishi, Y. Kitamura, **Effect of membrane preparation conditions on solute permeability in chitosan membrane**, J. Appl. Polym. Sci., 73(1999), 2715-2725

- Mauz, M., K. Kimmerle, and D.F. Huelser, **Concentration of native etheric oil aroma components by pervaporation**, *J. Mem. Sci.*, 118(1996), 145-150
- Mawasaki, T., T. Ohno, M. Taya, and S. Tone, **Separation of butanol from butanol-oleyl alcohol mixture by pervaporation with poly(dimethylsiloxane) hollow-fiber membrane**, *J. Chem. Eng. Jap.*, 25(1992), 257-262
- Meuleman, E.E.B., B. Bosch, M.H.V. Mulder, and H. Strathmann, **Modeling of liquid/liquid separation by pervaporation: Toluene from water**, *AIChE J.*, 45(1999), 2153-2160
- Michaels, A.S., **Polyelectrolyte complexes**, *Ind. Eng. Chem.*, 57(1965), 32-40
- Michell, A.J. and H.G. Higgins, **Conformation and intramolecular hydrogen bonding in glucose and xylose derivatives**, *Tetrahedron*, 21(1965), 1109-1120
- Millesime, L., C. Amiel, and B. Chaufer, **Ultrafiltration of lysozyme and bovine albumin with polysulfone membranes modified with quaternized polyvinylimidazole**, *J. Mem. Sci.*, 89(1994), 223-234
- Mishima, S. and T. Nakagawa, **Plasma-grafting of fluoroalkyl methacrylate onto PDMS membranes and their VOC separation properties for pervaporation**, *J. Appl. Polym. Sci.*, 73(1999), 1835-1844
- Mishima, S. and T. Nakagawa, **Sorption and diffusion of volatile organic compounds in fluoroalkyl methacrylate-grafted PDMS membrane**, *J. Appl. Polym. Sci.*, 75(2000), 773-783
- Miyata, T., T. Iwamoto, and T. Uragami, **Characteristics of permeation and separation for propanol isomers through polyvinyl alcohol membrane containing cyclodextrin**, *J. Appl. Polym. Sci.*, 51(1994), 2007-2014
- Miyata, T., J.-I. Higuchi, H. Okuno, T. Uragami, **Preparation of polydimethylsiloxane/polystyrene interpenetrating polymer network membranes and permeation of aqueous ethanol solutions through the membranes by pervaporation**, *J. Appl. Polym. Sci.*, 61(1996), 1315-1324
- Miyata, T., Y. Nakanishi, and T. Uragami, **Ethanol permselectivity of poly(dimethylsiloxane) membranes controlled by simple surface modifications using polymer additives**, *Macrom.*, 30(1997), 5563-5565
- Mochizuki, A., S. Amiya, Y. Sato, H. Ogawara, and S. Yamashita, **Pervaporation separation of water/ethanol mixtures through polysaccharide membranes IV. The relationships between the permselectivity of alginic acid membrane and its solid state structure**, *J. Appl. Polym. Sci.*, 40(1990), 385-400

- Moon, G.Y., R. Pal, and R.Y.M. Huang, **Novel two ply composite membranes of chitosan and sodium alginate for the pervaporation dehydration of isopropanol and ethanol**, *J. Mem. Sci.*, 156(1999), 17-27
- Moore, G.K. and G.A.F. Roberts, **Reactions of chitosan: 2. Preparation and reactivity of N-acyl derivatives of chitosan**, *Int. J. Bio. Macromol.*, 3(1981a), 292-296
- Moore, G.K. and G.A.F. Roberts, **Reactions of chitosan: 3. Preparation and reactivity of Schiff's base derivatives of chitosan**, *Int. J. Bio. Macromol.*, 3(1981b), 337-340
- Moore, G.K. and G.A.F. Roberts, **Reactions of chitosan: 4. Preparation of organosoluble derivatives of chitosan**, *Int. J. Bio. Macromol.*, 4(1982), 246-249
- Mulder, M.H.V., F. Fruitz, C.A. Smolders, **Separation of isomeric xylenes by pervaporation through cellulose ester membranes**, *J. Mem. Sci.*, 11(1982), 349-363
- Musale, D.A. and S.S. Kulkarni, **Effect of membrane-solute interactions on ultrafiltration performance**, *J. Macromol. Sci.-Rev. Macromol. Chem. Phys.*, C38(1998), 615-636
- Muzzarelli, R.A.A., **Natural chelating polymers: Alginic acid, Chitin and Chitosan**, Pergamon Press, 1973
- Muzzarelli, R.A.A., **Chapter 6. Chitin in The polysaccharides**, Vol. 3 edited by Aspinall, G.O., Academic press, Inc., 1985
- Muzzalupo, R., G.A. Ranieri, G. Golemme, E. Drioli, **Self-diffusion measurements of organic molecules in PDMS and water in sodium alginate membranes**, *J. Appl. Polym. Sci.*, 74(1999), 1119-1128
- Nabe, A., E. Staube, and G. Belfort, **Surface modification of polysulfone ultrafiltration membranes and fouling by BSA solutions**, *J. Mem. Sci.*, 133(1997), 57-72
- Nawawi, M. Ghazali M. and R.Y.M. Huang, **Pervaporation dehydration of isopropanol with chitosan membranes**, *J. Mem. Sci.*, 124(1997), 53-62
- Nawawi, M. Ghazali M., **Pervaporation dehydration of isopropanol-water systems using chitosan membranes**, PhD dissertation, University of Waterloo, 1997
- Nagase, Y., K. Ishihara, and K. Matsui, **Chemical modification of poly(substituted-acetylene). II. Pervaporation of ethanol/water mixture through poly(1-trimethylsilyl-1-propyne)/poly(dimethylsiloxane) graft copolymer membrane**, *J. Polym. Sci., Part B: Polym. Phys.*, 28(1990), 377-386

- Nagase, Y., Y. Takamura, and K. Matsui, **Chemical modification of poly(substituted-acetylene). V. Alkylsilylation of poly(1-trimethylsilyl-1-propyne) and improved liquid separating property of pervaporation**, *J. Appl. Polym. Sci.*, 42(1991), 185-190
- Nam, S.Y. and Y.M. Lee, **Pervaporation of ethylene-glycol-water mixtures I. Pervaporation performance of surface crosslinked chitosan membranes**, *J. Mem. Sci.*, 153(1999a), 155-162
- Nam, S.Y. and Y.M. Lee, **Pervaporation separation of methanol/methyl t-butyl ether through chitosan composite membrane modified with surfactants**, *J. Mem. Sci.*, 157(1999b), 63-71
- Neel, J., **Chapter 1. Introduction to pervaporation** in *Pervaporation membrane separation processes* edited by Huang, Elsevier, NY, 1991, 1-109
- Neel, J., Q.T. Nguyen, R. Clement, and D.J. Lin, **Influence of downstream pressure on the pervaporation of water-tetrahydrofuran mixtures through a regenerated cellulose membrane (Cuprophane)**, *J. Mem. Sci.*, 27(1986), 217-232
- Neumann, A.W., R.J. Good, C.J. Hope, and M. Sejpal, **An equation-of-state approach to determine surface tensions of low-energy solids from contact angles**, *J. Colloid Interf. Sci.*, 49(1974), 291-304
- Nguyen, Q.-T., C. Leger, P. Billard, and P. Lochon, **Novel membranes made from a semi-interpenetrating polymer network for ethanol-MTBE separation by pervaporation**, *Polym. Adv. Tech.*, 8(1997), 487-495
- Nguyen, Q.-T., R. Clement, I. Noezar, P. Lochon, **Performance of poly(vinylpyrrolidone-co-vinyl acetate)-cellulose acetate blend membranes in the pervaporation of ethanol-ethyl tert-butyl ether mixtures, Simplified model for flux prediction**, *Sep. Pur. Tech.* 13(1998), 237-245
- Nijhuis, H.H., M.H.V. Mulder, and C.A. Smolders, **Removal of trace organics from aqueous solutions. Effect of membrane thickness**, *J. Mem. Sci.*, 61(1991), 99-111
- Nii, S., Z.G. Mao, and H. Takeuchi, **Pervaporation with sweeping gas in polymeric hollow fiber membrane module. Separation of alcohols from aqueous solution**, *J. Mem. Sci.*, 93(1994), 245-253
- Nishi, N., J. Noguchi, S. Tokura, and H. Shiota, **Studies on chitin. I. Acetylation of chitin**, *Polym. J.*, 11(1979), 27-32
- Noble, R.D. and S.A. Stern, **Membrane separations technology, Principles and applications**, Elsevier Science B.V., The Netherlands, 1995

- Nunes, S.P. and K.V. Peinemann, **Ultrafiltration membranes from PVDF/PMMA blends**, *J. Mem. Sci.*, 73(1992), 25-35
- Ober, C.K. and G. Wegner, **Polyelectrolyte-surfactant complexes in the solid state: Facile building blocks for self-organizing materials**, *Adv. Mat.*, 9(1997), 17-31
- O'Brien, D.J., J.C. Craig, Jr., **Ethanol production in a continuous fermentation/membrane pervaporation system**, *Appl. Microbiol. Biotechnol.*, 44(1996), 699-704
- O'Brien, D.J., L.H. Roth, A.J. McAloon, **Ethanol production by continuous fermentation-pervaporation: a preliminary economic analysis**, *J. Mem. Sci.*, 166(2000), 105-111
- Ohya, H., K. Matsumoto, T. Negishi, T. Hino, and H.S. Choi, **Separation of water and ethanol by pervaporation with PVA-PAN composite membranes**, *J. Mem. Sci.*, 68(1992), 141-148
- Okada, T. and T. Matsuura, **A new transport model for pervaporation**, *J. Mem. Sci.*, 59(1991a), 133-150
- Okada, T., M. Yoshikawa, and T. Matsuura, **A study on the pervaporation of ethanol/water mixtures on the basis of pore flow model**, *J. Mem. Sci.*, 59(1991b), 151-168
- Olsson, J. and G. Tragardh, **Influence of temperature on membrane permeability during pervaporative aroma recovery**, *Sep. Sci. Tech.*, 34(1999), 1643-1659
- Parthasarathy, A., C.J. Brumlik, C.R. Martin, G.E. Collins, **Interfacial polymerization of thin polymer films onto the surface of a microporous hollow-fiber membrane**, *J. Mem. Sci.*, 94(1994), 249-254
- Pawlish, C.A., **Measurement of the diffusivity and thermodynamic interaction parameters of a solute in a polymer melt using capillary column inverse gas chromatography**, PhD dissertation, University of Massachusetts, Amherst, 1985
- Pawlish, C.A., A. Macris, and R.L. Laurence, **Solute diffusion in polymers. 1. The use of capillary column inverse gas chromatography**, *Macrom.*, 20(1987), 1564-1578
- Pawlish, C.A. J.R. Bric, and R.L. Laurence, **Solute diffusion in polymers. 2. Fourier estimation of capillary column inverse gas chromatography data**, *Macrom.*, 21(1988), 1685-1698
- Park, C.K., B.-K. Oh, M.J. Choi, and Y.M. Lee, **Separation of benzene/cyclohexane by pervaporation through chelate poly(vinyl alcohol)/poly(allyl amine) blend membrane**, *Polym. Bull.*, 33(1994), 591-598

- Park, H.C., R.M. Meertens, M.H.V. Mulder, C.A. Smolders, **Pervaporation of alcohol-toluene mixtures through polymer blend membranes of poly (acrylic acid) and poly (vinyl alcohol)**, J. Mem. Sci., 90(1994), 265-274
- Park, H.C., R.M. Meertens, and M.H.V. Mulder, **Sorption of alcohol-toluene mixtures in poly(acrylic acid)-poly(vinyl alcohol) blend membranes and its role on pervaporation**, Ind. Eng. Chem. Res., 37(1998), 4408-4417
- Pereira, C.C., A.C. Habert, R. Nobrega, C.P. Borges, **New insight in the removal of diluted volatile organic compounds from dilute aqueous solution by pervaporation process**, J. Mem. Sci., 138(1998), 227-235
- Perlin, A.S. and B. Casu, **Chapter 4. Spectroscopic methods in the polysaccharides**, Vol. 1 edited by G.O. Aspinall, Academic press, 1982
- Perterson, R.J., **Composite reverse osmosis and nanofiltration in membranes; Review**, J. Mem. Sci., 83(1993), 81-150
- Pesek, S.C. and W.J. Koros, **Aqueous quenched asymmetric polysulfone membranes prepared by dry/wet phase inversion**, J. Mem. Sci., 81(1993), 71-88
- Pinnau, I. and W.J. Koros, **Structures and gas separation properties of asymmetric polysulfone membranes made by dry, wet, and dry/wet phase inversion**, J. Appl. Polym. Sci., 43(1991), 1491-1502
- Qin, R., H.P. Schreiber, and A. Rudin, **Assessment of degree of fusion of rigid PVC from IGC measurements**, J. Appl. Polym. Sci., 56(1995), 51-56
- Qunhui, G., H. Ohya, Y. Negishi, **Investigation of the permselectivity of chitosan membrane used in pervaporation separation II. Influence of temperature and membrane thickness**, J. Mem. Sci., 98(1995), 223-232
- Qureshi, N. and H.P. Blaschek, **Butanol recovery from model solution/fermentation broth by pervaporation: evaluation of membrane performance**, Biomass and Biology, 17(1999a), 175-184
- Qureshi, N. and H.P. Blaschek, **Production of acetone butanol ethanol (ABE) by a hyper-producing mutant strain of Clostridium beijerinckii BA 101 and recovery by pervaporation**, Biotechnol. Prog., 15(1999b), 594-602
- Raghunath, B. and S.-T. Hwang, **Effect of boundary layer mass transfer resistance in the pervaporation of dilute organics**, J. Mem. Sci., 65(1992), 147-161
- Rautenbach, R. and R. Albrecht, **Membrane processes**, J. Wiley and Sons, 1989

- Rautenbach, R. and R. Albrecht, **On the behavior of asymmetric membrane in pervaporation**, J. Mem. Sci., 19(1984), 1-22
- Rautenbach, R. and R. Albrecht, **The separation potential of pervaporation. Part 1. Discussion of transport equations and comparison with reverse osmosis**, J. Mem. Sci., 25(1985), 1-23
- Ray, R., R.W. Wytcherley, D. Newbold, S. McCray, D. Friesen, and D. Brose, **Synergistic, membrane-based hybrid separation systems**, J. Mem. Sci., 62(1991), 347-369
- Ray, S.K., S.B. Sawant, J.B. Joshi, and V.G. Pangarkar, **Development of new synthetic membranes for separation of benzen-cyclohexane mixtures by pervaporation: A solubility parameter approach**, Ind. Eng. Chem. Res., 36(1997), 5265-5276
- Ray, S.K., S.B. Sawant, J.B. Joshi, and V.G. Pangarkar, **Methanol selective membranes for separation of methanol-ethylene glycol mixtures by pervaporation**, J. Mem. Sci., 154(1999), 1-13
- Reineke, C.E., J.H. Jagodzinski, and K.R. Denslow, **Highly water selective cellulosic polyelectrolyte membranes for the pervaporation of alcohol-water mixtures**, J. Mem. Sci., 32(1987), 207-221
- Ren, J. and C. Jiang, **Transport phenomena of chitosan membrane in pervaporation of water-ethanol mixture**, Sep. Sci. Tech., 33(1998), 517-535
- Rhim, J.-W., **Pervaporation separation of binary organic-aqueous liquid mixtures using modified blended polymer membranes : A theoretical and experimental investigation**, PhD dissertation, University of Waterloo, Canada, 1989
- Rhim, J.-W., M.-Y. Sohn, and K.-H. Lee, **Pervaporation separation of binary organic-aqueous mixtures using crosslinked PVA membranes.II.Phenol-water mixtures**, J. Appl. Polym. Sci., 52(1994), 1217-1222
- Rhim, J.-W. and R.Y.M. Huang, **On the prediction of separation factor and permeability in the separation of binary mixtures by pervaporation**, J. Mem. Sci., 46(1989), 335-348
- Rhim, J.-W., S.-W. Yoon, S.-W. Kim, and K.-H. Lee, **Pervaporation separation and swelling measurement of acetic acid-water mixtures using crosslinked PVA membranes**, J. Appl. Polym. Sci., 63(1997), 521-527
- Rhim, J.-W. and Y.-K. Kim, **Pervaporation separation of MTBE-methanol mixtures using cross-linked PVA membranes**, J. Appl. Polym. Sci., 75(2000), 1699-1707

- Richau, K., H.-H. Schwarz, R. Apostel, D. Paul, **Dehydration of organics by pervaporation with polyelectrolyte complex membranes: some considerations concerning the separation mechanism**, *J. Mem. Sci.*, 113(1996), 31-41
- Rinaudo, M., M. Miles, and P.L. Dung, **Characterization of chitosan. Influence of ionic strength and degree of acetylation on chain expansion**, *Int. J. Biol. Macromol.*, 15(1993), 281-285
- Roberts, G.A.F., **Determination of the degree of N-acetylation of chitin and chitosan** in Chitin handbook edited by R.A.A. Muzzarelli, M.G. Peter, European Chitin Society, 1997
- Ruchenstein, E. and X. Zeng, **Macroporous chitin affinity membranes for lysozyme separation**, *Biotechnol. Bioeng.*, 56(1997), 610-617
- Ryabina, V.R., S.G. Starodubtsev and A.R. Khokhlov, **Interaction of polyelectrolyte networks with oppositely charged micelle-forming surfactants**, *Polymer Sci. U.S.S.R.*, 32(1990), 903-909
- Sampranpiboon, P., R. Jiratananon, D. Uttapap, X. Feng, R.Y.M. Huang, **Pervaporation separation of ethyl butyrate and isopropanol with polyether block amide (PEBA) membranes**, *J. Mem. Sci.*, 173(2000), 53-59
- Sander, U. and M. Janssen, **Industrial application of vapour permeation**, *J. Mem. Sci.*, 61(1991), 113-129
- Scharnagl, N., K.-V. Peinemann, A. Wenzlaff, H.-H. Schwarz, R.-D. Behling, **Dehydration of organic compounds with SYMPLEX composite membranes**, *J. Mem. Sci.*, 113(1996), 1-5
- Schäfer, T., G. Bengtson, H. Pingel, K.W. Böddeker, J.P.S.G. Crespo, **Recovery of aroma compounds from a wine-must fermentation by organophilic pervaporation**, *Biotech. Bioeng.*, 62(1999), 412-421
- Schwarz, H.-H., K. Richau, and D. Paul, **Symplex membranes for pervaporation**, Proc. 5<sup>th</sup> Intern. Conf. Pervaporation Proc. in the Chem. Ind., Heidelberg, Germany, March 11-15, 1991
- Semenova, S.I., H. Ohya, and K. Soontarapa, **Hydrophilic membranes for pervaporation: An analytical review**, *Desal.*, 110(1997), 251-286
- Shelden, R.A. and E.V. Thomson, **Dependence of diffusive permeation rates on upstream and downstream pressures. III. Membrane selectivity and implications for separation processes**, *J. Mem. Sci.*, 4(1978), 115-127

- Sheng, J., **Pilot scale brine concentration process using membrane pervaporation**, J. Mem. Sci., 87(1994), 131-137
- Shi, Y., X. Wang and G. Chen, **Pervaporation characteristics and solution-diffusion behaviors through sodium alginate dense membrane**, J. Appl. Polym. Sci., 61(1996), 1387-1394
- Shieh, J.-J. and R.Y.M. Huang, **Pervaporation with chitosan membranes II. Blend membranes of chitosan and polyacrylic acid and comparison of homogeneous and composite membrane based on polyelectrolyte complexes of chitosan and polyacrylic acid for the separation of ethanol-water mixtures**, J. Mem. Sci., 127(1997), 185-202
- Shieh, J.-J. and R.Y.M. Huang, **A pseudophase-change solution-diffusion model for pervaporation.I. Single component permeation**, Sep. Sci. Tech., 33(1998), 767-785
- Shieh, J.-J. and R.Y.M. Huang, **A pseudophase-change solution-diffusion model for pervaporation.II. Binary mixture permeation**, Sep. Sci. Tech., 33(1998), 933-957
- Shimidzu, T. and M. Yoshikawa, **Chapter 7. Synthesis of novel copolymer membranes for pervaporation** in Pervaporation membrane separation processes edited by Huang, Elsevier, 1991, 321-361
- Shirahama, K., **Chapter 4. The nature of polymer-surfactant interactions in polymer-surfactant systems** edited by J.C.T. Kwak, Marcel Dekker, 1998
- Schnabel, S., P. Moulin, Q.T. Nguyen, D. Roizard, and P. Aptel, **Removal of volatile organic components (VOCs) from water by pervaporation: separation improvement by Dean vortices**, J. Mem. Sci., 142(1998), 129-141
- Smolders, C.A., A.J. Reuvers, R.M. Boom, and I.M. Wienk, **Microstructures in phase-inversion membranes. Part 1. Formation of macrovoids**, J. Mem. Sci., 73(1992), 259-275
- Sourirajan, S., S. Bao, and T. Matsuura, **An approach to membrane separation by pervaporation** in Proc. Sec. Int. Conf. On pervaporation processes in the Chem. Ind., Bakish Materials Corp., Englewood, NJ, 1987, 9-12
- Sun, Y.-M., Y.-K. Chen, C.-H. Wu, and A. Lin, **Pervaporation for the mixture of benzene and cyclohexane through PPOP membranes**, AIChE, 45(1999), 523-534
- Surana, R.K., R.P. Danner, F. Tihminlioglu, and J.L. Duda, **Evaluation of inverse gas chromatography for prediction and measurement of diffusion coefficients**, J. Polym. Sci., PartB: Polym. Phys., 35(1997), 1233-1240

- Suto, S. and N. Ui, **Chemical crosslinking of hydroxypropyl cellulose and chitosan blends**, *J. Appl. Polym. Sci.*, 61(1996), 2273-2278
- Tabe-Mohammadi, A., **A review of the applications of membrane separation technology in natural gas treatment**, *Sep. Sci. Tech.*, 34(1999), 2095-2111
- Takegami, S., H. Yamada, and S. Tsujii, **Pervaporation of ethanol/water mixtures using novel hydrophobic membranes containing polydimethylsiloxane**, *J. Mem. Sci.*, 75(1992), 93-105
- Tan, Z., R. Jaeger, and J. Vancso, **Crosslinking studies of poly(dimethylsiloxane) networks: a comparison of inverse gas chromatography, swelling experiments and mechanical analysis**, *Polymer*, 35(1994), 3230-3236
- Tanihara, N., N. Umeo, T. Kawabata, K. Tanaka, H. Kita, and K. Okamoto, **Pervaporation of organic liquid mixtures through poly(ether imide) segmented copolymer membranes**, *J. Mem. Sci.*, 104(1995), 181-192
- Terbojevich, M., A. Cosani, and R.A.A. Muzzarelli, **Molecular parameters of chitosans depolymerized with the aid of papain**, *Carbohydr. Polym.*, 29(1996), 63-68
- Terbojevich, M. and A. Cosani, **Molecular weight determination of chitin and chitosan** in *Chitin Handbook* edited by R.A.A. Muzzarelli and M.G. Perter, European Chitin Society, 1997
- Tihminlioglu, F., R.K. Surana, R.P. Danner, and J.L. Duda, **Finite concentration inverse gas chromatography: Diffusion and partition coefficient**, *J. Polym. Sci., PartB: Polym. Phys.*, 35(1997), 1279-1290
- Tomihata, K. and Y. Ikada, **Crosslinking of hyaluronic acid with glutaraldehyde**, *J. Polym. Sci.: Part A: Polym. Chem.*, 35(1997), 3553-3559
- Triarte, C., J. Alfageme, A. Etxeberria, and J.J. Iruin, **Gas chromatographic measurements of solute diffusion in blends of phenoxy and poly(1,4-butylene adipate)**, *Eu. Polym. J.*, 31(1995), 609-614
- Tyagi, R.K., A.E. Fouda, and T. Matsuura, **A pervaporation model: membrane design**, *Chem. Eng. Sci.*, 50(1995), 3105-3114
- Ulbricht, M. and H.-H. Schwarz, **Novel high performance photo-graft composite membranes for separation of organic liquids by pervaporation**, *J. Mem. Sci.*, 136(1997), 25-33
- Uragami, T., Y. Ohsumi, and M. Sugihara, **Studies on syntheses and permeabilities of special polymer membranes: 35. Preparation and permeation characteristics of chitin membranes**, *Polymer*, 22(1981), 1155-1156

- Uragami, T., M. Saito, and K. Takigawa, **Comparison of permeation and separation characteristics for aqueous alcoholic solutions by pervaporation and new evapomeation methods through chitosan membranes**, Makromol. Chem., Rapid Commun., 9(1988), 361-365
- Uragami, T. and M. Saito, **Studies on synthesis and permeabilities of special polymer membranes. 68. Analysis of permeation and separation characteristics and new technique for separation of aqueous alcoholic solutions through alginic acid membranes**, Sep. Sci. Tech., 24(1989), 541-554
- Uragami, T. and K. Takigawa, **Permeation and separation characteristics of ethanol-water mixtures through chitosan derivative membranes by pervaporation and evapomeation**, Polymer, 31(1990), 668-672
- Uragami, T. and H. Shinomiya, **Concentration of aqueous alcoholic solutions through a modified silicone rubber membrane by pervaporation and evapomeation**, Makromol. Chem., 192(1991), 2293-2305
- Uragami, T. and H. Shinomiya, **Concentration of aqueous dimethyl sulfoxide solutions through a chitosan membrane by permeation with a temperature difference**, J. Mem. Sci., 74(1992), 183-191
- Uragami, T. and T. Morikawa, **Permeation and separation characteristics of alcohol-water mixtures through Poly(dimethyl siloxane) membrane by pervaporation and evapomeation**, J. Appl. Polym. Sci., 44(1992), 2009-2018
- Uragami, T., T. Matsuda, H. Okuno, T. Miyata, **Structure of chemically modified chitosan membranes and their characteristics of permeation and separation of aqueous ethanol solutions**, J. Mem. Sci., 88(1994), 243-251
- Uragami, T., S. Kato, and T. Miyata, **Structure of N-alkyl chitosan membranes on water-permselectivity for aqueous ethanol solutions**, J. Mem. Sci., 124(1997), 203-211
- Van't Hof, J.A., A.J. Reuvers, R.M. Boom, H.H.M. Rolevink, and C.A. Smolders, **Preparation of asymmetric gas separation membranes with high selectivity by a dual-bath coagulation method**, J. Mem. Sci., 70(1992), 17-30
- Van oss, C.J., J. Visser, D.R. Absolom, S.N. Omenyi, and A.W. Neuman, **The concept of negative hamaker coefficients. II. Thermodynamics, experimental evidence and applications**, Adv. Coll. Interf. Sci., 18(1983), 133-148
- Vankelecom, I.F.J., D. Depre, S. De Beukelaer, and J.B. Uytterhoeven, **Influence of zeolites in PDMS membranes. Pervaporation of water/alcohol mixtures**, J. Phys. Chem., 99(1995), 13193-13197

Vankelecom, I.F.J., B. Moermans, G. Verschueren, P.A. Jacobs, **Intrusion of PDMS top layers in porous supports**, *J. Mem. Sci.*, 158(1999), 289-297

Vankelecom, I.F.J., J.D. Kinderen, B.M. Dewitte, and J.B. Uytterhoeven, **Incorporation of hydrophobic porous fillers in PDMS membranes for use in pervaporation**, *J. Phys. Chem. B*, 101(1997a), 5182-5185

Vankelecom, I.F.J., S. De Beukelaer, and J.B. Uytterhoeven, **Sorption and pervaporation of aroma compounds using zeolite-filled PDMS membranes**, *J. Phys. Chem. B*, 101(1997b), 5186-5190

Villaluenga, J.P.G. and A. Tabe-Mohammadi, **A review on the separation of benzene/cyclohexane mixtures by pervaporation processes**, *J. Mem. Sci.*, 169(2000), 159-174

Vinogradov, S.N. and R.H. Linnell, **Chapter 3. Spectroscopic manifestations of hydrogen bonding in Hydrogen bonding**, Van Nostrand Reinhold Company, 1971

Volkov, V.I., S.A. Korotchkova, H. Ohya, and Q. Guo, **Self-diffusion of water-ethanol mixtures in polyacrylic acid-polysulfone composite membranes obtained by pulsed-field gradient nuclear magnetic resonance spectroscopy**, *J. Mem. Sci.*, 100(1995a), 273-286

Volkov, V.I., S.A. Korotchkova, I.A. Nesterov, H. Ohya, Q. Guo, J. Huang, and J. Chen, **Self-diffusion of water and ethanol mixtures in cellulose derivative membranes and particles with the pulsed-field gradient NMR data**, *J. Mem. Sci.*, 110(1995b), 1-11

Volkov, V.I., V.D. Skirda, E.N. Vasina, S.A. Korotchkova, H. Ohya, and K. Soontarapa, **Self-diffusion of water-ethanol mixture in chitosan membranes obtained by pulsed-field gradient nuclear magnetic resonance technique**, *J. Mem. Sci.*, 138(1998), 221-225

Vrentas, J.S. and J.L. Duda, **Diffusion in polymer-solvent systems. I. Reexamination of the free-volume theory**, *J. Polym. Sci. Polym. Phys. Ed.*, 15(1977a), 403-416

Vrentas, J.S. and J.L. Duda, **Diffusion in polymer-solvent systems. II. A predictive theory for the dependence of diffusion coefficients on temperature, concentration, and molecular-weight**, *J. Polym. Sci. Polym. Phys. Ed.*, 15(1977a), 417-439

Vrentas, J.S. and C.M. Vrentas, **Energy effects of solvent self-diffusion in polymer-solvent systems**, *Macrom.*, 26(1993), 1277-1281

Vrentas, J.S. and C.M. Vrentas, and I.H. Romdhane, **Analysis of inverse gas chromatography experiments**, *Macrom.*, 26(1993), 6670-6672

- Vrentas, J.S., J.L. Duda, and A.-C. Hou, **Segmentwise diffusion in molten polystyrene**, *J. Appl. Polym. Sci.*, 31(1986a), 739-745
- Vrentas, J.S., J.L. Duda, and W.J. Huang, **Regions of fickian diffusion in polymer-solvent systems**, *Macrom.*, 19(1986b), 1718-1724
- Vrentas, J.S. and H.-C. Ling, **Influence of the glass transition on solvent self-diffusion in amorphous polymers**, *J. Polym. Sci. Part B: Polym. Phys.*, 26(1988), 1059-1065
- Vrentas, J.S. and C.-H. Chu, **Predictive capabilities of a free volume theory for solvent self-diffusion coefficients**, *J. Polym. Sci. Part B: Polym. Phys.*, 27(1989), 1179-1184
- Vrentas, J.S., J.L. Duda, and H.-C. Ling, **Free volume theories for self-diffusion in polymer-solvent systems. I. Conceptual differences in theories**, *J. Polym. Sci. Polym. Phys. Ed.*, 23(1985), 275-288
- Vrentas, J.S. and C.M. Vrentas, **Influence of solvent size on the diffusion process for polymer-solvent systems**, *J. Polym. Sci. Part C: Polym. Lett.*, 28(1990), 379-383
- Wang, X.-P., Z.-Q. Shen, F.-Y. Zhang, and Y.-F. Zhang, **A novel composite chitosan membrane for the separation of alcohol-water mixtures**, *J. Mem. Sci.*, 119(1996), 191-198
- Wang, X.-P., Z.-Q. Shen, F.-Y. Zhang, Y.-F. Zhang, **Preferential separation of ethanol from aqueous solution through hydrophilic polymer membranes**, *J. Appl. Polym. Sci.*, 73 (1999), 1145-1151
- Wang, H., K. Tanaka, H. Kita, and K.-I. Okamoto, **Pervaporation of aromatic/non-aromatic hydrocarbon mixtures through plasma-grafted membranes**, *J. Mem. Sci.*, 154(1999), 221-228
- Watanabe, K. and S. Kyo, **Pervaporation performance of hollow-fiber chitosan-polyacrylonitrile composite membrane in dehydration of ethanol**, *J. Chem. Eng. Jap.*, 25(1992), 17-21
- Watson, J.M. and P.A. Payne, **A study of organic compound pervaporation through silicone rubber**, *J. Mem. Sci.*, 49(1990), 171-205
- Watson, J.M., G.S. Zhang, and P.A. Payne, **The diffusion mechanism in silicone rubber**, *J. Mem. Sci.*, 73(1992), 55-71
- Wei, Y.-C. and S.M. Hudson, **The interaction between polymer electrolytes and surfactants of opposite charge**, *Rev. Macromol. Chem. Phys.*, C35(1995), 15-45.
- Wei, Y. and R.Y.M. Huang, **Selective sorption of latex membranes with ethanol-water mixtures**, *Sep. Sci. Tech.*, 29(1994), 301-314

- Wei, Y.C., S.M. Hudson, J.M. Mayer, and D.L. Kaplan, **The crosslinking of chitosan fibers**, *J. Polym. Sci., Part A : Polym. Chem.*, 30(1992), 2187-2193
- Wenzlaff, A., K.W. Boddeker, and K. Haffenbach, **Pervaporation of water-ethanol through ion exchange membranes**, *J. Mem. Sci.*, 22(1985), 333-344
- Wesslein, M., A. Heintz, and R.N. Lichtenthaler, **Pervaporation of liquid mixtures through poly(vinyl alcohol)(PVA) membranes. II. The binary systems methanol/1-propanol and methanol/dioxane and the ternary system water/methanol/1-propanol**, *J. Mem. Sci.*, 51(1990), 181-188
- Wheatley, M.A., M. Chang, E. Park and R. Langer, **Coated alginate microspheres: Factors influencing the controlled delivery of macromolecules**, *J. Appl. Polym. Sci.*, 43(1991), 2123-2135
- Wijmans, J.G., A.L. Athayde, R. Daniels, J.H. Ly, H.D. Kamaruddin, I. Pinnau, **The role of boundary layers in the removal of volatile organic compounds from water by pervaporation**, *J. Mem. Sci.*, 109(1996), 135-146
- Will, B. and R.N. Lichtenthaler, **Comparison of the separation of mixtures by vapor permeation and by pervaporation using PVA composite membranes. I. Binary alcohol-water systems**, *J. Mem. Sci.*, 68(1992), 119-125
- Will, B. and R.N. Lichtenthaler, **Comparison of the separation of mixtures by vapor permeation and by pervaporation using PVA composite membranes. II. The binary systems ammonia-water, methylamine-water, 1-propanol-methanol and the ternary system 1-propanol-methanol-water**, *J. Mem. Sci.*, 68(1992), 127-131
- Wong, B., Z. Zhang, Y. P. Handa, **High-precision gravimetric technique for determining the solubility and diffusivity of gases in polymers**, *J. Polym. Sci. B*, 36(1998), 2025-2032
- Wytcherley, R.W. and F.P. McCandless, **The separation of meta- and para-xylene by pervaporation in the presence of CBr<sub>4</sub>, a selective feed complexing agent**, *J. Mem. Sci.*, 67(1992), 67-74
- Xie, L.Q., **Measurement of solute diffusion in polymers by inverse gas chromatography using fused-silica open tubular columns**, *Polymer*, 34(1993), 4579-4584
- Xie, H.A., Q.T. Nguyen, P. Schaetzel, and J. Neel, **Dehydration of amines and diamines by pervaporation with ionomer and PVA-based membranes**, *J. Mem. Sci.*, 81(1993), 97-108

- Yalpani, M., **Polysaccharides : Synthesis, modifications and structure/property relations**, Elsevier, 1988
- Yamaguchi, T., S. Nakao, and S. Kimura, **Design of pervaporation membrane for organic-liquid separation based on solubility control by plasma-graft filling polymerization technique**, *Ind. Eng. Chem. Res.*, 32(1993), 848-853
- Yamaguchi, T., S. Nakao, and S. Kimura, **Solubility and pervaporation properties of the filling polymerized membrane prepared by plasma-graft polymerization for pervaporation of organic-liquid mixtures**, *Ind. Eng. Chem. Res.*, 31(1992), 1914-1919
- Yamaguchi, T., S. Yamahara, S. Nakao, and S. Kimura, **Preparation of pervaporation membranes for removal of dissolved organics from water by plasma-graft filling polymerization**, *J. Mem. Sci.*, 95(1994), 39-49
- Yamasaki, A., T. Iwatsubo, T. Masuoka, and K. Mizoguchi, **Pervaporation of Ethanol/Water through a polyvinylalcohol/cyclodextrin(PVA/CD) membrane**, *J. Mem. Sci.*, 89(1994a), 111-117
- Yamasaki, A. and K. Mizoguchi, **Preparation of PVA membranes containing beta-cyclodextrin oligomer(PVA/CD membrane) and their pervaporation characteristics for ethanol/water mixture**, *J. Appl. Polym. Sci.*, 51(1994b), 2057-2062
- Yamasaki, A., T. Shinbo, and K. Mizoguchi, **Pervaporation of benzene/cyclohexane and benzene/n-hexane mixtures through PVA membranes**, *J. Appl. Polym. Sci.*, 64(1997), 1061-1065
- Yang, J.S., H.J. Kim, W.H. Jo, and Y.S. Kang, **Analysis of pervaporation of methanol-MTBE mixtures through cellulose acetate and cellulose triacetate membranes**, *Polymer*, 39(1998), 1381-1385
- Yang, J.-S. and G.-H. Hsiue, **C<sup>4</sup> olefin/paraffin separation by poly[(1-trimethylsilyl)-1-propyne]-graft-poly(acrylic acid)-Ag<sup>+</sup> complex membranes**, *J. Membr. Sci.*, 111(1996), 27-38
- Yang, J.-S. and G.-H. Hsiue, **Selective olefin permeation through Ag(I) contained silicone rubber-graft-poly(acrylic acid) membranes**, *J. Membr. Sci.*, 126(1997), 139-149
- Yang, J.-S. and G.-H. Hsiue, **Swollen polymeric complex membranes for olefin/paraffin separation**, *J. Mem. Sci.*, 138(1998), 203-211
- Yanagishita, H., C. Maejima, D. Kitamoto, and T. Nakane, **Preparation of asymmetric polyimide membrane for water/ethanol separation in pervaporation by the phase inversion process**, *J. Mem. Sci.*, 86(1994), 231-240

Yanagishita, H., D. Kitamoto, and T. Nakane, **Separation of alcohol aqueous solution by pervaporation using asymmetric polyimide membrane**, High Performance Polymers, 7(1995), 275-281

Yeom, C.K. and R.Y.M. Huang, **Modeling of the pervaporation separation of ethanol-water mixtures through crosslinked poly(vinyl alcohol) membrane**, J. Mem. Sci., 67(1992), 39-55

Yeom, C.K. and K.-H. Lee, **Study on permeation behavior of a liquid mixture through PVA membranes having a crosslinking gradient structure in pervaporation**, J. Appl. Polym. Sci., 59(1996a), 1271-1279

Yeom, C.K., J.G. Jegal, and K.H. Lee, **Characterization of relaxation phenomena and permeation behaviors in sodium alginate membrane during pervaporation separation of ethanol-water mixture**, J. Appl. Polym. Sci., 62(1996b), 1561-1576.

Yeom, C.K. and K.-H. Lee, **A study on desorption resistance in pervaporation of single component through dense membrane**, J. Appl. Polym. Sci., 63(1997), 221-232

Yeom, C.K. and K.H. Lee, **Characterization of sodium alginate membrane crosslinked with glutaraldehyde in pervaporation separation**, J. Appl. Polym. Sci., 67(1998a), 209-219

Yeom, C.-K. and K.-H. Lee, **Characterization of sodium alginate and poly(vinyl alcohol) blend membranes in pervaporation separation**, J. Appl. Polym. Sci., 67(1998b), 949-959

Yeom, C.K., C.U. Kim, B.S. Kim, K.J. Kim, and J.M. Lee, **Recovery of anionic surfactant by RO process. Part I. Preparation of polyelectrolyte-complex anionic membrane**, J. Mem. Sci., 143(1998c), 207-218

Yeom, C.K., H.K. Kim, and J.W. Rhim, **Removal of trace VOCs from water through PDMS membranes and analysis of their permeation behaviors**, J. Appl. Polym. Sci., 73(1999), 601-611

Yoshikawa, M., H. Yokoi, K. Sanui, and N. Ogata, **Selective separation of water-alcohol binary mixture through poly(maleimide-co-acrylonitrile) membrane**, J. Polym. Sci., Polym. Chem. Ed., 22(1984a), 2159-2168

Yoshikawa, M., H. Yokoi, K. Sanui, N. Ogata, and T. Shimidzu, **Polymer membrane as a reaction field. II. Effect of membrane environment on permselectivity for water-ethanol binary mixtures**, Polym. J., 16(1984b), 653-656

Yoshikawa, M., N. Ogata, and T. Shimidzu, **Polymer membrane as a reaction field. III. Effect of membrane polarity on selective separation of a water-ethanol binary mixture through synthetic polymer membranes**, J. Mem. Sci., 26(1986), 107-113

- Yoshikawa, M., T. Wano, and T. Kitao, **Specialty polymeric membranes 2. Pervaporation separation of aqueous lower alcohol solutions through modified polybutadiene membranes**, J. Mem. Sci., 89(1994), 23-36
- Yoshikawa, M., K. Tsubouchi, M.D. Guiver, and G.P. Robertson, **Modified polysulfone membranes. III. Pervaporation separation of benzene-cyclohexane mixtures through carboxylated polysulfone membranes**, J. Appl. Polym. Sci., 74(1999a), 407-412
- Yoshikawa, M., K. Tsubouchi, and T. Kitao, **Specialty polymeric membranes. VIII. Separation of benzene from benzene/cyclohexane mixtures with nylon 6-graft-poly(butyl methacrylate) membranes**, Sep. Sci. Tech., 34(1999b), 403-422
- Yoshikawa, M. and K. Tsubouchi, **Specialty polymeric membranes. 10. Separation of benzene from benzene/cyclohexane mixtures with modified nylon 6 membranes**, Sep. Purif. Tech., 17(1999c), 213-223
- Yoshikawa, M. and K. Tsubouchi, **Specialty polymeric membranes. 9. Separation of benzene/cyclohexane mixtures through poly(vinyl chloride)-graft-poly(butyl methacrylate)**, J. Mem. Sci., 158(1999d), 269-276
- Yoshikawa, M., T. Yoshioka, J. Fujime, A. Murakami, **Pervaporation separation of MeOH/MTBE through agarose membranes**, J. Mem. Sci., 178(2000), 75-78
- Zander, A.K., M.J. Semmens, and R.M. Narbaitz, **Removing VOCs by membrane stripping**, J. Am. Water Works Assoc., 81(1989), 76-81
- Zeng, X. and E. Ruchenstein, **Control of pore sizes in macroporous chitosan and chitin membranes**, Ind. Eng. Chem. Res., 35(1996), 4169-4175
- Zeng, X. and E. Ruchenstein, **Macroporous chitin affinity membranes for wheat germ agglutinin purification from wheat germ**, J. Mem. Sci., 156(1999), 97-107
- Zhaikov, G.E., A.P. Iordanskii, and V.S. Markin, **Chapter 3 in Diffusion of electrolytes in polymers**, VSP, Utrecht, The Netherlands, 1988
- Zhang, L., D. Zhou, H. Wang, and S. Cheng, **Ion exchange membranes blended by cellulose cuoxam with alginate**, J. Mem. Sci., 124(1997), 195-201
- Zhang, L., J. Guo, J. Zhou, G. Yang, Y. Du, **Blend membranes from carboxymethylated chitosan/alginate in aqueous solution**, J. Appl. Polym. Sci., 77(2000), 610-616
- Zhang, Q., L. Liu and F. Wang, **Preparation and characterization of collagen-chitosan composites**, J. Appl. Polym. Sci., 64(1997), 2127-2130

**Zhao, X.P. and R.Y.M. Huang, Pervaporation separation of ethanol-water mixtures using crosslinked blended polyacrylic acid-nylon 66 membranes, J. Appl. Polym. Sci., 41(1990), 2133-2145**

**Zhou, M., M. Persin, and J. Sarrazin, Methanol removal from organic mixtures by pervaporation using polypyrrole membranes, J. Mem. Sci., 117(1996), 303-309**

## **APPENDIX**

# **THE MEASUREMENT OF VISCOSITY AVERAGE MOLECULAR WEIGHT OF CHITOSAN MEMBRANES. A STUDY ON DEPOLYMERIZATION IN ACETIC ACID**

---

## **INTRODUCTION**

Chitosan has been known to be depolymerized according to the specific activities of enzyme such as papain [Terbojevich et al., 1996] and acid such as nitrous acid [Allan and Peyron, 1988]. In this experiment, the effect of acetic acid concentration in the chitosan solution on the depolymerization was investigated in terms of the viscosity average molecular weight. Measurements of solution viscosity were carried out using a Cannon-Ubbelohde dilution viscometer.

## **MATERIALS AND METHOD**

First, 1.1% chitosan (Flonac-N) flakes were dissolved in 10 wt% and 4 wt% acetic acid solutions, respectively. 10% acetic acid solutions were dissolved in room temperature and 60 °C to know the depolymerization effect according to the temperature increase. Chitosan solution was filtered to remove the undissolved portion or impurities using the

glass filter. The membranes were prepared by casting the polymer solution onto a clean glass plate using a casting knife designed in this laboratory. The casting membranes were dried at room temperature for 24 hours in a dust free, environmentally controlled chamber. The dried membrane was peeled off from the plate, and then treated in 0.8M NaOH solution containing 50 vol% ethanol solution for 24 hours at room temperature, washed thoroughly to completely remove NaOH, dried at room temperature for further use. To prepare the chitosan solution for the measurements of viscosity average molecular weight, chitosan membrane of 0.5 g's prepared in 10% and 4% acetic acid solutions was dissolved in 0.5 M acetic acid (AcOH) solution of 100ml and then 0.2 M sodium acetate (AcONa) of 100 ml was added into the chitosan solution to make 0.0025 g/ml (that is, 0.25 g/dl) solution. These three different solutions which contain the chitosan membranes originally prepared in 10% (temperatures are 25 °C and 60 °C) and 4% acetic acid solutions (at 25 °C), respectively were tested in the viscometer.

Intrinsic viscosity can be calculated as follows.

$$[\eta] = \frac{-t_1 + 4t_{1/2} - 3t_0}{c_1 t_0} \quad (1)$$

Here,  $t_0$  denotes the average flow time of pure solvent (50 vol% 5 M acetic acid/50 vol% 2 M sodium acetate), while  $t_1$ ,  $t_{1/2}$  are the flow times of the chitosan solutions of concentration  $c_1$  ( $=0.25\text{g/dl}$ ) and  $(c_1)/2$ , respectively. The  $t_{1/2}$ 's were obtained as follows. Once  $t_1$  was measured, the pure solvent of the same amount with the chitosan solutions was added to make  $\frac{c_1}{2}$  solution. The resulting solutions were mixed well by bubbling air through the viscometer for one minute, and then  $t_{1/2}$ 's were measured.

After calculating the intrinsic viscosity,  $[\eta]$ , the relationship between the viscosity average molecular weight of a polymer and its intrinsic viscosity is given by Mark-Houwink-Sakurada (MHS) equation:

$$[\eta] = KM^a \quad (2)$$

Here,  $K$  and  $a$  are constants which depend on the polymer, solvent, and solution temperature. For chitosan in 0.5M acetic acid-0.2M sodium acetate the  $K$  and  $a$  values are found to be  $3.5 \times 10^{-4}$  and 0.76 [Terbojevich and Cosani, 1997; Terbojevich et al., 1996; Rinaudo et al., 1993].

#### MEASUREMENT OF MOLECULAR WEIGHT

From the experimental data, intrinsic viscosities,  $[\eta]$ , are 9.2064 dl/g for 4% acetic acid, 8.6744 dl/g and 8.157 dl/g for the dissolving temperature 25 °C and 60 °C of 10% acetic acid solution, respectively. The viscosity average molecular weights of two kinds of chitosan membranes are calculated using MHS equation and listed in below Table. For the 10% acetic acid solution, there is 7% difference in molecular weight between room temperature and 60 °C.

	Chitosan membrane prepared in 10 % acetic acid solution at 25 °C	Chitosan membrane prepared in 10 % acetic acid solution at 60 °C	Chitosan membrane prepared in 4 % acetic acid solution
$M_v$	<u><math>6.0 \times 10^5</math></u>	<u><math>5.58 \times 10^5</math></u>	<u><math>6.5 \times 10^5</math></u>

**PHYSICOCHEMICAL PROPERTIES OF INVESTIGATED  
SOLVENTS IN THIS DISSERTATION**

---

<i>Solvents</i>	<i>MW</i> (g/mol)	<i>Specific</i> <i>Gravity</i>	<i>Solubility in</i> <i>Water</i> (g/100g <i>H<sub>2</sub>O</i> )	<i>Solubility</i> <i>Parameter</i> ( $\delta$ ) (cal/cm <sup>3</sup> ) <sup>0.5</sup>	<i>b.p.</i> (°C)	<i>Vapor</i> <i>Pressure,</i> mmHg (20 °C)
Water	18	1	-	23.4	100	
Methanol	32	0.81	$\infty$	14.3	64.7	96
Ethanol	46	0.79	$\infty$		78	44
Isopropanol	60	0.79	$\infty$		82.3	33
MTBE	88.15	0.7405	5.1	-	55.2	249 @25
Toluene	92	0.806	Minimal		111	22
Ethyl butyrate	116.16	0.875	6460 ppm		120	17.3 @25

## PUBLICATIONS, PRESENTATIONS AND PATENT

---

Publications and presentations resulting from this thesis and PhD program were listed below.

### PUBLICATIONS IN REFEREED JOURNALS

1. **G.Y. Moon**, R. Pal and R.Y.M. Huang, Novel two ply composite membranes of chitosan and sodium alginate for the pervaporation dehydration of isopropanol and ethanol, *Journal of Membrane Science*, 156(1999), 17-27
2. R.Y.M. Huang, R. Pal and **G.Y. Moon**, Crosslinked chitosan composite membrane for the pervaporation dehydration of alcohol mixtures and enhancement of structural stability of chitosan/polysulfone composite membranes, *Journal of Membrane Science*, 160(1999), 17-30
3. R.Y.M. Huang, R. Pal and **G.Y. Moon**, Characteristics of sodium alginate membranes for the pervaporation dehydration of ethanol-water and isopropanol-water mixtures, *Journal of Membrane Science*, 160(1999), 101-113
4. R.Y.M. Huang, R. Pal and **G.Y. Moon**, Pervaporation dehydration of aqueous ethanol and isopropanol mixtures through alginate/chitosan two ply composite

- membranes supported by poly(vinylidene fluoride) porous membrane, *Journal of Membrane Science*, 167(2000), 275-289
5. A. Chanachai, R. Jiraratananon, D. Uttapap, **G.Y. Moon**, W.A. Anderson and R.Y.M. Huang, Pervaporation with chitosan/hydroxyethylcellulose(CS/HEC) blended membrane, *Journal of Membrane Science*, 166(2000), 271-280
  6. R.Y.M. Huang, **G.Y. Moon**, and R. Pal, N-acetylated chitosan membranes for the pervaporation separation of alcohol/toluene mixtures, *Journal of Membrane Science* for the publication, 176(2000), 223-231
  7. R.Y.M. Huang, **G.Y. Moon**, and R. Pal, Chitosan/anionic surfactant complex membranes for the pervaporation separation of methanol/MTBE and characterization of polymer/surfactant system, Accepted in *Journal of Membrane Science* for the publication, August, 2000
  8. **G.Y. Moon**, R.Y.M. Huang, R. Pal, EPDM membranes for the pervaporation separation of aroma compound, In the preparation for the publication, 2000

#### **PRESENTATIONS AT SCIENTIFIC AND ENGINEERING CONFERENCES**

1. **G.Y. Moon**, R. Pal and R.Y.M. Huang, Novel two ply composite membranes of chitosan and sodium alginate for the pervaporation dehydration of isopropanol

- (PrOH) and ethanol (EtOH), International Congress on Membranes and Membrane processes, June 12-18, 1999, Toronto, Canada
2. **G.Y. Moon**, R.Y.M. Huang and R. Pal, N-acetylated chitosan membrane for the pervaporation separation of ethanol/toluene mixture, 49<sup>th</sup> Canadian Chemical Engineering Conference, October 3-6, 1999, Saskatoon, SK, Canada

## **PATENT**

1. R.Y.M. Huang, R. Pal and **G.Y. Moon**, Novel composite membrane, Canadian patent application, March 11, 1999; US patent and PCT application

## EXPERIMENTAL ERRORS

---

Experimental errors involved in pervaporation experiments were studied with pure chitosan membranes for aqueous ethanol mixtures at 60 °C. Three membranes which were believed to be identical in the chemical and physical properties were prepared from the same membrane sheet and were tested for the dehydration of alcohol. Since the membrane properties were generally constant for three membranes, the deviation in experimental results were due to the experimental errors, such as the collection of the permeate and the measurement of permeate concentration using GC. Figure A1 shows deviation of the permeation fluxes increases with the increase of water content in the feed from 1% for 95% EtOH mixture to 11% for 50 % EtOH mixture. When water content in the feed increases, the membrane swells significantly so that the pervaporation time is shortened. The less the operation time is, the larger the experimental error of the permeation flux is. However the non-constant phenomenon was observed for the separation factor vs. the feed concentration as can be seen in Figure A2. This was most likely due to limited amounts of permeate and inaccuracies in GC analysis and refractive index resulted.

Overall, the pervaporation experiments require careful experimental work in order to obtain the reliable data. In this thesis, special efforts were made to collect the experimental data using standardized experimental procedure and careful measurements.

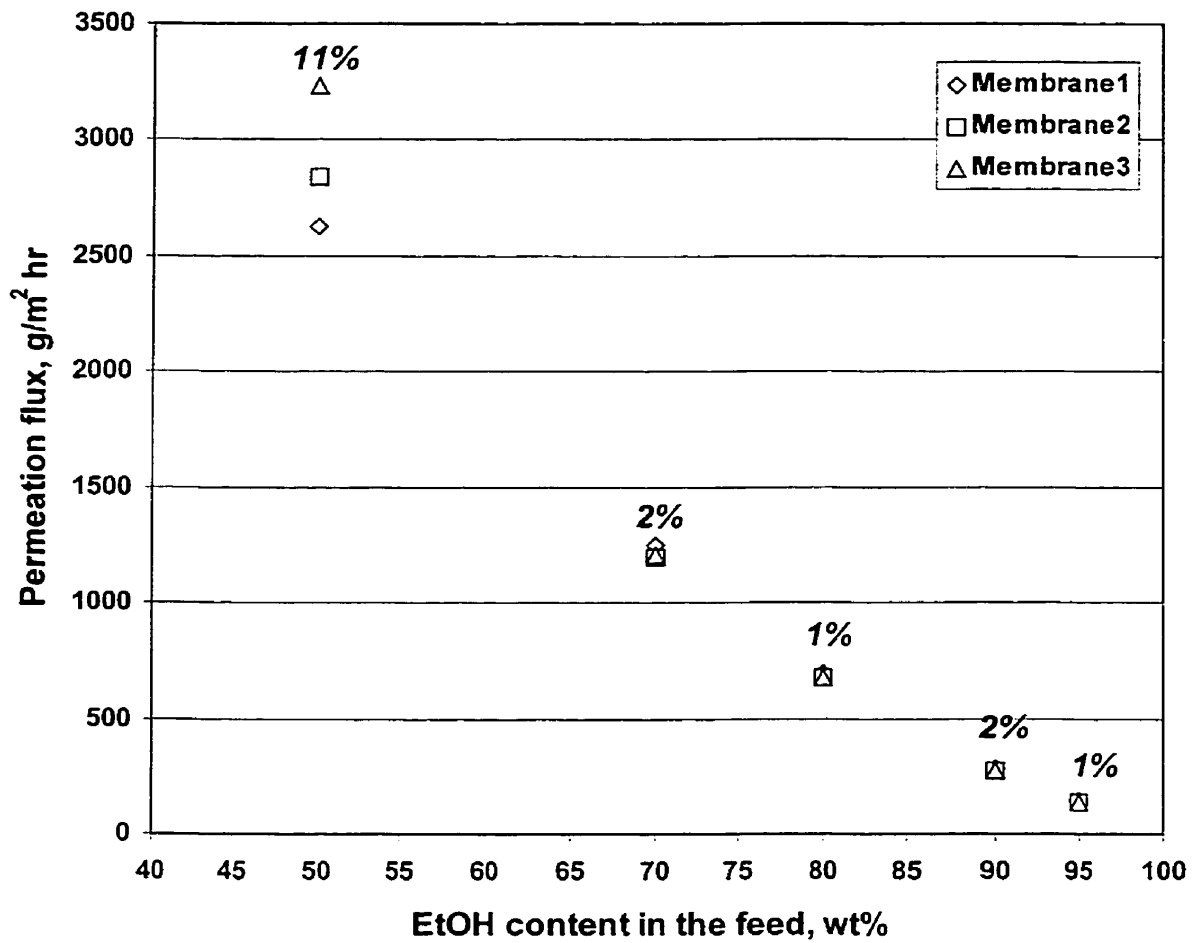


Figure A1 Effect of the feed concentration on the permeation flux for EtOH mixtures at 60 °C and the deviation

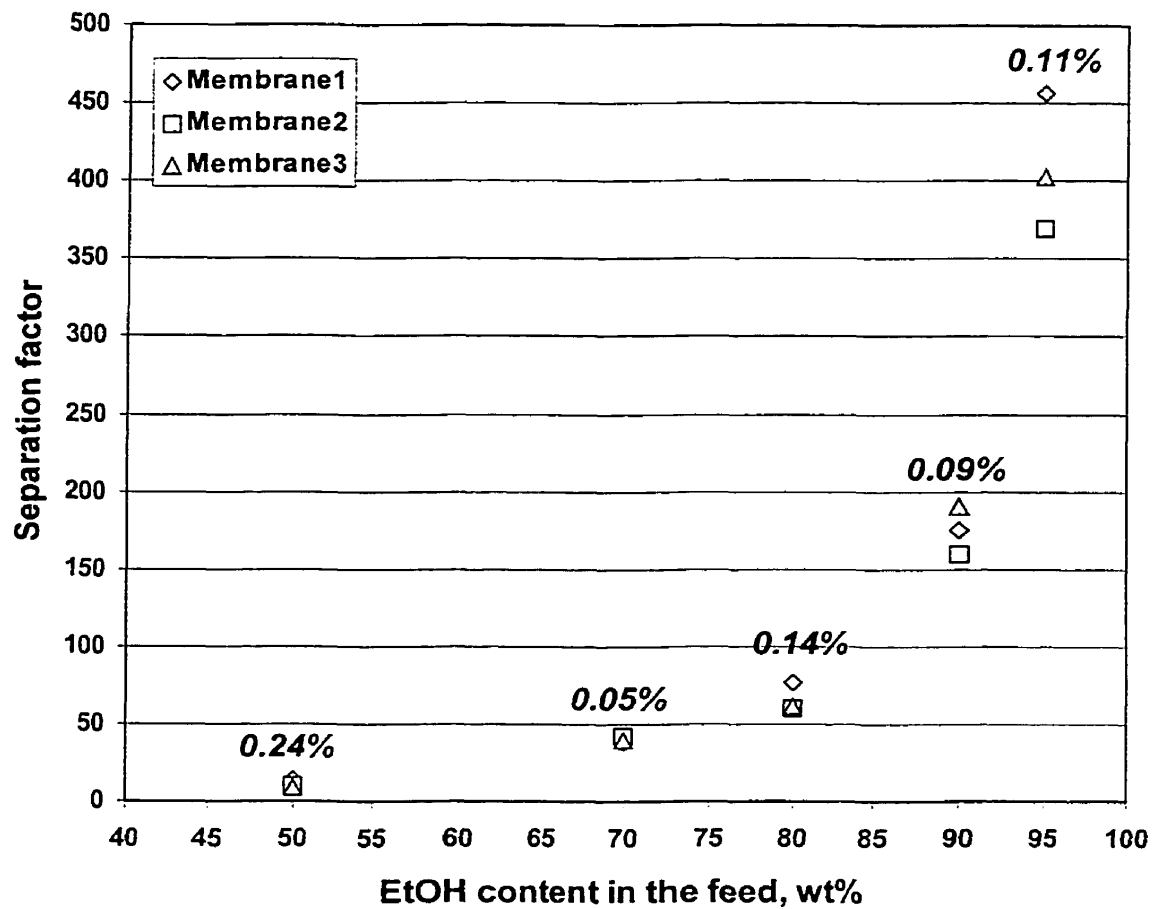


Figure A2 Effect of the feed concentration on the separation factor for EtOH mixtures at 60 °C and the deviation

## EXPERIMENTAL DATA

---

Those who are interested in the experimental data can access to the data files at Membrane Laboratory in Department of Chemical Engineering of University of Waterloo with the permission of Professor Robert Y.M. Huang ([ryhuang@engmail.uwaterloo.ca](mailto:ryhuang@engmail.uwaterloo.ca)).